The Role of the Immune Microenvironment in Mesothelioma and Lung Cancer

By

Suzanne Graef

A thesis submitted to

The University of Birmingham

for the degree of

DOCTOR OF PHILOSOPHY

Institute of Immunology and Immunotherapy

College of Medical and Dental Sciences

The University of Birmingham

February 2019

Abstract

Mesothelioma develops on a background of chronic inflammation, promoting a cytokine rich environment which can alter the profile and function of the immune system. Immunomodulatory treatments have transformed prognosis of many cancers, while mesothelioma outcomes remain poor. Understanding the immunobiology of mesothelioma may unlock resistance and drive progress.

The immune microenvironment of mesothelioma and NSCLC were examined to determine whether T cell immunity could be impaired through myeloid induced T cell tolerance and direct tumour and T cell interactions. Evaluation of peripheral blood and tumour specimens revealed abnormal blood profiles, with high percentages of CD15 and CD14 positive cells and reduced T cell percentages. Mesothelioma tumour cells allowed assessment of the cytokine profile, demonstrating that GM-CSF induced production of reactive oxygen species by granulocytes, leading to T cell inactivation. T cell and dendritic cell dysfunction were also directly induced by mesothelioma, driven by induction of STAT3, as demonstrated by partial rescue with AZD9150.

Sequential peripheral blood profiles were assessed in MATRIX and PEPS2 clinical trials of check-point inhibition in NSCLC. A high neutrophil-to-lymphocyte ratio was significantly predictive of poorer outcome, specifically following the first cycle of treatment. These findings support the theory that immune competence is required for optimal response to immunomodulatory treatments.

Acknowledgements

I would like to thank my supervisors Carmen De Santo and Gary Middleton for all their help and support throughout the last four years. They have provided me with a huge amount of knowledge, support and inspiration, and continue to do so. Such positivity, insight and drive constantly reminds me why I chose to take this time to complete my PhD.

I would also like to thank the wider group in the De Santo/Mussai lab, particularly Frank, Livingstone, Sarah and Sylvia. Their patience, help and guidance during the course of this PhD has been invaluable.

I would like to thank all of the patients and healthy volunteers who gladly gave their blood and tissue, as without their cooperation, there would be no research. I hope that we can provide them with hope and continued faith that progress is being made.

I would like to thank my husband, Jon, for putting up with me during the times that this research caused so many frustrations and, more recently, for being so unbelievably understanding when so many hours were devoted to this project. I could not have managed this without your support. A final thank you is for my daughter, Harper, who joined us during this journey. You have helped make life outside of this PhD so much fuller; you have kept me going.

Table of contents

List of figures

List of tables

Abbreviations

ALK	Anaplastic lymphoma kinase gene
AMP	Adenosine monophosphate
AP-1	Activator protein 1
APC	Antigen presenting cell
BAP1	BRCA associated protein 1
BRCA	Breast cancer 1 gene
CA-125	Cancer antigen 125
CALGB	Cancer and leukaemia group B
CCL	C-C Motif Chemokine Ligand
CD	Cluster of differentiation
CDKN2A	Cyclin dependent kinase inhibitor 2A
cDNA	Complementary DNA
CEA	Carcinoembryonic antigen
COX	Cyclo-oxygenase
CRP	C reactive protein
CT	Computerised tomography
CTLA-4	Cytotoxic T lymphocyte associated antigen 4
CXCL	Chemokine (C-X-C motif) ligand
DAMP	Damage associated molecular patterns
DC	Dendritic cells
DNA	Deoxyribonucleic acid
EGFR	Epidermal growth factor receptor
EMA	Epithelial membrane antigen
EMT	Epithelial to mesenchymal transition
EORTC	European organisation for the research and treatment of cancer
ERK	Extracellular signal related kinases
FOXP3	Forkhead box P3
GCSF	Granulocyte colony stimulating factor
GMCSF	Granulocyte macrophage colony stimulating factor
HBME-1	Hector Battifora Mesothelioma
HDAC	Histone de-acetylase
H_2O_2	Hydrogen peroxide

HLA-DR	Human leucocyte antigen DR
HMGB1	High mobility group box protein 1
HNSCC	Head and neck squamous cell cancer
ICAM	Inter-cellular adhesion molecule
IDO	Indoleamine 2,3-dioxygenase
IFN-γ	Interferon gamma
IHC	Immunohistochemistry
IL	Interleukin
iNOS	Inducible nitric oxide synthase
IRF-1	Interferon regulatory factor 1
JAK	Janus Kinase
LAG-3	Lymphocyte antigen gene-3
MAPK	Mitogen activated protein kinase
MATRIX	National lung MATRIX trial
MCP-1	Monocyte chemoattractant protein-1
MDSC	Myeloid derived suppressor cells
MHC	Major histocompatibility complex
MIP-2	Macrophage inflammatory protein 2
MLR	Mixed leucocyte reaction
MMP	Matrix metalloproteinase
MT-1 MMP	Membrane type 1 matrix metalloproteinase
MTAP	Methylthioadenosine phosphorylase
mTOR	Mammalian target of rapamycin
NALP3	NACHT, LRR and PYD domains containing protein
NF2	Neurofibromatosis 2 gene
NF-κB	Nuclear factor kappa-light-chain-enhancer of activated B cells
NK cell	Natural killer cell
NLR	Neutrophil Lymphocyte Ratio
NO	Nitric Oxide
NP57	Neutrophil elastase
NPM	Nucleophosmin gene
NSCLC	Non-small cell lung cancer
OS	Overall survival
PAMPs	Pathogen associated molecular patterns

PD-1	Programmed cell death protein 1
PD-L1	Programmed cell death protein ligand 1
PDGF	Platelet derived growth factor
PET	Positron emission tomography
PFS	Progression free survival
PG-E2	Prostaglandin E2
PI3K	Phosphoinositide 3-kinases
PMA	Phorbol 12-myristat 13-acetate
PRR	Pattern recognition receptors
PS	Performance status
PTEN	Phosphatase and tensin homolog gene
RB	Retinoblastoma protein
ROS	Reactive Oxygen Species
SASP	Senescence associated phenotype
SOCS3	Suppressor of cytokine signalling 3 protein
STAT	Signal transducer and activator of transcription
TAM	Tumour associated macrophage
TAN	Tumour associated neutrophil
TCR	T cell receptor
Th cells	T helper cells
TIGIT	T-cell immunoreceptor with Ig and ITIM domains
TIM-3	T cell immunoglobulin-3
TLR	Toll like receptors
TNM	Tumour, lymph node and metastases
Treg	Regulatory T cell
TTF-1	Thyroid transcription factor 1
TGF-β	Transforming growth factor beta
TNF-α	Tumour necrosis factor alpha
TP53	Tumour protein 53
VEGF	Vascular endothelial growth factor
WT-1	Wilms' tumour 1

Chapter 1: Introduction

1.1 Mesothelioma

1.1.1 The Incidence and Epidemiology of Mesothelioma

Malignant mesothelioma is an aggressive tumour which primarily affects the pleura and peritoneum (1). It was first identified as an asbestos related disease in the late 1950's following epidemiological observations in South Africa, with cases almost exclusively seen in men and women exposed to environmental asbestos and working in the asbestos industry (2). It has since been shown throughout industrialised countries that overall consumption levels of asbestos are highly correlated to increased incidence of mesothelioma (3). Patterns of mesothelioma incidence further localise to areas of naturally occurring asbestos and areas with high industrial use (4,5). The incidence of mesothelioma climbed markedly following the 1960's, owing to increases of the mining and production of asbestos related products in the preceding 25 years, peaking in the early 1970's (3). Asbestos uses included building products, cement, pipes, insulation, roofing materials and tiles; with the UK seeing a particular use of asbestos in the ship building industries. Mortality rates in the UK saw a greater than ten-fold increase between 1968 and 2001, and trends in the ages of those affected began to change, with increased numbers reported before the age of 60 (5,6). Following epidemiological studies, mesothelioma incidence has been shown to be highest amongst males. However, risk is also increased in female contacts of male asbestos workers (7) and occurs in equal prevalence where early environmental exposure has occurred (8). These findings support the

fact that increased male incidence is caused through increased exposure within male dominated professions, rather than a genetic predilection for this disease.

Following acceptance of asbestos as a class I carcinogen, its use was banned within the UK in 1985. However, due to the significant latency period between exposure and the development of mesothelioma, a predicted peak incidence of mesothelioma in the UK is due between 2015 and 2020 (6,9). In many Western countries asbestos use is now strictly prohibited and regulated, however worldwide, it continues to be used as a low cost construction material and resistance to regulation has been seen in countries with high levels of production (10,11). Worldwide incidence is predicted to continue to rise in correlation with the use per capita of asbestos following extrapolation from data within developed countries although accurate information on recorded cases in developing countries is limited (12). With 2 million tons of recorded asbestos production worldwide in the year 2000, a significant worldwide health burden is predicted (3,10).

Although asbestos is by far the biggest driver of mesothelioma, cases have also been associated with environmental erionite exposure (13), ionising radiation (14) and simian virus 40 (SV40) (15). Erionite is a naturally occurring fibrous mineral which, when inhaled, can lead to respiratory diseases similar to those induced by asbestos. Cases were originally identified relating to environmental exposure in Turkey (16), leading to classification as a group 1 carcinogen; however, erionite has since been identified widely in western USA (17,18). Concerns have been raised regarding possible environmental and occupational exposure, yet no legal regulations regarding its use are in place (17).

Links with ionising radiation were identified when increased incidence was observed in populations treated for testicular cancer and Hodgkin's Lymphoma (9,14,16,19) and, more

controversially, the association with SV40 and mesothelioma, was proposed following the contamination of a large number of polio vaccines with live SV40 within the 1950's and 1960's (20). SV40 has been demonstrated to have oncogenic potential, with a link to the development of mesothelioma proposed following detection of SV40 DNA sequences within mesothelioma specimens (15,21). This causal relationship has however, never been proven and there remains considerable doubt regarding the true risk of SV40 contamination (22).

Approximately 2700 cases of mesothelioma were diagnosed within the UK 2015, accounting for less than 1% of cancer diagnoses within the UK overall. Incidence is significantly higher in males, accounting for 85% of the diagnoses. Over the last 20 years there has been a large increase in combined age standardised incidence, although this has begun to slow since 2005. Within the last 10 years, incidence in women within the UK has been climbing at a higher rate than males, seeing a 16% increase, whereas in males it has remained largely stable (23), Figure 1.1. The highest increases in incidence have been seen in the most elderly populations, with those over 80 years seeing incidence per 100,000 increase from 17% to 26%, compared to a falling incidence in those under 60, reflecting the changing patterns of exposure. Once diagnosed, mesothelioma is almost universally fatal, with average survival between 9 and 12 months (24) and 5 year survival rates of only 5%. These survival outcomes are among the poorest outcomes for all cancer sites, second only to pancreatic carcinoma (25). Mortality rates have therefore risen steadily in line with increases in incidence, with dramatic increases from 0.4 per 100,000 to 4.4 per 100,000 seen since the 1970's (Figure 1.2).

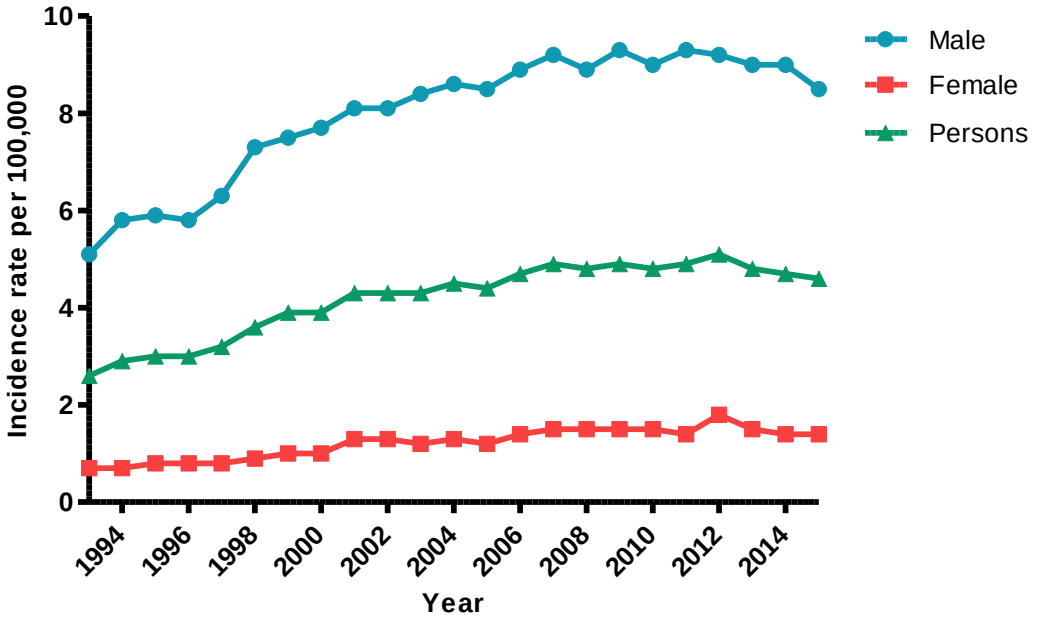

Figure 1. 1. Mesothelioma Age-Standardised Incidence Rates within the UK between 1993-2015. Adapted from Cancer Research UK (20).

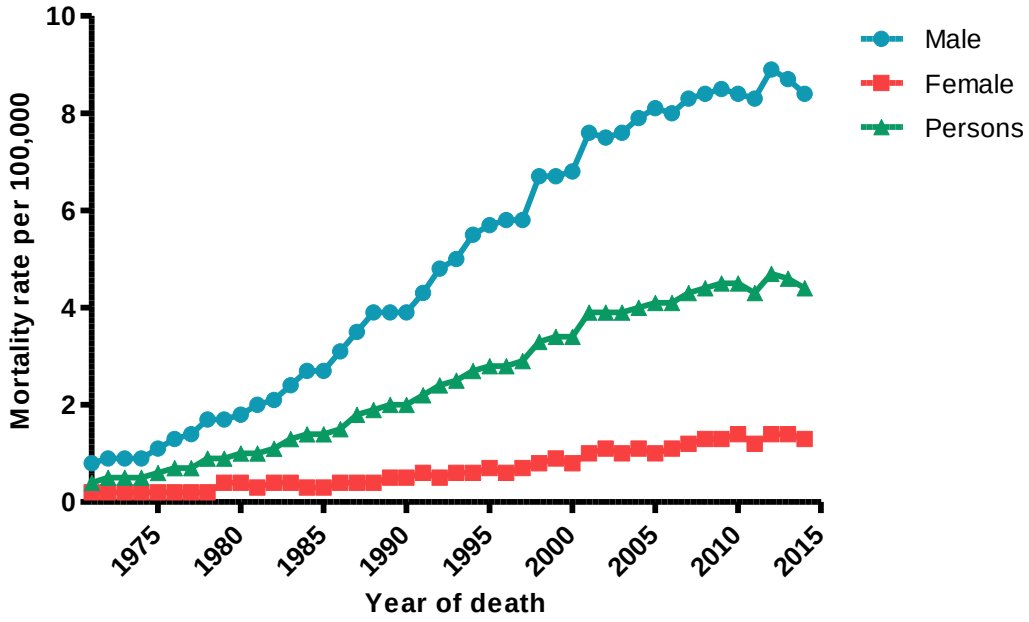

Figure 1. 2. Mesothelioma Age-Standardised Mortality Rates within the UK between 1971-2015. Adapted from Cancer Research UK (23).

1.1.2 The Normal Mesothelium

The mesothelium consists of a single layer of mesothelial cells lying above a basement membrane, with connective tissue layers which form a protective layer covering the pleura, pericardium and peritoneum. Within the pleural cavity the mesothelial layer comprises either the parietal pleura, which covers the thoracic wall, mediastinum, heart and diaphragm; or the visceral pleura, which covers the lungs (26). Mesothelial cells originate from the mesoderm however, they have a mixed phenotype once developed, expressing both mesenchymal filaments vimentin and desmin, as well as cytokeratins classically seen on epithelial tissues (27). The pleural mesothelium has a variety of functions; it creates a lubricated surface to allow movement of organs with reduced friction, provides a barrier to infective agents, in addition to a system of transport for fluid and cells both in and out of the pleural cavity (28). There is also a prominent role for mesothelial cells in the inflammatory response following infection and inflammation, with the production of a wide range of inflammatory mediators which induce the migration of monocytes, neutrophils and macrophages into the pleural space (29). T cell responses can also be regulated through mesothelial activation, with up regulation of HLA-DR and ICAM1 (CD54) seen following infection, and induction of a robust CD4 T cell response (30).

In a normal environment mesothelial cells proliferate minimally however, following stimulation by inflammatory factors produced following mesothelial injury, a rapid increase in proliferation occurs (31,32). The behaviour of mesothelial cells during wound healing sets them apart from normal epithelium. In contrast to epithelial cells, which proliferate from the wound edges only, mesothelial cells distant from the wound are able to proliferate, detach from their original site and repopulate the wound site (33). In addition, mesothelial cells are

able to alter their phenotype from epithelial to mesenchymal following stimulation through injury or by certain growth factors. In studies of the behaviour of mesothelial cells during peritoneal dialysis, up regulation of the repressive transcription factor, *snail*, is driven by TGF-β and interleukin-1β (IL-1β). The activity of *snail* down regulates cytokeratins and E-cadherin and the resultant fibroblast-like cells lose their contact inhibition and adopt a higher migratory capacity (34). This epithelial to mesenchymal transition, often described in malignant processes, therefore provides a platform for pathogenic processes.

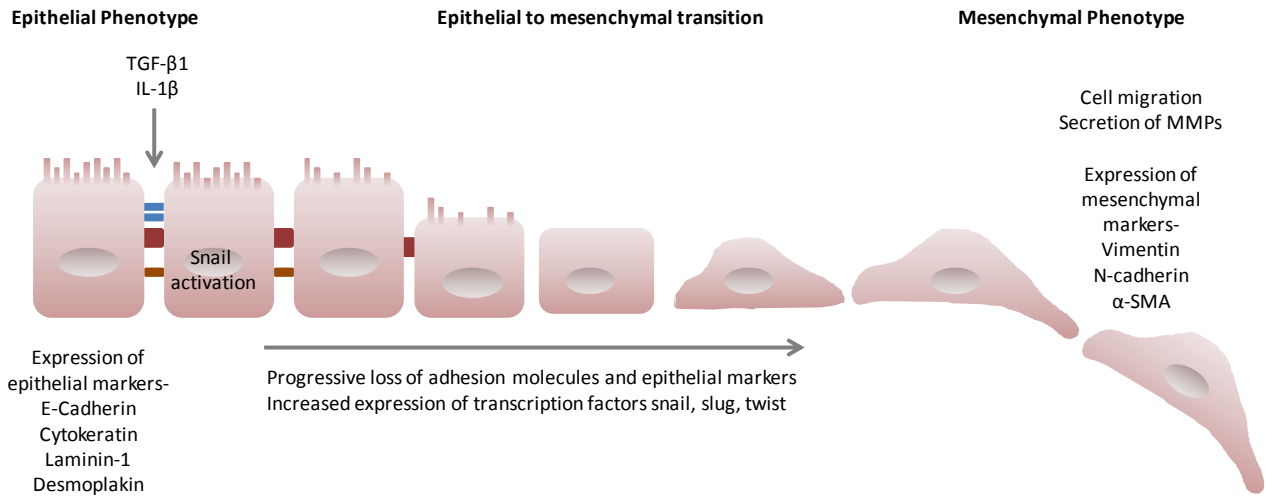

Figure 1. 3. Epithelial to mesenchymal transition (EMT).

Adapted from Aroeira *et al* (35). Mesothelial cells have been demonstrated to show EMT properties during healing processes. IL-1β and TGF-β were shown to activate the snail transcription factor in epithelial-like cells and trigger gradual loss of adhesion molecules and epithelial markers, leading to the development of mesenchymal-like cells. This process is often described in the development of malignant cells and the path to metastatic disease.

1.1.3 Non-Malignant Asbestos Related Disease

The role and behaviour of the mesothelium in initiation of inflammatory responses provides the inflammatory basis for the pathogenesis of asbestos-associated disease. Following exposure to asbestos, inhaled fibres are deposited within the lungs, triggering inflammatory responses. Once present, fibres are capable of persistence for decades and have been detected within pathological specimens of the lungs, pleura and lymph nodes years after presumed exposure (36). The toxicity of asbestos fibres is not universal, with some subtypes more widely associated with the origin of disease. The most commonly used type of asbestos, chrysotile, forms part of the serpentine group based on its curled fibre shape, with amosite and crocidolite making up the most commonly used fibres of the amphibole group.

Historically, amphibole asbestos was believed to be the most damaging to health, due to its shorter, needle shaped fibres however, clear evidence demonstrates that chrysotile is also a significant carcinogen (37,38). Chrysotile fibres were also the most commonly detected form of asbestos within mesothelioma specimens in a study by Suzuki *et al*, highlighting its carcinogenic properties (39).

Pleural disease is currently the most frequently diagnosed asbestos-related disease, affecting between 20 and 40% of exposed individuals after a latency period of 20-30 years (40). Pleural plaques are the predominant feature, formed through the deposition of collagen along the pleural surface and can be associated with fibrosis when involvement of the visceral pleural occurs. These plaques show little evidence of inflammation and may have central calcification. There is no evidence to suggest that malignant transformation occurs within pleural plaques however, they are associated with increased risk of developing mesothelioma, due to the association with asbestos exposure (41). The second most frequent asbestos associated disease is asbestosis, defined as the interstitial pneumonitis and fibrosis caused by inhalation of asbestos fibres. Pathological diagnosis is by the observation of acinar changes and the presence of asbestos bodies and it is further classified by severity in to 4 sub-groups, with the most severe showing alveolar collapse, with fibrous and honeycomb remodelling of the lung (42). Differentiating asbestosis from other forms of diffuse pulmonary fibrosis can be difficult, therefore history of exposure to asbestos is critical in forming the diagnosis. As with pleural plaques, there is a significant latency period of 15-20 years however, the cumulative extent of exposure appears to be a more prominent risk factor (40). The presence of asbestos bodies or asbestos fibres aids diagnosis in those cases where histological sampling is viable although this invasive test is not routine practice (43).

1.1.4 The Pathogenesis of Mesothelioma

The presence of asbestos fibres within the lung and pleura rapidly stimulates an inflammatory reaction, with the accumulation of alveolar macrophages and neutrophils attempting to clear the foreign fibres. Upon exposure to asbestos, alveolar macrophages have been shown to produce a number of cytokines including TGF-β, which aids inflammatory cell recruitment and collagen and fibronectin deposition, along with the production of further pro-inflammatory cytokines IL-1β and TNF- α (44). The inflammatory environment induced by asbestos fibres also promotes free radical release, which is believed to be one of the major determinants of asbestos induced lung and mesothelial injury (45). Oxygen radicals can be released from alveolar macrophages and neutrophils, as well as through direct reactions with asbestos minerals. Release from inflammatory cells occurs during the respiratory burst triggered by phagocytosis, and is enhanced through failure to engulf larger asbestos particles, described as frustrated phagocytosis (46,47). Free radical release from asbestos itself, results from the interaction of hydrogen peroxide (H_2O_2) with iron cations within its crystalline structure. This leads to production of the reactive hydroxyl radical in a process is known as the Fenton Reaction (48). In addition to oxygen radicals, reactive nitrogen species are also believed to have a role in asbestos related inflammation. Nitric oxide, a required cellular signalling molecule, is produced by the inducible nitric oxide synthase (iNOS) catalysed reaction of L-arginine to L-citrulline. Its presence in combination with oxygen radicals can result in the formation of peroxynitrite ($ONOO^-$), a potent oxidant capable of cellular damage. Asbestos has been shown to induce the production of nitric oxide and expression of iNOS in both macrophages and mesothelial cells, particularly in the presence of additional inflammatory cytokines such as IL-1β (49,50). The formation of reactive nitrogen and oxygen species can

subsequently lead to a number of damaging cellular processes including nitration of tyrosine residues, resulting in signalling modifications (51), induction of cell damage through lipid peroxidation, as well as direct DNA damage by hydroxylation of DNA bases (48). Nitric oxide and reactive oxygen are also capable of activation of the proto-oncogenes *c-fos* and *c-jun,* required for cell cycle progression, along with activation of the transcription factor activator protein 1 (AP-1). Interestingly, asbestos fibres themselves are capable of inducing prolonged phosphorylation of mitogen activated protein (MAP) kinases and extracellular signal-regulated kinases (ERK) 1 and 2 via the epidermal growth factor receptor (EGFR), which also lead to nuclear translocation and drive activation of *c-fos and c-jun* (52). These asbestos driven processes again lead to the transactivation of AP-1, which drives proliferation and apoptosis and subsequently the malignant transformation of mesothelial cells (53).

Asbestos fibres are also implicated in the production of chromosomal abnormalities which are a commonly observed feature in mesothelioma (54,55). Fibres are shown to cause direct physical interference within cell mitosis, causing spindle deformation and chromosomal breaks (56). Cytokinesis failure also occurs as a direct result of asbestos exposure, resulting in the production of bi-nucleated cells and subsequent aneuploidy in daughter cells (57). Specific chromosomal aberrations in mesothelioma have been detected, with recurrent findings involving chromosomes 1, 3, 7, 9 and 22 (54,58,59). Additional chromosomal defects are seen in chromosome 19 in a number of asbestos associated lung cancers (60). Within mesothelioma, one of the most commonly observed chromosomal abnormalities is monosomy of chromosome 22 (59). This prompted further investigation into possible involvement of the known tumour suppressor gene, neurofibromatosis 2 (NF2), which is located on chromosome 22q. The function of NF2 as tumour suppressor gene and acquisition

of its name, was discovered due to its association with neurofibromatosis, a disease characterised by tumours involving the brain and nervous system. However, mutated forms of this gene have since been detected in melanoma, breast cancer and colon cancer (61). The NF2 gene was found to be mutated in approximately 40% of mesothelioma tumours and 40-53% of tested mesothelioma cell lines (61,62). In-frame deletions or premature stop codons were most commonly identified abnormalities, leading to the loss or truncation of the NF2 protein (62). Other frequently recognised genetic drivers in mesothelioma include BRCA1 associated protein 1 (BAP1) and cyclin dependent kinase inhibitor 2A (CDKN2A) (63) however, a greater number of recurrent mutations have also recently been identified through sequencing of over 200 mesothelioma tumours (64). CDKN2A is the most common mutation observed in mesothelioma and encodes two cell cycle regulatory proteins, p16 and p14ARF which form pathways involved in the regulation of retinoblastoma (RB) protein, a prominent oncogene, and the tumour suppressor gene p53 (65). Mutations in CDKN2A are seen in 74% of mesothelioma cases, commonly in conjunction with methylthioadenosine phosphorylase (MTAP) mutations, rendering them dependent on de novo synthesis of purine derivatives for the generation of adenosine monophosphate (AMP) (66). BAP1 inactivation has been identified in approximately 23% of tumours and is the most recent significant genetic driver to be identified in 2011 (67). The role of BAP1 as a tumour suppressor gene has since been further defined as a crucial component in the DNA double strand break repair process. BAP1 functions as a de-ubiquitinase, with its phosphorylation in the presence of DNA damage leading to the appropriate recruitment and function of homologous recombination proteins BRCA1 and RAD51 (68). The recent work by Raphael Bueno *et al* looking at 206 mesothelioma tumours highlighted a number of additional significantly mutated genes in mesothelioma. This was in addition to identifying inactivating gene fusions and splice alterations in the pre-

determined genetic drivers BAP1 and NF2. Interestingly, this study demonstrated that despite the presence of a number of genetic abnormalities, mesothelioma has few mutations which lead to direct alterations of protein structures, above only acute myeloid leukaemia and thyroid carcinoma. The genetic alterations observed allowed classification into 4 distinct groups, which closely matched the current classification of epithelioid, sarcomatoid and biphasic subtypes. Although previously identified in mesothelioma, this study also provided further insight into tumour protein 53 (TP53) mutations, with detection in 8% of tumours, exclusively within sarcomatoid and biphasic subtypes. In accordance with this, TP53 conferred poorer prognosis (64). Further analysis and data collection on mutational rates of other detected genes within this study may provide further insights into the genetic basis of mesothelioma.

1.1.5 The Inflammatory Basis of Asbestos Related Pleural Injury

Along with the production of reactive oxygen species by inflammatory mediators, cytokine release also has a significant role in the pathogenesis of asbestos induced lung injury and malignant transformation. Asbestos is known to have direct cytotoxic effects against mesothelial cells, with the necrotic response leading to release of damage associated molecular patterns (DAMP), particularly the high mobility group box protein 1 (HMGB1). Release of this DAMP leads to macrophage activation (69) and the combined macrophage stimulation by HMGB1 and exposure to asbestos fibres leads to the release of the pro-inflammatory cytokines TNF-α and IL-1β. This process is also augmented by the presence of free radicals (70,71). The origins of IL-1β production are due to activation of the NALP3 inflammasome, a multi-protein complex which can be activated by exposure to various pathogens and toxins. The main activator of the NALP3 inflammasome in this setting has been

shown to be macrophage derived ROS, following frustrated phagocytosis (72). The release of chemotactic factors such as TGF-β, PDGF and EGF are also important in the initial inflammatory response, attracting further inflammatory cells and recruiting fibroblasts, which precipitate the initiation of fibrotic changes within the lung and pleura (73-75). Specific to the effect of asbestos within the pleura, an in vitro study by Acencio *et al* demonstrated that exposure was also able to drive the production of IL-1β, IL-6 and macrophage inflammatory protein 2 (MIP-2) from pleural mesothelial cells. The combination of asbestos exposure and cytokine production induced necrosis and cell death, with IL-1β and IL-6 having the most significant effect (76). This toxic effect of asbestos is clearly of significant interest, as if cell death is occurring following asbestos exposure, this precludes malignant transformation. This question was addressed by Yang *et al*, who demonstrated the interplay between mesothelial cells and their microenvironment, showing that macrophage derived TNF-α provides human mesothelial cells with survival signals via NF-κB activation (77), again emphasising the important cross-talk occurring between mesothelial cells and their microenvironment. The inflammatory environment created plays a significant role in malignant transformation and tumour development, with Adachi *et al* showing evidence that IL-6 is a strong driver of mesothelioma cell growth, and further driver of continued IL-6 production. In addition, IL-6 was a direct promoter of VEGF production (78). Although VEGF has not consistently been shown to have a direct effect on mesothelial cell growth, it is likely that the production enhances tumour development through induction of angiogenesis (79). Additional factors supporting tumour development, also induced by inflammatory cytokines TGF-β and PDGF, include matrix metalloproteinase (MMP) 2 and membrane type 1 (MT-1) MMP. Through activation of the p38 MAP-kinase, the expression of MMP-2 and MT-1 MMP aid in the degradation of the extra-cellular matrix and facilitate migration and invasion of mesothelioma

cells (74). Finally, along with the induction of numerous cytokines, the inducible enzyme cyclo-oxygenase 2 (COX-2) is also implicated in the pathogenesis of mesothelioma. This enzyme is of interest in a malignant setting due to its ability to stimulate cell proliferation and produce a forward feedback loop via the epidermal growth factor receptor (EGFR), inducing prostaglandin E2 production and further stimulating COX2 activity (80). COX-2 over production has been documented in multiple studies of mesothelioma, with its production stimulated by the cytokine milieu induced by asbestos (81,82). Highlighting the importance of factors such as VEGF and COX-2 in the development and progression of mesothelioma is also their association with prognosis. Tumoural production of COX-2, detected by immunohistochemical staining, was associated with independent prognostic value in two studies of over 30 mesothelioma specimens and importantly retained its prognostic value when added to the currently accepted prognostic scoring systems of the CALGB and EORTC (82,83). Similarly, both tumoural and serum detection of VEGF has been associated with survival, with tumours showing increased VEGF production in response to tissue necrosis. In addition, an incremental VEGF increase in serum was associated with asbestos exposure, early and late stage mesothelioma (84,85).

1.1.6 STAT3 Signalling in Mesothelioma

STAT3 activation has also been shown to be up regulated within mesothelioma tumour specimens (86) and to have a pivotal role in the regulation of pathways including IL-6 driven VEGF production (78). In a study of 44 mesothelioma specimens STAT3 cytoplasmic expression was detected in 79.5% of specimens, with 61.4% showing detectable phosphorylated STAT3. The highest levels of expression were detected in biphasic subtypes

and in addition, a trend towards greater expression in more advanced disease was detected within tissue of NSCLC obtained within the study (86). As described above, IL-6 has been shown to have a significant role in the pathogenesis of mesothelioma and the role of STAT3 in IL-6 signalling is now widely accepted. Adachi and colleagues demonstrated a significant role of IL-6 in tumour proliferation, in addition to the activation of VEGF transcription. Through the introduction of a dominant negative STAT3 phenotype they demonstrated that IL-6 signalling via STAT3 was responsible for both VEGF production and enhanced cell proliferation. Interestingly, VEGF production was not found to be significantly involved in cell proliferation in this setting however, its availability within the tumour environment is highly likely to support tumour growth through angiogenesis. This pathway of IL-6/JAK/STAT activated growth in mesothelioma was further supported by the use of the suppressor of cytokine signalling 3 protein (SOCS3). SOCS proteins, demonstrated to be negative activators of STAT signalling, are capable of suppressing the pathway through both blockade of the cytokine receptor and binding of Janus kinase (JAK) proteins to inhibit their function (87). STAT3 signal blockade through the use of an adenovirus vector expressing high levels of SOCS3, led to a reduction in mesothelioma cell proliferation and, within a mouse xenograft model, mesothelioma tumour progression was inhibited (88). Not only defined by its effects on growth in mesothelioma, STAT3 has also been implicated in the development of a senescence associated phenotype (SASP) and the development of resistant clones. SASP has been described in a number of malignant phenotypes and defines a senescent stress response associated with the production of inflammatory cytokines and mitogenic factors, which aid in malignant transformation, particularly related to epithelial to mesenchymal transition (86). Canino *et al* demonstrated that the SASP phenotype can be triggered in mesothelioma following treatment with the chemotherapeutic agent pemetrexed, the most commonly used

drug in this cancer type. Mesothelioma cells were shown to enhance production of a number of pro-inflammatory cytokines including IL6, IL8, VEGF-A, IFN-γ and CXCL1, in addition to developing a mesenchymal phenotype. These subpopulations also showed intense resistance to treatment with pemetrexed. Phosphorylation of STAT3 was significantly enhanced within these SASP populations and its prominent role in their development was confirmed through STAT3 silencing. This both inhibited the development of the SASP phenotype and enhanced sensitivity to chemotherapy treatment (89). These findings demonstrate a prominent role for STAT3 in signalling pathways leading to the growth, transformation and resistance of mesothelioma.

1.1.7 Clinical Presentation, Diagnosis and Management of Mesothelioma

Presentation

Despite advances in management and survival rates of many other malignancies, mesothelioma has remained largely treatment-resistant and outcomes have remained poor, with an average survival of 12 months from diagnosis (90,91). This is compounded by the invariably late presentation of many patients due to the insidious nature of early symptom progression. The primary presenting complaint is chest wall pain, occurring in approximately 60% of patients. Upon investigation, many of these patients will have a co-existing pleural effusion, the most common clinical sign, therefore the combination of chest wall pain and pleural effusion should always prompt investigation for mesothelioma. Accompanying symptoms may include breathlessness, secondary to the presence of a pleural effusion, malaise and weight loss. Such constitutional symptoms however are often a sign of late stage disease. Following tumour invasion, involvement of lymph nodes may occur, leading to

clinically palpable disease. In addition, spread within the thoracic cavity can lead to superior vena cava obstruction, cardiac tamponade and spinal cord compression (92). A rare presentation of malignant pleural mesothelioma is also miliary disease, with metastases spread diffusely within the lungs (93,94). Interestingly, a recent report by Purek *et al* described 2 cases of late miliary recurrence following initial treatment of mesothelioma, possibly indicating an alteration of the natural progression of this disease induced by systemic therapy (95). Other forms of mesothelioma may occur in the peritoneum, the pericardium and tunica vaginalis of the testes. Peritoneal mesothelioma accounts for approximately 20-30% of mesothelioma cases diagnosed annually (96) and symptoms are classically abdominal distension secondary to ascites and abdominal pain (92). Pericardial and tunica vaginalis mesothelioma are much rarer forms, presenting with constrictive pericarditis, pericardial effusion or cardiac tamponade (97,98); or a painless scrotal mass or hydrocele (99), respectively. For the purpose of this thesis, I will focus only on the diagnosis and management of pleural mesothelioma.

Diagnosis and management

Diagnosis of mesothelioma occurs through a combination of CT imaging and sampling of pleural fluid or tissue for cytological assessment. Often pleural biopsy is required to confirm the histological diagnosis as fluid cytology may be negative in malignant disease (100). Even with a good tissue biopsy, diagnosis can still be difficult due to similarities with other cancers such as poorly differentiated adenocarcinoma and sarcoma. It is therefore important that a strict panel of immunohistochemical markers are used to confirm the diagnosis. These typically include epithelial membrane antigen (EMA), calretinin, Wilms' tumour 1 (WT-1), Hector Battifora mesothelial-1 (HBME-1), mesothelin and cytokeratin 5 and 6. Markers used

to exclude adenocarcinoma should also be used, including TTF-1, CD15 and CEA, which are almost always negative in mesothelioma (101). Following diagnosis, staging is carried out in cases of mesothelioma which may undergo surgical resection however, it has limited impact on systemic treatment. The initial staging system was derived from the tumour, lymph node, metastases (TNM) lung cancer staging system in use in the early 1990's (102), however this has undergone revision and updates as part of the American Joint Committee on Cancer (AJCC) staging manual as mesothelioma management has progressed (103). TNM staging allows separation into 4 pathological stages of which stage I-III are all amenable to surgical resection if the patient is physically fit enough and the surgical procedure can be offered. To determine resectability standard CT of the thorax and abdomen and PET-CT can be used initially, although disease is often under-staged using imaging techniques (104) and confirmation requires surgical exploration. Those patients with stage IV disease, or those who are not candidates for surgical resection due to fitness or comorbid disease should be offered chemotherapy.

Despite recommendations for surgical resection in current clinical guidelines for all patients with stage I-III disease, there is considerable controversy as to whether surgery in mesothelioma significantly improves survival outcomes. It is still suggested that by the correct identification of suitable surgical candidates and adequately experienced specialist surgical team, survival may be enhanced through surgery (105). However, present trial evidence has conversely demonstrated that some forms of surgery do not provide a significant survival benefit over more conservative treatments (106), or that outcomes in comparable patients are similar when receiving surgery or multimodal therapy versus chemotherapy alone (107). It is accepted that surgery for mesothelioma will not achieve complete removal of all cancer

cells (R0 resection), and a macroscopic complete resection is therefore the intended goal for surgery (108). Achieving a near R0 resection is much more likely if patients undergo a more extensive extra-pleural pneumonectomy, which removes the entirety of the involved pleura, lung, diaphragm and pericardium. However, complications following this procedure are unacceptably high, with mortality and morbidity of almost 7% and 62%, respectively (109). A preferred management option is extended pleurectomy and decortication (P/D) or the less aggressive P/D, which removes only the involved pleural and macroscopic tumour, along with any involved diaphragm and pericardium if the extended P/D is performed (109). To date there is no firm conclusion as to whether overall, surgery provides better survival outcomes than chemotherapy, or which surgical procedure should be preferred. A feasibility study to assess whether it was acceptable to assign patients to surgery or no surgery has been previously carried out. Recruitment to this trial was very slow, with only 50 participants in 3 years. Surgical outcomes within the 24 patients allocated to P/D in this study were poor, with survival of 14.4 months versus 19.5 months in the non-surgical arm, therefore initial conclusions stated that surgical intervention may be harmful to patients (110). A revised version of this study has recently been carried out (ClinicalTrials.gov Identifier: NCT02040272) and results are awaited. Whether conclusions can be drawn from this study regarding the benefits of surgery will again be controversial however, as survival remains a secondary endpoint due to the low number of patients expected in this trial.

Despite recommendations for surgery, many patients with mesothelioma do not receive surgical intervention due to disease stage or co-morbidities precluding surgery. Chemotherapy has therefore remained the mainstay of treatment in current practice. A standard of care was established in 2003 in a pivotal trial using the chemotherapy doublet of

cisplatin and pemetrexed. This combination led to an overall survival benefit of 3 months, with a response rate of 41% (111). Over the 15 years since this combination therapy was established as best practice, little progress has been made. Only one phase III study has successfully demonstrated survival benefit with the addition of bevacizumab (an angiogenesis inhibitor targeting VEGF) to standard treatment. This trial demonstrated a 2.7 month survival benefit with this three drug combination over standard chemotherapy, increasing average survival to 18.8 months (112). Radiation therapy is generally not recommended for use in mesothelioma, except as part of multi-modal therapy following surgical resection. This is due to the usually large surface area affected by pleural mesothelioma and toxicity associated with thoracic radiation therapy (113).

1.1.8 Developments in the Treatment of Mesothelioma

Targeted therapies

Excluding the use of the VEGF antibody Bevacizumab, targeted therapies have not shown benefit in the treatment of mesothelioma despite a number of clinical trials. Targets investigated have included the EGFR pathway, histone de-acetylase (HDAC) modification, NF-κB pathway inhibition and the mammalian target of rapamycin (mTOR) pathway (114-117). EGFR over-expression is possibly one of the most frequent molecular changes seen in mesothelioma, detected in 75 to 97% of patients and is implicated in de-regulated cell signalling and tumour growth in many cancer types (118,119). Despite this frequent de-regulation, trials targeting the EGFR with inhibitors gefitinib and erlotinib have not shown clinical benefit (114,120). Histone de-acetylases are also currently believed to impact mesothelioma development due to their role in epigenetic regulation of gene transcription.

Early trials of HDAC inhibition appeared promising, with some evidence of response (121), leading to the initiation of a phase III trial to assess the effectiveness of vorinostat as a second or third line therapy in mesothelioma. Despite the early suggestion of activity, no survival benefit was seen in this trial (115). Similarly, neither NF-κB inhibition with ranpirnase and bortezomib, nor mTOR inhibition with everolimus led to any meaningful treatment benefit (116,117,122).

Immune modulation as a treatment for mesothelioma

Areas of treatment development which may be showing some promise of benefit include the development of immune-targeted therapies, either alone or as a combined therapy targeting tumour surface molecules such as mesothelin or WT-1. Mesothelin has provided considerable interest over the past 2 decades due to its expression on mesothelioma tumour specimens and detection within the serum of up to 70% of patients with active mesothelioma (123). Mesothelin is a glycophosphatidylinositol (GPI)-linked cell-surface glycoprotein with an initial structure forming a 71kDa protein. This structure is subsequently cleaved to produce a 40kDa membrane bound protein and a 31kDa portion which is shed into the bloodstream, thus detectable in peripheral blood sampling (124). The role of mesothelin expression in mesothelioma and other cancers is unclear however, there is evidence that it is able to up-regulate the production of matrix-metalloproteinases (MMP), which degrade the extra cellular matrix. This process therefore aids in the invasive potential of malignant cells (125). In ovarian cancer, membrane bound mesothelin has also been shown to bind to the cancer antigen CA-125 and promote cell adhesion, possibly contributing to peritoneal spread of malignancy in this setting (126). In addition to cellular migration, mesothelin has also been shown to act as an autocrine growth factor in the setting of pancreatic carcinoma through the

induction of IL-6 production and increased levels of the soluble IL-6 receptor (127). The mesothelin protein may therefore be used in treatment development as both a specific target for malignant cells and as a functional target, with disruption of malignant processes occurring through its removal or blockade.

To date, a number of mesothelin targeted drugs have entered into clinical trials including the monoclonal antibodies amatuximab (128) and anetumab ravtansine (129) , the immunotoxins SS1P and LMB-100 (130) and the cancer vaccine CRS-207 (131). As the majority have only reached phase I trials, further data is required prior to assessment of their therapeutic potential however, early phase trials of SS1P in combination with chemotherapy have shown promise. This recombinant protein is fused to the Pseudomonas exotoxin A and has a single chain variable fragment with high affinity for mesothelin (132). Once bound, the toxin is internalised by the cell and induces apoptosis. Problems have arisen in early trials due to anti-body formation neutralising the toxin, limiting the number of possible doses (133). Pre-treatment with an immunosuppressive regime of pentostatin and cyclophosphamide dramatically reduced this occurrence (134). This pilot study led to major responses in 3 previously chemotherapy refractory patients, with prolonged response duration of over 15 months (134). Due to the immunogenicity of SS1P a new formulation of this immunotoxin, LMB-100, has been produced with removal of the majority of the B and T cell epitopes (135). This formulation should be much less likely to induce antibody formation and is currently under assessment in a phase I clinical trial (ClinicalTrials.gov identifier NCT02798536).

Immune checkpoint blockade

There is significant interest in the use of checkpoint blockade in mesothelioma although to date, no check-point inhibitors have been licensed for use in this cancer. The first trial of

checkpoint inhibition was with the CTLA-4 inhibitor tremelimumab. This was a phase II trial examining tremelimumab as a second line treatment following progressive disease after platinum chemotherapy. Only 2 of 29 patients had objective responses to treatment, although stable disease was achieved in 9 patients (31%) and median overall survival was 10.7 months (136). Further trials have examined the use of PD-1 blockade, with more promising outcomes. The KEYNOTE-028 trial demonstrated that the PD-1 antibody pembrolizumab produced responses in 5 of 25 patients (20%) and a further 13 (52%) had stable disease, with an overall median survival of 18 months (137). Combination treatment with PD-1 and CTLA-4 inhibition has also been assessed within the MAPS2 phase II trial, where the PD-1 antibody nivolumab was assessed alone and in combination with the CTLA-4 antibody ipilimumab. This trial recruited 125 patients with 1:1 randomisation to each arm. Response rates with nivolumab alone were slightly inferior to those seen with pembrolizumab, at 18.5% however, the combination arm reported a response rate of 27.8% (138). Consistent with these response rates, nivolumab alone led to an overall survival of 13.6 months, with the combination arm not reaching median OS after 15 months of follow up (139). Interestingly, within this study the PD-L1 positivity of tumours did not correspond to response rates or overall survival, indicating that the PD-L1 status of the tumour is not the primary factor contributing to the immune dysfunction in this setting. Further phase III trials are ongoing in mesothelioma examining the use of pembrolizumab in the second line setting (ClinicalTrials.gov Identifier: NCT02991482) and, in addition, CHECKMATE 743 is currently assessing the use of the combination treatment nivolumab and ipilimumab as a first line therapy in place of standard chemotherapy (ClinicalTrials.gov Identifier: NCT02899299). The use of immunotherapy drugs in the first line metastatic setting have revolutionised treatment outcomes in diseases such

as melanoma (140-142), lung cancer (143-145) and renal cell carcinoma (146), therefore this trial provides significant hope to mesothelioma patients.

In addition to the use of checkpoint blockade there are a number of additional immunotherapy-based treatments being examined in mesothelioma, including dendritic cell (DC) vaccines and chimeric antigen receptor T cell therapies. The use of dendritic cell vaccines has been under investigation for many years, with the aim of antigen presenting cell (APC) activation of cytotoxic T cells leading to a targeted immune response against the tumour (147). Pre-clinical studies have demonstrated the feasibility of targeting mesothelioma with dendritic cell therapy with a promising human study leading to responses in 6 of 10 patients treated with mesothelioma pulsed DC (148). Attempts to improve the efficacy of DC based vaccines are being examined, including the use of cyclophosphamide to reduce the immunosuppressive effect which may be occurring through tumour infiltrating regulatory T cells (149). Following the promising results of pre-clinical studies, a further phase I/II study is currently on going examining the use of a WT-1 based DC vaccine, in combination with chemotherapy (ClinicalTrials.gov Identifier: NCT02649829).

With this slow and limited progression of therapeutic options over the past decade and ongoing poor survival rates, there is clearly a true unmet need for research development in mesothelioma. The use of immunotherapy in this setting appears to be emerging as the most promising area of therapeutic benefit and as such, emphasises the need to understand the wider immune microenvironment of this cancer.

1.2 The Role of the Innate Immune System in the Control of Malignancy

1.2.1 Dendritic Cells

Dendritic cells are known to be the most potent antigen presenting cells within the innate immune system and are capable of presentation of a large number of antigens in order to engage T cell responses. In addition to presentation of microbial material, DC also present tumour antigens and are believed to be critical in defending the host from the development of cancer and conversely, critical in the development of tolerance. Dendritic cells exist in both immature and activated forms, performing different roles within each stage. In addition, their roles are also defined by their origin and subset.

1.2.2 Dendritic Cell Subtypes

Circulating dendritic cells are divided into 2 major subsets, conventional (myeloid) DC and plasmacytoid DC, defined by surface marker expression and functional profiles (150). These broad subdivisions have recently challenged by Villani *et al,* who identified further divisions in DC subsets through single cell RNA sequencing analysis (151).

Conventional DC (cDC) are the major fraction of DCs in blood, tissue and lymphoid organs, and are further subdivided into two groups dependent on their expression of CD1c or CD141. Both express CD13 and CD33, defining their myeloid origin. cDC are distinct from pDC due to their ability stimulate naïve T cell responses and are capable of presentation through both MHC class I and class II molecules. cDC are also defined by their unique ability to present exogenous antigen via the MHC class I pathway, a process termed cross-presentation (Bevan, 1976). Villani *et al* identified a further division within the CD1C+ population, demonstrating a population, termed CD1C+_A DC, with higher MHC class II expression, which were capable of

secreting higher levels of inflammatory mediators CCL19, IL-10, IL-12B, and IL-18 upon activation. The second subgroup, CD1C+_B DC demonstrated higher expression of chronic inflammatory genes CD14, S100A9 and S100A8 (151).

Plasmacytoid DCs (pDC) classically express CD123, CD68 and CD303 and play a prominent role in the type 1 interferon response to virus (152). pDC have a lower capacity to prime naive T cells, although have been shown to produce CD4+ T cell activation within lymph nodes following antigen stimulation (153). Though no further subdivision in this population was identified by Villani and colleagues, a population with similar a gene expression profile to pDC was identified within their work. It was later determined that this population was distinct from pDC and termed AXL+SIGLEC6+ (AS) DC. This novel DC subset was shown to more closely resemble cDC in terms of morphology and in contrast to pDC expressed high levels of CD86 and were capable of stimulation of both CD4+ and CD8+ T cell proliferation.

Tissue resident DCs are again a distinct population of DC termed Langerhans Cells. They are located within the stratified squamous epithelium of the skin, bronchus and mucosal membranes. They display the surface markers CD1a, CD207, and Langerin. Upon activation they are capable of migration to lymphoid organs and produce potent cross presentation to T cells for a select range of pathogens (150). Also found within tissues, a variety of monocytic DCs have been characterised. These cells, which show CD14, MHC class II and CD11c positivity, lack the myeloid DC markers CD1, CD141 and co-stimulatory molecules (154). Monocytic DCs are distinct in their gene expression profiles to cDC (151) and lack the ability to stimulate naive T cells (155). Additional markers expressed, such as DC-SIGN (CD209) and the macrophage

markers FXIIIA and CD163, are suggestive of development in environments promoting immune tolerance (156).

1.2.3 The Role of Dendritic Cells in cancer

Dendritic cells play a major role in the function of the innate immune system and are deemed vital for the initiation of an appropriate host response to the presence of microbial pathogens and in addition, are believed to be crucial in early anti-tumour immunity. Although tumours provide predominantly "self" antigens, there is strong evidence that the abnormal stress and cell death occurring within tumours produces substances which act as activation signals to APC, such as DCs. This model, originally proposed by Matzinger in 1994, described not just the recognition of "non-self" signals, but the release of alarm or danger signals from host cells, which led to APC activation in a similar manner. These signals, classified as damage associated molecular patterns (DAMPs) (157), were initially shown to be released through the abnormal necrotic cell death occurring within cancer cells (158). However, continued research has shown that DAMPs can be released during cell death in both necrosis and apoptosis (159). Since this initial identification of DAMPs, a theory of immunogenic cell death as developed which has demonstrated the activation of DC by self-antigens, released in the process of cell death, particularly of cancer cells (160). Such processes have been shown to be induced by chemotherapy agents and the immunological response observed correlates with response to therapy (161,162). The properties of immunological cell death include endoplasmic reticulum (ER) stress, leading to the expose of calreticulin and other ER proteins at the cell surface. These proteins signal and activate local DC through CD91, TLR4 and P2RX7 expressed on the

DC cell surface (160). As cells begin to undergo either apoptosis or necrosis, further DAMPs, including heat shock proteins (163), HMGB1 (164) and double stranded DNA (165), induce DC activation. It is now accepted that DAMPs, released through both apoptosis and necrosis, are capable of leading to immunogenic cell death through DC activation against tumour cells (159).

Multiple DC subtypes are shown to be active in the setting of cancer, including monocytic DC, pDC and myeloid DC, although the role of each subpopulation is less clear. Monocytic DC have been shown to infiltrate murine melanoma tumours as the predominant DC population and these tumour-infiltrating DC were shown to be fully competent in their ability to act as APC. When activated, a protective effect was demonstrated against melanoma growth in mice (166). Despite the initial perception of a limited role of plasmacytoid DC in cancer immunity, murine tumour in-vitro models have also demonstrated that pDC developed effective anti-tumour immune responses through the activation of antigen-specific CD8+ T cells. In melanoma models, pDC production of IL-12 and type I interferon led to T cell activation, with increased expression of T cell homing markers and T cell IFN-γ expression. pDC were also detected in human melanoma samples, supporting their potential role (167). The important role of conventional DC was demonstrated by Fuertes *et al* with CD8α+ DC confirmed as the population priming antigen specific CD8+ T cells in murine cancer models. Following exposure to B16 melanoma cells, a population of primed, IFN-γ producing CD8+ T cells was detected in the spleens of exposed mice. The generation of these antigen specific T cells was shown to be reliant on the production of Type 1 IFNs and importantly, induced by cross-presentation by DC. This was demonstrated through the depletion of DC by treatment with diphtheria toxin, as this population of primed T cells could no longer be detected (168).

The above findings highlight the importance of varying DC populations in the control of tumour growth and, in human cancer patients, a greater understanding of the role of DC subtypes has emerged in recent years. This is particularly important in the development of DC based cancer vaccination. Due to the challenges of extracting naturally occurring DC subsets, early research in DC vaccination has favoured ex-vivo generation of monocytic DC. The use of this method has shown promise, demonstrating induction of tumour immunity, however, limitations are seen with DC migration. Only 1-5% of injected DC were shown to survive or migrate to nodal sites (169,170) and actual tumour responses were observed in less than 10% of patients (171). Recent insights have been obtained into the superiority of naturally occurring DC (nDC) over in vitro generated monocytic DC (171), therefore further research into the use of naturally occurring myeloid or plasmacytoid DC has been a matter of focus, particularly owing to the improvements in cell isolation over recent years (172).

The use of both mDC and pDC as part of cancer vaccination techniques has been explored extensively with clinical trials. Tel *et al* demonstrated successful isolation of pDC from patients, followed by ex-vivo activation and loading of pDC with melanoma peptides. pDCs were able to induce Type 1 IFN responses and enhanced expression of IFN induced genes. Antigen specific CD4+ and CD8+ T cell responses were also detected. Although a feasibility study, review of the treated cases did reveal a substantial increase in overall survival when compared to matched untreated controls (173). The use of CD1+ mDC have been trialled both alone and in combination with pDC or additional immunotherapies (174-176). It is believed that the delivery of mDC in combination with immunotherapies leads to the exposure to tumour antigen and the capture and processing by DC, negating the need for maturation and antigen loading ex-vivo. In one small study of 14 patients with metastatic melanoma, antigen

loaded mDC were able to produce antigen specific T cell responses in one third of patients, with an association between their presence and patient survival (176).

In human cancer patients these findings have resulted in the first phase III trial in patients with stage III melanoma, which is exploring the use of nDC in the adjuvant setting. This trial compared the use of combination pDC and CD1+ mDC vaccines to placebo. Although recruitment to this trial was prematurely halted due to the availability of alternative adjuvant therapies, robust survival data should be achieved following recruitment of 150 patients (174).

1.2.4 The Development of Self-Tolerance

The above data supports the role of DC in T cell priming in the setting of cancer; however, it is evident that tumours are not controlled successfully by the host immune system. Although early DC activation may be occurring, there is ineffective DC priming and activation of tumour specific T cells in the setting of cancer. Immune tolerance then ensues, preventing effective T cell responses. The reasons for the defective functions of DC are multiple, with development of both self-tolerance and dysfunction caused by the tumour microenvironment implicated.

Self-tolerance is an important mechanism within a healthy immune system, required to prevent overwhelming immune reactions and tissue damage. For this reason, multiple mechanisms exist outside of the setting of cancer to allow this to occur. The determination of self-tolerance occurs primarily within the thymus, where frequent presentation of self-antigens by DCs occurs. Here, deletion of T cells which have high affinity for self-antigens occurs within the thymic medulla (177). Peripheral tolerance also appears to be partly

dependent on circulating DCs, with deletion of auto reactive CD8+ T cells occurring when introduced into mouse models (178). The mechanisms behind this self-regulation are not fully elucidated however, the concept that an activated T cell response requires a combination of antigen presentation, co-stimulation and a cytokine response from DCs demonstrates the importance of cell-cell cross talk within the innate and adaptive immune system.

These mechanisms of self-tolerance become particularly pertinent when trying to establish the failings of the immune system to recognise and mount an adequate immune response in the setting of malignancy. There are a number of mechanisms now defined, in particular, ineffective CD8 T cell responses and abnormalities in T cell regulation, however, another vital aspect in this setting is the inadequate development and function of DCs. The factors leading to both self-tolerance and immune suppression are numerous, therefore I will address important mechanisms, most pertinent to this research.

1.3 Immune Dysfunction in a Malignant Environment

A competent immune response is a vital way of eliminating abnormal cells which may have the capability of malignant transformation and this concept has long been accepted as an ongoing immune-surveillance process (179). The mechanism of immune escape is therefore of great interest in the development of malignancy and is now accepted as an emerging cancer hallmark (180). The fact that appropriate immune function is vital in reducing the occurrence of cancer is supported by evidence that the incidence of malignancy in immunosuppressed transplant recipients is 3 times higher than in the normal population, with over 20 different cancer types showing significantly increased incidence (181). In addition,

mouse models with deficiencies in T cell function are much more susceptible to the development of malignancy (182).

This concept is supported within mesothelioma, with evidence that the presence of differing T cell subsets can significantly alter tumour progression. In a study of 302 mesothelioma tumours, the presence of an increased number of CD4+ infiltrating T cells and a lower number of NP57+ neutrophils and FOXP3+ Tregs, detected through immune-histochemical staining, were independently associated with improved survival (183). Examination of a smaller subset of tumours by Yamada *et al* demonstrated that increased numbers of tumour infiltrating CD4+ and CD8+ T cells predicted improved survival in those patients undergoing surgical resection for mesothelioma (184). There was also a trend for improved survival all patients with high CD8+ infiltration (receiving surgery or chemotherapy) however, this did not reach significance ($p=0.10$). In contrast to the positive effect of T cell infiltration in mesothelioma, poor prognosis has been associated with increased neutrophil counts, with the neutrophil-lymphocyte ratio forming an independent prognostic indicator in two large retrospective studies of mesothelioma patients (185,186). This parameter was also shown to increase steadily with disease stage from 2.8 at stage I to 3.7 at stage IV (186). These studies highlight the importance of the immune system in directing the path of tumour progression and begin to suggest that certain mechanisms are employed by cancer cells to subvert the normal immune response and allow tumour growth.

1.3.1 Immunosuppressive Mechanisms Employed by Cancer

As introduced above, within a normal host there is continuous immune surveillance carried out by cells of the innate immune system, such as NK cells and macrophages, which detect transformed cells and initiate an immune response. The release of IFN-γ and breakdown of tumour cells releases tumour antigens which can be processed and presented by APCs, initiating T cell stimulation and an adaptive immune response with targeted cytotoxic T lymphocytes. During this process, some tumour cells with less immunogenic surface proteins may escape initial killing and lead to outgrowths of tumour populations which are hidden from the activated T cells and more resistant to killing. Overtime, these outgrowths gain more mutations and, following interaction with inflammatory cytokines, are more likely to produce additional factors which are capable of dampening down the immune responses occurring. Ultimately the tumour outgrowths which are most hidden and most immunosuppressive will persist and overcome the host immune response, leading to the clinical appearance of cancer. This process is described as a continuum of elimination, equilibrium and escape, termed immunoediting (182).

1.3.2 Regulatory T cells

Regulatory T cells (Tregs) are a subpopulation of CD4+ T cells which can be recruited to tumour sites through tumour and macrophage secreted chemokines such as CCL22 (187) or induced by tumour related factors including TGF-β production and the presence of immature DCs (188). The presence of Tregs within a tumour environment has multiple effects on conventional T cells, suppressing their function through release of the immunosuppressive cytokines TGF-β and IL-10 (189,190), along with the induction of IDO production (191) and the T cell inhibitory molecule B7-H4 on APCs (192) . The presence of intra-tumoural Tregs has

been shown to reduce overall survival in a number of cancer subtypes (193) and in addition, cancer associated Tregs have been shown to have a more potent suppressive phenotype when detected in the peripheral blood of cancer patients, compared to healthy controls (194). The presence of inhibitory T cells is currently a factor under investigation in patients who lack responses to immunotherapy, as it is believed that the ongoing regulatory activity within a tumour may inhibit successful re-activation of immune function. Sutmuller *et al* demonstrated this effect using a murine model of the B16-BL6 melanoma tumour, clearly showing that the concomitant blockade of regulatory T cells, alongside tumour vaccination, was able to enhance the rejection of tumour growth. Antibodies against CD25 clearly demonstrated reduction in numbers of circulating regulatory T cells and both anti-CD25 and anti-CTL4-4 treatments were capable of enhancing the action of tumour vaccination. In addition, their effects were synergistic when both antibodies were given together (195). An additional mechanism of Treg depletion is the use of low dose cyclophosphamide, which has been shown in human subjects to successfully reduce numbers of CD25+ T reg cells. Ghiringhelli *et al* investigated increasing doses of cyclophosphamide, demonstrating that a low dose regimen is required to selectively target Treg populations, while maintaining the number and function of other T cell groups (196). Further studies using two murine models of mesothelioma demonstrated that using this method of cyclophosphamide Treg depletion led to enhanced tumour responses to both chemotherapy with gemcitabine and DC based vaccination (149,197).

1.3.3 Tumour Associated Myeloid Cells

In addition to regulatory T cell populations the tumour microenvironment also harbours regulatory DC, along with inhibitory myeloid populations including M2 macrophages, inhibitory neutrophils and myeloid derived suppressor cells (MDSC).

Inhibitory Dendritic Cells

Mature DC are the most potent APC within the immune system, capable of activating cytotoxic T cells and initiating anti-tumour immune responses (198), however, the numbers of detectable DC in the blood and tumours of cancer patients are significantly reduced (199,200). In addition to reduced numbers, the cytokine rich tumour microenvironment is capable of impairing DC development, creating cells incapable of T cell stimulation and with numerous immunosuppressive functions. The production of increased levels of VEGF, detectable in patient serum, is associated with both decreased intra-tumoural and circulating dendritic cells in cancer patients (201,202). Tumour associated VEGF and IL-6 have also both been shown to affect DC maturation, leading to reduced class II MHC expression and subsequent reduction in T cell priming ability (203,204). GM-CSF is also commonly released within the tumour microenvironment and in the setting of DC function this cytokine currently appears to have conflicting roles. In certain settings, GM-CSF has been shown to augment the tumour immune response, producing DC with higher expression of co-stimulatory molecules and inducing a strong cytotoxic T cell responses (205). It also appeared to drive clinical responses to tumour vaccination which were not observed in the absence of GM-CSF (206). In contrast to these findings, GM-CSF has a prominent role in the in vitro development of MDSC (207) and has been shown to enhance these populations when given in conjunction with tumour vaccines, impairing their effectiveness (208). In addition to tumour-related

cytokines, a number of cancers, including lung cancer and mesothelioma, demonstrate high COX-2 activity with resultant prostaglandin-E2 (PGE2) production (209-211). PGE2 is most frequently thought of as a pro-inflammatory molecule however, exposure of DC to PGE2 at early stages of development can lead to inhibition of DC differentiation and loss of stimulatory function (212). Tumour related factors can also induce the expression of the immunosuppressive molecule B7-H1 (PD-L1) and B7-H4, both inhibitors of T cell function (192,213). The role of B7-H1 or, now more widely used, PD-L1, has been extensively characterised in the setting of cancer and is capable of reducing T cell IFN-γ and IL-2 production, enhancing production of the immunosuppressive cytokine IL-10 and inhibiting T cell anti-tumour responses (213,214). Krempski *et al* also demonstrated that in addition to the PD-L1/PD-1 interaction occurring between DC and T cells, DCs are also able to express both suppressive surface markers which lead to a self-regulatory feedback loop, decreasing the production of inflammatory cytokines and maintaining an immature phenotype (214). The induction of B7-H4 as an inhibitory molecule on DC is less well described, with its identification and role in T cell inhibitory function occurring in 2003 (215). It has since been shown that DC expression of B7-H4 is induced through IL-10 release, which can be stimulated by regulatory T cells (192). A further immunosuppressive DC mechanism includes the release of indoleamine 2,3-dioxygenase (IDO). IDO is the enzyme responsible for the catabolism of tryptophan, an amino acid required to allow T cell progression through the cell cycle and therefore essential for T cell proliferation (216). Signalling between regulatory T cell CTLA-4 and the co-stimulatory DC molecules CD80 and CD86 has been shown to enhance IDO expression in DCs (191,217). IDO can be released by both mature and immature DC however, upon IFN-γ activation, IDO expression is lost. In contrast, in the presence of the

immunosuppressive cytokines IL-10 and TGF-β, IDO production persists and DC lose their ability to stimulate T cell proliferation (218).

Tumour Associated Macrophages

As with DC, macrophages are capable of both pro- and anti-tumour effects and with the progression of cancer, their roles as tumour promoters appears to increase. The recruitment of monocytes and macrophages into the tumour environment occurs at an early stage, particularly in those cancers with an inflammatory basis such as mesothelioma (219). This is further enhanced by tumour related cytokines and chemokines which recruit monocytes and macrophages to the site of the tumour. Monocyte chemoattractant protein-1 (MCP-1 or CCL2), is one of the most commonly detectable chemokines released by tumour cells and is associated with enhanced numbers of tumour infiltrating macrophages (220-222). Once present within the tumour their roles are determined by the presence of immunomodulatory cytokines which, most commonly in the setting of malignancy, drive macrophages to an alternative M2 phenotype. Classically activated M1 macrophages form an integral part of the innate immune system and in the presence of IFN-γ and IL-12, released by Th1 cells and APCs, respectively, are capable of significant cytotoxic effects through the release of NO and TNF-α (223,224). In the presence of Th2 cytokines IL-4 and IL-13, macrophages are instead driven towards an M2 phenotype. These M2 cells release suppressive IL-10 in place of IL-12 and demonstrate enhanced arginase activity (225). Tumour associated macrophages (TAM) share similar features to alternatively activated M2 macrophages, with enhanced expression of immunosuppressive cytokines IL-10 and TGF-β. They also produce chemokines such as CCL2, to enhance further macrophage migration. Conversely, TAM also express chemokines known to induce IFN-γ release, demonstrating that this subpopulation is diverse from the classic M2

macrophage phenotype (226). Once the TAM phenotype is established within tumours, their roles become even further diversified, contributing not just to immunosuppression, but to vascularisation of the tumour due to VEGF release in response to tumour hypoxia (227-229) and tissue remodelling (230), demonstrating a wide role in the promotion of tumour growth.

Tumour Associated Neutrophils

In parallel to the divergence of macrophages within the tumour microenvironment, it has recently become apparent that neutrophils are also capable of polarisation into an N1 versus N2 phenotype which demonstrate tumour promotion. It is now accepted that high numbers of both circulating neutrophils and tumour infiltrating neutrophils have a negative impact on prognosis in cancer (183,231,232), however, the local and systemic mechanisms behind this have not been fully described. In addition to this, the distinction between tumour associated N2 neutrophils and granulocyte-myeloid derived suppressor cells (G-MDSC) is not well defined, leading to considerable overlap in their definition in many studies. Abnormal neutrophil populations have been detected in multiple cancers including head and neck cancer (HNSCC) (233), melanoma (234), lung, breast and gastrointestinal cancer (235) and I will attempt to draw together conclusions regarding their underlying mechanisms. Trellakis and colleagues investigated neutrophil populations in patients with HNSCC. They detected higher percentages of circulating neutrophils in HNSCC, compared to healthy subjects, and a correlation between increasing neutrophil counts and T stage or nodal status. Increased levels of chemokines involved in neutrophil chemotaxis including CXCL8 (IL-8), CCL4 and CCL5 were detected, along with CRP, a marker of systemic inflammation. The increases in CRP were again correlated with T stage and nodal involvement. In addition, following stimulation with tumour conditioned supernatants neutrophils rapidly released lactoferrin and MMP-9, both markers

of degranulation, indicating neutrophil activation was stimulated by HNSCC (233). Interestingly, MMP-9 has also been implicated in the initiation of angiogenesis in a tumour model of pancreatic cancer (236). In additional work, this group demonstrated that this population of neutrophils was functionally impaired, with reduction in ROS production following induction by phorbol 12-myristat 13-acetate (PMA). These cells were also comparatively resistant to apoptosis and displayed a predominant immature phenotype of CD66b+CD16 low/negative (237). In partial agreement of this study, Choi *et al* detected populations of CD16 low neutrophils in the blood of cancer patients with late stage tumours. In this study, the CD16 low population was believed to represent activated granulocytes, with loss of CD16 expression occurring upon activation. This population of CD16 low neutrophils was shown to be immunosuppressive through contact dependent induction of T cell apoptosis, although no mechanism was defined (235). In contrast to both of these observations Pillay *et al*, reported the detection of a mature, CD16 bright population, which through the release of hydrogen peroxide led to suppression of T cell function (238). This mechanism of T cell suppression has been further verified by a number of studies which demonstrate that the release of reactive oxygen species by neutrophils results in inhibition of the expression of the T cell receptor (TCR) zeta chain (required for T cell activation signalling), reduced cytokine production and subsequent inhibition of T cell proliferation (239-241). The divergence in these neutrophil phenotypes may be due to the differentiation between immature G-MDSC and N2 neutrophils, demonstrating the possibility of 2 distinct populations within the setting of cancer.

Along with difficulties in the description of the N2 phenotype, the mechanisms of N2 neutrophil induction within the tumour microenvironment are also unclear. One favoured

mechanism is through the actions of TGF-β, which has been shown to reduce the cytotoxic abilities of neutrophils through reduced degranulation and contribute to neutrophil suppressive activity (242,243). Work by Fridlender *et al* supports this mechanism and this group successfully demonstrated the complex interplay between N1 and N2 neutrophils through the blockade of TGF-β. This study demonstrated that, in the presence of TGF-β, neutrophils display a pro-tumour phenotype with restricted activation of intra-tumoural CD8+ T cells. Blockade of TGF-β led to increased activation of intra-tumoural CD8+ T cells. This was not found to be simply due to the removal of immunosuppressive cells, but the reversal of intra-tumoural neutrophils to an N1 phenotype (243). The method employed by neutrophils to suppress T cell activity was not identified within this study however, the N2 neutrophils had higher arginase activity, an important mechanism of T cell suppression (244). An additional mechanism of N1 to N2 polarisation proposed by De Santo *et al*, is the action of serum amyloid A (SAA). This marker of systemic inflammation was detected in high concentrations in patients with melanoma and was shown to be the mechanism behind neutrophil polarisation in this setting. Polarised neutrophils demonstrated enhanced production of IL-10, a potent immunosuppressive cytokine, IL-8 and increased arginase activity. Polarised neutrophils were capable of T cell suppression, determined by mixed leucocyte reaction (MLR), and this was shown to be IL-10 dependent (234).

An additional feature of N2 neutrophils is their loss of cytotoxic activity towards tumour cells, observed by Mishalian *et al* in models of lung cancer and mesothelioma. This study found that neutrophils detected in early cancers were more in line with classic N1 neutrophils, producing the inflammatory cytokine TNF-α and releasing nitric oxide and H_20_2 and demonstrating tumour directed cytotoxicity. As tumours progressed, the inflammatory activity of neutrophils

was significantly reduced, implying polarisation to an N2 phenotype (245). In concordance with these findings, Fridlender also observed enhanced tumour cell cytotoxicity following TGF-β blockade due to enhanced inflammatory activity and release of reactive oxygen species (243). This role of ROS in TAN is of great interest as its effects on tumour toxicity and T cell function are clearly divergent, with the balance of effects possibly going someway to explaining the suppression of these neutrophil functions within a tumour setting. In addition to decreased immune stimulation and cytotoxicity, N2 neutrophils are also associated with tumour promotion, enhancing tumour growth and implicated in mechanisms of angiogenesis. In a murine model of pancreatic carcinoma, the presence of intra-tumoural neutrophils was shown to be responsible for the angiogenic switch through the production of MMP-9. Neutrophil MMP-9 led to the release of VEGF from pancreatic islets, permitting signalling and initiation of angiogenesis (236). Intra-tumoural neutrophils have also been found to independently upregulate VEGF expression (245) and be responsible for systemic release of VEGF in the blood of patients with oral cancers (246). It is therefore evident that neutrophils, altered from their classic phenotype, have a significant role in tumour progression in relation to both immune suppression and active pro-tumoural mechanisms.

Myeloid derived suppressor cells

Myeloid derived suppressor cells are a further subset of immunosuppressive or regulatory cells that have been identified in the tumour microenvironment and peripheral blood of cancer patients. These cells, initially termed immature myeloid cells (iMCs), are believed to be myeloid precursors, capable of differentiation into myeloid subsets including macrophages, granulocytes and dendritic cells; however, unlike in a healthy individual, these cells are not restricted to residing within the bone marrow until differentiation.

Suppressive immature myeloid cells were first identified in mouse tumour models by Young *et al*, through observations that mice bearing Lewis Lung Carcinomas developed a population of immunosuppressive cells within the bone marrow in a setting of enhanced haematopoiesis (247). Following this pivotal discovery, many more authors described the presence of large numbers of immature myeloid cells within tumour bearing mice and human subjects within the peripheral circulation, lymphoid organs and within tumour tissue itself (248,249). It is now accepted that these cells are not an isolated population of cells triggered by the presence of malignancy, but rather a heterogeneous group of immature myeloid cells which develop in many disease settings including sepsis (75), tuberculosis (76) and autoimmune disease (77). The term now adopted for these cells is myeloid derived suppressor cells (MDSCs). There are currently 2 major subsets identified in human subjects, which include monocytic MDSC (m-MDSC) and granulocytic MDSC (g-MDSC) although, as touched on above, due to the fact that this population are myeloid precursors, there are considerable difficulties in the differentiation of these cells from other groups of regulatory myeloid cells including suppressive DC, TAM and TAN. Recent attempts have been made to produce a defined phenotype although to date, there is no single set of surface markers or cellular characteristics that can definitely identify these populations in humans (250). Murine MDSC are more accurately identified due to the presence of a specific set of surface markers which are not detectable on other cell populations. Initially defined by the surface expression of Gr1+ and CD11b+ (251) and now sub-divided into monocytic MDSC and granulocytic MDSC, determined by their expression of Ly6C or Ly6G, respectively (252-254).

1.3.4 Checkpoint Activation and its Role in the Tumour Environment

CTLA-4

The understanding of the role of check points in the tumour environment has boomed over the last decade, with considerable successes occurring in targeting these pathways to release the brakes they place on the host immune system. Understanding their role in the development of malignancy is essential for the understanding of how the drugs targeted against them have managed to herald such success in a relatively short period.

The role of checkpoints, as their name would allude, is to provide the appropriate "checks" during immune activation, balancing the stimulatory and inhibitory signals to allow an effective immune response, while preventing serious harm resulting from the actions of the effector cells. Throughout the immune system there are mechanisms of negative feedback, allowing only the most appropriate level of response to occur. T cells, during their initial activation, require co-stimulation via two cell surface proteins, which trigger a cascade of intracellular signals. The first surface protein requiring engagement is the T cell receptor (TCR) itself, with stimulation through presentation of antigen bound to MHC molecules. This binding triggers a cascade of signalling within the cell, leading to early transcription of IL-2 (255), which is then augmented through binding of the co-stimulatory molecule CD28 to CD80 (B7-1) or CD86 (B7-2) expressed on the antigen presenting cell (256). Only after this second signal does transcription of IL-2 mRNA become stable and its production is increased 30 fold (256). At initial activation of the T cell, CD28 expression is transiently increased (257) however, shortly after the ligation of both the TCR and CD28, CD28 mRNA and surface expression begins to be down regulated (258). Within this period, CTLA-4 expression is markedly increased and begins to competitively bind to CD80 and CD86 in place of CD28, and with markedly higher

affinity (259). Due to the high detected affinity for CD80/CD86 binding, CLTA-4 was initially believed to be an additional co-stimulatory factor however, it was later demonstrated that this transition in expression was in fact a mechanism of T cell regulation, slowing down the activation and proliferation initially triggered. This concept was clearly demonstrated in murine models deficient for CTLA-4. These mice demonstrated a fatal lymphoproliferative disease, which was halted through the administration of CTLA-4Ig, providing evidence that CTLA-4 expression was required to maintain T cell tolerance (260). It has since been demonstrated that the highest expression of CTLA-4 is found on regulatory T cells, further confirming its role in immune regulation (261).

PD-1

The second most prominent regulatory molecule in T cell signalling is PD-1. PD-1 was first identified as a negative immune regulator following studies within mouse models. The absence of PD-1 expression was associated with the development of autoimmune lupus-like arthritis and glomerulonephritis syndromes, in addition to autoimmune cardiomyopathy (262,263). PD-1 expression was shown to be induced following T cell and B cell activation, with its primary inhibitory function being associated with T cell expression (264,265). The ligand for PD-1 was identified by Freeman *et al*, who demonstrated that PD-L1:PD-1 binding inhibited T cell proliferative responses (266). T cell inhibition could be overcome through higher T cell co-stimulatory binding of the TCR and CD28, in addition to higher levels of IL-2 however, with prolonged PD-L1:PD-1 binding this pathway appeared to show dominance (267). PD-1 activation alters the profile of cytokine production, with a reduction in IL-2 and increased IL-10 secretion from activated T cells (268); also altering the expression of

transcription factors involved in cell cycle progression, T cell effector function and cell survival signalling (269).

PD-L1 is expressed on a variety of cell types including T cells, B cells and the antigen presenting cells, macrophages and DC. This presence is interesting as it has been shown that its ligation not only impairs T cell function, but also alters the stimulatory functions of APCs (270). A second ligand to PD-1, PD-L2, is much less frequently found and was initially believed only to be inducible on macrophages and DC in response to inflammatory cytokines such as GM-CSF, IFN-γ and IL-4 (271,272). Further work has since demonstrated that a far more diverse population of cells can express PD-L2, with detection on alveolar epithelial cells, in response to respiratory syncytial virus (RSV) infection and the presence of IFN-γ and IL-4 (273); colonic fibroblasts (274); and, most interestingly, tumour associated fibroblasts in NSCLC, with a range of expression from 13-82% (275). Fibroblasts are able to act as non-professional APC and therefore, may be capable of altering immune responses. Within the colonic environment it was demonstrated that PD-L2 expression on fibroblasts was capable of inducing T cell inhibition via a reduction in IL-2 production (274). Within the environment of NSCLC, this role was also confirmed, with a reduction in T cell suppression occurring with the use of PD-L2 inhibitory antibodies (275) .

LAG-3, TIM-3 and TIGIT

In addition to CTLA-4 and PD-1, further signalling molecules including TIM3, LAG-3 and TIGIT, are also implicated in the mechanisms of immune homeostasis through T cell inhibition. Lymphocyte antigen gene-3 (LAG-3) was originally discovered as a T cell molecule with structural homology to the CD4 co-receptor. LAG-3 was shown to bind competitively to class II MHC molecules, displacing CD4-MHC binding (276) and to be responsible for the control of

T cell expansion following activation (277). Similarly to CTLA-4, LAG-3 expression is also found in higher concentrations on regulatory T cells, with loss of this expression leading to loss of control of T cell regulation, in addition to loss of regulation of macrophages, granulocytes and dendritic cells (278). T cell immunoglobulin-3 (TIM-3), identified in 2002, was again implicated in control of T cell activation (279). Through antibody binding of TIM-3 its negative regulatory properties were identified, with its absence strongly associated with the development of auto-immune disease (280,281). TIM-3 has been found to have a number of ligands, although most implicated in its role as a negative regulator of T cells are galectin-9 and high mobility group protein B1 (HMGB1), leading to induction of cell death and inhibition of innate immune activation, respectively (282,283). The most recently identified of these three additional inhibitory proteins is T-cell immunoreceptor with Ig and ITIM domains (TIGIT). Identified in 2009, TIGIT is expressed on activated T cells, in addition to NK cells and Tregs. TIGIT was shown to inhibit proliferative functions of T cells through impaired TCR signalling, in addition to the suppression of Th1 function by regulatory T cells (284,285). Interestingly, TIGIT has also been shown to affect DC function, leading to a switch in cytokine production from pro-inflammatory IL-12 to inhibitory IL-10 and resulting in T cell inactivation (286).

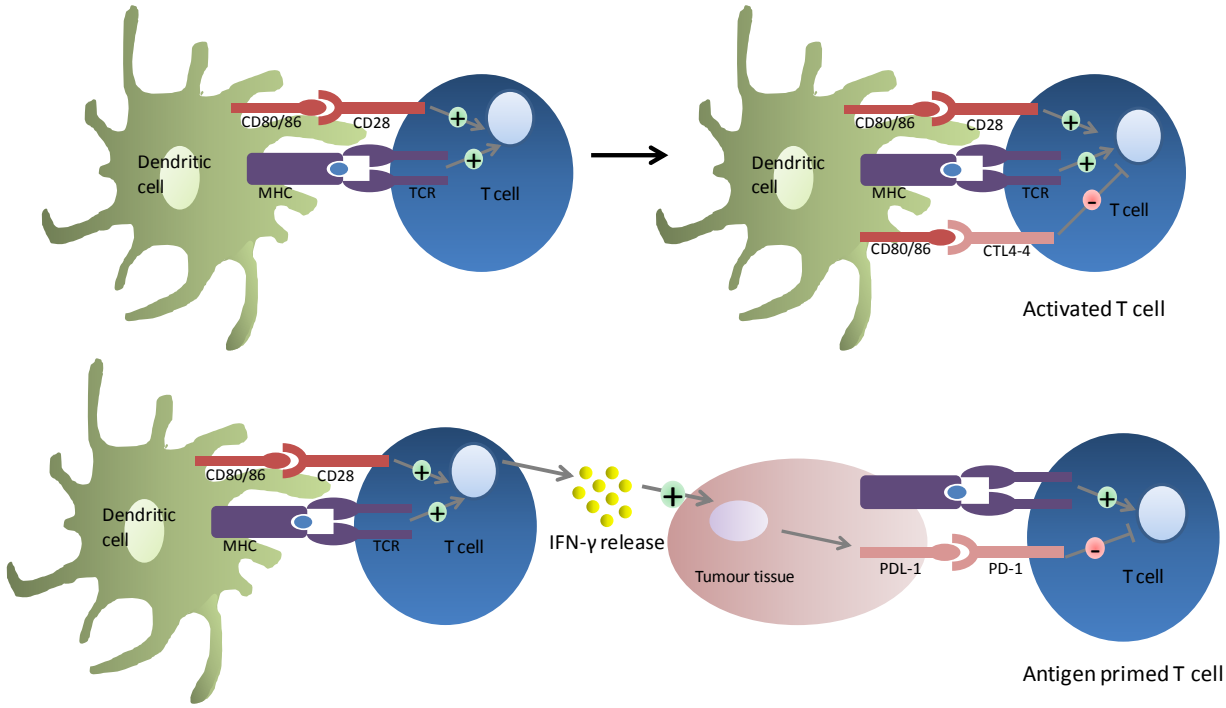

Figure 1. 4. Mechanisms of T cell regulation by CTL4-4 and PD-1.

T cell activation occurring via MHC:TCR binding and co-stimulation by CD28:CD80/86 leading to T cell activation. Activation of the TCR triggers the translocation of CTLA-4 molecules to the cell surface which competitively bind to CD80/86 and dampen the activation. The PD-1 pathway can be activated following initial T cell activation, which leads to IFN-γ release. IFN-γ triggers signalling within tumour and healthy tissue, leading to the transcription and up-regulation of PD-L1. PD-1:PD-L1 binding then acts to down-regulate T cell activation and minimise tissue damage. (Adapted from Pardoll, 2012 (287).

Check points within the tumour environment

Following the discovery of inhibitory check points within the immune system, thoughts rapidly gravitated to the prospects of signal manipulation in order to treat disease. The function of these molecules was therefore extensively investigated within the tumour microenvironment and the possibility of releasing the brakes on the immune system, in order to target cancer, has since become a reality. The study of check point expression within the tumour microenvironment rapidly demonstrated that PD-L1 expression and signalling is a commonly

found feature within multiple cancers including mesothelioma, lung cancer, melanoma, urothelial cancers, amongst others (274,288-291) .

PD-L1 expression on normal systemic tissues is low, however, within the tumour environment activation of intracellular pathways leads to up-regulated expression on the cell surface. Early research demonstrated that PD-L1 could be detected on a number of human cancer cell lines, and that expression could be further enhanced through the presence of inflammatory molecules such as IFN-γ, highlighting the role of PD-L1 in immune regulation. IFN-γ signalling was shown to lead to activation of the transcription factor interferon regulatory factor 1 (IRF-1), leading to enhanced binding to the PD-L1 promoter. Furthermore, the role of the JAK/STAT pathway was also demonstrated, with inhibition of JAK/STAT signalling significantly reducing the expression of PD-L1 (292). Further evidence that PD-L1 was important in cancer mediated regulation of the immune system was shown by its regulation in NMP/ALK+ T cell lymphomas. The NMP/ALK rearrangement is a proven oncogene whose activation leads to constitutive expression of STAT3 and promotion of proliferation and survival (293). Marzec *et al* further demonstrated that NMP/ALK activation of STAT3 was also responsible for the enhanced expression of PD-L1, thus enhancing the ability of T cell lymphoma cells to deactivate inflammatory immune signalling and invade immune detection (294,295). Similar enhanced PD-L1 expression has also been shown in gliomas, in response to PI3K signalling, following the loss of the phosphatase and tensin homolog (PTEN) gene (296). In human lung cancer, activation of PD-L1 signalling was shown to be regulated by both IFN- γ stimulated STAT3 activation and an alternative pathway, involving PI3K, ALK and mTOR signalling. mTOR was shown to have a strong role in PD-L1

expression, demonstrated by reduction in PD-L1 expression following the use of the mTOR inhibitor rapamycin. This inhibition also resulted in decreased rates of tumour growth (297).

The enhanced level of expression of PD-L1 in tumour tissues, undoubtedly disrupts immune activation within the tumour environment. Tumour T cell infiltrates have been shown to be significantly lower in tumours with high levels of PD-L1 expression in patients with resected NSCLC (288). Although no correlation to pathological features or post-surgical outcome could be detected within this study of NSCLC, Nakanishi *et al* demonstrated significant correlation between PD-L1 expression and both tumour grade and post-operative tumour recurrence in urothelial cancer (290). Similar associations were detected within both gastric and breast carcinomas. In gastric cancer, 42% of tumours were positive for PD-L1 expression with tumour size, invasion, presence of lymph node metastases and overall survival all significantly associated with PD-L1 expression (298). Higher grades of breast cancer and the poor prognostic feature of triple negative breast cancer were also associated with PD-L1 expression (299).

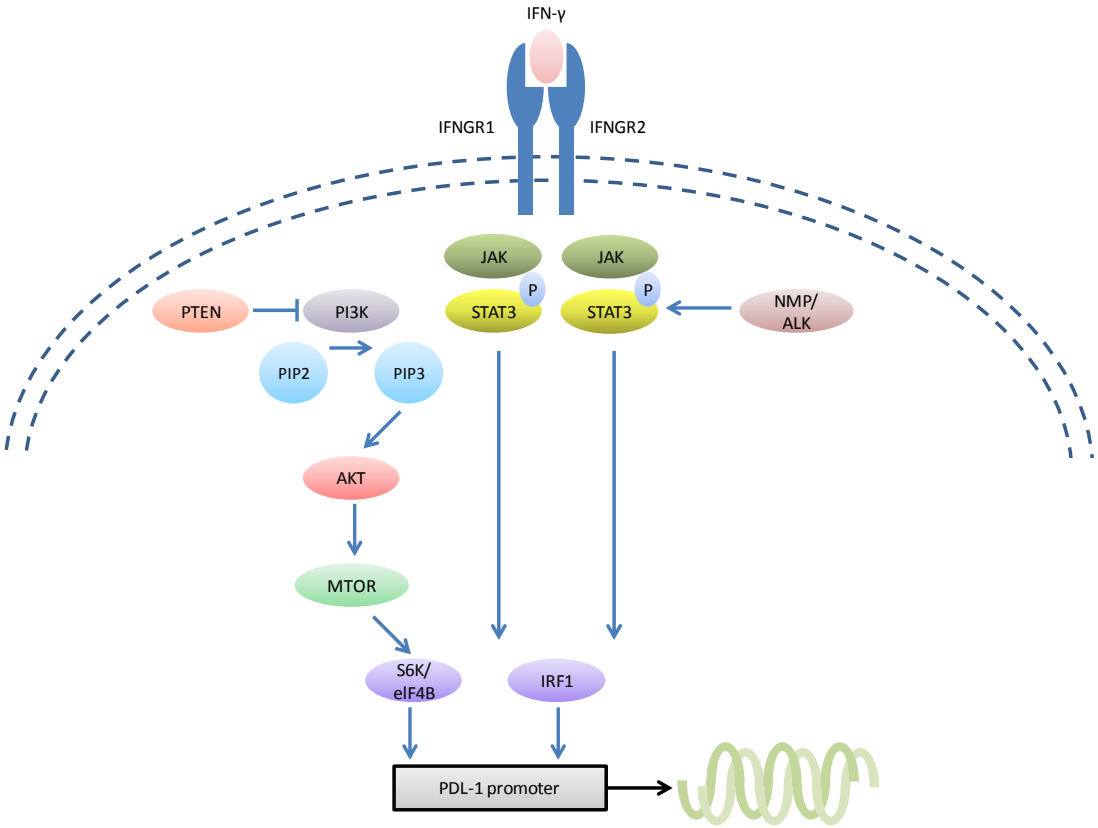

Figure 1. 5. The multiple signalling pathways of PD-L1 expression.

Signalling via the IFN gamma receptor leads to signalling via JAK and STAT3 leading to downstream signalling and binding of IRF1 to the PD-L1 promoter. Enhanced PD-L1 expression has also been shown in response to PI3K signalling, following loss of the PTEN gene. This leads to ALK and mTOR signalling, again driving binding of transcription factors to the PD-L1 promoter.

(Adapted from Ritprajak and Azuma, 2015 (300)).

1.4 Using Checkpoint Inhibition in the Treatment of Lung Cancer

1.4.1 The Role of PD-1/PD-L1 Blockade in the Management of Lung Cancer

Lung cancer has been one of the most successful tumour subtypes for the integration of checkpoint inhibition into clinical practice, with huge changes in clinical practice occurring in recent years. Early trials demonstrated excellent response rates in patients with advanced lung cancer, and where conventional chemotherapy could expect to provide only minimal gains in survival, PD-1 blockade led to survival beyond that ever seen before in this setting. The first trial to demonstrate these outcomes was KEYNOTE 010, which improved overall survival outcome in patients receiving PD-1 inhibition versus standard chemotherapy. Analysis of those patients with PD-L1 positivity greater than 50%, survival was more than doubled, from 8.2 months to 17.3 months (301). Three pivotal trials in lung cancer further paved the way for the introduction of immunotherapy into mainstream practice, with demonstration of an overall survival benefit in both the first line and second line setting. Within KEYNOTE 024 patients with advanced NSCLC were enrolled to receive either immunotherapy with pembrolizumab, or standard chemotherapy at diagnosis. Patients receiving Pembrolizumab saw increased response rates of 44.8% compared to 27.8% with chemotherapy, in addition to significantly longer progression free survival of 10.3 months compared to 6 months (143). Patients with this trial were permitted to cross over following progression on chemotherapy, weakening overall survival data. In the second line setting, the PD-1 antibody Nivolumab again provided significant improvements in response rates, increasing from 9% with chemotherapy to 20% with Nivolumab. In addition, a clear survival advantage was demonstrated in 2 separate phase III studies, with median OS improving from 6 to 9.2 months but, most dramatically, 2 year OS improving from 8% to 23% (302).

Promisingly, unlike with some of the earlier immunotherapy trials with CTLA-4 antibodies, PD-1 blockade seemed to be well tolerated with a favourable toxicity profile over standard chemotherapy. Most recently, immunotherapy with pembrolizumab has been licensed for use in combination with standard chemotherapy, following clinical trial results that demonstrated further improvements in response rates, progression free and overall survival, compared to immunotherapy alone (303). Response rates within the combination arm were 47.6% compared with 18.9% within the chemotherapy-alone arm, with disease control 84.6% compared to 70%. PFS was almost doubled, from 4.9 to 8.8 months with combination treatment, and this translated to a significant OS benefit, with a hazard ration for death of 0.49. At 12 months a 20% survival difference was detected, with 69.2% of patient alive in the combination arm compared with 49.4% with chemotherapy alone. Such dramatic improvements in response and survival are rarely seen in clinical trials in cancer, and truly mark a changing landscape.

Despite these huge leaps forward treatment in all trials and in licensing was restricted to patients of performance status (PS) 0 or 1. This restriction excludes a large number of lung cancer patients, as the age of presentation and association with smoking means that a large number of patients are likely to carry comorbidities which exclude them from access. A retrospective study carried out on 20,561 Polish patients with lung cancer demonstrated that within both males and females, the percentage of PS2 patients were 29 and 31%, respectively (304). Previous research has clearly proven that treatment of PS2 patients with standard chemotherapy agents does lead to improved survival outcomes (305,306), therefore with proven lower toxicity rates, immunotherapy should be opened up to this broader population.

The study incorporated within this PhD examined the use of Pembrolizumab within a PS2 population. As part of this study, we wished to explore whether inflammatory profiles and T cell function were associated with response to treatment or prognosis. (ClinicalTrials.gov Identifier: NCT02733159).

In addition to analysis of patient samples from PEPS2, we were also able to perform analysis on blood samples obtained from an additional clinical trial assessing the function of the PD-L1 antibody, Durvalumab. This patient cohort was a subgroup from the national lung matrix trial (MATRIX), a precision medicine trial aimed at enabling the analysis of multiple targeted treatments, without the need for individual trials (ClinicalTrials.gov Identifier: NCT02664935). Following the recent success of EGFR and ALK targeting in lung cancer it became evident that further detectable mutations within lung cancer may also provide actionable targets (307,308). Through the stratified medicine programme, MATRIX aims to identify small sub-populations of patients with lung cancer who carry actionable mutations and partner them with available treatments. As these cohorts alone are small, sometimes accounting for only 1-2% of an unselected population, individual trials would struggle to recruit numbers to provide statistically significance in outcomes. MATRIX aims to analyse treatment efficacy, not comparing to a standard treatment arm. Where patients do not carry any targetable mutations, they will be offered treatment with the PD-L1 antibody Durvalumab.

The access to samples from an additional population receiving treatment aimed at disrupting the PD-1/PD-L1 pathway provides a useful comparator and an opportunity to confirm any potential observed findings. In addition, the differentiation between patients of PS 0-1 enrolled within MATRIX and those of PS2 within PEPS2 provides a novel insight into the

changing immune patterns in patients with advanced cancer with significant comorbidity.

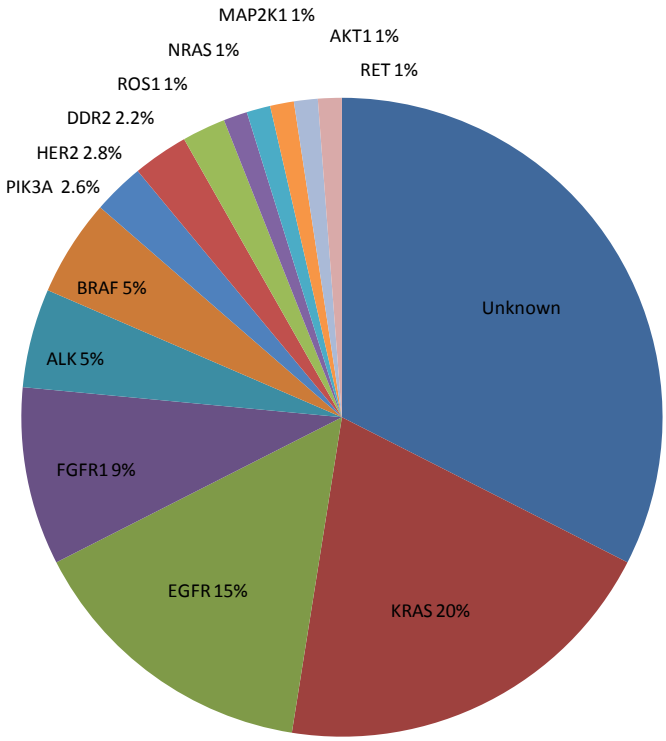

Figure 1. 6. Molecular subtypes in NSCLC.

There are now a large number of identified activating mutations in both adenocarcinoma and squamous cell lung cancer. Targetable mutations can lead to improved treatment responses and survival in selected patient populations. The MATRIX trial aims to improve the testing and delivery of targeted treatments to determine efficacy in small cohorts, which would otherwise not enter clinical trials.

(Adapted from Pao and Hutchinson 2012 and Oxnard *et al* 2013 (307,309)).

1.4.2 Predictive Biomarkers Associated with Response to Immunotherapy

Despite the treatment revolution that immunotherapy has provided, not all cancer patients respond to this therapy and there are few accepted biomarkers which can be predictive of response or risk of toxicity. Several recent studies have examined clinical and biological parameters to aid in this stratification of patients, but to date this knowledge is limited. The most commonly used tool to assess the chances of clinical response to anti-PD-1 therapy is the assessment of tumour PD-L1 expression, with early trials of check point inhibition clearly demonstrating an association between high PD-L1 expression and tumour responses in many cancer types (310). This association continued to be observed within lung cancer trials, with response rates of 50% seen in those patients with PD-L1 expression levels greater than 50%, compared to only 28% in those with levels of 1% or more (311). Interestingly, trials in melanoma did not find a significant association between PD-L1 expression and response (312), leading to the variations in drug licensing criteria for these tumour types. The difficulties in the ability to predict responses accurately using PD-L1 expression alone has since led to alterations in PD-L1 measurement, with the prevalence of PD-L1 on the surrounding immune infiltrate now being considered as an equally important biomarker. This biomarker adoption stemmed from a trial of the PD-L1 antibody atezolizumab, where the investigators un-expectantly found that higher PD-L1 expression on the immune infiltrate had a greater association with response than tumour PD-L1 expression. PD-L1 was detected on a number of immune cells including macrophages, dendritic cells and T cells and 83% of tumours with an immune infiltrate IHC score of 3 responded to treatment. Herbst and colleagues were able to obtain on-treatment biopsies within this study and clearly demonstrated that responding tumours showed a dense infiltrate of immune cells with high

PD-L1 expression. Non-responding tumours were seen to have little or no infiltrate, with poor PD-L1 expression (313).

Finding such as those by Herbst *et al* have led to the development of scoring systems such as the combined positive score (CPS), which incorporates both the tumour and immune cell prevalence of PD-L1 positivity. Early forms of this test in melanoma incorporated tumour cell expression of PD-L1, in addition to staining of mononuclear inflammatory cells. Significant associations between high scores and both response rates and progression free survival were demonstrated (289). Developments of this scoring method subsequently produced the CPS assay, which is defined as the percentage of tumour cells, macrophages, or lymphocytes expressing PD-L1 in a tumour biopsy, relative to the total number of tumour cells (314). This test has been validated through a number of clinical trials and is now set as the standard in more recent trials assessing tumour responses to PD-1 inhibition (315,316). The adoption of this broader assessment of PD-L1 detection clearly signifies the importance of the immune infiltrate in tumour immune evasion and in determining responses to treatment.

The finding that the expression of PD-L1 on the immune infiltrate in cancers is important is no surprise and raises further questions about the predictive value of the types and numbers of immune cells within both the tumour microenvironment and peripheral blood. The most frequently examined immune cell types in this setting are both tumour infiltrating T cells and Tregs, with evidence to suggest that response to treatment is associated with higher levels of infiltrating T cells, and in the setting of CTLA-4 antibodies, the presence of Treg cells is significantly predictive of response (317). In two separate studies by Martens *et al* baseline characteristics, in addition to dynamic changes in blood parameters, were examined in patients receiving ipilimumab, to assess their association with response and overall survival.

They observed that low percentages of both baseline monocytes and HLA-DR negative monocytic-MDSC were predictive of long term survival, in addition to a positive association between high relative eosinophils counts and patient outcomes (317). When examining dynamic changes, the most striking changes were seen CD4+Ki67+ and CD8+Ki67+ circulating T cells, with increased frequencies detected in 84% and 96% of patients, respectively. Increases in frequencies of circulating CD4+CD25+FoxP3+ T regs and a reduction in classical monocytes were also detected. When correlated to patient outcome, the most striking association with improved OS was seen when patients demonstrated early increases in absolute lymphocyte counts, with an associated delayed increase in CD4+ cells. When compared to patients who had neither finding, this combination of outcomes saw a dramatic increase in 1 year survival from 9.6% to 78.3% (318).

These findings clearly demonstrate that alterations within the immune system are vital in the mechanisms used by tumours to evade detection. The presence of PD-L1 on tumour cells is most certainly not the only factor determining response to PD-1/PD-L1 inhibition and it is now widely accepted that assessment of the immune infiltrate should be a part of initial tumour assessment. The role of circulating immune biomarkers are, however, less well accepted and it is unclear whether these parameters can be reliably associated with response and outcome. Through this PhD this is a question I plan to further explore.

1.5 Project Aims

As discussed within the introduction, mesothelioma is a cancer with very poor prognosis and limited treatment options. Further research is required to fully understand the environment in which this cancer develops, in order to aid in the development of targeted and successful treatments.

Through the first part of this thesis I plan to assess the peripheral and tumour immune profile of a cohort of mesothelioma patients at diagnosis. This will be achieved through the sampling of patient tissue and blood during either surgical biopsy or resection. I plan to primarily examine the myeloid compartment, to identify abnormal populations by comparison with healthy control blood samples. Tissue analysis will be aimed at identifying the presence of infiltrating myeloid or T cells. My aim is to determine whether an identified population displays significant functional differences to healthy controls and has the ability induce T cell tolerance. The mechanisms behind this will be sought.

Secondly, I wish to examine the effect of mesothelioma on T cell immunity. T cell dysfunction has a prominent role in the patterns of immune escape within malignancy and the immune profile within mesothelioma has the potential to drive T cell dysfunction through direct interaction as well as through altered APC function. I plan to examine the role of STAT3 in this setting, aiming to explore the effects of mesothelioma in T cells with both functioning STAT3 and inhibited STAT3 signalling.

My final aim is to assess whether the peripheral immune profile can be used to predict response to checkpoint blockade and to determine whether checkpoint blockade can affect

or normalise this profile. From this information, I hope to establish markers predictive of response to immune modulation or survival within mesothelioma or NSCLC.

Chapter 2: Materials and Methods

2.1 Healthy donor and patient blood and tissue preparation

2.1.1 Patients and Donors

Samples were obtained from 44 patients with suspected mesothelioma who were attending for diagnostic biopsy at Heartlands Hospital, Birmingham, and from 7 patients with confirmed mesothelioma attending for resection at Glenfield Hospital, Leicester. Clinical information was obtained through case note review at the source hospital by members of the local research teams. Written informed consent was obtained before sample collection with ethical approval obtained from the London Ethics Committee (reference number 14/LO/1527) and through the Midlands Lung Tissue Consortium (reference number 07/MRE08/42).

For the work carried out within the PEPS2 clinical trial ethical authorisation was obtained from the West midlands Research Ethics committee (reference number 16/WM/0010). For work carried out as part of the National lung MATRIX trial ethical authorisation was obtained through the National Research and Ethics committee South, Central and Oxford (reference number 14/SC/1346).

Healthy donor samples were obtained from volunteers at the University of Birmingham and were collected under the previously held ethics of Dr Francis Mussai (reference number 10/H0501/39).

For patient samples, venepuncture was carried out at varying times of the day, prior to surgery or biopsy, or at time of attendance for treatment. No exact timings were recorded, although due to the

nature of the attendance to hospital, most venepuncture was performed prior to 12noon. All were within working hours of 9am to 5pm. Healthy donor samples were taken primarily between 9am and 12 noon.

2.1.2 Sample Preparation

40ml of whole blood, collected in heparinised vacutainers, and matched fresh tissue samples were obtained where possible. Samples were transported on the day of collection to the University of Birmingham.

2.1.3 Plasma Collection

Blood samples collected in heparinised tubes were allowed to stand for 1 hour at room temperature to allow natural separation. Plasma was collected and centrifuged for 5 minutes at 500xg then transferred to a clean Eppendorf tubes prior to storage at -80°C.

2.1.4 Whole Blood and Peripheral Blood Mononuclear Cell (PBMC) Processing

PBMCs from both patients and healthy donors were isolated from whole blood through gradient separation. For certain experiments aphaeresis leukocyte-depleted cones, purchased from the National Blood Service, were used to obtain CD14+ monocytic cells or T cells. Blood was diluted in RPMI-1640 (Sigma Aldrich) 1:1 for patient or healthy donor samples and 1:4 for aphaeresis cones, before layering onto Lymphoprep (Stemcell technologies). Samples were then centrifuged for 30minutes at 900xg with the brake off. PBMCs were collected from the plasma:Lypmphoprep interface. PBMCs were washed with RPMI for 15minutes at 500xg. The supernatant was discarded, and the cells washed with RPMI for 10minutes at 270xg.

To enrich for CD14+ cells and CD15+ cells, the PBMC pellet was resuspended in 500µl MACS buffer with 50µl CD14 or CD15 magnetic beads (Miltenyi). Samples were mixed and placed at 4°C for 20 minutes. Samples were washed in MACS buffer (phosphate buffered saline (PBS) 1X, 2% BSA (≤0.1ng/mg endotoxin) , 2 mM EDTA), centrifuged for 5 minutes at 500xg and the

pellet re-suspended. MACS LS columns (Miltenyi) were inserted into a magnetic separator and prepared by rinsing with 3ml MACS buffer. The cell suspension (500 μl) was then added and the column washed 3 times with 3ml of buffer. The column was removed from the magnetic field and the magnetically labelled cells flushed out using a plunger within 5ml RPMI. Negative fractions were centrifuged for 5 minutes at 500xg and resuspended in fresh medium. Cells were further sorted if required, or frozen for future use.

For granulocyte isolation, visible cells were harvested from the top of the red cell pellet using a suction pipette, following gradient separation. Approximately 500μl of cells were diluted in 5ml of lysis buffer and RBC lysis performed over 10 minutes at room temperature. Lysis buffer was diluted with RPMI and the sample centrifuged, to reveal a leukocyte pellet. The pellet was further purified through magnetic bead separation as described above, using CD15+ beads (Miltenyi).

2.1.5 Tumour Tissue Processing

Tissue samples were obtained during biopsy or surgical resection procedures and placed as fresh tissue into RPMI. They were stored at 4°C until collection, transported on ice and stored again at 4°C within our laboratory until processing. Samples were processed within 12 hours of receipt. Specimen pots were opened within a sterile culture hood and tissue diced into small pieces in a petri dish before transfer to MACS C-tubes (Miltenyi) in 7ml of RPMI. Tissue was further mechanically digested using the gentle MACS cell dissociator (Miltenyi). The resultant cell suspension was filtered and washed with RPMI and centrifuged for 5minutes at 500xg. Samples were then stained using the following anti human antibodies in 300 μl FACS Buffer (PBS 1X (Sigma) +10% foetal bovine serum (FBS, Sigma)): CD45, CD14, CD15 and CD3 (All antibodies were produced by Biolegend). The samples were incubated with the antibodies

at 4°C for 30 minutes. The samples were washed twice in FACS Buffer, re-suspended in 500 μl of FACS Buffer and sorted with the FACS Aria cell sorter. The positive cells were collected in 10% RPMI.

Negative cells were collected and cryopreserved as "tumour cells" for future use.

2.2 Cell Culture

2.2.1 Growth and Maintenance of Tumour Cell Lines

The mesothelioma cell line MSTO211 was obtained as a gift from Professor Fennell, University of Leicester, and 5 additional mesothelioma cell lines, Meso 15, Meso 26, Meso 30, Meso 34 and Meso 43, were purchased from MesobanK UK (Table 2.1). Cell lines were verified using Northgene DNA short-tandem repeat analysis and were routinely tested and negative for mycoplasma. All mesothelioma cell lines were cultured in complete medium consisting of RPMI-1640 (Sigma), 10% heat inactivated Foetal Bovine Serum (FBS, Sigma), 1% penicillin/ streptomycin (Life Technologies), 1% sodium pyruvate (Life Technologies) and 1% L-glutamine (Life Technologies). Cells were grown at 37°C in 5% CO_2 in 25cm^2 flasks and split twice per week. Cells were split using 1x TrypLE Express (Gibco), 1ml per flask, for 5 minutes. Cells were then harvested by agitation and dilution in RPMI, centrifuged for 5 minutes at 500xg and re-plated at a density of 1 x 10^6 per 25cm^2 flask in 10ml complete medium.

For the purpose of extracting tumour conditioned media (TCM), cells were plated as described above and cultured for 72 hours until approximately 90% confluent. Cell line conditioned media was then removed and filtered prior to use.

2.2.2 Cryopreservation of Cells

When cell lines were not in use they were cryopreserved at -80°C. Cells were centrifuged for 5 minutes at 500xg. All media was removed from pellets prior to re-suspension in freezing media consisting of FBS and 10% dymethyl sulfoxide (DMSO, Sigma) and transfer to 1.5ml cryovials. Cryovials were placed in an isopropanol filled Mr Frosty (Nalgene) and placed in a -80°C freezer. Cells were moved from the Mr Frosty into cryo-boxes after at least 4 hours.

To thaw frozen vials, they were gently washed in warm media, prior to dilution in 5ml RPMI and centrifuged at 500xg for 5 minutes to remove freezing media. Cell pellets were re-suspended in the desired media prior to use.

2.2.3 Transwell Assays and Polarisation of Isolated Myeloid Cells

Monocytes were extracted from an aphaeresis cone and granulocytes were extracted from healthy donor blood samples following gradient separation, as described above. For the development of dendritic cells (DC), CD14+ cells were plated at a concentration of $1x10^6$ per ml (3 ml per well) in 6 well plates (Costar) in the presence of GMCSF (50ng/ml) (Peprotech) and IL-4 (100ng/ml) (Peprotech) and cultured at 37°C in 5% CO_2 for 6 days. To polarise cells, DC were generated in the presence of 25% TCM for 6 days, granulocytes were cultured in 12 well plates in a total of 2ml media, in the presence of 25% TCM for 24-48 hours. Where transwell assays were used, mesothelioma cell lines were plated in a 24 well plate at a concentration of $0.1x10^6$ and returned to the incubator to allow adherence to the plate. After 4 hours, a 0.4µm transwell permeable support containing $0.5x10^6$ neutrophils was placed on top of the plated cells. Cells were cultured for 24 or 48 hours, depending on the experimental design.

2.2.4 T Cell Proliferation and Suppression Assays

Two methods of T cell functional assays were used during this PhD; a mixed leucocyte reaction (MLR) using DC to stimulate T cell proliferation and T cell suppression assays using anti-CD3 and anti-CD28 stimulation. In both cases we used a 96 flat bottom well plate (Falcon), and cells were cultured in 200 μl of medium.

For MLR using DC, 50,000 DCs, generated as described above, were co-cultured with 200,000 allogeneic T cells for 96 hours. Suppressive activity was determined by the addition of reducing concentrations of immunosuppressive cells (CD15+ cells purified from patients or healthy donors, and TCM polarised CD15 + cells) to a DC: T cell MLR, with at ratios of 1:1 to 1:0.125, T cells:CD15+ cells. Unstimulated, immature DC were used within these culture conditions, previously demonstrated to effectively stimulate T cell proliferation (319).

For T cell suppression assays, anti-CD3 monoclonal antibody (eBioscience) was plated approximately 12 hours before the assay was begun to allow time for fixation of the plate bound CD3 (3μg/ml). Following cell preparation, reducing concentrations of either patient derived or polarised CD15+ cells were then plated alongside allogeneic T cells at ratios of 1:1 to 1:0.25. Further T cell stimulation was achieved through the addition of anti-CD28 antibodies (2μg/ml) (eBioscience). T cells cultured in absence of suppressive cells were used as a proliferation control. Unstimulated T cells were used as a negative control. Where T cell function was being assessed in isolation, anti-CD3 and anti-CD28 were used to stimulate T cell proliferation, without the addition of other cell populations.

Following culture for 96 hours proliferation was assessed through ^{3}H-thymidine incorporation. Thymidine was added to all wells at a concentration of 0.5μCi per well and

incubated at 37°C for 16 hours to allow incorporation into cellular DNA during mitotic cell division. Plates were subsequently frozen at -20°C. Plates were defrosted and harvested onto glass fibre filters prior to reading using a TopCount Scintillation counter (Perkin Elmer), with results displayed as counts per minute (CPM). The results were represented as percentage of T cell proliferation in the presence of suppressive cells relative to the control (stimulated T cell in absence of suppressive cells).

2.2.5 T Cell Proliferation by CFSE Labelling

5-Carboxyfluorescein diacetate succinimidyl ester (CFSE) labelling (eBioscience) was also used to assess T cell proliferation. CFSE is known to cross intact cell membranes and once inside the cell, intracellular esterases cleave the acetate groups to produce the fluorescent carboxyfluorescein molecule, which can be detected via flow cytometry with a peak excitation wavelength of 494nm and peak emission of 521nm.

In order to perform CFSE labelling, T cells were resuspended at a concentration of 8 x 10^6 per ml and washed twice with PBS to remove serum. CFSE was added to a final concentration of 1µM. The solution was mixed immediately and incubated at room temperature (20°C) in the dark for 10 minutes. The reaction was quenched by adding 5 x volume of cold, complete RPMI (10% serum). Cells were then washed 3 times in complete media before plating.

T cells were plated at concentration of 4 x 10^6 per ml in the presence of anti-CD3 and anti-CD28 as described above. Proliferation was assessed at 96 hours by harvesting the well and examining CFSE intensity via flow cytometry. Unstimulated T cells were used as a positive control and unlabelled T cells as a negative control. Proliferation was demonstrated by CFSE dilution, with successive halving of the fluorescence intensity of CFSE indicating cell division.

For both thymidine incorporation and CFSE assays, where no T cell proliferation occurred in control wells, the assay could not be analysed and was therefore removed from the analysis.

2.2.6 STAT3 Inhibition using a STAT3 Antisense Oligonucleotide

For T cell and DC experiments examining the function of STAT3, inhibition was achieved with the use of an antisense oligonucleotide, AZD9150, obtained from Astrazeneca. T cells were plated at a concentration of $2x10^6$ per ml within 6 well plates, with direct addition of the antisense oligonucleotide at a concentration of 5µM. This was following initial dose titrations as per manufacturer guidance. Cultures were carried out for 48 hours with or without the presence of tumour conditioned media. Where necessary a control ASO was added at equivalent concentrations, also provided by Astrazeneca. To attempt to enhance uptake, the transfection agent Fugene6 was used as per the manufacturer protocol.

The STAT3 ASO was also added directly to culture with DC on day one of generation, at a concentration of 5µM, with or without the presence of TCM. The use of Fugene6 was not required or tested within this population.

Table 2. 1. Tumour cell lines

Cell line	Origin	Tumour Subtype	Supplier
Meso 15	Male 68 years	Epithelioid mesothelioma	MesobanK UK
Meso 43	Male 56 years	Epithelioid mesothelioma	MesobanK UK
Meso 30	Male 60 years	Epithelioid mesothelioma	MesobanK UK
Meso 26	Male 66 years	Biphasic mesothelioma	MesobanK UK
Meso 34	Male 53 years	Sarcomatoid mesothelioma	MesobanK UK
MSTO-211H	Male 62 years	Biphasic mesothelioma	ATCC
NCI-H1299	Male 43 years	Non-small cell lung cancer	ATCC

2.3 Flow Cytometry

Whole blood and tumour tissue were analysed by multi-colour flow cytometry using the Cyan flow cytometer (Beckman Coulter). RBC lysis was performed on 500µl of whole blood from patients and healthy donors, prior to washing and centrifugation at 500xg for 5 minutes. Cell pellets were re-suspended in 500µl FACS buffer. Small aliquots of digested tumour tissue were taken from the cell pellet, washed and analysed as per whole blood.

50µl of diluted cell suspension was added to wells in a 96 well round bottom plate and centrifuged at 500xg for 5 minutes. Supernatant was removed by flicking the plate gently into the sink. Cell pellets were stained using a panel of antibodies including common myeloid surface markers CD14, CD15, CD33, CD11b, CD66b, CD16, HLA-DR and PD-L1, and T cell surface markers CD3, CD4 and CD8. In a subgroup of patients, expression of the T cell exhaustion markers LAG3, TIM3 and PD-1 were also investigated. The panel of cell surface markers used is displayed in table 2.2. Staining was carried out for 30 minutes at 4°C prior to washing in 100µl FACS buffer. The stained cell pellets were re-suspended in 200µl FACS buffer and transferred to 5ml FACS tubes for acquisition. All flow cytometry was performed immediately following staining. Analysis was carried out using FlowJo software.

Table 2. 2. Antibodies used within multi-colour flow cytometry

Target	Fluorochrome	Clone	Host	Dilution	Manufacturer
CD14	FITC	61D3	Mouse	1:100	eBioscience
CD15	Violet 1	H198	Mouse	1:100	eBioscience
CD33	Pe-Cy5	HIM3-4	Mouse	1:200	eBioscience
CD11b	Pe-Cy7	1CRF44	Mouse	1:400	eBioscience
CD16	APC-Cy7	CB16	Mouse	1:400	eBioscience
CD66b	APC	G10F5	Mouse	1:400	Biolegend
CD3	APC	UCHT1	Mouse	1:100	BD
CD8	FITC	RPAT4	Mouse	1:100	BD
CD4	PE	HIT8a	Mouse	1:100	BD
HLA-DR	PE	G46-6	Mouse	1:50	BD
CD45	PE	H130	Mouse	1:100	Biolegend
PD1	PE	EH12.2H7	Mouse	1:100	Biolegend
PDL1	PE	29E.2A3	Mouse	1:100	Biolegend

LAG3	FITC	11C3C65	Mouse	1:100	Biolegend
LOX1	PE	15C4	Mouse	1:100	Biolegend
CD83	FITC	HB15e	Mouse	1:100	eBioscience
CD86	APC	IT2.2	Mouse	1:100	Biolegend
CD80	PE	2D10.4	Mouse	1:100	Biolegend
CD40	FITC	5C3	Mouse	1:100	Biolegend
CD54	APC	HA58	Mouse	1:100	Biolegend

2.4 Molecular Biology

2.4.1 RNA Extraction and Generation of cDNA

Following experiments any cells to be preserved for RNA analysis were lysed in RLT lysis buffer (Qiagen) with 1% 4.3M β-mercaptoethanol and frozen at -80°C. Upon thawing, the RNEasy mini kit (Qiagen) was used to extract RNA following the manufacturer's instructions. Briefly, the lysis solution was mixed with an equal volume of 70% ethanol and placed onto an RNEasy spin column. The sample was washed twice using manufacturer provided buffers and the spin column dried by a final spin without buffer. RNA was then eluted using purified RNAse- free water and quantified using the NanoDrop Fluorospectrometer (Thermo Scientific).

To generate cDNA, up to 400ng of RNA was added to a reverse transcription reaction using the Promega Reverse Transcription System as per the manufacturer's instructions. Following the initial heating of RNA to 70°C for 10 minutes, RNA was added to the reaction mix (see table 2.3) and heated to 42°C for 15 minutes, 95°C for 5 minutes, followed by 4°C for 5 minutes.

Table 2. 3. PCR reagents

Component	Volume
MgCl2, 25mM	4µl
Reverse Transcriptase 10x buffer	2µl
dNTP mixture, 10mM	2µl
RNasin Ribonuclease inhibitor	0.5µl
AMV reverse transcriptase	0.5 µl
OligoDT Primer	1 µl
Nuclease free water	To a total volume of 20 µl

2.4.2 Quantitative Real Time Polymerase Chain Reaction (RT-qPCR)

RT-qPCR allows for quantification of gene expression during the PCR through the measurement of increasing fluorescence, emitted by an amplified probe. For each reaction, 10-50ng of cDNA (dependent on the quantity of cDNA obtained in individual experiments) was combined with forward and reverse primers of the gene of interest and a PCR master mix (SYBR green (Roche) or TaqMan (Invitrogen), dependent on PCR probes used) in a total volume of 20µl. For each reaction the house-keeping gene, GAPDH, was also amplified for normalisation. Primer sequences or assay ID are documented in table 2.4. Once plated, PCR was carried out using the Fast 7500 RT PCR system (Applied Biosystems). Samples were then

subjected to heating to 95°C for 20 seconds to activate the polymerase enzyme, followed by 40 cycles of 95°C for 3 seconds to denature the cDNA and 60°C for 30 seconds for primer annealing and elongation. For TaqMan probes an additional first step of 50°C for 2 minutes was added for optimal uracil-N glycosylase (UNG) activity.

Analysis of data was carried out using the 7500 PCR system and further calculated according to $2^{-\Delta T}$ method, displayed as units of mRNA of interest relative to GAPDH.

Table 2. 4. Primer sequences

Gene of Interest	Forward primer	Reverse Primer	Manufacturer
NOX2	CAAGATGCGTGGAAACTA	TCCCTGCTCCCACTAACA	Eurofins
GAPDH	CCAGCCGAGCCACATCGCTC	ATGAGCCCCAGCCTTCTC	Eurofins
STAT3	Assay ID Hs 00374280_ml		TaqMan
STAT5	Assay ID Hs00559637_gl		TaqMan
STAT1	Assay ID Hs01013996_ml		TaqMan
GAPDH	Assay ID Hs02758991_gl		TaqMan

2.4.3 Protein Extraction and Electrophoresis

To enable protein extraction cells were pelleted by centrifugation at 500xg for 5 minutes, and all media removed prior to washing with PBS. The pellet was re-suspended in 40µl 1x RIPA buffer (ThermoFisher), comprising 25mM Tris HCl pH 7.6, 150mM NaCl, 1% NP-40, 1% sodium deoxycholate, 0.1% SDS. PhosStop phosphatase inhibitors (Roche) and a protease inhibitor cocktail (Sigma) were added to RIPA buffer prior to cell lysis. Cells were vortexed and placed on ice for 20minutes, with a further vortex at 10 minutes. Cells were then centrifuged for 30 minutes at 14,000xg. Supernatants were removed and transferred to clean Eppendorfs and pellets discarded. Protein quantities were determined using the Bradford method using Coomassie Protein Assay Reagent (Pierce). Protein quantities were determined by comparison to the colour response of bovine serum albumin (BSA) dilutions as a protein assay standard.

20µg of protein was then diluted with 4xLamellli Buffer (Bio-Rad), which comprised 62.5 mM Tris-HCl, pH 6.8, 10% glycerol, 1% LDS, 0.005% Bromophenol Blue, to produce a total volume of 25µl. Samples were heated to 95°C for 5 minutes to denature proteins.

Samples were loaded into wells of a precast Criterion™ TGX™ gel alongside a protein ladder (ThermoScientific) to allow accurate determination of protein size. A 25Mm Tris, 192mM glycine, 0.1% SDS buffer (pH 8.3) was used to perform electrophoresis. Gels were run at 100V until protein aliquots entered the gel, then 150V for approximately 60 minutes, or until complete protein separation was achieved.

2.4.4 Western Blotting

Following gel electrophoresis proteins were transferred using the Trans-Blot Turbo transfer system (Bio-Rad). Trans-Blot Turbo polyvinylidene difluoride (PVDF) membrane packs, containing buffer-saturated ion reservoir stacks and a pre-wetted PVDF membrane, were used to perform the transfer using a pre-determined protocol of 7 minutes at 1.3A, 25V.

Following protein transfer, membranes were blocked in PBS/1% Tween (Sigma) (PBS-T) with 5% Bovine Serum Albumin (BSA) for 1 hour at room temperature to prevent non-specific binding of antibodies. Incubation with primary antibody was then performed overnight at 4°C (see table 2.5 for specific antibodies and dilutions). Following overnight protein detection, blots underwent 3 x 15-minute washes in PBS-T, prior to the addition of a secondary antibody for 1 hour. Appropriately matched secondary antibodies were conjugated to horseradish peroxidise (HRP) for chemiluminescent detection. Blots underwent a further 3 washes in PBS-T prior to examination for protein detection using Clarity ECL substrate (Bio-Rad), which catalyses a reaction between HRP and Luminol to release light. Luminescence was then detected by exposure to Xray film.

Table 2. 5. Antibodies used within western blot

Protein Target	Molecular Weight	Source	Manufacturer
STAT3	79.86 kDa	Rabbit	Cell Signalling
Phospho-STAT3 (Tyr705)	79.86 kDa	Rabbit	Cell Signalling
STAT5	90 kDa	Rabbit	Cell Signalling
β-Actin	45 kDa	Rabbit	Cell Signalling

2.5 Enzyme Linked Immunosorbent Assay (ELISA)

2.5.1 Standard Sandwich ELISA Techniques

For the detection of cytokines in human plasma and released during cell culture experiments ELISAs were commonly performed. Specific ELISA detection plates (Corning) were pre-coated with primary capture antibody diluted in carbonate coating buffer, pH 9.5 (Biolegend) and incubated over night at 4°C. The following day, the capture antibody was removed by flicking the plate into the sink and plates were washed 4 times with PBS/0.05% Tween, prior to blocking in PBS/0.05% Tween/10%FBS for a minimum of 2 hours at room temperature. Plates were washed again 3 times with PBS/0.05% Tween, followed by blotting against paper towels to remove residual wash buffer. Standards were added at reducing concentrations, as per manufacturer directions, and samples were added in 25µl volumes. The plate was sealed and incubated at 4°C overnight. Plates were washed a further 4 times in PBS/0.05% Tween, with

blotting on paper towels to remove excess, prior to the addition of the appropriate biotin labelled detection antibody for 1 hour at room temperature. Washing was repeated prior to adding the Avidin-HRP conjugate for 30 minutes at room temperature. Plates were protected from light from this point. A final 4 PBS/0.05% Tween washes were performed prior to adding tetramethylbenzidine (TMB) substrate to observe colour development. Once colour development was optimal, the reaction was stopped by the addition of TMB stop solution. Optical density was read using a micro-plate reader (Bio-Rad) at 450nm. Concentrations were calculated following the construction of a standard curve using the plated standards. Where sample concentration fell below the standard curve, results were deemed to be negative, if above, these samples were excluded from the analysis or re-tested with dilution of the primary sample.

2.6 Quantification of ROS Production via Amplex Red Assay

During patient sample collection and CD15+ cell polarisation experiments the production of reactive oxygen species was determined using the 2', 7'– dichlorofluorescein diacetate (DCFDA) cellular ROS detection assay kit (Abcam). CD15+ cells were incubated with 2.5µM DCFDA for 30 minutes at 37^{o}C followed by removal of any residual dye. The presence of ROS within cells is detected by the oxidation of DCFDA by ROS into the highly fluorescent compound 2', 7' –dichlorofluorescein (DCF). TCM polarized cells were also incubated with 30ng/ml Phorbol 12-myristate 13-acetate (PMA) during the staining with DCFDA as a positive control.

The stained cells were analysed on the Cyan flow cytometer (Beckman Coulter) through detection of a FITC signal, with excitation and emission at 495nm and 529nm, respectively.

Quantification of H_2O_2 production in polarised CD15+ cells was measured using the Amplex Red Hydrogen Peroxidase assay kit (Invitrogen). Following culture in TCM for 24 hours, cells were washed twice in RPMI, counted and plated in Krebs–Ringer phosphate buffer. A second plate was prepared containing 100µl per well of reaction mixture (50 µM Amplex® Red reagent and 0.1 U/mL HRP in Krebs–Ringer phosphate) and pre-warmed at 37°C for 10 minutes. The reaction mixture was plated both with and without PMA. 20µl of cells were then added to each well and warmed for 10 minutes. A H_20_2 standard curve was used to allow quantification. Detection of H_2O_2 was carried out using a microplate reader detecting absorbance at 560nm.

2.7 Immunohistochemistry

Mesothelioma sections were obtained from diagnostic tumour biopsies and slides were prepared and provided by the hospital pathology department. Slides were deparaffinised by placing into Histoclear (National diagnostics) for 5 minutes, followed by ethanol for 5 minutes. They were then rehydrated by washing with water. Endogenous peroxide block was performed using 0.3% hydrogen peroxide for 15 minutes. Slides were then washed again in water. Antigen retrieval was performed in 10 mM sodium citrate buffer (pH 6.0). Slides were placed in a pre-heated buffer and further heated for 20 minutes in a microwave oven. Slides were cooled for 15 minutes and washed in running tap water for 2 minutes. Protein blocking in 5X Caesin (ThermoFisher) was carried out for 30 minutes at room temperature. Sections

were then incubated over night with primary antibody, rabbit anti-GM-CSF (Novus Biologicals), diluted in PBS at a concentration of 1:200. The following day sections were washed three times in Tris-buffered saline/0.1% Tween 20 (TBS-T), each for 5 minutes. Secondary antibody (Universal ImmPRESS antibody, Vector Laboratories) was added at room temperature for 30 minutes as per the manufacturer's instructions. Three further washes of 5 minutes with TBS-T were performed, followed by the addition of DAB substrate (ImmPACT DAB, Vector Laboratories) for 5 minutes. Slides were washed in running water for 5 minutes, then counterstained with Harris haematoxylin (Sigma) for 1 minute, prior to washing in warm water for 5 minutes. Slides were dehydrated using ethanol and Histoclear and mounted using Omnimount (National diagnostics). Following drying, slides were examined and photographed using a Nikon Eclipse 400 microscope.

2.8 Statistical Analysis

Statistical analysis was carried out with the advice of a university statistician. Analysis was performed using the PRISM 6.0 software programme (GraphPad). For the initial interrogation of data, histograms were performed to assess for normality. Normality testing was also carried out using the D'Agostino and Pearson omnibus normality test within the GraphPad programme. Where data was found to be non-normal in distribution non-parametric tests were applied. For most data, comparisons between two groups were therefore analysed using a non-parametric Mann Whitney U test. Median values are demonstrated within figures as a better representative of central tendency, when data is not normally distributed. Where multiple variables were analysed, analysis of variance (ANOVA) was carried out, with post-

test correction. The exact method of correction was dependent on the primary test applied. Specific tests for individual experiments are reported within each figure legend.

Chapter 3: The Immune Microenvironment in Mesothelioma

3.1 Introduction

As discussed in depth within the introduction, the treatment of mesothelioma has fallen behind many other solid tumours during the past 2 decades. There has been little improvement in survival outcomes over this period and prognosis remains poor, with average survival between 12 and 18 months and less than 5% living beyond 5 years (320,321). This limited clinical progress is consistent with the fact that treatment has remained unaltered since the 2003 phase III trial comparing pemetrexed and cisplatin, to cisplatin alone. Combination treatment extended survival by 2.8 months and this was established as the gold standard medical treatment for mesothelioma (111). Although a modest benefit, this has been the largest increase in survival outcomes seen in almost 15 years of clinical trials. The VEGF antibody, Bevacizumab, is the only drug during this period to have demonstrated significant overall survival advantages, with a similar survival benefit of 2.7 months (112); however, it has not been adopted into routine clinical practice in the UK. The poor development in the field of mesothelioma is further emphasized by the significant incremental improvements seen in cancers such as NSCLC and melanoma, brought about through the introduction of targeted therapies (322-324) and checkpoint inhibitors (143,301).

Results from early phase trials examining the efficacy of check-point inhibitors have shown evidence of prolonged survival, with CTLA-4 inhibition alone (136,325), and in combination with PD-1 blockade (139,326). Trials in progress include a phase III trial comparing check point inhibition to current standard of care (ClinicalTrials.gov Identifier: NCT02899299). A further

area being explored extensively in mesothelioma is the engineering of T cell activity through vaccines or by chimeric antigen (CAR) T cell therapy. Targets being explored include mesothelin (327), fibroblast activation protein (FAP) (328), ErbB (329), Wilms Tumour 1 peptide (WT-1) (330), and PD-1 (331). This area is of particular interest due to previous data suggesting that increased neutrophil-to-lymphocyte ratios confer poor prognosis in MPM, highlighting probable T cell dysfunction (185,332). These findings are supported by a recent study examining immune cell infiltrates in a large sample of 302 mesothelioma tumours. Authors concluded that the presence of a lower number of NP57+ neutrophils and FOXP3+ Tregs, and increased numbers of CD4+ infiltrating T cells, were all factors independently associated with improved survival (183). Similar observations in surgical patients, following resection for mesothelioma, suggest that increased numbers of tumour infiltrating CD8+ T cells predict improved clinical outcomes (184). These studies imply that the presence of both an appropriate number of T cells and an environment permitting T cell function are vitally important for an effective immune response against tumour cells.

In addition to the prognostic effects of altered immune profiles, mesothelioma has also been shown to induce populations of myeloid cells with altered functional abilities. Monocytes derived from mesothelioma patients were shown to be incapable of appropriate antigen processing and differentiation (199), in addition to being directed towards TAM differentiation by factors released by mesothelioma including CCL2 and M-CSF (333,334). Tumour associated neutrophils have also been implicated in the pathogenesis of murine mesothelioma, with a pro-tumoural “N2” phenotype being induced by TGF-β (335). N2 neutrophil numbers were shown to increase within tumour tissues as their pro-tumour phenotype develops, with reduction in cytotoxic properties due to reduced TNF-α and H_2O_2

production. However, a mixed picture of cytokine release was detected, with both IL-10 and IL-12 up-regulated. Interestingly, early neutrophil depletion from murine mesothelioma tumour models had no effect on tumour growth, yet depletion of N2 neutrophils slowed growth dramatically, demonstrating their propensity to develop a pro-tumoural effect (245). Highlighted by these studies is the plasticity that neutrophils demonstrate within a tumour environment and the possibility of sub-populations of tumour-induced neutrophils. Available data within this area has been obtained within murine studies, therefore the distinction between tumour induced neutrophils and granulocytic MDSC in human subjects is of interest. There are no current surface markers which clearly differentiate TAN from MDSC; however, Fridlender *et al* recently demonstrated through transcriptomics that normal neutrophils, TAN and G-MDSC display differing mRNA profiles (336). Variations in gene expression related to cytotoxic function, mobilisation, cytokine and chemokine production, and antigen presentation were all demonstrated (336).

The presence of dysfunctioning myeloid populations and immunosuppressive cells is likely to impact on the ability of tumours to achieve robust responses to immunotherapy treatments. This can be highlighted by the demonstration that tumour vaccination using a PD-1 DNA based vaccine led to a reduction in circulating MDSC and enhanced the function of antigen specific CD8+ T cells (331,337). The mechanism leading to an enhanced CD8+ population and associated reduction in MDSC was not elucidated, but the findings demonstrate the complex interaction between systemic and tumour residing immune populations in cancer. Through targeting of both sides of this double-edged sword, the success of cancer immunotherapy may be enhanced.

In view of this breadth of somewhat conflicting data regarding the effect of myeloid populations in mesothelioma, we sought to further assess the presence of immunosuppressive populations in human subjects, with a particular focus on immune-suppressive granulocytes which have received less focus to date. We proposed to identify the predominant tumour induced myeloid populations and to determine their phenotype, function and possible mechanisms of immune suppression utilised in mesothelioma.

3.2 Results

3.2.1 Mesothelioma patients

Between August 2014 and September 2017 patients undergoing diagnostic biopsy or definitive surgery for mesothelioma were consented to take part in this study. Patients were recruited from 2 collaborating sites, Heartlands Hospital, Birmingham, and Glenfield Hospital, Leicester. Of the patients undergoing diagnostic biopsy, 15 of the 49 enrolled patients were later confirmed to have mesothelioma. All 7 patients undergoing resection had a prior confirmed histological diagnosis of mesothelioma. All patients with no histological diagnosis of mesothelioma were excluded from the analysis. From each enrolled patient 40ml of blood was collected, alongside a tumour specimen where possible. For 1 patient, a tumour specimen was collected without a matched blood sample due to difficulties with venepuncture. The median age of this cohort of patients was 71, ranging from 61-83 years and 86.4% were male. 20 patients (90.9%) had a histological diagnosis of epithelioid mesothelioma, 1 (4.5%) biphasic and 1 (4.5%) sarcomatoid. All patients were diagnosed with

pleural mesothelioma. Of those undergoing diagnostic biopsies, all were treatment naive. Two patients (9.1%) had undergone neo-adjuvant chemotherapy prior to surgical resection. A summary of patient characteristics is found in table 3.2.

3.2.2 Healthy samples

Healthy donor blood samples were collected in order to provide comparators to blood samples from patients with mesothelioma. No "healthy" tissue could be obtained as patients with a negative diagnosis for mesothelioma were invariably diagnosed with other pleural conditions such as pleural plaque or pleural infections. Healthy volunteers were recruited from the University of Birmingham. Median age was 33 (range 33-69), with 57.1% male and 42.9% female.

Table 3. 1. Healthy Donor Characteristics

Healthy donor characteristics (n=18)	
Variable	**n (%)**
Age	
Median (range)	33(27-69)
Sex	
Male	8 (57.1)
Female	6 (42.9)

Table 3. 2. Patient Characteristics

Patient characteristics (n=22)	
Variable	**n (%)**
Age	
Median (range)	71 (61-83)
Sex	
Male	19 (86.4)
Female	3 (13.6)
Histology	
Epithelioid	20(90.9)
Biphasic	1 (4.6)
Desmoplastic	0
Sarcomatoid	1 (4.6)
Unknown	0
Site of primary disease	
Pleural	22 (100)
Peritoneal	0
Prior debulking surgery	0
Neoadjuvant chemotherapy	2 (9.1)
Prior immunotherapy*	0

3.2.3 Detection of abnormal frequencies of lymphocytes and myeloid cells in patients with mesothelioma

A primary aim for this study was to determine whether there was a variation in the frequency and characteristics of circulating myeloid cells in patients with mesothelioma and to determine whether these populations could act to suppress T cell function and proliferation. Staining of whole blood revealed that mesothelioma patients consistently displayed reduced percentages of circulating T cells when compared with healthy controls. In patients, mean frequencies of CD3+ lymphocytes, CD4+ lymphocytes and CD8+ lymphocytes were 14%, 16.3% and 12.8%, respectively, compared with 29%, 24.3% and 24.4% in healthy comparators. These findings were highly significant. Statistical analysis of the differences in whole blood cell frequency was performed using a Mann Whitney non-parametric T test (Figure 3.1, A-C). When examining the function of patient T cells, they were found to have reduced proliferative capacity when compared to healthy controls (Figure 3.1, D).

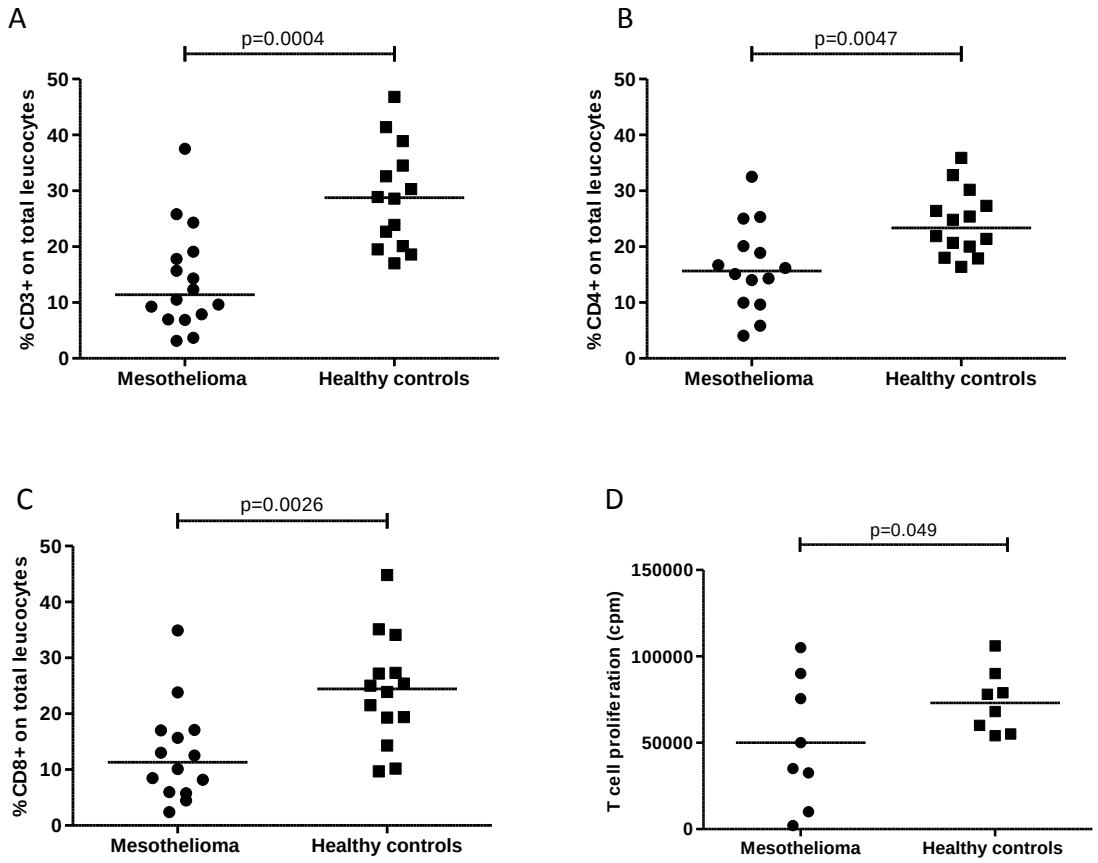

Figure 3. 1 Flow cytometry analysis of whole blood compared to healthy controls

(A-C) Flow cytometry analysis of whole blood from patients with mesothelioma demonstrating T cell surface expression of CD3 (n=16), CD4 (n =14) and CD8 (n=14). Comparative staining was carried out in healthy controls (n=14). Percentage of positive cells within the total leucocyte gate is demonstrated, median percentage is indicated by horizontal lines. (D) Patient (n=8) and healthy (n=8) CD3+ T cells were purified and stimulated with anti-CD3 and anti-CD28 for 4 days. T cell proliferation was determined by thymidine incorporation over 16 hours. Counts per minute (cpm) is proportional to the number of proliferating cells. Statistical analysis has been carried out using a Mann Whitney, non-parametric U test.

Analysis of whole blood myeloid cells was carried out using a pre-determined gating strategy, demonstrated in Figure 3.2 A and B. Consistent with the reduction in T cell frequency, we detected increased percentages of both CD11b+CD14+ monocytes and CD11b+CD15+ granulocytes in whole blood of patients with mesothelioma. These differences again were significant, with average percentages of 5.7% and 50.8% for patient monocytes and granulocytes, respectively, compared to 2.4% and 36.5% in healthy subjects (Figure 3.3, A, B), (analysed by Mann Whitney non-parametric U test). As a result of these alterations of granulocyte percentages, patients demonstrated increased neutrophil lymphocyte ratios (NLR). Increases in NLR have previously been detected in patients with mesothelioma, along with other cancers, and these changes have been associated with both increased stage of disease and poor prognosis (185,186). Patient populations demonstrated ratios of up to 5 times that of healthy donors, with the average ratio of 6.2 compared to 1.5 in healthy comparators ($p=0.0003$) (Figure 3.3, C).

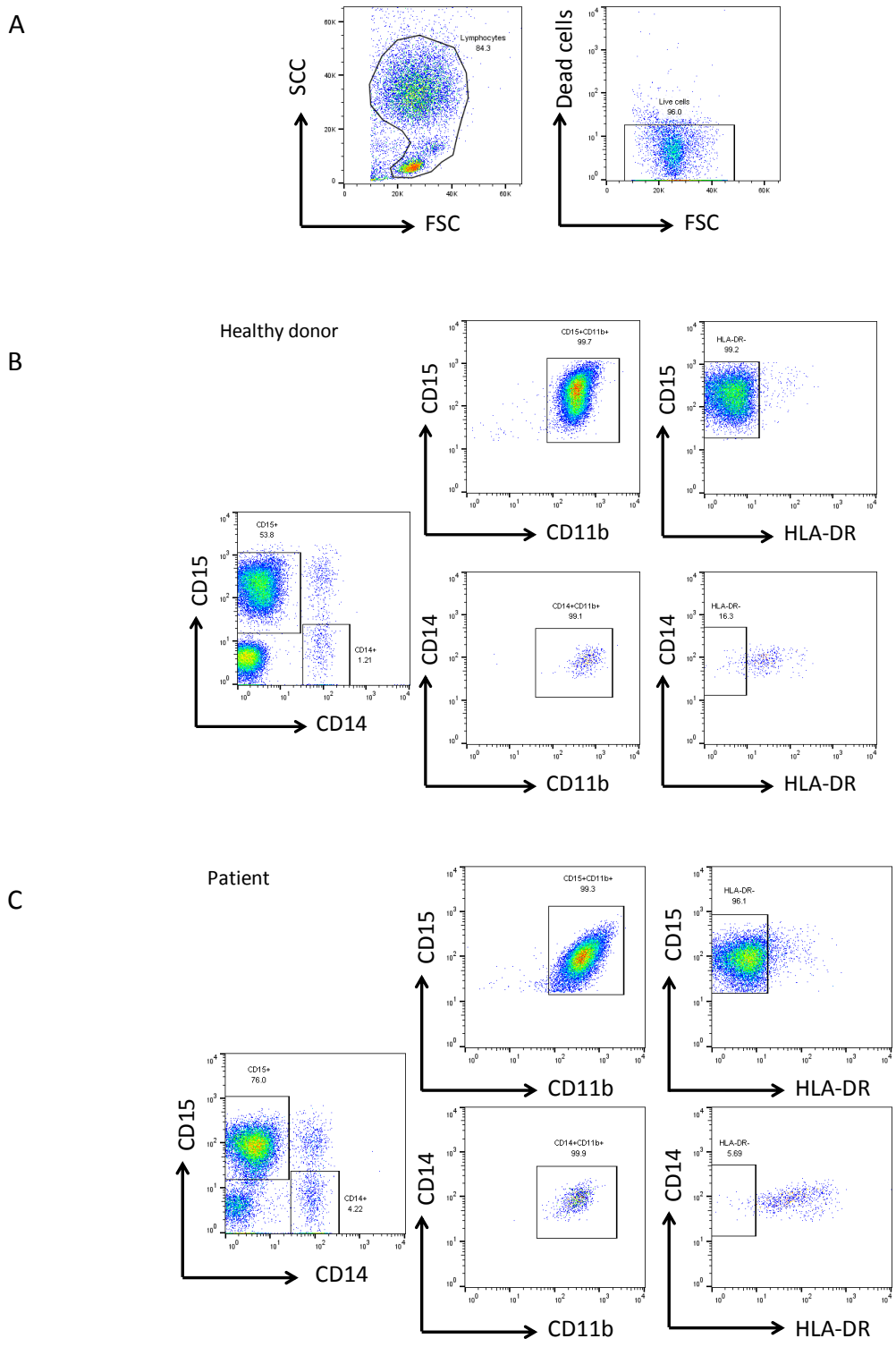

Figure 3. 2. Flow cytometry gating strategy.

(A) Flow cytometry was used to analyse blood and tumour samples. Cells were gated using morphology by forward scatter (FSC) and side scatter (SCC). Dead cells were excluded using the live dead stain Hoechst. (B, C) Cell phenotype was determined using a panel of cell surface markers including CD14, CD15, CD11b and HLA-DR. Representative samples from one healthy donor and one patient sample are shown.

A

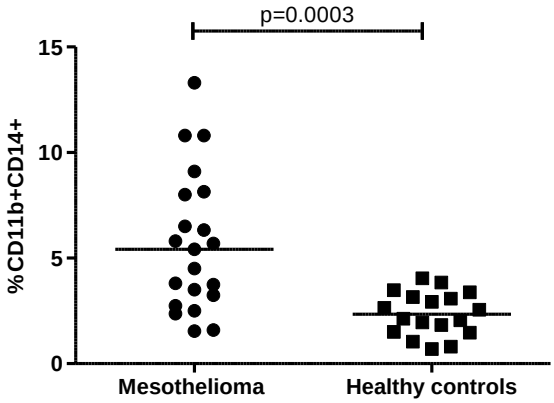

B

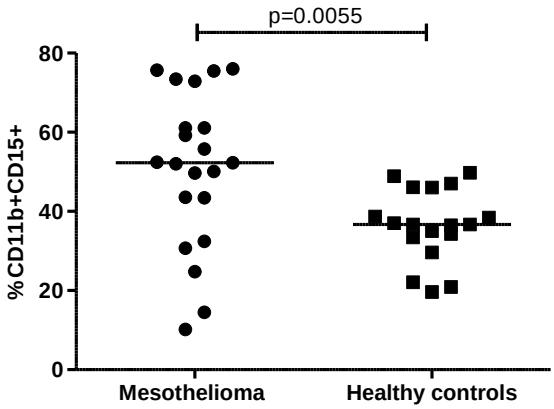

C

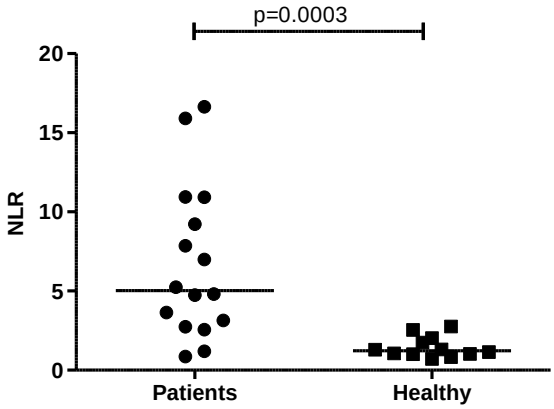

Figure 3. 3. Myeloid populations in mesothelioma patients compared to healthy controls

Whole blood was subjected to surface marker analysis by flow cytometry. Mesothelioma patients (n=21) were analysed alongside healthy controls (n=18). Percentage frequency of the surface markers CD14+ (A) and CD15+ (B) were detected on CD11b+ cells. (C) The Neutrophil Lymphocyte Ratio (NLR) was calculated using frequencies of CD15+ and CD3+ lymphocytes in patient (n=16) and healthy (n=12) samples. Horizontal lines represent median values. Statistical analysis has been carried out using a Mann Whitney, non-parametric U test.

In view of the detection of abnormal frequencies of myeloid cells in patients with mesothelioma, we wished to investigate whether they could be representing myeloid derived suppressor cells (MDSC). MDSC of both granulocytic and monocytic lineage are classically defined as being low density cells, which reside in the mononuclear cell layer following gradient separation using Ficoll or Lymphoprep™. Phenotypically there is still much debate on their preferred classification due to the fact there are no definitive markers. However, MDSC are classically HLA-DR (class II MHC) low or negative (250), therefore low surface HLA-DR expression was used to define MDSC in this setting. Following gradient separation of blood samples, cells were isolated from the low-density interface ("PBMC ring") between Lymphoprep™ and plasma, prior to analysis by flow cytometry.

Within the PBMC ring the percentage of detected CD11b+CD15+ cells was higher in patients compared to healthy controls however, the CD11b+CD14+ population did not differ. Percentages of low density CD11b+CD15+ cells were variable between patients, with a range of 2.8% to 24.9%, compared with 0.6% to 10.3% in healthy donors ($p=0.0011$) (Figure 3.4, A, B). When comparing HLA-DR expression within the PBMC ring there was no significant difference between patients and healthy controls in the monocytic sub-group. Patient granulocytes in the PBMC layer showed lower expression, $p=0.0384$ (Figure 3.4, C, D). In view of the non-significant difference in numbers of PBMC monocytes and lack of differential HLA-DR expression between patient and healthy monocytes, the HLA-DR expression of monocytic cells in whole blood was analysed, to ensure that expression was not being altered by the process of gradient separation. Again, no significant difference in monocyte HLA-DR expression was detected (Figure 3.4, E); this population was therefore not classified as classic monocytic-MDSC. The expression of HLA-DR in the whole blood granulocytic population again

showed lower HLA-DR expression than healthy granulocytes, but this did not reach significance, p=0.0512 (Figure 3.4, F).

As no significant differences in monocyte phenotype were detected, further investigation was focussed on granulocytes. To investigate both high and low density granulocyte populations further, additional markers associated with neutrophil maturation were examined including CD11b, CD16 and CD66b. Expression of CD11b and CD66b on granulocytes is associated with activation, with both acting as adhesion molecules to allow neutrophil migration into sites of inflammation, therefore a reduction may indicate a loss of neutrophil activity. In contrast, prior research has associated the marked loss of CD16 expression with states of acute inflammation and premature bone marrow release (338), in addition to granulocyte activation (235,339).

When these markers were examined in mesothelioma patient samples, greater variability in surface marker expression was seen in granulocytes from patient whole blood, compared with healthy controls, although no significant differences between the two groups were observed. Low density granulocytes showed lower intensity of expression of CD11b, CDD16 and CD66b; however, these differences were non-significant (Figure 3.5, A, B).

Overall, these findings indicated that there was a profoundly altered inflammatory profile in patients with mesothelioma, with reduced T cell frequency and a predominant abnormal population of granulocytes, representing an average of 50.8% of circulating lymphocytes.

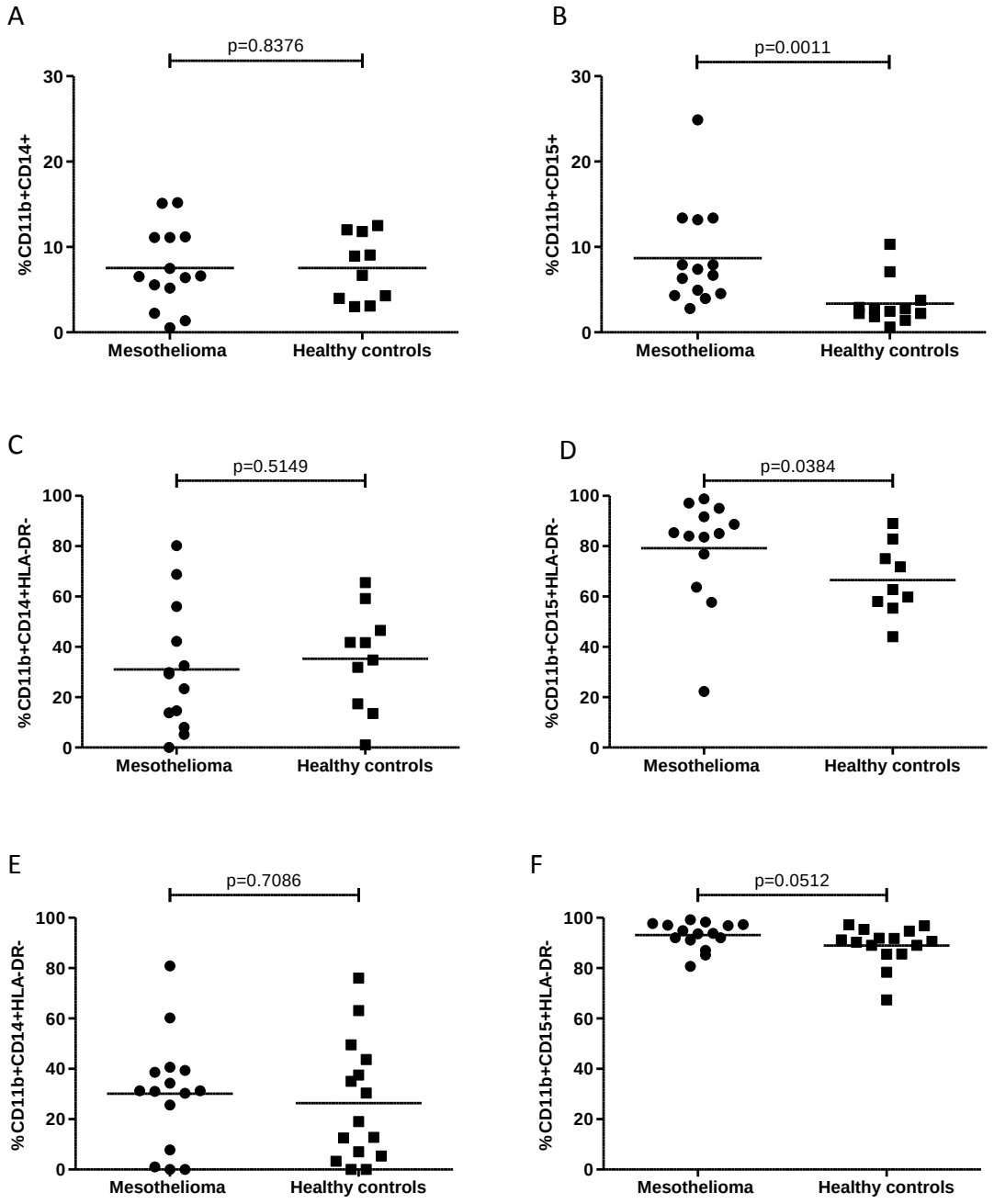

Figure 3. 4. Flow cytometry analysis of myeloid cells within the PBMC layer and whole blood

Gradient separation of whole blood allowed isolation of low density cells within the PBMC layer. Patient (n=14) and healthy (n=10) samples were analysed. (A, B) Flow cytometry analysis of cell surface markers demonstrated frequencies of CD14+CD11b+ monocytic cells and CD15+CD11b+ granulocytes. (C, D) Surface expression of HLA-DR on CD14+CD11b+ and CD15+CD11b+ populations extracted from the PBMC ring are shown. (E, F) Whole blood analysis of HLA-DR expression on CD14+ and CD15+ populations was also performed in patient (n=15) and healthy (n=15) samples. Horizontal line represents median frequency. Statistical analysis was carried out using the Mann Whitney non-parametric U test.

A

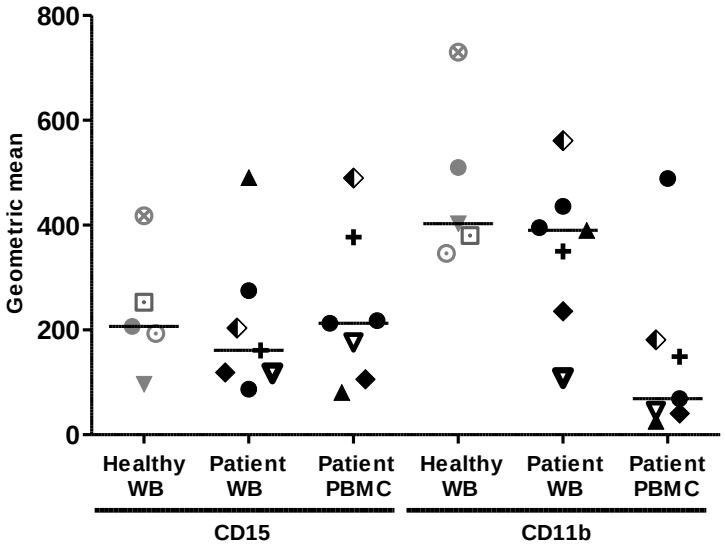

B

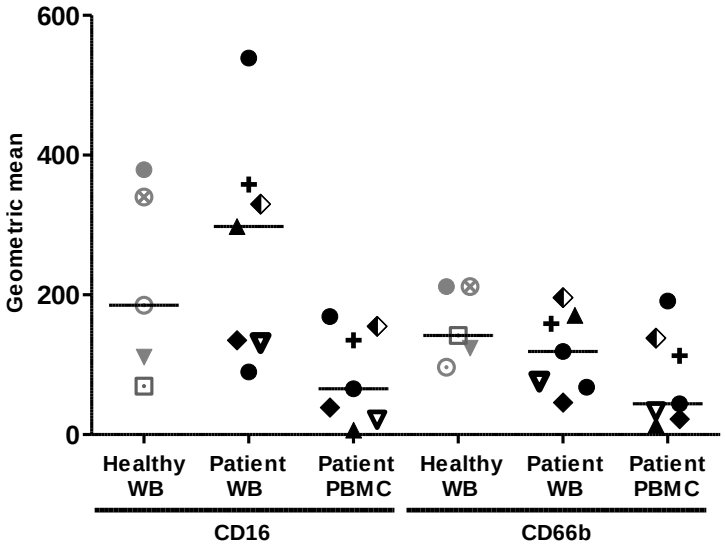

Figure 3. 5. Surface marker expression profiles on granulocytes

Further analysis of granulocyte surface marker expression was carried out by flow cytometry. Differential expression of CD15 and CD11b (A), and CD66b and CD16 (B) were analysed on healthy (n=5) and patient (n=7) whole blood samples and patient PBMC (n=7). Surface expression is represented as geometric mean with horizontal line demonstrating median expression. Statistical analysis of differences between groups was carried out using the Kruskal-Wallis ANOVA, with Dunn's correction for multiple comparisons. No statistically significant differences were observed.

3.2.4 Detection of tumour infiltrating lymphocytes

Following classification of myeloid cells and lymphocytes within the blood of mesothelioma patients, we wished to assess the presence of tumour infiltrating immune cells. Following digestion of fresh tissue samples, cells were stained by flow cytometry using the cell surface marker panel described for blood. In addition, to corroborate our findings 38 mesothelioma tissue sections were stained by IHC, for the presence of tumour infiltrating myeloid cells.

Digested tumour tissue was investigated for the presence of infiltrating CD14+ monocytes, CD15+ granulocytes and CD3+ T cells. All 3 subgroups were found within mesothelioma tumour tissues. Displayed as a percentage of live cells following tumour digestion, CD3+ lymphocytes were the most predominant population (average 20.7%), with an average of 8.8% of CD15+ granulocytes and 3.9% CD14+ monocytes (Figure 3.6, A). In a small population of tumour samples, more detailed analysis of tumour infiltrating myeloid cells was carried out, to allow comparison with circulating cells within whole blood. This revealed numbers of HLA-DR negative tumour infiltrating myeloid cells were reduced in monocytic and granulocytic populations (Figure 3.6 A, B).

The presence of immune check point markers was also investigated within tumour infiltrating lymphocytes. The relationship between immunosuppressive cells including DC, TAM, TAN and MDSC and checkpoint activation in T cells has been widely studied, producing evidence that immunosuppressive populations utilise this mechanism to reduce T cell immune responses (212). Obermajer and colleagues demonstrated that PD-L1 expression was enhanced on a population of immature DC, and MDSC have also been shown to the enhanced PD-L1 expression on pancreatic tumour cells, leading to PD-1:PD-L1 signalling and T cell inhibition (340). In view of the limited information on PD-L1 status and function in myeloid populations

in mesothelioma, this was included an additional aspect of phenotype analysis. In circulating and tumour residing myeloid cells the expression of PD-L1 was greater on CD14+ populations than CD15+. Median expression on circulating cells was 16.8% on CD14+ and 7.8% on CD15+. Upon tumour residing myeloid cells median expression was 35.3% and 10.1%, respectively. Healthy populations showed median PD-L1 expression of 25.4% on CD14+ populations and 12.9% on CD15+ granulocytes (Figure 3.6 C, D). Although lower PD-L1 expression was observed in circulating populations, there were no significant differences between healthy controls, patient circulating myeloid cells or tumour infiltrating myeloid cells. In contrast, striking differences were observed in the expression of PD-1 on tumour infiltrating CD3+ T cells, with PD-1 expression within the tumour up to 5 times higher than that of peripheral T cells (Figure 3.6, E). This finding was statistically significant with a p value of <0.05 (analysis performed using the Kruskal-Wallis test, with correction using Dunn's multiple comparisons). This finding may imply that T cells within the tumour microenvironment are reaching a state of exhaustion, with signalling via PD-L1 on myeloid populations or tumour cells, leading to inactivation and dysfunction.

To further confirm the finding of tumour infiltrating myeloid cells, 38 human mesothelioma tumour sections were analysed by immunohistochemistry. Sections were stained to detect CD15-positive, infiltrating myeloid cells, within a clinical laboratory at Heartlands Hospital. The degree of CD15 positive staining varied between patients. There was also marked intra-tumoural variation in the distribution of CD15 positive cells. Sections were reviewed with the assistance of a Consultant Histopathologist to confirm the findings. The density and distribution of positive cells was assessed, and staining was classified into categories as abundant, moderate or sparse. Categorisation was based on numbers of cells within 5 high

power fields. Abundant staining was represented by greater than 25 cells, moderate between 10 and 25 and sparse, less than 10. A representation of sections within each staining category is demonstrated in Figure 3.7, A. Overall, 35 sections could be assessed, of these 5 showed abundant staining, 13 stained moderately and 17 stained sparsely (Figure 3.7, B). Figure 3.7, C, demonstrates sections of epithelioid mesothelioma at high magnification. Within these images, CD15 positive migratory cells are observed. The presence of polylobated nuclei support neutrophil morphology.

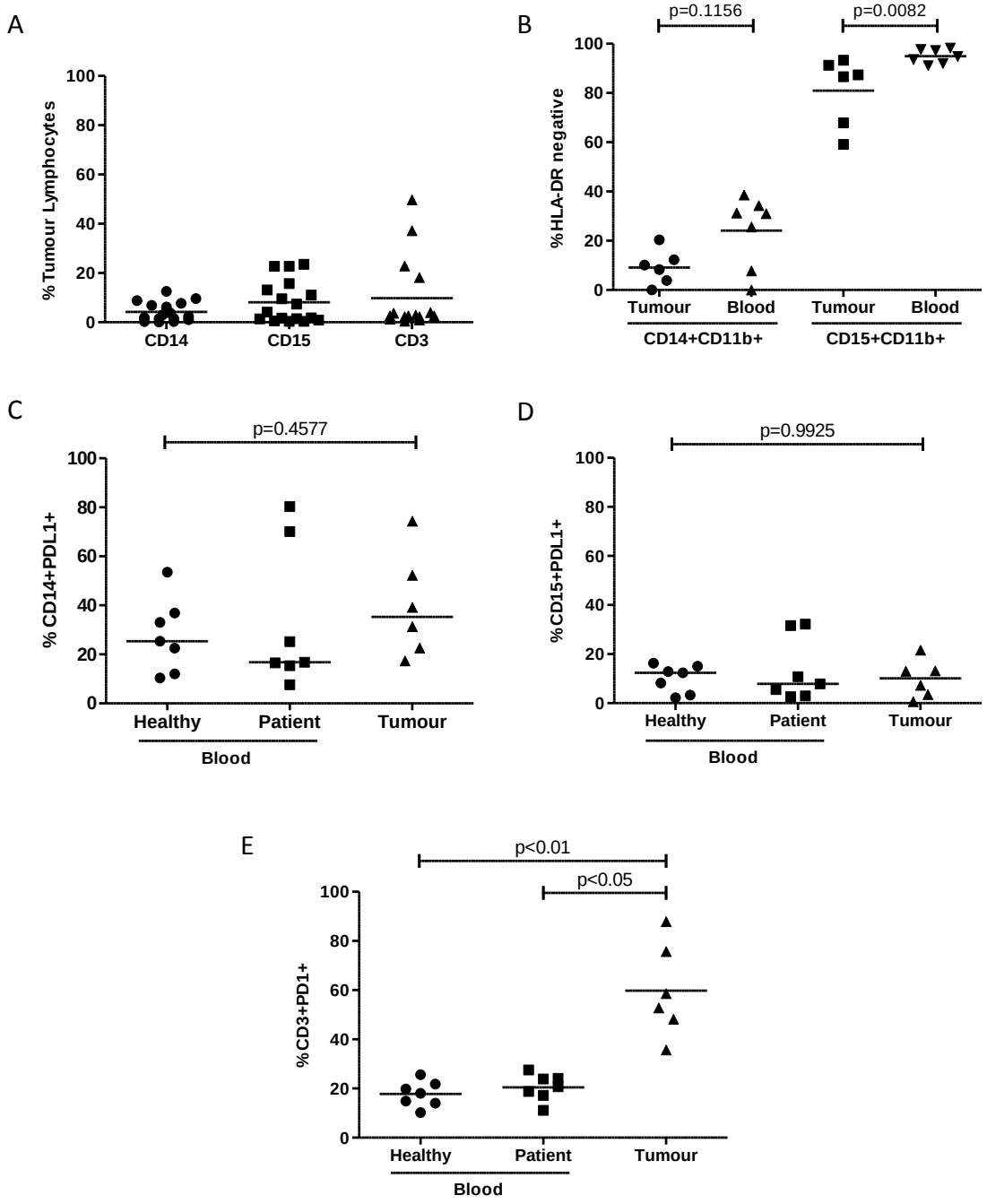

Figure 3. 6. Tumour infiltrating immune cells in mesothelioma.

Analysis of tumour infiltrating immune cells was carried out by flow cytometry. (A) Following tumour tissue digestion, surface marker expression of CD14, CD15 and CD3 was assessed on CD45+ cells. (B)Expression of HLA-DR was assessed on a subset of samples (n=6), with comparison of expression between blood and tumour specimens carried out. (C, D) PD-L1 surface expression was assessed on a subgroup of CD14 and CD15 positive cells (n=6).(E) PD-1 surface expression was assessed on CD3+ cells (n=6). Horizontal lines represent median values. Statistical analysis between 2 groups was carried out using the Mann Whitney non-parametric U test. The Kruskal-Wallis test was used to compare multiple groups, with Dunn's post-test correction.

A

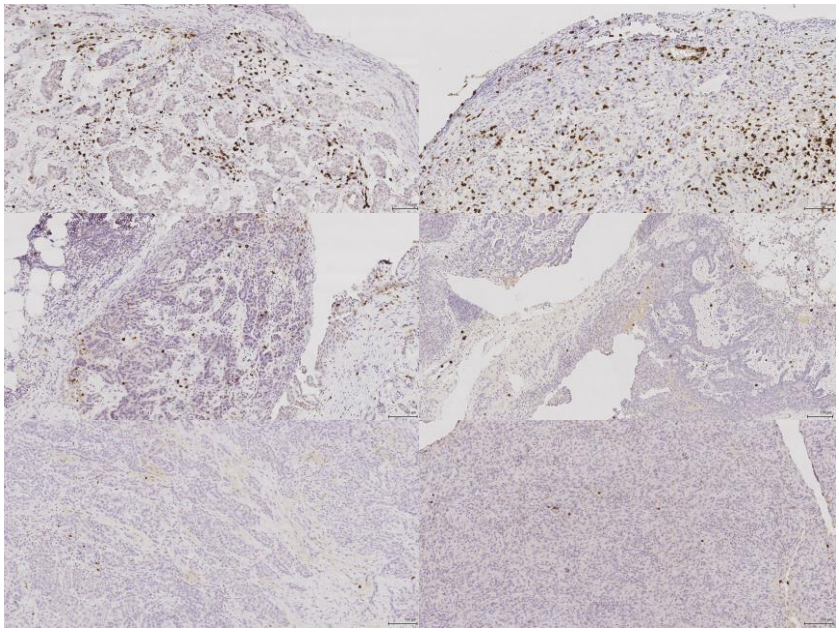

B

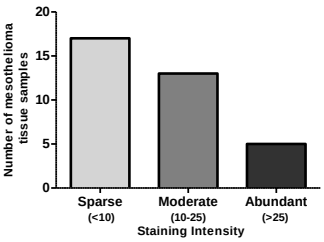

C

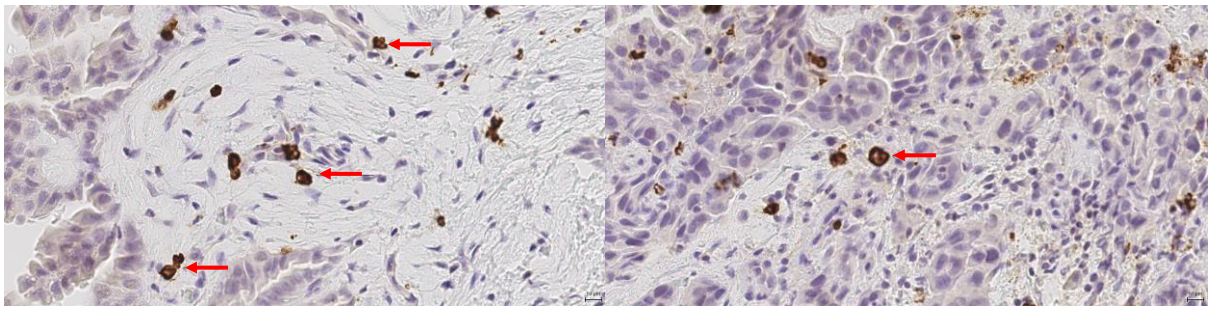

Figure 3. 7. Tumour infiltrating granulocytes demonstrated by IHC

Immunohistochemical staining was carried out on 38 mesothelioma tumour samples to detect infiltrating CD15+ cells. (A) Brown cytoplasmic and membranous staining shows CD15 positive cells. Staining was detected within tumour stroma and tumour tissue. Samples were reviewed and staining classified as abundant (top 2 images), moderate (middle 2 images) or sparse (bottom 2 images). Images taken at 10x magnification. (B) Following quantification staining was sparse in 17 specimens, moderate in 13 and abundant in 5. (C) High power magnification views of epithelioid malignant mesothelioma depicting small numbers of individually disposed CD15-positive migratory cells, mostly occupying the interstitium. These possess polylobated nuclei stained in negative relief, contrasted against brown cytoplasmic & membranous immunoperoxidase positivity, supportive of neutrophil polymorphs. Images taken at 40x magnification.

3.2.5 Granulocytes from mesothelioma patients release reactive oxygen species

In the first part of this chapter increased frequencies of circulating granulocytic cells were detected in patients with mesothelioma, with resultant increased NLR, in addition to evidence of tumour infiltrating granulocytes. We therefore wished to assess whether these populations of CD15+ granulocytes were functionally diverse when compared to CD15+ granulocytes from healthy controls, and to determine whether this abnormal population was capable of impairing T cell function.

Granulocytes have previously been shown to lead to T cell dysfunction through multiple mechanisms including enhanced arginase activity (244,341), release of immunosuppressive cytokines (234) and the release of reactive nitrogen and oxygen species (239). Our primary investigation was therefore focussed on these established mechanisms. Granulocytes were harvested from the surface of the red blood cell pellet following centrifugation and purified using magnetic bead isolation. Between 10 and 20 $x10^6$granulocytes were isolated from each 50ml sample. During counting viability was assessed and further experiments carried out if viability was over 80%. For analysis by PCR, $10x10^6$ granulocytes were used for RNA extraction. Through qPCR the activity of arginase I and iNOS in patient granulocytes was investigated. No significant differences in iNOS or arginase I expression were detected when comparing patient granulocytes to healthy equivalents (Figure 3.8, A). Following granulocyte isolation, the capacity to release ROS was assessed using the Amplex Red Hydrogen Peroxide Assay, which enables detection and quantification of hydrogen peroxide (H_2O_2) release. Isolated cells were counted to assess viability and $1.5x10^4$ plated per well. Granulocytes isolated from mesothelioma patients produced significantly higher concentrations of H_2O_2 when compared to granulocytes obtained from healthy donors (Figure 3.8, B). This data was subsequently

extended through collaboration with a research group within the National Institute of Health (NIH), USA, and can be reviewed in a collaborative publication (342).

To confirm that ROS production by granulocytes could be stimulated by mesothelioma tumours, in-vitro experiments were carried out using tumour conditioned media derived from patient tumour specimens and mesothelioma cell lines. Purified healthy CD15+ granulocytes were cultured in the presence of 25% tumour supernatant for 24 hours, with a control population cultured in the presence of complete RPMI alone. The production of ROS was then assessed by flow cytometry using H_2DCFDA. This compound is capable of intracellular ROS detection due to conversion of non-fluorescent H_2DCFDA to highly fluorescent DCF upon cleavage of acetate groups by oxidation. Following culture in the presence of tumour derived supernatants, enhanced ROS production was detected by flow cytometry, when compared to unexposed granulocytes (Figure 3.8 C, D). To confirm ROS production, further experiments were carried out to quantify the release of H_2O_2 species released in culture using the Amplex Red Hydrogen Peroxide Assay. Cell line and tumour supernatants led to enhanced detection of H_2O_2 in culture (Figure 3.8, E).

The mechanism resulting in enhanced ROS production was explored through investigation of nicotinamide adenine dinucleotide phosphate (NADPH) oxidase activity, known to be the enzyme responsible for mediating ROS production within granulocytes. Upon activation, NADPH catalyses the production of the superoxide anion (O^-_2) within granulocytes, leading to formation of reactive oxygen species (343). The NADPH enzyme is made up of 2 transmembrane components, p22phox and gp91phox/NOX2, along with three cytosolic proteins and a GTPase (344). Up-regulation of all components can be used to study the status of NADPH activity therefore, the activity of the transmembrane component NOX2 was

examined by qPCR. Consistent with this mechanism, up regulation of NOX2, in conjunction with ROS production, was seen in neutrophils cultured in the presence of mesothelioma cell line supernatants. One representative experiment including cells treated with 3 different mesothelioma supernatants is shown (Figure 3.8, F).

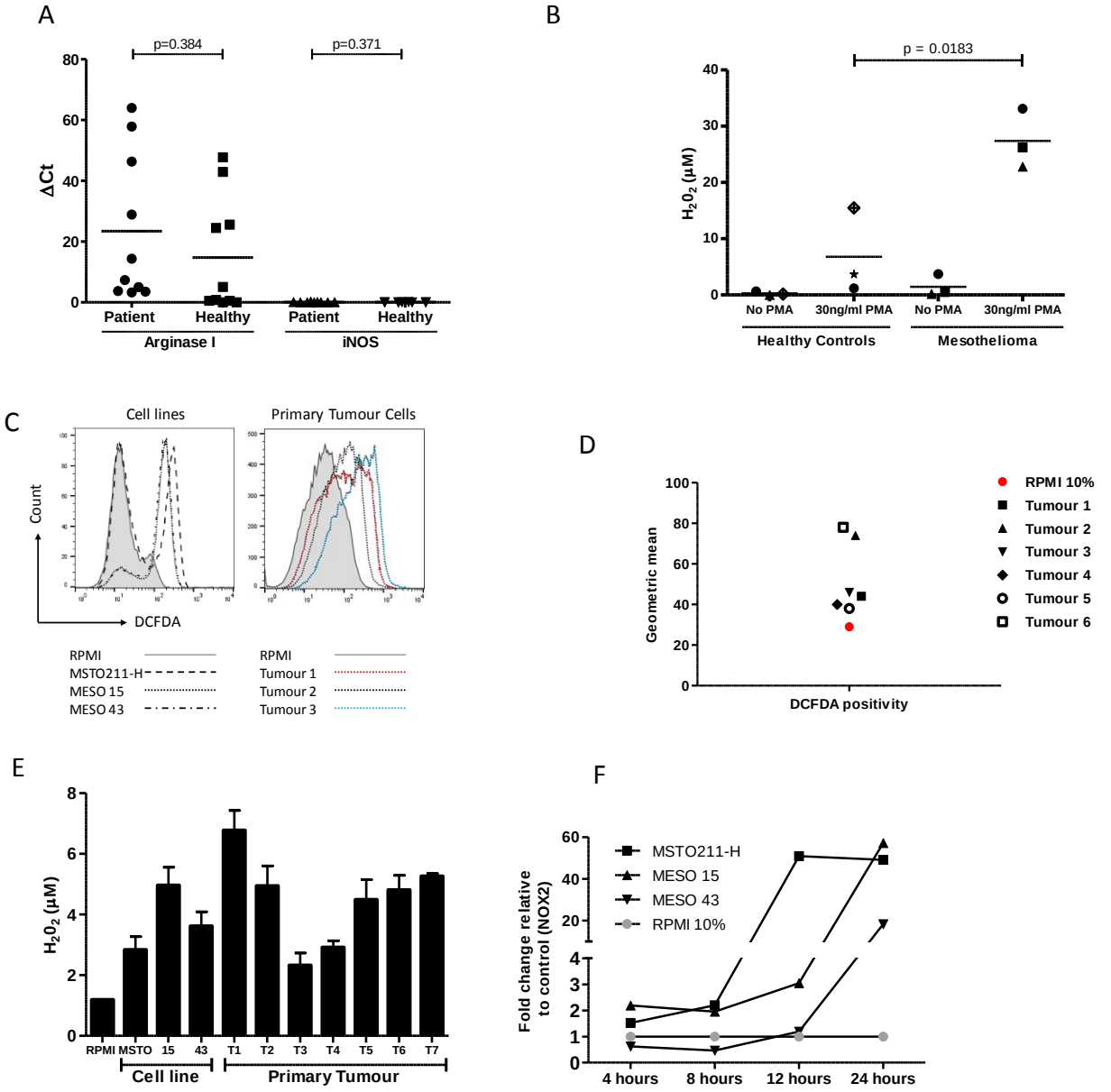

Figure 3. 8. Granulocyte expression of immune mediators Arginine I, iNOS and reactive oxygen species (ROS).

(A) qPCR was carried out on granulocytes extracted from mesothelioma patients (n= 10) and healthy controls (n=10) to determine mRNA expression of Arginase I and iNOS. ΔCt values demonstrate expression relative to internal housekeeping control. (B) Freshly isolated granulocytes from mesothelioma patients (n=3) and healthy controls (n=3) were tested for baseline release of hydrogen peroxide (H2O2) using the Amplex® Red Assay, pre- and post-PMA stimulation. Statistical analysis was carried out using an unpaired t-test. (C) Healthy granulocytes were exposed to supernatants conditioned with 3 mesothelioma tumour cell lines and tumour from 3 donors. ROS were detected at 24 hours through flow cytometry by DCFDA oxidation. Healthy granulocytes cultured in RPMI 10% were used as control. (D) Healthy granulocytes were exposed to supernatants conditioned by tumour from 6 donors. The geometric mean of DCFDA oxidation, detected at 24 hours through flow cytometry, shows an increase in ROS in TCM exposed cells. Healthy granulocytes cultured in RPMI 10% were used as control. (E) ROS production was quantified through the measurement of H2O2 within the Amplex® Red Assay. (F) Granulocytes were extracted from cultures at serial timepoints for assessment of NADPH enzyme activity, determined by NOX2 detection. NOX2 expression is expressed as fold change relative to RPMI control. 1 of 3 replicate experiments displayed.

3.2.6 Granulocytes from patients with mesothelioma are suppressive to T cell function

Following demonstration of enhanced ROS production in granulocytes exposed to mesothelioma, their ability to impair T cell function was assessed. Granulocytes were isolated from blood obtained from mesothelioma patients and healthy donors as described above. CD15+ populations were also extracted from digested tumour specimens. Due to the composition of digested tumour specimens, single cell sorting was chosen as the mechanism to purify myeloid populations. This was achieved through fluorescent labelling of the populations of interest using anti-CD15 antibodies.

The effect on T cell function was measured through T cell suppression assays. Assays were performed in 96 well plates by plating decreasing concentrations of granulocytes in the presence of stimulated allogeneic T cells. A representative single sample suppression assay is shown in Figure 3.9 A. Ratios of T cells to granulocytes of 1:1 to 1:0.125 were used in all assays in order to examine the potency of T cell suppression. The ratio of 1:0.5 was chosen for statistical analysis as a 1:1 ratio of T cell: myeloid cell interaction was not deemed to be a physiological representation. A reduction in T cell proliferation was induced by both low density and high density CD15+ granulocytes however, the suppression observed was significant with CD15+ granulocytes isolated from the high density compartment, with significant suppression occurring at the ratio of 1:0.5 (2 T cells to 1 myeloid cell), with a p value of 0.0195 (analysed using the non-parametric Mann Whitney U test). When examining CD15+ populations extracted from tumour tissue, suppressive activity was also observed, with an average reduction in T cell proliferation of 42% (Figure 3.9, B). There appeared to be a broad variation in the suppressive activity in both blood and tumour derived cells which

could not be explained through observations of increased circulating myeloid cell number or by cell phenotype, specifically, suppression did not correlate with higher numbers of HLA-DR negative circulating CD15+ cells. There was no correlation observed in the subsets examined from blood or tumour infiltrating cells (Figure 3.9, C).

To further corroborate these findings, in-vitro experiments were again carried out using tumour derived supernatants. Granulocytes cultured in the presence of tumour conditioned supernatants showed strong suppressive activity against T cell proliferation. In contrast, granulocytes cultured in complete media (R10%), were not capable of T cell suppression (Figure 3.10, A).

In order to test the hypothesis that ROS production by granulocytes was the mechanism leading to T cell dysfunction, the ROS scavenger N-acetylcysteine (NAC) was added to proliferation experiments. The addition of this compound to proliferation assays containing high density granulocytes led to rescued T cell proliferation, implying that the release of ROS could be the mechanism behind T cell suppression in this setting (Figure 3.10, B, C).

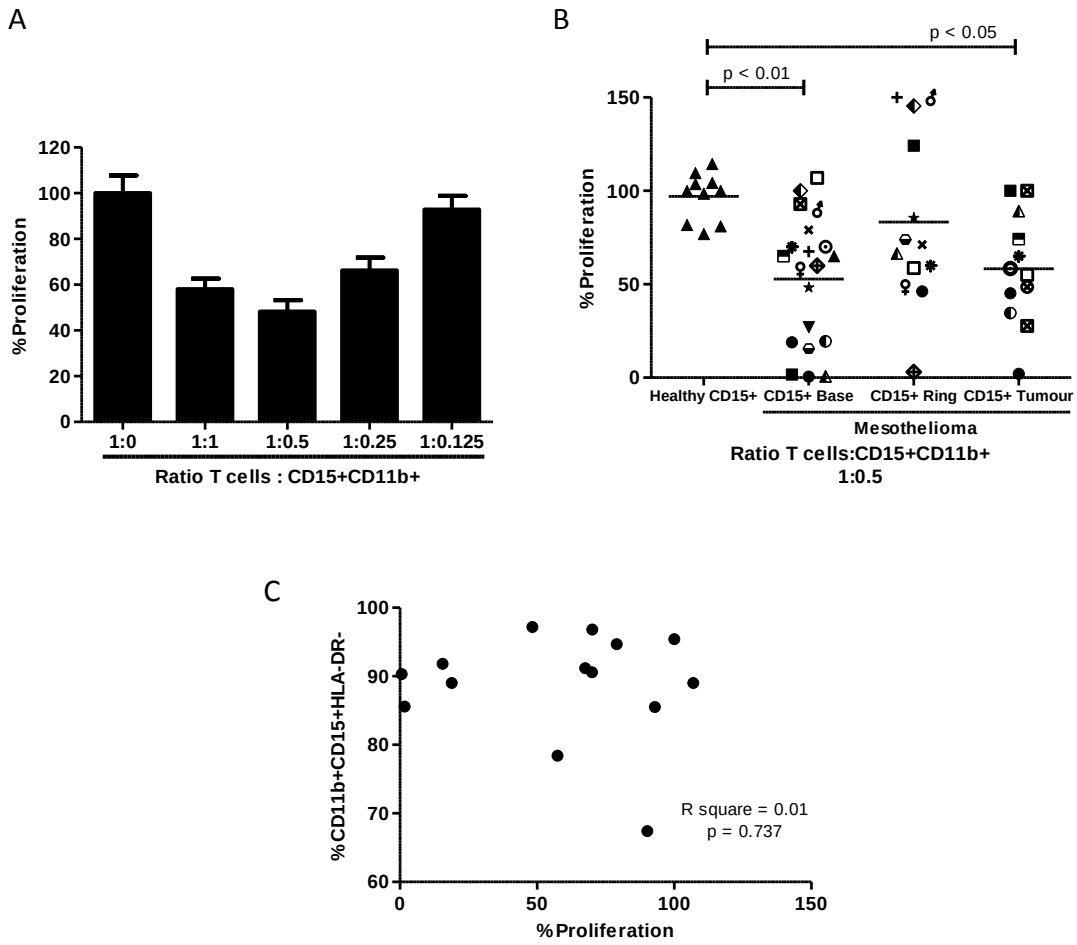

Figure 3. 9. Assessment of the impact of CD15+ granulocytes on T cell proliferation

CD15+ cells isolated from patient blood (low density n=13, high density n=20) and tumour (n=12) were plated in proliferation assays at decreasing concentrations alongside allogeneic T cells to assess potency of suppression. Healthy CD15+ cells (high density, n=10) were used as an experimental control. (A) Representative experiment demonstrating all concentrations plated. A concentration of 1:0.5 (T cell: CD15+ granulocyte) was chosen in group analysis. (B) Group analysis of T cell proliferation assays. Proliferation was determined by thymidine incorporation and is expressed relative to T cell control. Statistical analysis was performed using the Kruskal-Wallis test, with Dunn's correction for multiple comparisons. (C) Expression of the surface marker HLA-DR on CD15+ cells was examined to determine any correlation with T cell suppression.

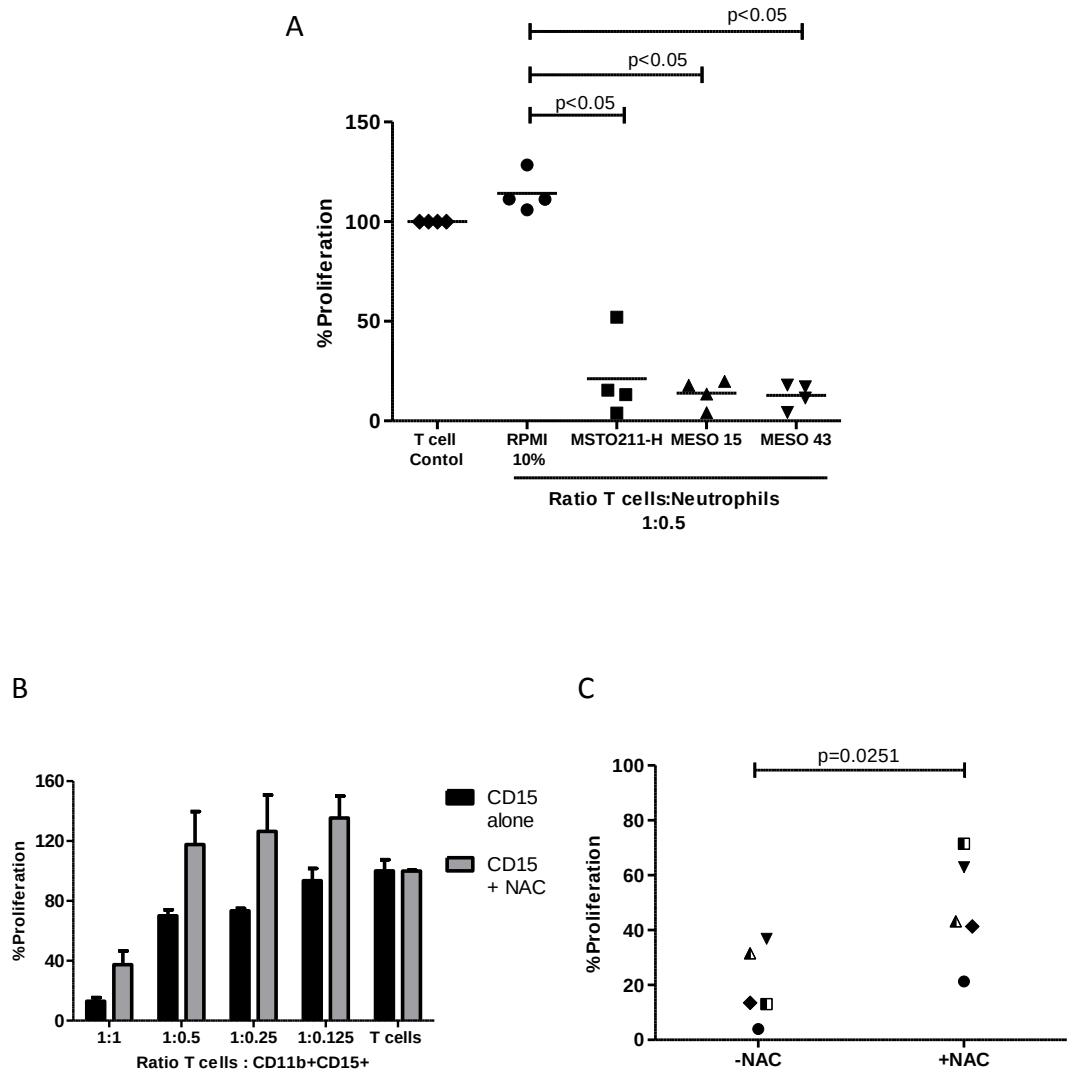

Figure 3. 10. The effect of N-acetyl cysteine on T cell proliferation

(A) Healthy granulocytes were cultured in the presence of tumour conditioned media from 3 mesothelioma cell lines for 24 hours, prior to plating within T cell proliferation assays. Granulocytes cultured in RPMI 10% for 24 hours were used as a control. T cell proliferation was determined by thymidine incorporation and is expressed relative to T cells alone (control). Four replicate experiments are shown. Statistical analysis was performed using the Kruskal-Wallis test with Dunn's correction for multiple comparisons. (B) The ROS scavenger N-acetyl cysteine was added to T cell proliferation assays to determine the effect of ROS on T cell proliferation. One representative experiment demonstrates the effect of NAC at all T cell: granulocyte concentrations. (C) Five replicate experiments at the ratio 1:0.5 (T cell: Granulocyte), demonstrate proliferation relative to T cell control, with and without the addition of NAC. Statistical analysis was performed using a paired T test.

3.2.7 Production of an immunosuppressive environment by mesothelioma

As we successfully demonstrated that mesothelioma supernatants were able to drive ROS production by granulocytes, we went on to establish what factors within mesothelioma were responsible for this polarisation. The fact that supernatants alone were able to polarise granulocytes confirmed that this mechanism was not contact dependent. It was therefore likely that the nature of this crosstalk was related to a factor released into the micro-environment. To further determine the nature of this factor, mesothelioma cell line supernatants were boiled to denature all proteins and identical suppression experiments were carried out. These experiments clearly showed that granulocytes cultured in the presence of boiled supernatants completely lost their ability to suppress T cell proliferation (Figure 3.11, A). This is consistent with the presence of a soluble protein released by mesothelioma cell lines. ELISAs were performed to detect common proteins which may be implicated in immune modulation. This established that the microenvironment of mesothelioma was rich in cytokines capable of neutrophil attraction and activation such as IL-8 and VEGF (345,346), along with the immune modulatory cytokines GMCSF, GCSF, IL-6 and PGE2. Soluble mesothelin, which has been implicated in the polarisation of tumour infiltrating macrophages (347), was also detectable in a number of supernatants (Figure 3.11, B). Within patient plasma raised concentrations of mesothelin, IL-6 and VEGF were detected however, plasma GMCSF was not detected (Figure 3.11, C). Further neutrophil associated chemokines GROα and Midkine were also detected in a broader chemokine array examining cell line supernatants only. Although these chemotactic factors are not directly implicated in the activation of granulocytes and ROS release, the presence of cytokines with a strong role in chemotaxis of granulocytes supports the hypothesis that this population of cells has a

significant role in the pathogenesis of mesothelioma induced immune modulation (348,349) (Figure 3.12, A-C).

A

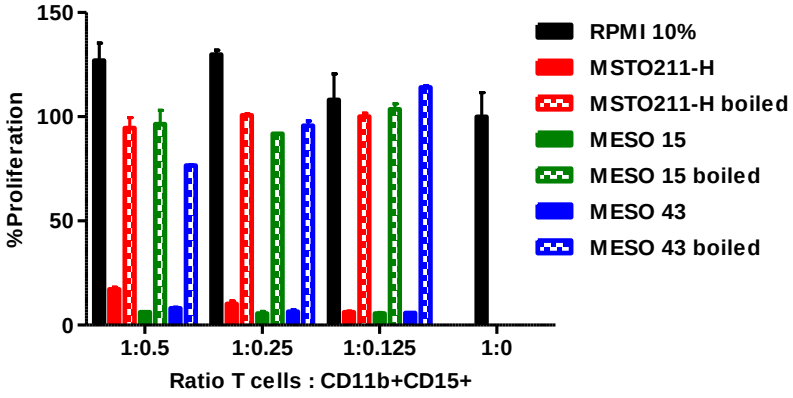

B

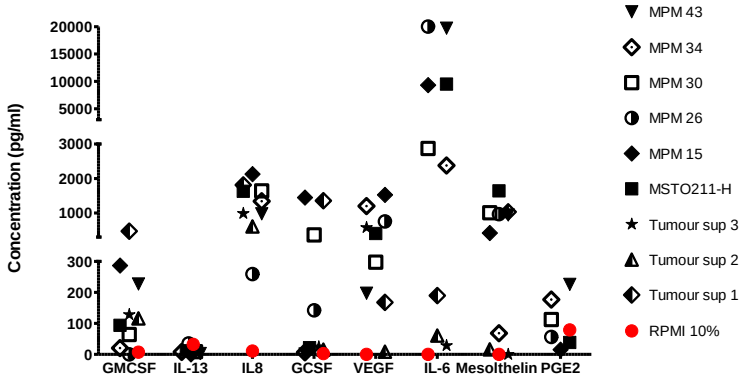

C

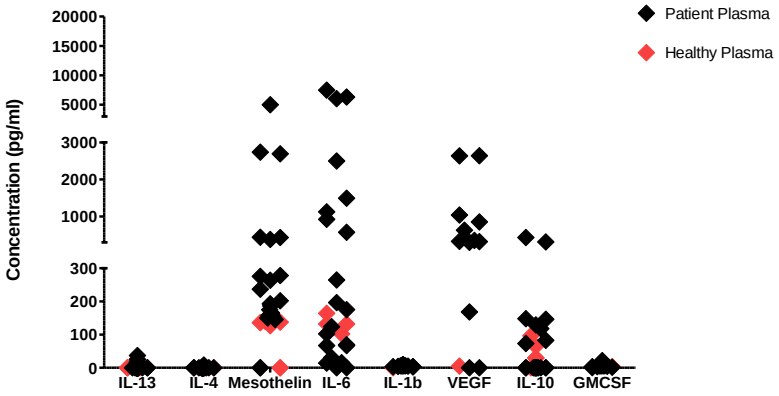

Figure 3. 11. Cytokine profiles within mesothelioma supernatants

(A) Granulocytes were cultured in the presence of fresh and boiled tumour conditioned media (TCM), obtained from three mesothelioma cell lines. Granulocytes from each condition were then used within T cell suppression assays to assess whether the denaturing of proteins altered the effects of TCM (one of 3 representative experiments shown). Improved T cell proliferation was observed when granulocytes were cultured in the presence of boiled TCM. (B) Tumour (n=3) and cell line (n=6) supernatants were screened for the presence of cytokines GMCSF, IL-13, IL-8, GCSF, VEGF, IL-6, mesothelin by individual ELISAs. (C) Patient (n=23) and healthy donor (n=5) plasma samples were screened for the presence of IL-13, IL-4, Mesothelin, IL-6, IL-1β, VEGF, IL-10 and GMCSF using individual ELISAs.

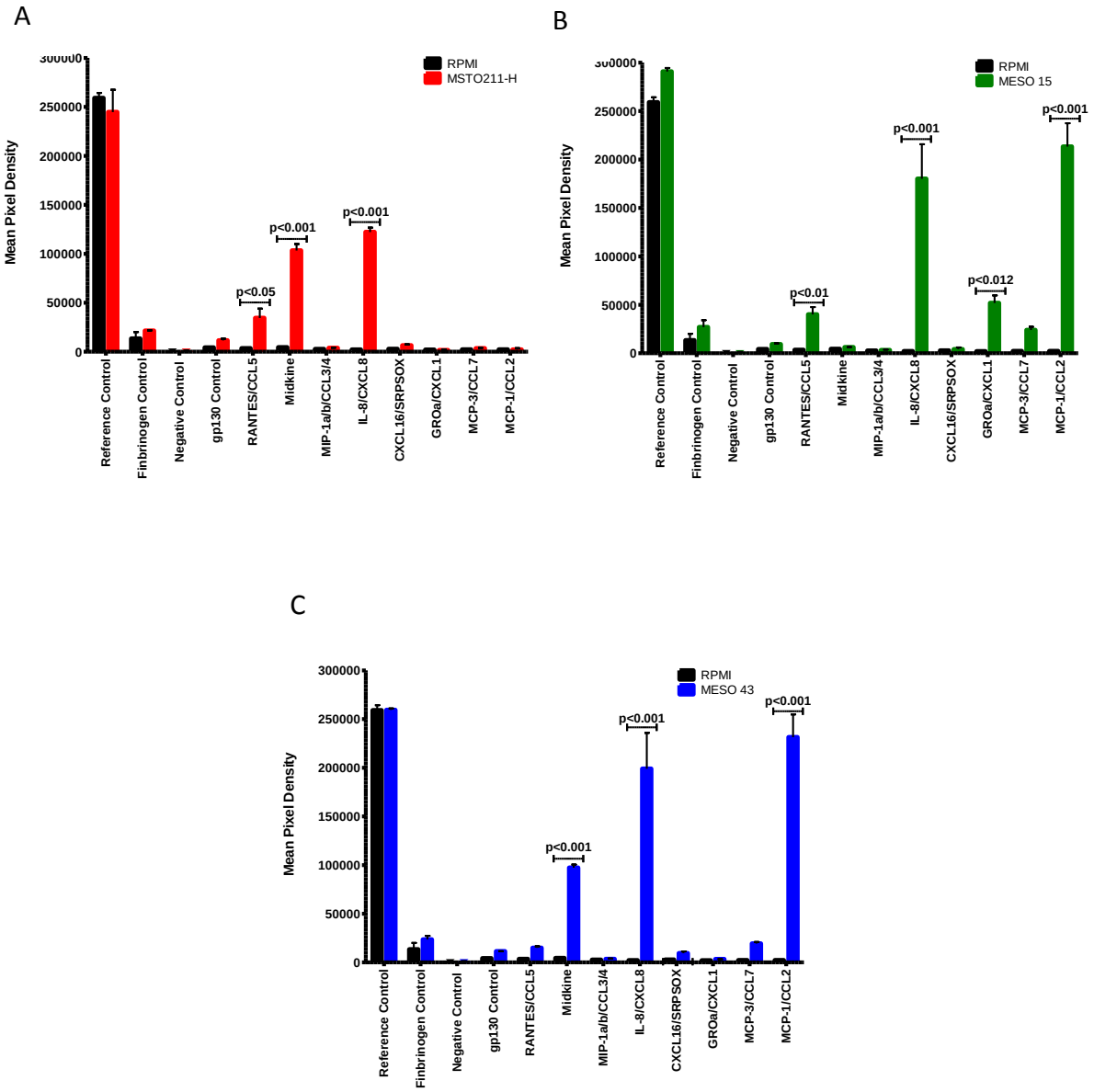

Figure 3. 12. Inflammatory mediators detected in mesothelioma supernatants

Tumour conditioned media from 3 cell lines (MSTO211-H (A), MES0-15 (B) and MESO-43 (C)) were further analysed using a human chemokine array. Following extraction from culture, TCM was incubated with the array membrane as per the manufacturer instructions. Chemokines were detected in duplicate. RPMI 10% was incubated with a separate membrane alongside TCM as a control. Following membrane development, pixel densities were obtained, and statistical analysis performed using a two-way ANOVA, with Bonferroni post-tests to correct for multiple analyses. Significant results are demonstrated, with relevant p values shown.

We then investigated whether any of the identified cytokines were capable of enhancing ROS production to the same degree as mesothelioma supernatants. Healthy CD15+ granulocytes were purified and cultured in the presence of varied concentrations of IL-6, VEGF, GCSF, GMCSF, PGE2 and IL-8. For all cytokines, concentrations varying from 100pg/ml to 1ng/ml were tested, with IL-6 and IL-8 tested at 2ng/ml and 5ng/ml in addition, due to higher detected levels of cytokines within mesothelioma supernatants. Of all tested cytokines GMCSF led to the highest increase in ROS production, comparable to tumour supernatants, and consistently enhanced ROS when tested at concentrations from 2ng/ml to 100pg/ml (Figure 3.13, A-C). In order to determine whether GMCSF was responsible for the enhanced ROS production in mesothelioma tumour exposed granulocytes, supernatants were cultured for 6 hours in the presence of an anti-GMCSF neutralising antibody. Treated supernatants were then added to granulocytes in culture for 24 hours, prior to detection of ROS, as described above. Treatment with an anti-GMCSF antibody led to a reduction in ROS production, which when analysed using the Wilcoxon matched pairs rank test showed a significant reduction ($p=0.0313$) (Figure 3.14, A, B). Quantification of released H_2O_2 species supported these findings, with reduction in granulocyte released H_2O_2 in the presence of the anti-GMCSF antibody (Figure 3.14, C).

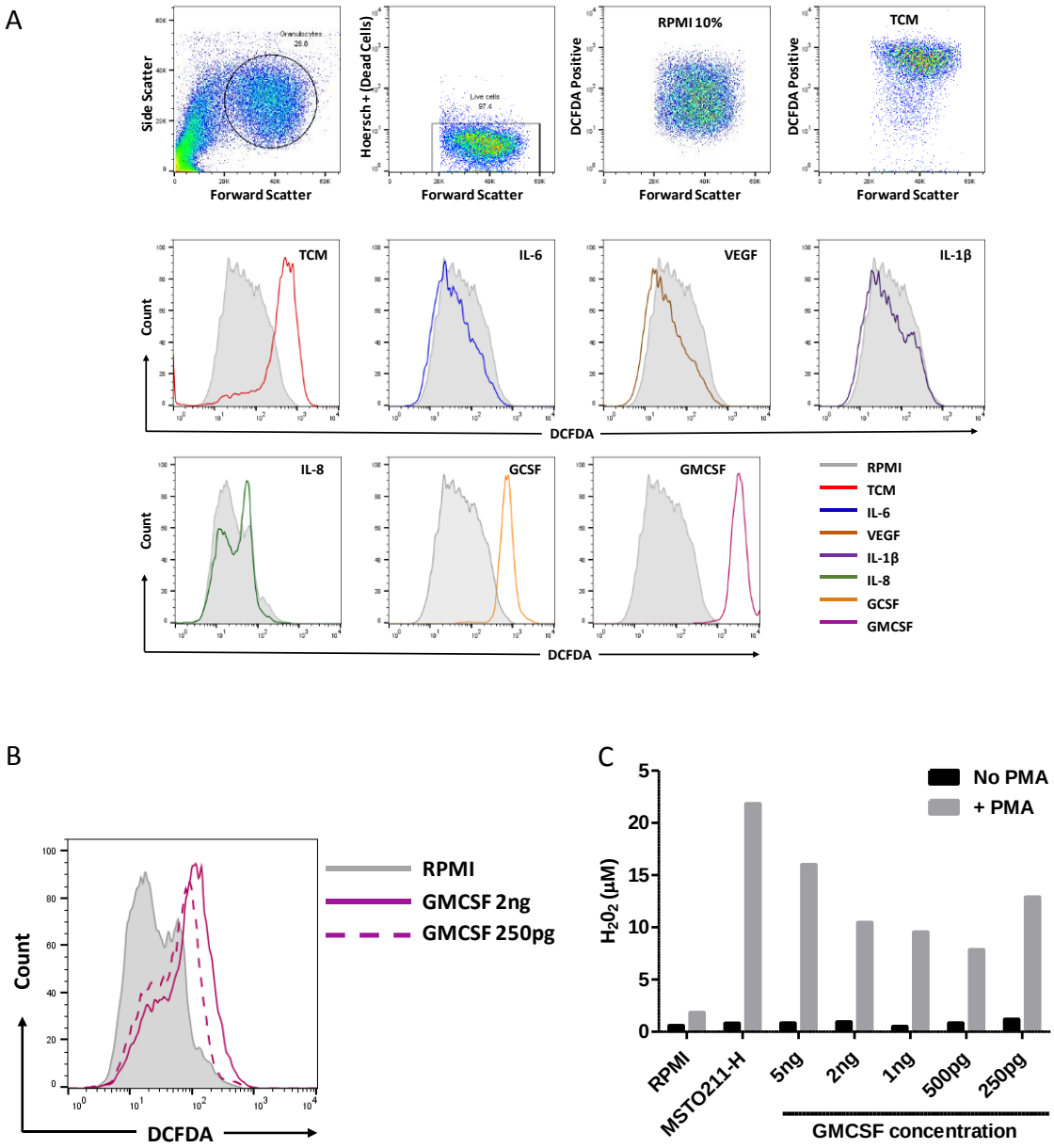

Figure 3. 13. Cytokine driven production of reactive oxygen species

Freshly isolated healthy granulocytes were exposed to a panel of cytokines in culture for 24 hours. Cytokines were tested at a concentration of 1ng/ml. (A) Flow cytometry analysis was performed on live granulocytes to detect ROS production through oxidation of H2DCFDA to the fluorescent compound DCF. Granulocytes cultured in RPMI 10% were used as a control. (B) Reducing concentrations of GMCSF (5ng-250pg) were added to granulocyte cultures prior to ROS detection to determine the minimal concentration required to induce an increment of ROS. ROS activity was detected through DCF detection by flow cytometry. (C) The quantification of ROS was detected by the production of H_2O_2, using the Amplex Red H_2O_2 assay.

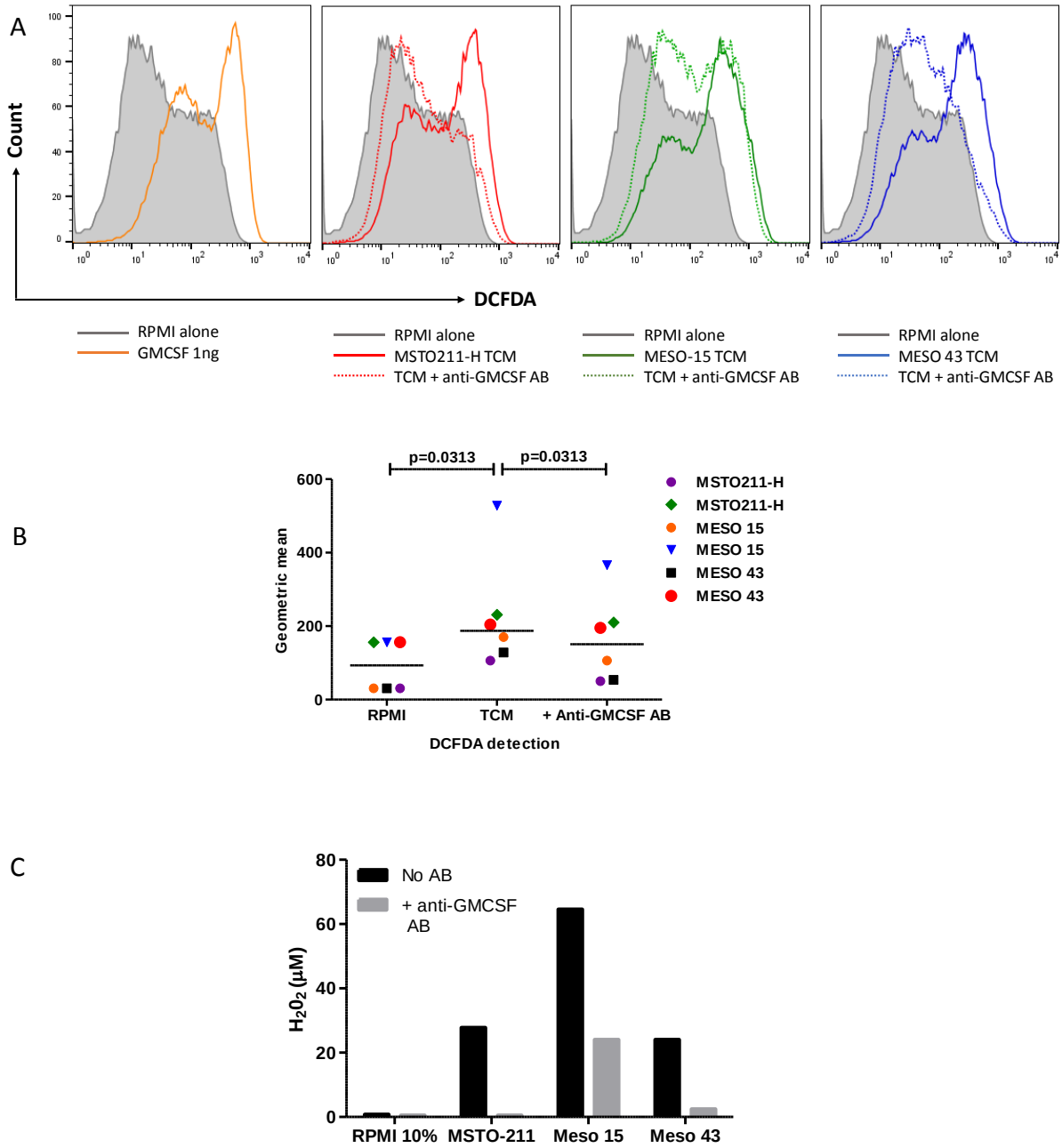

Figure 3. 14. Inhibition of ROS production through GMCSF blockade

(A) Healthy granulocytes were exposed to TCM alone or in the presence of a GMCSF antibody prior to detection of ROS activity by flow cytometry. (B) Geometric means of fluorescence detection were calculated for statistical analysis using Wilcoxon matched pairs rank test. Two replicate experiments shown. (C) Analysis of H_2O_2 production by granulocytes was also performed in a third replicate experiment, to determine the effect of anti-GMCSF blockade on H_2O_2 production. These reductions were not significant using the Wilcoxon matched pairs rank test.

To determine whether GMCSF generation of ROS was the mechanism leading to suppression of T cell function, anti-GMCSF neutralising antibodies were added to neutrophil polarisation cultures, prior to performing T cell proliferation assays. Rescue of proliferation was observed, confirming the hypothesis that neutrophil polarisation, driven by GMCSF released by mesothelioma, disrupted T cell function (Figure 3.15, A). To further confirm whether tumour derived GMCSF could drive granulocytes to suppress T cell proliferation, along with enhancing granulocyte ROS production, granulocytes were treated for 24 hours with recombinant GMCSF (1ng/ml). This led to a reduction in T cell proliferation, consistent with the effect seen with mesothelioma supernatants (Figure 3.15, B). The ROS scavengers catalase and N-acetylcysteine were added to culture and led to rescued T cell proliferation, suggesting that granulocyte ROS production was leading to T cell dysfunction. This was significant with the use of catalase; however, significance was not met with NAC when post-test correction was applied using the Kruskal Wallis test (Figure 3.15, C).

Following these findings, we wished to examine the presence of GMCSF in a larger cohort of mesothelioma patients to determine the proportion of patients with mesothelioma that this mechanism may relevant. 10 tissue sections were stained with anti-GMCSF antibody and detected the presence of GMCSF in all tumours (Figure 3.16, A-E). These findings were supported through data held within the R2 database, which revealed by transcriptomics that approximately 50% of mesotheliomas express GMCSF (350).

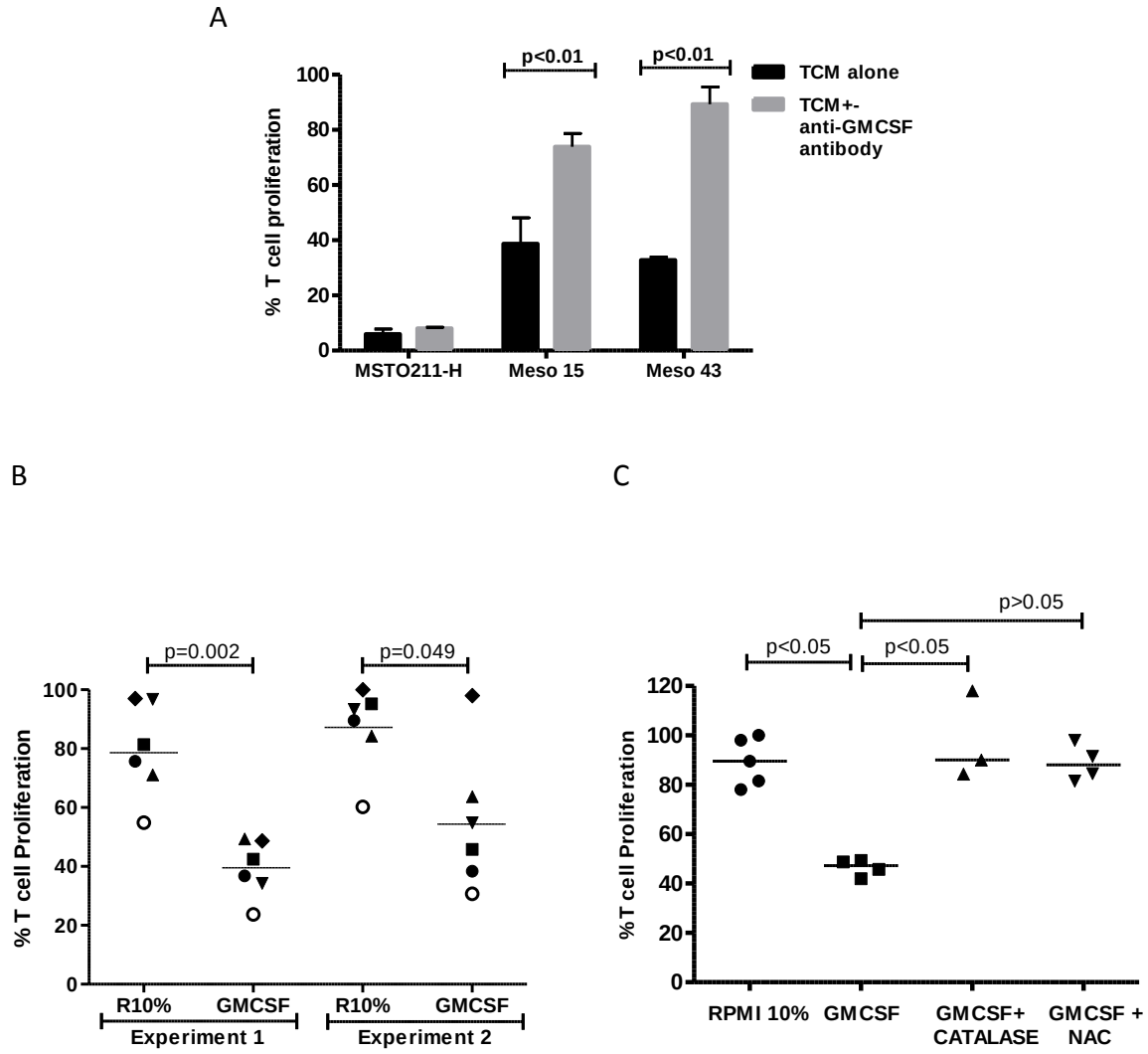

Figure 3. 15. GMCSF derived ROS production and effects on T cell proliferation

(A) Granulocytes were cultured in the presence of TCM, with or without the addition of a GMCSF antibody for 24 hours, prior to culture in T cell proliferation assays. Cell viability was confirmed by flow cytometry. The effect of GMCSF blockade was observed using 3 different cell lines. (B) Granulocytes were cultured in the presence of 1ng GMCSF for 24 hours, prior to culture in T cell proliferation assays, to observe the independent effect of GMCSF treated granulocytes on T cell function. (Two experiments were performed with 6 replicate wells). Horizontal bars show median values. Statistical analysis was performed using a Mann Whitney U test. (C) The ROS scavengers catalase (500units/ml) and N-acetylcysteine (5mM) were added to T cell: granulocyte proliferation assays to observe for any effect on T cell function by the removal of ROS. Horizontal bars show median values. Statistical analysis was performed using the Kruskal-Wallis ANOVA, with Dunn's correction for multiple comparisons.

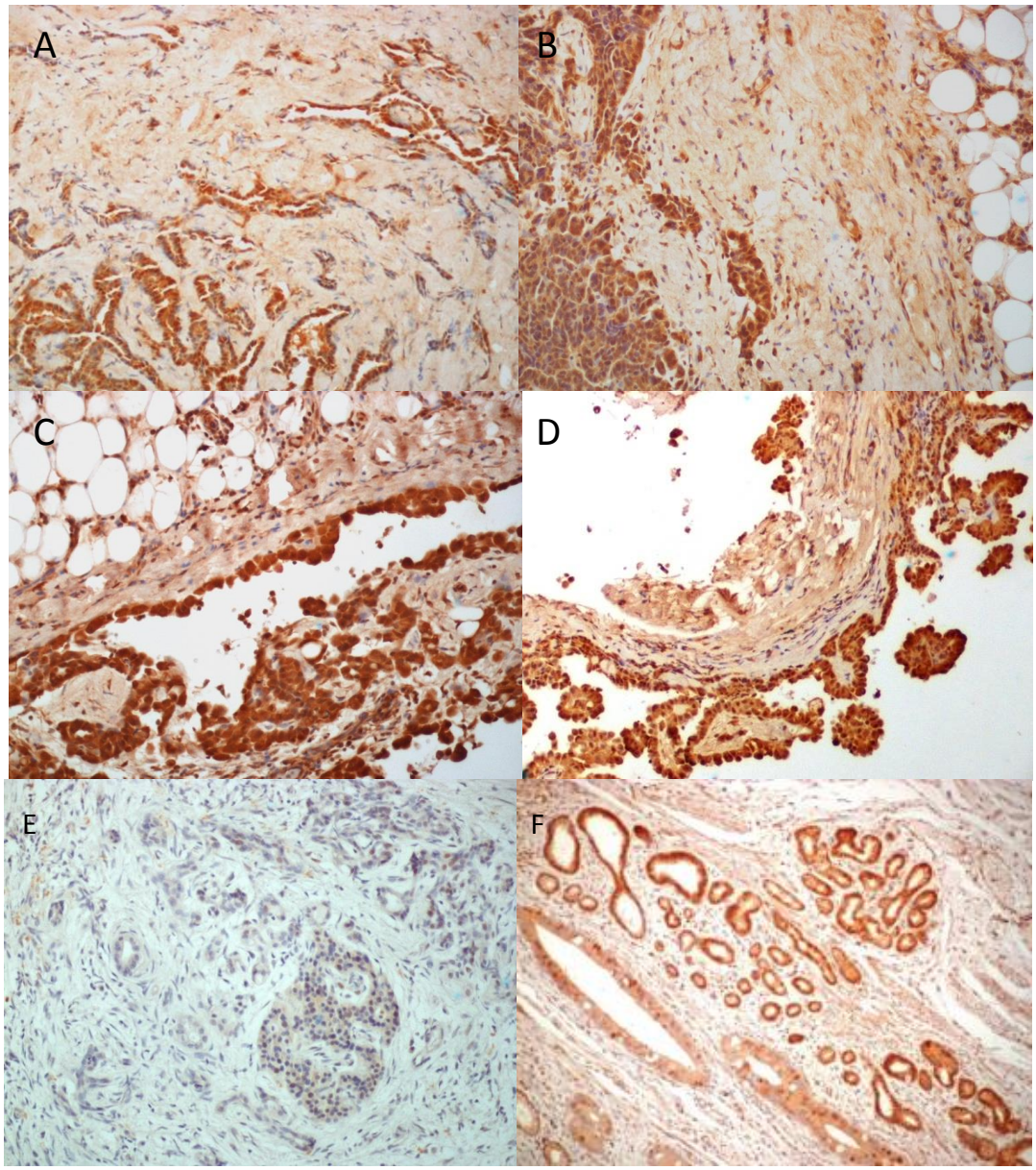

Figure 3. 16. Immunohistochemical staining of human mesothelioma tumour specimens

Immunohistochemical staining of human mesothelioma tumour sections was performed to examine for the presence of GMCSF. (A) Malignant Mesothelioma, adenomatoid type, showing strong cytoplasmic positivity of the tumour cells for GMCSF. (B) Epithelioid mesothelioma demonstrating sheets of solid epithelioid tumour cells, showing diffuse positive staining for GMCSF. (C) Malignant Mesothelioma, adenomatoid type, showing strong cytoplasmic positivity of the tumour cells in diffuse pattern for GMCSF. (D) Mesothelioma, with papillary fronds, displaying strong cytoplasmic staining in diffuse pattern. (E) Secondary antibody alone. (F) Positive control pancreatic tissue.

3.3 Discussion

The impact of the tumour microenvironment on the function of immune cells is highly relevant to current practice in oncology, owing to the successful introduction of immunomodulatory therapies. Certain cancer types, including NSCLC and melanoma, have seen large gains achieved in patient outcomes due to the use of checkpoint inhibitors such as PD-1, PD-L1 and CTLA-4 (143,351,352) however, these benefits have not yet been seen with all cancer types (353-355). An understanding of the variation in response may be gained from a greater appreciation of the complex interactions occurring between a patients' tumour and immune system, from which the tumour is successfully escaping.

Throughout the development of asbestos related disease and the subsequent development of mesothelioma, an inflammatory environment is present. Mesothelial, stromal and inflammatory cells produce a number of immunomodulatory cytokines, including IL-1β, IL-6, TNF-α and TGF-β (69,76,78); growth and angiogenesis drivers, VEGF and PDGF (74,85); in addition to factors which are capable of altering the tissue cytoskeleton such as MMP-2 and MMP-9 (74,125). This cytokine milieu therefore provides and environment which supports and enhances malignant transformation, tumour growth and invasion.

In this study we confirm that a strong inflammatory phenotype is associated with mesothelioma through the interrogation of both primary tumour samples and mesothelioma cell lines. Of particular interest, increased concentrations of pro-inflammatory cytokines IL-6, GM-CSF and PGE2 were demonstrated, in addition to the neutrophil chemotactic factors and angiogenesis drivers IL-8, VEGF, Midkine and GRO-α. Consistent with an enhanced inflammatory cytokine profile, it was shown that patients with mesothelioma harbour a significantly altered systemic blood profile, with reduced T cell and raised neutrophil

percentages. This peripheral blood profile significantly differed from healthy controls and supports previous data which has shown markedly raised neutrophil to lymphocyte ratios within this tumour type (332,356).

The intra-tumoural immune environment in mesothelioma has received increased focus in recent years, with a large study carried out by Ujiie and colleagues investigating patterns of lymphocyte invasion revealing the presence of tumour infiltrating macrophages. An increased ratio of this population to CD8+ lymphocytes conferred prognostic significance; however, this study did not assess other myeloid populations which may also have been present within tumours (357). A similar, larger investigation, examining 302 tumour sections, also included surface markers for neutrophil detection. This study supported the findings of Ujiie *et al*, that high numbers of tumour infiltrating macrophages conferred poorer prognosis, but also demonstrated that neutrophil infiltration had negative prognostic implications and remained a significant indicator in multivariate analysis (183). The majority of functional studies carried out in this setting have been within murine models, which provide supporting evidence of a polarising environment promoting M2 macrophage infiltration (333,334), immunosuppressive myeloid cells (331) and tumour associated neutrophils (243,245). However, despite the prognostic associations of the NLR, little research has focussed on the functional role of tumour associated neutrophils in human mesothelioma patients.

Within this study both low density CD15+ cells found in the PBMC ring, along with high density CD15+ cells collected from the RBC pellet were examined. Numbers of CD15+ cells within the PBMC ring were significantly higher in patient blood, indicating the presence of an abnormal population of cells not present in healthy controls. However, both high and low density populations demonstrated suppressive activity in T cell proliferation experiments. High

density neutrophils were more abundant and demonstrated more potent suppressive activity, therefore focus was towards this group in ongoing experiments. Consideration was given as to whether this population could be classified as G-MDSC however, the fact that this population was of high density, determined by their separation from those within the PBMC ring, prevented this classification and identifies them as a distinct population (250). This distinction between G-MDSC and tumour associated neutrophils has been the subject of much debate and there is no current agreement as to how to delineate these populations phenotypically. Recently produced transcriptomic evidence strongly supports the existence of at least two distinct groups of tumour associated neutrophils which show loss of normal neutrophil characteristics (336).

Despite discordance in relation to nomenclature, it is widely accepted that increased numbers of circulating, "cancer-associated" neutrophils lead to worse patient outcome in a number of different tumour settings, with poor outcomes attributed to pro-tumour effects of neutrophils such as inflammation and immune tolerance (243,358), induction of angiogenesis (359,360) and tumour cell mobilisation (361). Therefore, the presence of such an enhanced neutrophil population in mesothelioma is highly pertinent.

Primarily, this study was interested in the immunological functions of abnormal neutrophils as it has previously been shown that neutrophils are capable of inducing T cell tolerance as a mechanism of tumour escape (234,244). Mechanisms utilised by immunosuppressive neutrophils in cancer have been investigated, with the two most frequently described being arginase-I expression (362,363) and ROS production (240). Both mechanisms can affect T cell function through impaired MHC signalling due to both down regulation of the CD3 zeta chain and nitration of tyrosine residues present on the T cell receptor. These conformational

changes result in reduced flexibility and render it less responsive to interaction with MHC molecules (364,365). We therefore investigated whether either of these documented mechanisms could be occurring in this setting. Enhanced ROS production by neutrophils was shown to be the mechanism of T cell suppression. This enhanced ROS production was driven by increased NADPH activity and the suppressive role of ROS was confirmed through rescue with ROS scavenging agents NAC and catalase.

The mechanism driving neutrophil ROS production was shown to be tumour derived GMSCF, which enhanced ROS production to a much greater degree than other expressed cytokines and remained able to stimulate production at varied concentrations. Raised levels of GMCSF were not detected in patient serum however. The effect of GMCSF on neutrophils was therefore thought to be occurring within the local tumour environment and as such, not represented by circulating GMCSF concentrations. Serum GMCSF, when detected in the setting of cancer, has also been reported at low levels, with concentrations in the range of 40pg/ml (366), lower than those detected within the tumour culture environment in this study.

GMCSF is a commonly encountered cytokine in malignancy and the role of GMCSF in neutrophil priming has been previously documented, with Dang *et al* demonstrating that GMCSF could drive NADPH activity through p47phox phosphorylation (367). Interestingly, some studies have shown that although GMSCF strongly primes neutrophils for ROS release, a second signal is required to induce the respiratory burst (368); however, in our study and the work by Dang *et al*, GMCSF was shown to be an independent inducer of ROS production. A wider role of GMCSF as a driver of immunosuppression in the setting of cancer is also well established, with GMCSF being one of the most commonly implicated factors in the

development of MDSC (207,369,370). Inhibition of GMCSF in combination with chemotherapy treatment reduced both number and suppressive function of G-MDSC in an vitro culture model (371) and in support of these findings Serafini *et al* demonstrated that the delivery of GMCSF alongside a tumour vaccine in murine melanoma, led to increased numbers of suppressive myeloid cells and a reduction in vaccine efficacy (208). These findings have significant implications in current practices as GMCSF is often delivered in combination with tumour vaccines and is used alongside many chemotherapy agents to support the immune system during treatment. In mesothelioma, at least two historical trials have described the use of GMCSF as part of chemotherapy protocols (372,373) and it has also been utilised as a mechanism of stimulating immune responses in conjunction with vaccine therapy in mesothelioma (330,374). In these trials there were either no comparator arms or, in the most recent trial using a WT-1 peptide vaccine, GMCSF was delivered alongside both the treatment and control vaccines. It is therefore not possible to determine the effect of GMCSF in these trials. A further study examined the delivery of GMCSF direct to the tumour bed in mesothelioma patients in attempts to stimulate a local immune reaction. The delivery of GMCSF led to neutrophilia and neutrophil activation in patients, determined by enhanced CD11b expression; however, only 1 of 14 patients demonstrated a response to this treatment, implying that local GMCSF likely does not improve the local immune response. Again, the demonstration of a negative effect in this trial caused by GMCSF is not possible (375). One area where the negative phenomenon of exogenous or tumour derived GMCSF has been studied more intensely is within head and neck cancer, following a study which implicated the prophylactic delivery of G-CSF as a poor prognostic factor for local disease control (376). Both GMCSF and GCSF have subsequently been shown in murine head and neck cancer models to

promote angiogenesis, support increased and persistent infiltration of neutrophils and macrophages, and to drive tumour growth (377).

The possibility of targeting tumour associated GMCSF is something that can now be considered in view of a recent trial which demonstrated the safe and effective delivery of Mavrilimumab, a human monoclonal antibody targeting the GMCSF receptor, to a cohort of patients with severe rheumatoid arthritis (378). Patients treated with the GMCSF receptor antibody saw meaningful and significant responses in terms of disease severity, demonstrating its effectiveness in man. Although no studies have yet been completed in the setting of cancer, the concept of an over stimulated immune response leading to neutrophil dysfunction can be paralleled and this provides another possible approach to immune modulation as a treatment for cancer.

This research highlights the extremely complex interplay between cancer and the immune system and demonstrates the high plasticity that neutrophils exhibit. Our novel findings, that a population of suppressive granulocytes, induced by tumour-derived GMCSF, are present in the patients of mesothelioma, provides a new insight into the poor immune responses to mesothelioma, and to the association of high neutrophil numbers with poor prognosis. In addition, these findings also help to guide understanding of failures in responses to treatments aimed at enhancing T cell function. Releasing T cells from the suppressive effects of granulocyte-derived ROS may have significant implications in the success of many therapies currently under investigation including check-point blockade, tumour vaccines and CAR T cell therapy. Releasing the brake applied by the surrounding tumour environment, may create a profound change in treatment response and ultimately alter the outcome in this complex

tumour. The mechanism of tumour derived GMCSF driving granulocyte T cell suppression has not to our knowledge previously been shown in the setting of mesothelioma.

Chapter 4: STAT3 mediated immune dysfunction in mesothelioma

4.1 Results

4.1.1 T cell function is impaired following culture in the presence of mesothelioma

During the analysis of mesothelioma patient blood profiles, a reduction in frequency of 3 common T cell subsets (CD3, CD4 and CD8) was observed. This prompted further investigation into the direct impact of mesothelioma on the function of T cells, and in addition, the ability of APCs such as dendritic cells (DC) to create a functional immune synapse in this setting.

As discussed within the introduction, the pleiotropic cytokine, IL-6, and its activation of STAT3 has been widely implicated in immune dysfunction in the setting of malignancy, specifically in the alteration of T cell function. We therefore targeted our investigation toward the effects of IL-6 and STAT3 hyperactivation in the setting of mesothelioma.

Due to the findings in chapter three of a significant reduction in the percentage of circulating T cells in patients with mesothelioma, in addition to data demonstrating T cell infiltration in mesothelioma tissues was of prognostic relevance (183-185,332), our initial focus was the direct effect of mesothelioma on T cell function in vitro. In order to carry out this investigation, mesothelioma cell lines were used to provide a tumour conditioned supernatant (TCM), as described in chapter 3 and the methods section. T cells were isolated from healthy donors or leukocyte cones and purified using a pan-T cell isolation kit (Miltenyi). To investigate whether tumour cells impair direct cell function, T cells were cultured in the presence of TCM from 3 mesothelioma cell lines for 48 hours, prior to stimulation with PMA and ionomycin. T cells cultured in RPMI 10% were used as a control. Production of a Th1 response was subsequently

assessed through IFN-γ release, measured by flow cytometry. Culture in the presence of TCM from MSTO211-H, Meso 15 and Meso 43 reduced the production of IFN-γ in repeated experiments however, only the reduction of IFN-γ production induced by MSTO211-H and Meso 15 was significant. Four replicate experiments were performed analysing IFN-γ release from CD3 positive T cells and statistical analysis performed using a repeated measures ANOVA, with Dunnett's correction for multiple comparisons (Figure 4.1 A, B).

The function of TCM treated T cells was further assessed by their ability to proliferate following non-antigen specific stimulation using anti-CD3 and anti-CD28. T cells were cultured with complete RPMI (RPMI 10%), or complete RPMI plus 25% TCM, for 48 hours. Cells were then removed, washed and viability assessed, prior to plating. T cells were plated at a concentration of $4x10^6$/ml, in the presence of anti-CD3 and anti-CD28 for 96 hours, with proliferation assessed by thymidine incorporation. Proliferation was suppressed by all 3 cell line conditions, with MSTO-211H and Meso 15 showing significant levels of suppression when analysed using the Kruskal-Wallis ANOVA, with Dunn's correction for multiple comparisons. Results are expressed relative to proliferation of T cells cultured in RPMI 10%, (Figure 4.2).

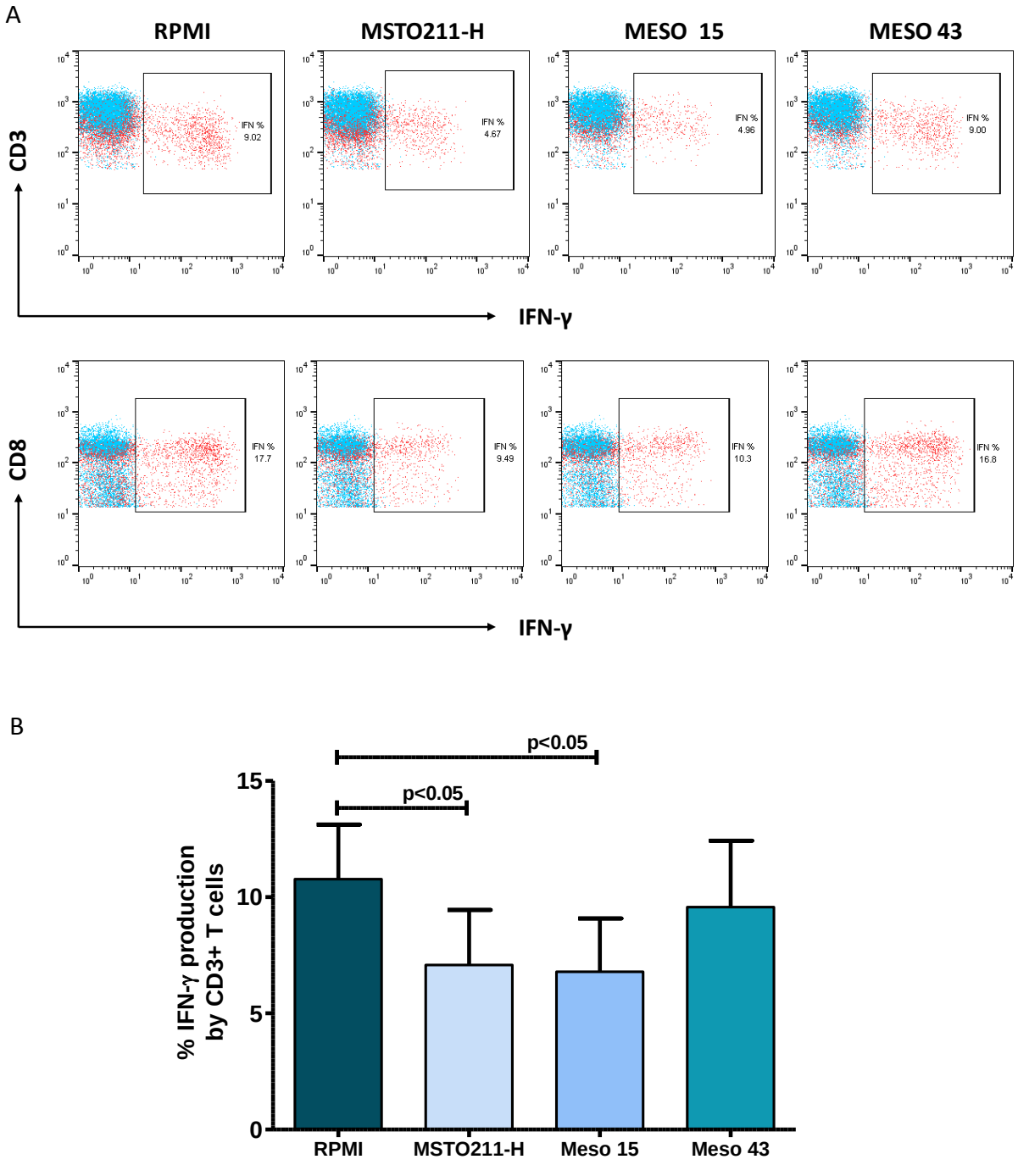

Figure 4. 1 The effect of mesothelioma tumour conditioned media on T cell production of IFN- γ

(A) Healthy T cells were cultured in the presence of TCM from 3 mesothelioma cell lines for 48 hours, prior to stimulation with PMA and ionomycin. Production of a Th1 response was assessed through IFN-γ release, measured by flow cytometry. IFN-γ release was measured from CD3 positive and CD8 positive T cells. (B) Four replicate experiments were performed analysing IFN-γ release from CD3 positive T cells. Results were combined for statistical analysis which was performed using a repeated measures ANOVA, with Dunnett's correction for multiple comparisons.

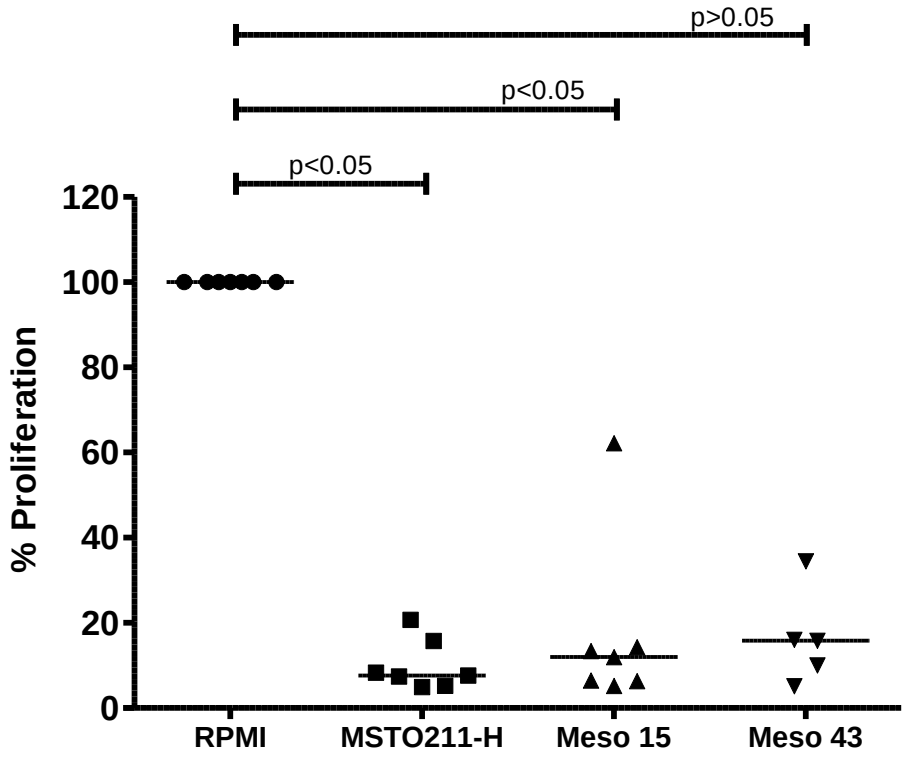

Figure 4. 2. The effect of mesothelioma tumour conditioned media on T cell proliferation

Healthy T cells were cultured in the presence of tumour conditioned media for 48 hours, prior to T cell proliferation assays. Treated T cells were assessed for viability and replated at densitiies of $4x10^6$ per ml, prior to stimulation with with anti-CD3 and anti-CD28. Function was assessed by measurement of proliferation, detetced by thymidine incorporation, at 96 hours. Healthy T cells cultured in 10% RPMI were used as a proliferation control and proliferation of treated T cells expressed relative to this. Experiments were replicated with TCM from 3 mesothelioma cell lines, (MSTO211-H n=7, Meso 15 n=7, Meso 43 n=5). Horizontal lines demonstrate median proliferation. Differences in proliferation were analysed using the Kruskal-Wallis test, with Dunn's correction for multiple comparisons.

4.1.2 Mesothelioma activates T cell STAT3

To determine whether hyperactivation of STAT3 could be involved in the dysfunction of T cells, we next examined the expression of phosphorylated STAT3 and total STAT3 through quantitative PCR (qPCR) and western blot. In initial experiments T cell expression of STAT3 mRNA was assessed following exposure to TCM for 24 hours. Equal numbers of T cells were cultured in complete RPMI (RPMI 10%) or in the presence of 25% MSTO211-H, Meso 15 or Meso 43 TCM, with all wells harvested at 24 hours. This experiment demonstrated small increases in STAT3 mRNA in T cells exposed to TCM at 24 hours; however, these increases were not significant when analysed using a repeated measures ANOVA, with Dunnett's post-test for multiple comparisons (Figure 4.3, A).

The detection of abnormal phosphorylation of STAT3 may also be relevant to T cell function, as it is through this process that STAT3 is able to activate cellular signalling, with constitutive phosphorylation implicated in pathogenic STAT3 function. Analysis of phosphorylated STAT3 was performed as a time course, to determine whether phosphorylation was occurring differentially in T cells exposed to TCM, compared to those in RPMI alone. T cells were plated as described above, and wells were harvested at time points of 5, 15, 30, 60 and 90 minutes. Upon harvesting, cells were immediately washed, pelleted and placed on ice, prior to freezing at -20°C. Once all time points were complete protein lysates were produced, in order to allow western blots to be performed in parallel. Early STAT3 phosphorylation was detected in T cells exposed to TCM at 5 minutes and persisted to the final time point of 90 minutes. No phosphorylation of STAT3 was observed in T cells cultured in RPMI (Figure 4.3 B, C).

In order to identify the mechanism which may be leading to STAT3 phosphorylation, the effects of cytokines known to be present in the supernatants of mesothelioma tumours and

cell lines were assessed (Figure 3.10 & 3.11), along with additional cytokines known to have immunomodulatory actions. IL-1β, VEGF, Mesothelin, GM-CSF, GCSF, IL-8, IL-10, PGE2 and IL-6 were added to complete RPMI in the presence of T cells. T cells were harvested and pelleted for western blot after exposure for 30 minutes. Only IL-6 was capable of early STAT3 phosphorylation and was equivalent to mesothelioma TCM (Figure 4.4, A). To investigate whether the presence of IL-6 within TCM could be inducing STAT3 phosphorylation, soluble IL-6 blocking antibody was added to the mesothelioma TCM for 6 hours, before being added to T cell culture. Blocking IL-6 led to a marked reduction in the level of STAT3 phosphorylation in T cells, implying that activation of STAT3 may be occurring via an IL-6 dependent mechanism (Figure 4.4, B).

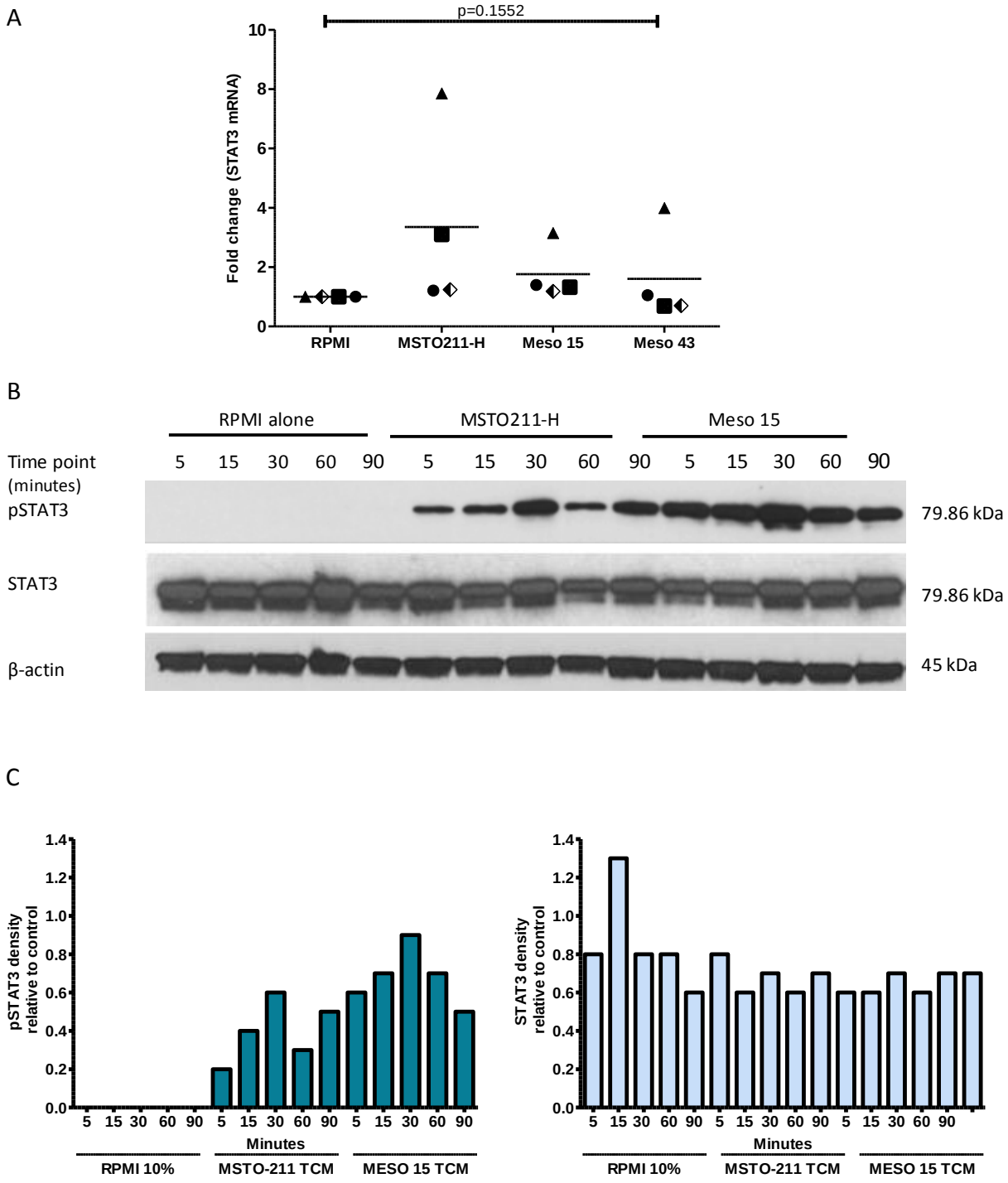

Figure 4. 3. The effect of mesothelioma on STAT3 expression

(A) T cells were cultured in the presence of tumour conditioned media (TCM) from 3 mesothelioma cell lines for 24 hours prior to assessment of total STAT3 mRNA expression. Four replicate experiments are shown, with horizontal line representing mean. Analysis was performed using a repeated measures ANOVA, with Dunnett's correction for multiple comparisons. (B) STAT3 phosphorylation and total STAT3 were assessed by western blot at multiple time points, from 5 to 90 minutes. (C) Densitometry was performed on protein bands to allow for assessment of expression relative to β-actin control.

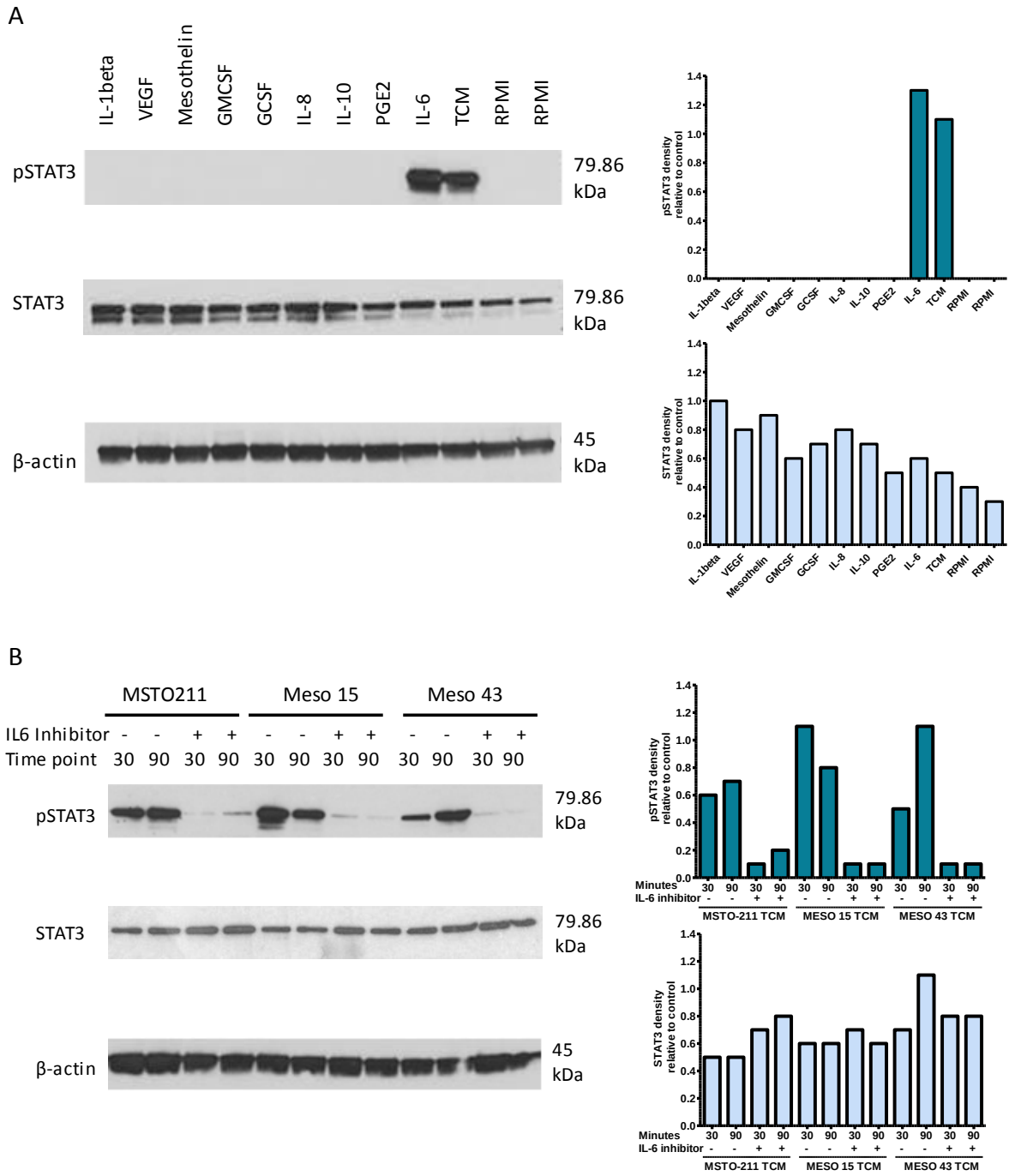

Figure 4. 4. The induction of STAT3 phosphorylation by soluble factors in mesothelioma

(A) Healthy T cells were exposed to immunomodulatory cytokines (IL-1β, VEGF, Mesothelin, GM-CSF, GCSF, IL-8, IL-10, PGE2 and IL-6) for 30 minutes, prior to assessment of pSTAT3 activity by western blot. Tumour conditioned media (TCM) was used as a positive control for pSTAT3 induction. Western blot and relative protein expression, determined by densitometry, are displayed. (B) To determine whether IL-6 present in TCM was inducing STAT3 phosphorylation, soluble IL-6 was blocked using an IL-6 antibody, prior to detection of pSTAT3. Experiments were performed using TCM from 3 cell lines. Representative western blots of 3 replicate experiments are shown.

4.1.3 STAT3 inhibition is achieved through an antisense oligonucleotide and enhances T cell function

As it was demonstrated that STAT3 phosphorylation occurs following exposure to TCM we wished to investigate what functional effect this could be having on T cells within the tumour microenvironment. In order to investigate this, the STAT3 antisense oligonucleotide (ASO), AZD9150, was obtained as a gift from Astrazeneca to inhibit STAT3 activation in the presence of mesothelioma conditioning. Dose titrations were carried out following instructions from the manufacturer regarding recommended dose regimens. Despite detection of moderate reductions in STAT3 mRNA (Figure 4.5, A), visible reductions in STAT3 protein were small and variable (Figure 4.5, B). It was thought that the lack of protein reduction may be related to limited uptake of the ASO, therefore we attempted to enhance the uptake into T cells using the non-liposomal transfection agent Fugene6. This did not result in any significant improvement in ASO function, in terms of STAT3 protein expression (Figure 4.6, A). Due to the difficulties in obtaining robust STAT3 knockdown in human T cells, we tested the ASO in additional cell types. When tested with the human T cell leukaemia cell line, JURKAT, treatment with the STAT3 ASO led to marked knockdown of protein expression when compared to untreated cells. This indicated that lack of STAT3 protein reduction in T cells was not a functional defect in the ASO itself, but likely a problem with the uptake of the molecule into human T cells (Figure 4.6, B).

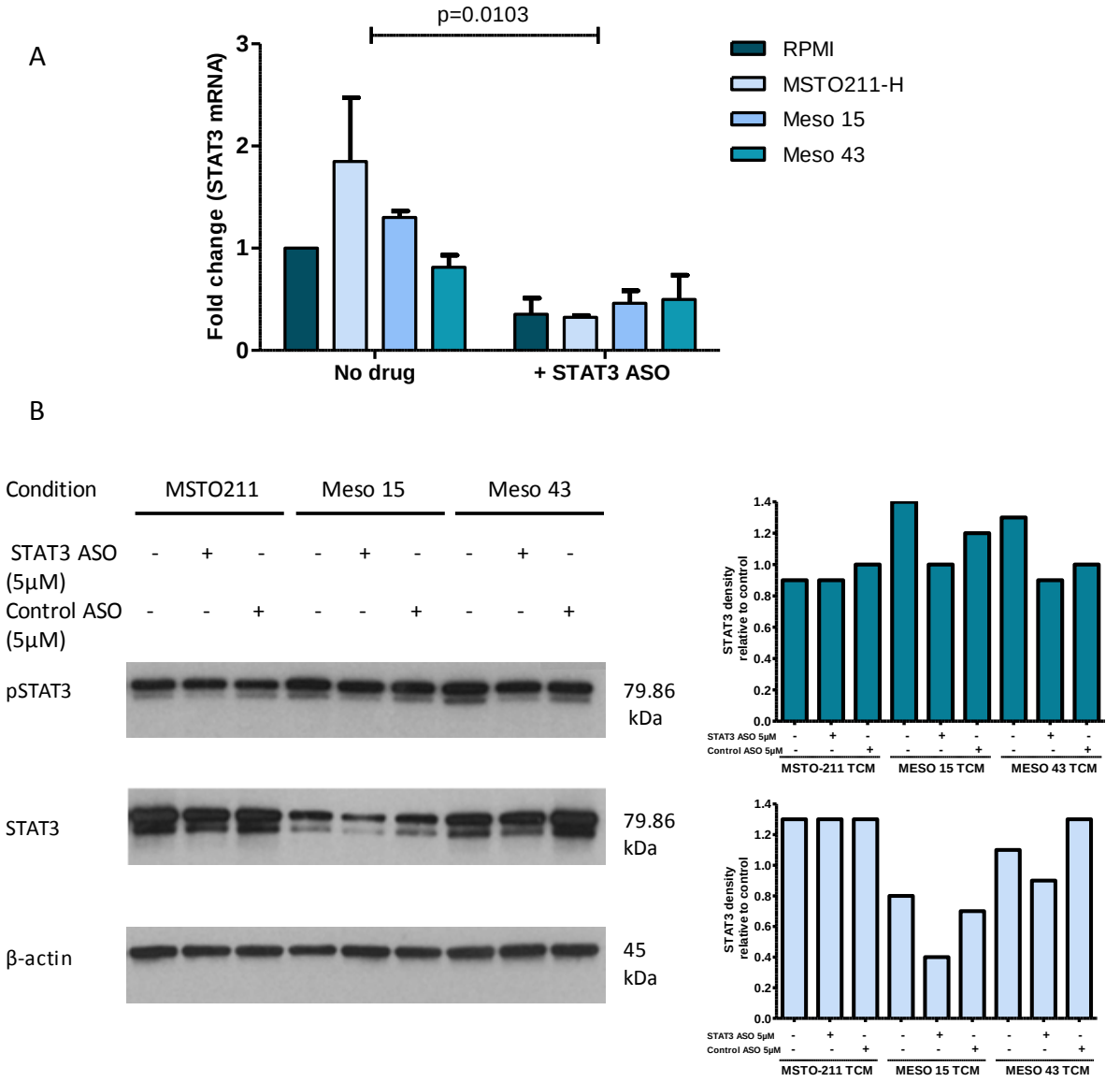

Figure 4. 5. The use of an antisense oligonucleotide to inhibit STAT3 function

Healthy donor T cells were isolated and cultured in RPMI 10% and TCM from 3 mesothelioma cell lines in the presence of the anti-sense oligonucleotide, AZD9150, targeted to STAT3. AZD9150 was used at a concentration of 5µM, directly added to media. Cells were treated for 48 hours then harvested for analysis. The effect of the oligonucleotide was assessed through STAT3 mRNA detection (A) and protein expression (B). Statistical analysis of the ASO effect on STAT3 mRNA expression was carried out using a paired T test. One of three replicate experiments is shown.

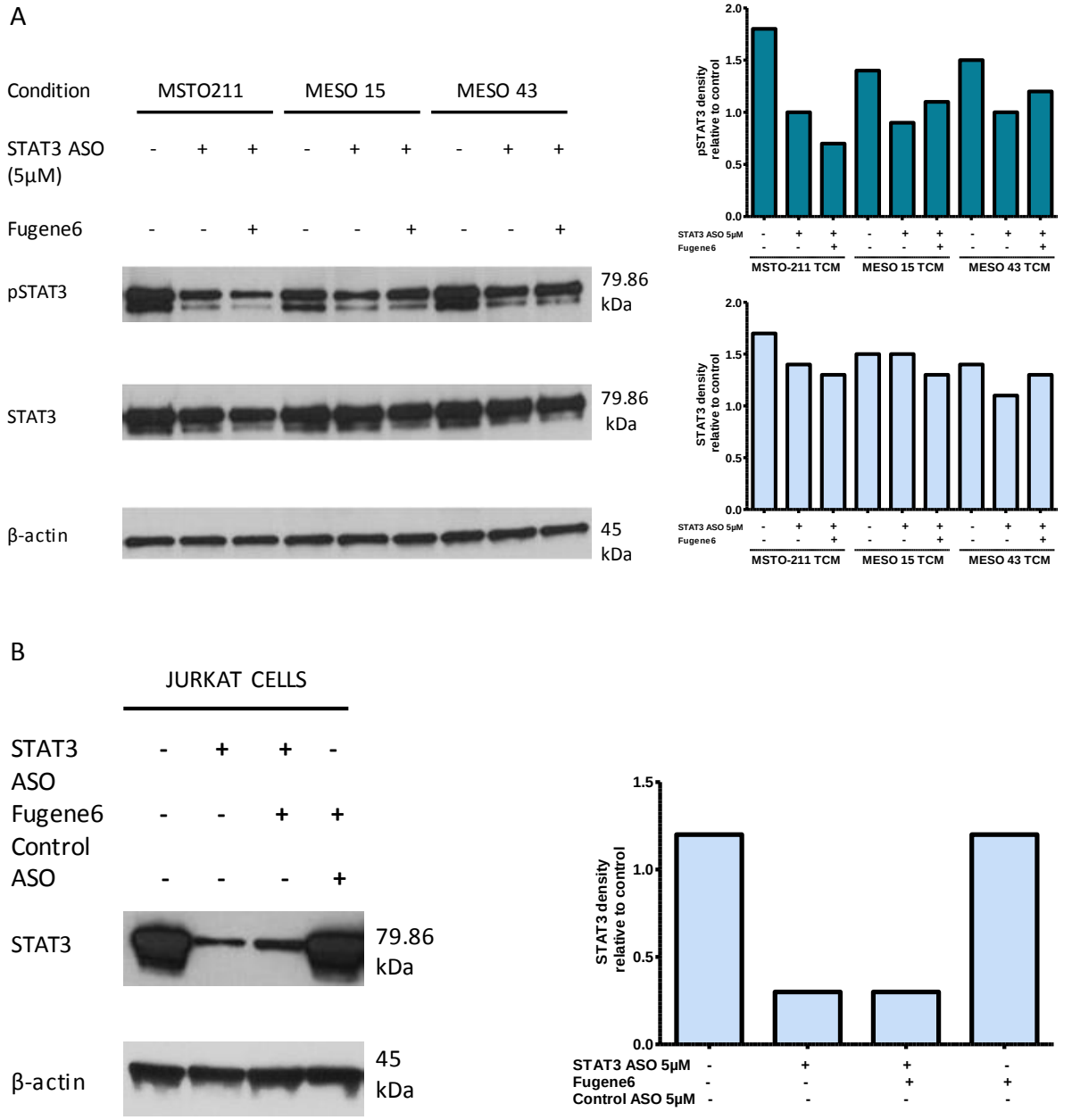

Figure 4. 6. Enhancing the effect of the STAT3 antisense oligonucleotide

(A) To attempt to enhance the efficacy of the STAT3 antisense oligonucleotide, the transfection agent Fugene6 was used in T cell culture experiments. T cells were cultured in the presence of TCM from 3 separate cell lines. TCM alone, TCM plus STAT3 ASO (5µM) and TCM plus STAT3 ASO in the presence of Fugene6 were assessed. Total STAT3 and phosphorylated STAT3 protein expression for all conditions were determined by western blot. Representative of 3 replicate experiments. (B) The function of the STAT3 ASO was tested in the T cell leukaemia cell line, JURKAT, to determine whether a more robust reduction in protein expression could be achieved. Total STAT3 was assessed by western blot.

Despite the very modest reduction in STAT3 protein expression in human T cells, STAT3 ASO treatment was able to produce an improvement in T cell function in cells cultured in the presence of mesothelioma TCM. T cells were treated with the STAT3 ASO and control ASO, prior to exposure to TCM for 48 hours. Proliferation assays were performed, as previously described. Improvement in T cell proliferation was achieved in T cells cultured in mesothelioma TCM from MSTO211-H and Meso 43; however, when analysis was performed using the Kruskal-Wallis ANOVA, these improvements were not significant (Figure 4.7 A-C). To investigate whether improvements in T cell function could be achieved through targeting the STAT3 pathway at an upstream activation point the JAK2 inhibitor, ruxolitinib, was used to perform equivalent experiments. JAK2 is a vital component of the cytokine signalling pathway, permitting intracellular phosphorylation of STAT3, following the binding of cytokines to their receptors and activation of the signal transducer gp130 (379). The addition of ruxolitinib to T cells was able to reduce STAT3 expression, determined by mRNA and protein detection. The reduction in STAT3 was significant over three replicate experiments, when analysed using a repeated measures ANOVA ($p<0.01$). This reduction was equivalent to that achieved with the STAT3 ASO (Figure 4.8, A). Interestingly, equivalent protein reduction was not observed, with significant changes in total STAT3 band density seen with the STAT3 ASO ($p<0.01$, analysed using repeated measures ANOVA), but not observed with ruxolitinib in duplicate experiments (Figure 4.8, B). Following treatment with ruxolitinib, the function of T cells was also assessed through proliferation assays. No rescue was observed with the use of ruxolitinib, in contrast to the STAT3 ASO (Figure 4.9, A). It is possible that the lack of rescue in this scenario was related to the non-specific effect of ruxolitinib which, in contrast to an ASO, has the capability to affect pathways of other STATs, reliant on JAK2 for intracellular signalling. The mRNA expression of STAT1 and STAT5 were therefore examined within T cells following

treatment with both drugs. Dramatic decreases in STAT1 expression ($p<0.001$), but not STAT5, were observed in cells treated with ruxolitinib. No significant changes in STAT1 or STAT5 were seen following treatment with the ASO (Figure 4.9, B). The findings that ruxolitinib severely impairs STAT1 expression may explain the inability to rescue T cell proliferation in T cells, despite similar levels of STAT3 blockade. STAT1 has been shown to play a vital role in CD8+ T cell function, with its activation observed in response to type 1 interferons and successful CD8+ T cell expansion and survival dependent on this signalling process (380,381). The absence of this molecule in combination with reduction in STAT3, therefore appears to prevent T cell rescue. Interestingly, T cells not treated with TCM did not experience a reduction in proliferative capability, implying a potential additive effect of mesothelioma tumour conditions and STAT1 inhibition resulting in this effect.

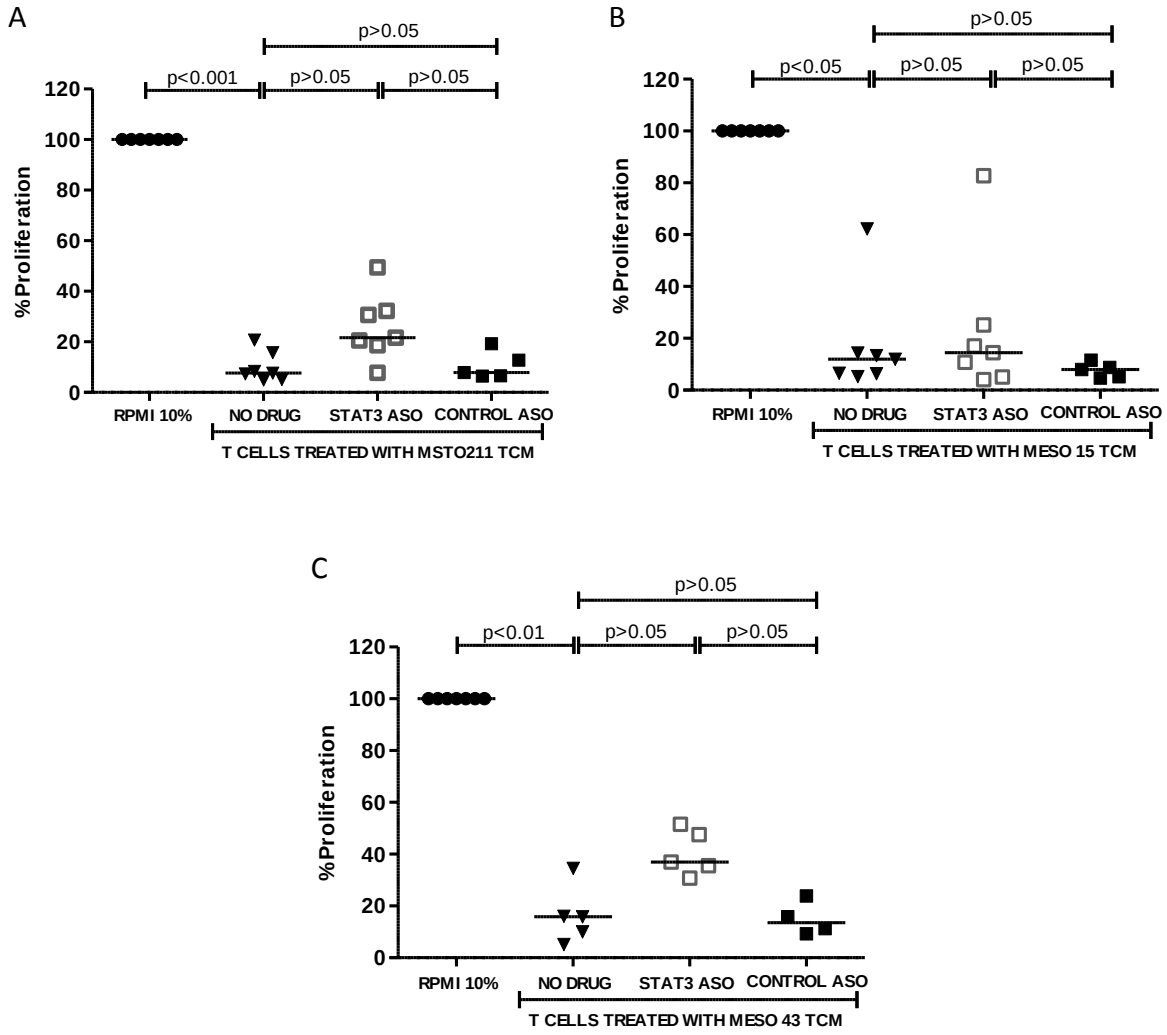

Figure 4. 7. The effect of STAT3 inhibition on T cell proliferation

Healthy T cells were treated with the STAT3 ASO, AZD9150, or control ASO, prior to addition of TCM, and remained in culture for 48 hours. Treated T cells were assessed for viability and replated at densitiies of $4x10^6$ per ml, prior to stimulation with with anti-CD3 and anti-CD28. Function was assessed by measurement of proliferation, detetced by thymidine incorporation, at 96 hours. Healthy T cells cultured in RPMI 10% were used as a proliferation control and proliferation of treated T cells expressed relative to this. Experiments were replicated with TCM from 3 mesothelioma cell lines, (A) T cells cultured in MSTO211-H TCM with STAT3 and control ASO (n=7), (B) T cells cultured in Meso 15 TCM with STAT3 and control ASO (n=7), (C) T cells cultured in Meso 43TCM with STAT3 and control ASO (n=5). Horizontal lines demonstrate median proliferation. Differences in proliferation were analysed using the Kruskal-Wallis ANOVA with Dunn's correction for multiple comparisons.

A

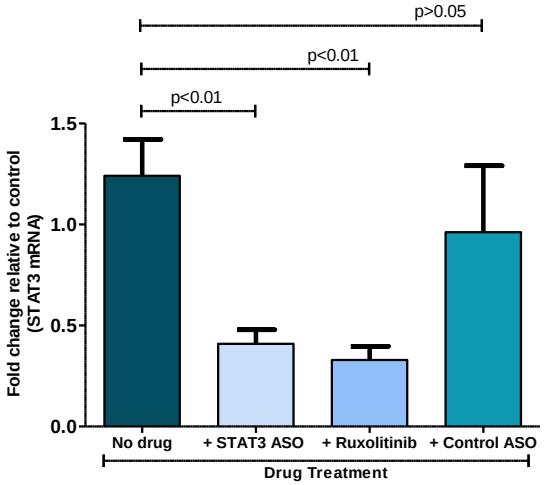

B

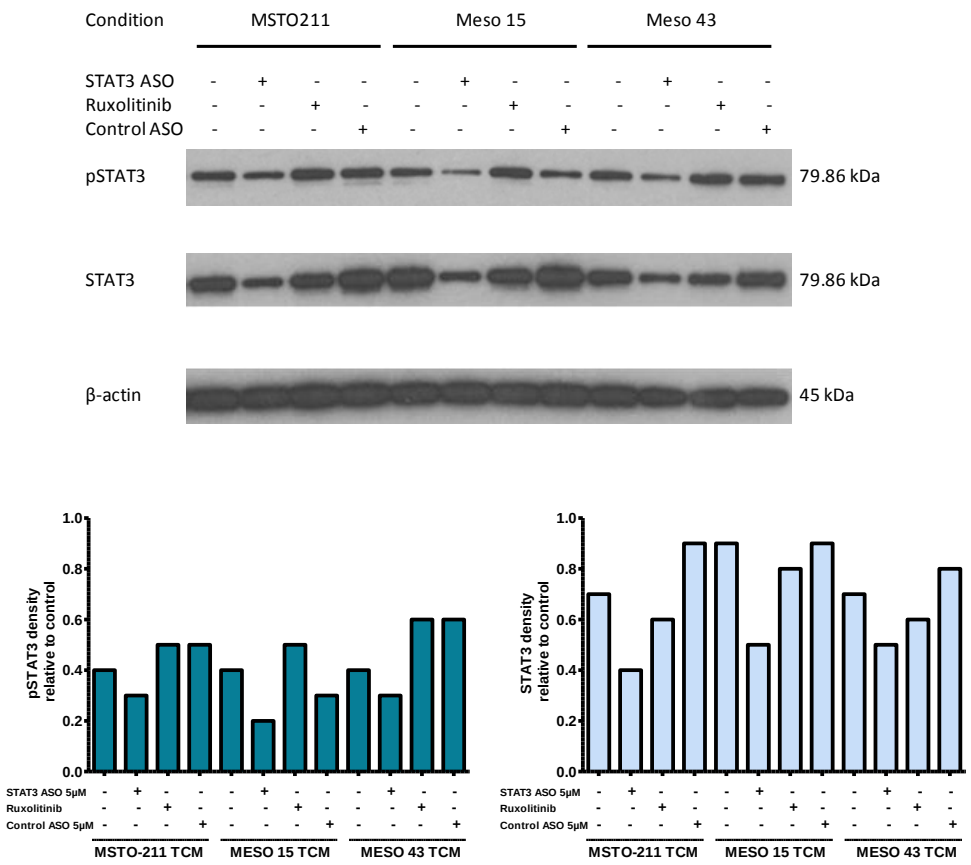

Figure 4. 8. The effect of JAK2 versus STAT3 inhibition on STAT3 mRNA and protein expression

T cells were treated with the JAK2 inhibitor ruxolitinib, to observe whether blockade of upstream STAT3 pathways led to improved T cell function. (A) The effect of ruxolitinib was assessed through detection of total STAT3 mRNA and STAT3 protein. Significant reduction in mRNA was observed with both ruxolitinib ($p<0.01$) and STAT3 ASO ($p<0.01$), analysed using repeated measures ANOVA. (B)Protein reduction in T cell groups did not correspond to mRNA reduction, with significant changes in STAT3 band density observed only with the STAT3 ASO ($p<0.01$), analysed using repeated measures ANOVA. (One of three representative experiments shown).

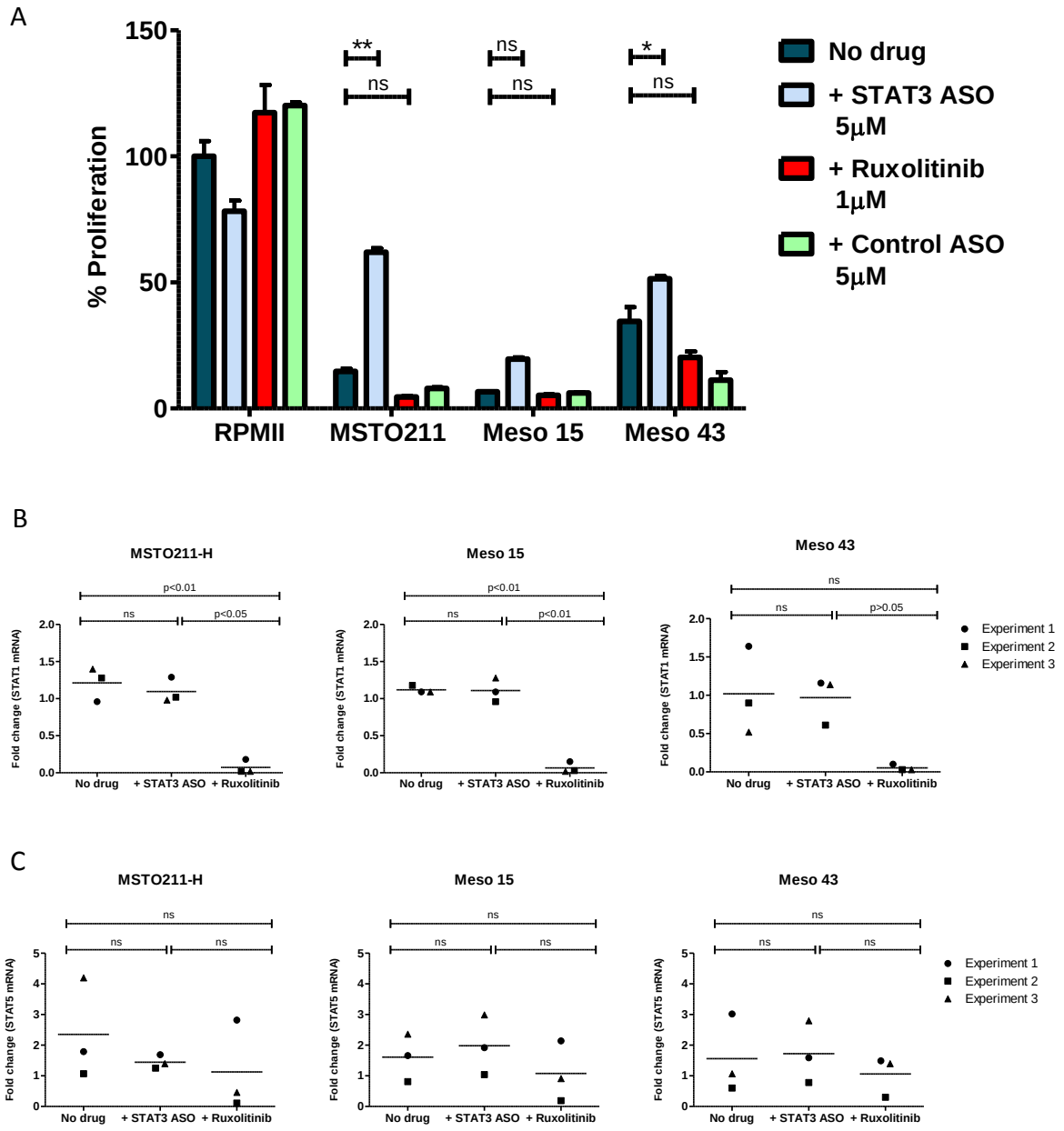

Figure 4. 9. The effect of JAK2 versus STAT3 inhibition on T cell function

(A) T cells were treated with both the JAK2 inhibitor, ruxolitinib, and the STAT3 ASO, in the presence of TCM, prior to T cell proliferation assays. T cells were cultured in RPMI 10% as a control, in the presence of all drug conditions. Three replicate wells were plated for each condition. Analysis was performed using a two-way ANOVA. Inhibition of STAT3 using the ASO (pale blue bars) led to significant proliferation rescue in cells treated with MSTO211 and Meso 43 TCM. No significant rescue was observed with ruxolitinib (red bars) in any condition. (B) T cells cultured for 48 hours in the presence of TCM, in addition to the STAT3 ASO or ruxolitinib, were examined for STAT1 mRNA expression. Three replicate experiments are shown for each TCM condition. A significant reduction in STAT1 mRNA was observed with ruxolitinib treatment. (C) T cells were simultaneously examined for STAT5 expression. No significant changes were observed. Statistical analysis was performed using a repeated measures ANOVA.

4.1.4 DC function is impaired following culture in the presence of mesothelioma

Following the observations that mesothelioma cell lines were capable of altering T cell function through modulation of STAT3, we attempted to assess the effect on dendritic cells (DC) within this environment. DC are known to be negatively modulated by STAT3 hyperactivation. It has previously been shown by Nefedova *et al* that STAT3 activation, induced by treatment with colon carcinoma TCM, had the ability to impair DC development and diverge cells from a group of functionally important APC, to cells that resemble MDSC. This population of MDSC lacked DC maturation markers and expressed CD14, consistent with an immature myeloid population (382). We hypothesised that impaired T cell function within mesothelioma may similarly be compounded by the presence of a functionally impaired population of DC within a tumour environment.

DC were generated from healthy CD14+ cells, in the presence of IL-4 and GM-CSF, as described within the methods section. DC culture was supplemented with 25% TCM from 2 mesothelioma cell lines, MSTO211-H and Meso 15. Following generation, their ability to stimulate T cell proliferation was assessed within a T cell proliferation assay using a ratio of 50,000 DC to 200,000 allogeneic T cells. Cells were plated in co-culture for 96 hours and T cell proliferation measured by thymidine incorporation. DC generated in the presence of GM-CSF and IL-4 and RPMI 10% were able to stimulate T cell proliferation. In contrast, DC cultured in the presence of TCM were significantly impaired in their ability to stimulate T cell proliferation. $p<0.05$ for both MSTO211 and Meso 15 TCM (Figure 4.10, A).

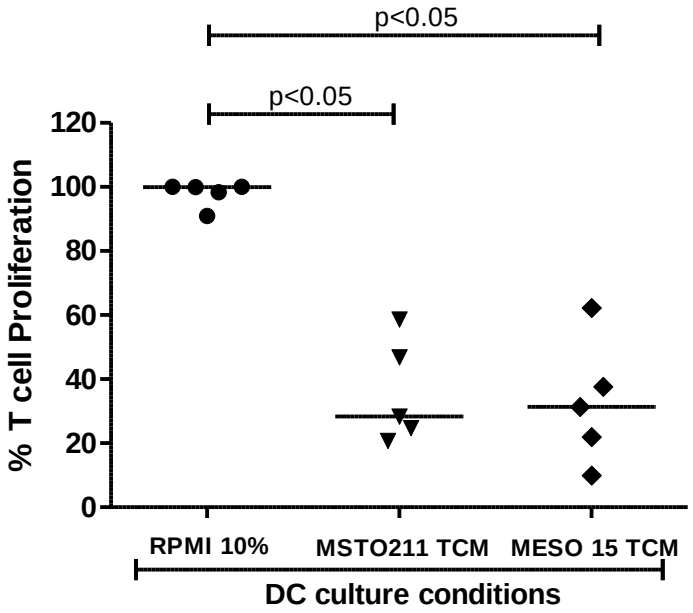

Figure 4. 10. Mesothelioma impairs DC ability to stimulate T cell proliferation

DC were generated from healthy CD14+ monocytes, isolated from a leucocyte cone, in the presence of GM-CSF and IL-4. Control DC were generated in the presence of RPMI 10%. The effect of TCM was tested through the addition of 25% TCM from 2 mesothelioma cell lines to DC cultures. Following 6 days, DC were harvested, and viability assessed, prior to re-plating in T cell proliferation assays. 50,000 DC were added to 200,000 allogeneic T cells and proliferation determined by thymidine incorporation at 96 hours. Proliferation is expressed relative to T cells stimulated by DC cultured in the presence of RPMI 10%. Five replicate experiments are shown. Horizontal line demonstrates median proliferation. Differences in proliferation were analysed using the Kruskal-Wallis ANOVA, with Dunn's correction for multiple comparisons. DC cultured in the presence of MSTO211 and Meso 15 TCM were significantly impaired in their ability to stimulate T cell proliferation, $p<0.05$.

4.1.5 Impaired T cell stimulation may be caused by DC STAT3 dysfunction in the presence of mesothelioma TCM

During development monocyte derived DC lose their expression of CD14 and CD33 and begin to express markers of maturation and co-stimulatory molecules including CD40, CD54, CD80, CD86, CD83. Maturation can be initiated through inflammatory stimuli and interaction with foreign peptides. During this process DC also relocate Class I and II MHC molecules from endosomal and lysosomal compartments to their cell surface, allowing antigen presentation (383). Their level of maturation determines their ability to interact and prime circulating T cells, and therefore, their ability to drive T cell activation and proliferation.

To determine whether the mechanism leading to poor DC function in the presence of mesothelioma TCM could be impaired DC maturation, the phenotype of these cells was further analysed by flow cytometry. DC were generated as described, followed by LPS stimulation overnight on day 6. Flow cytometry analysis was performed on day 7. Surface expression of maturation and co-stimulatory molecules CD83, CD86, CD80, CD54, CD40 and Class II MHC (HLA-DR), along with CD14 and CD33, markers suggesting immaturity, were assessed in three experiments. Within the first experiment performed, there were no observed differences in the expression of CD14 or CD33, and costimulatory molecules were expressed at similar levels in all groups. Within experiment 2, both CD14 and CD33 expression persisted on TCM treated DC, with reduction of the expression of costimulatory molecules HLA-DR, CD80 and CD86, particularly in those DC exposed to Meso 15 TCM. Both CD40 and CD54 were also reduced in TCM exposed DC, again more marked in those exposed to Meso 15 TCM (Figure 4.11 A, B). Within the third experiment, CD14 expression again persisted on DC treated with TCM; however, no changes in expression of CD33 were observed.

Costimulatory and maturation markers did not differ significantly between culture conditions. All 3 experiments are depicted, with geometric mean of surface marker expression reported for DC cultured in RPMI 10%, MSTO211-H TCM and Meso 15 TCM for each experiment in Figure 4.12, A. As persistence of markers of immaturity could not be consistently observed in TCM exposed DC, and markers of maturation and co-stimulation did not differ significantly between each condition, it was concluded that these changes could not account for the impaired ability of DC to stimulate T cells. The cause of inter-experimental variability is due to the response of different donor cells to the effects of TCM over the prolonged culture time of DC. More experiments with a larger number of healthy donors will be necessary to reduce the donor viability and obtain clear evidence of the TCM effect on DC maturation.

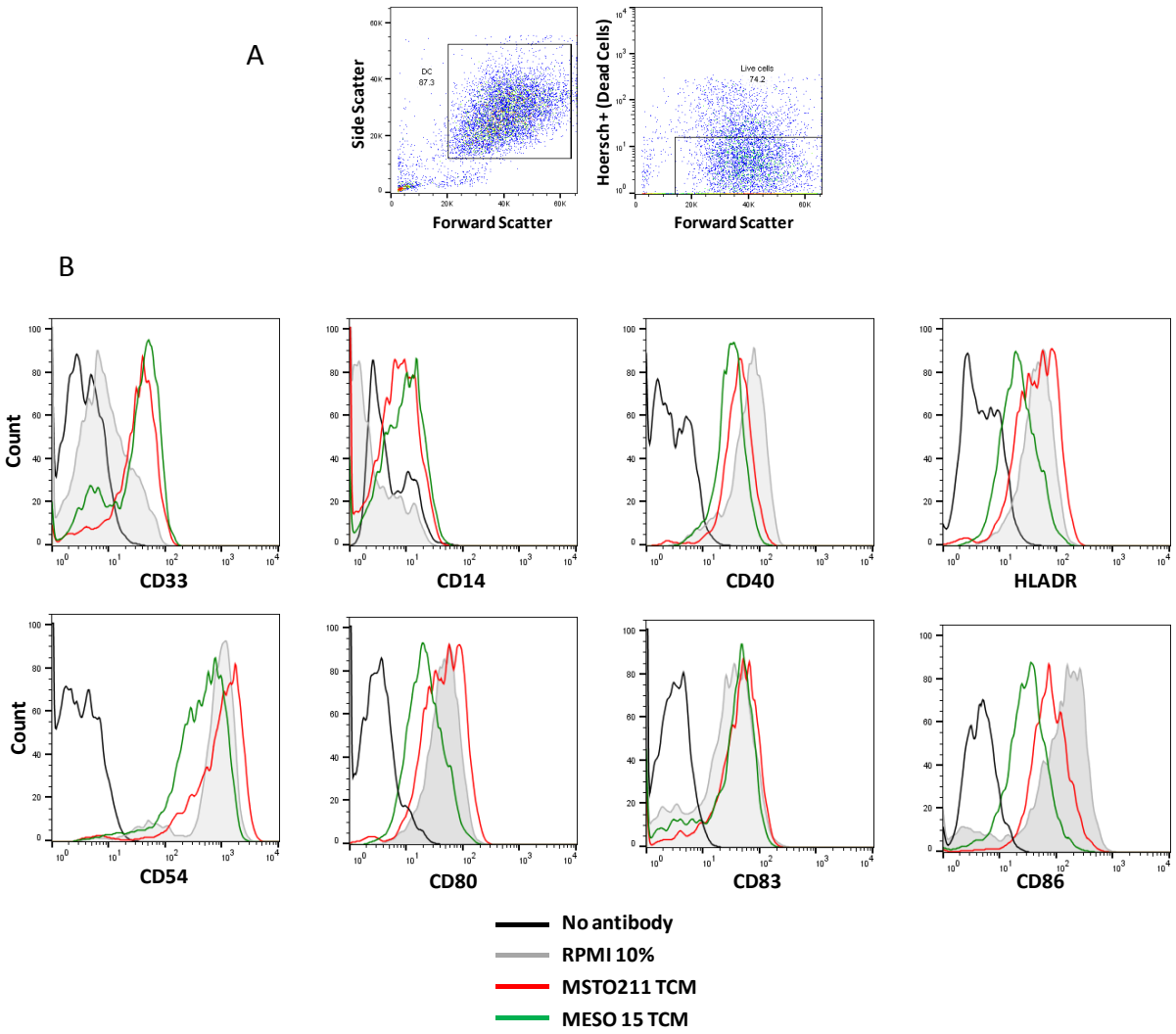

Figure 4. 11. The effects of mesothelioma tumour conditioned media on DC maturation (i)

DC were generated from healthy CD14+ monocytes, isolated from a leucocyte cone, in the presence of GM-CSF and IL-4. Control DC were generated in the presence of RPMI 10% and the effect of TCM tested through the addition of 25% TCM from 2 mesothelioma cell lines to cultures. Cells were treated with LPS for 12 hours on day 6 and examined by flow cytometry on day 7. (A) Gating of live DC. (B) Expression of surface markers of DC maturation (CD40, HLA-DR, CD54, CD80, CD83, CD86) and immaturity (CD14, CD33) were examined. Histograms show expression of markers on DC cultured in RPMI 10% (grey), MSTO211-H TCM (red) and Meso 15 TCM (green). Black histogram (No antibody) represents unstained DC.

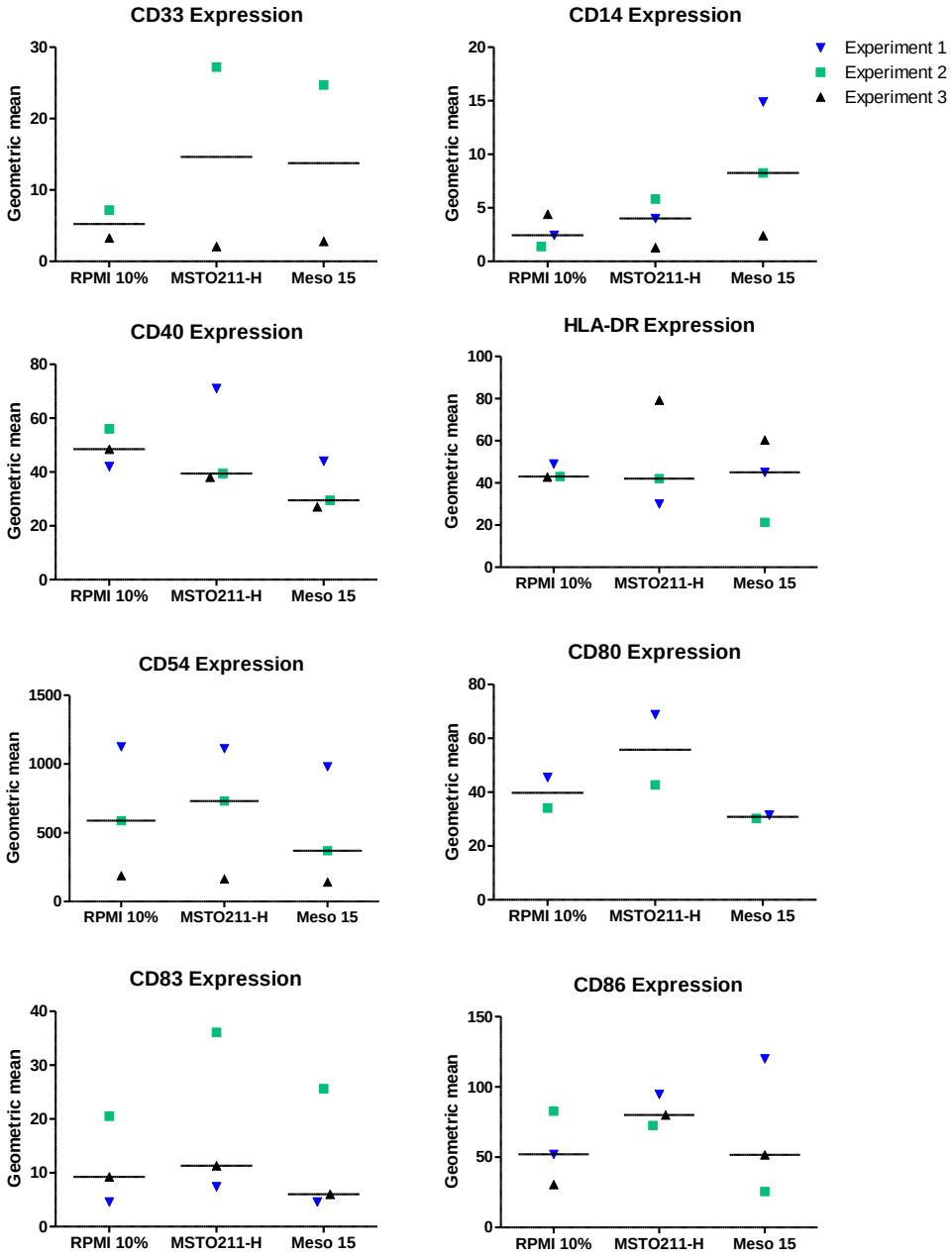

Figure 4. 12. The effects of mesothelioma tumour conditioned media on DC maturation (ii)

DC surface marker expression, following culture in TCM (as described in figure 4.11), was assessed in 3 separate experiments. Surface expression is represented as geometric mean with horizontal line demonstrating median expression. Statistical analysis of differences between groups was carried out using the Kruskal-Wallis test, with Dunn's correction for multiple comparisons. No statistically significant differences were observed.

As there were no significant differences in the surface expression of co-stimulatory molecules this could not account for the poor ability of TCM exposed DC to activate T cell proliferation. We therefore sought to determine whether STAT3 activation could be implicated as the mechanism behind impaired DC function and signalling.

The level of STAT3 expression was first assessed by qPCR and western blot following mesothelioma TCM exposure. Within DC exposed to TCM, an increase in STAT3 mRNA was observed, which was confirmed by western blot (Figure 4.13 A, C). Density ratios for STAT3 protein expression were 0.6 for DC cultured with no TCM exposure, compared to 1.0 and 0.9 for MSTO211-H and Meso 15 TCM, respectively. This did not reach significance following duplicate experiments, however, ($p=0.355$).

Within parallel experiments DC were treated with the STAT3 ASO. Significant reductions in both STAT3 mRNA and STAT3 protein were observed in all DC groups, $p=0.0034$ and $p<0.0001$, respectively (Figure 4.13 B, C). Analysis of the difference in STAT3 expression was carried out using a paired T test. Following this STAT3 knockdown, DC from both MSTO211 TCM and Meso 15 TCM groups demonstrated improvements in function, determined by their ability to stimulate T cell proliferation, suggesting a role of STAT3 in this mechanism. The observed rescue in DC cultured in the presence of TCM did not reach significance however, when analysed the Kruskal-Wallis ANOVA, with Dunn's correction for multiple comparisons (Figure 4.14 A, B).

To determine whether disruption of STAT3 signalling at different points within its pathway could also affect DC function, the JAK2 inhibitor, ruxolitinib, was also added to the culture of DC. In initial experiments significant toxicity was observed when added at the concentration

titrated within T cell experiments. Further titration required a dose 10 times lower than that used in T cell culture, implying a significant toxic effect caused by disruption of JAK2 signalling during DC maturation. T cell stimulation by DC was impaired by ruxolitinib when added to DC cultured in RPMI 10% and no rescue in proliferation was achieved by the addition of ruxolitinib to DC culture in the presence of MSTO211 or Meso 15 TCM (Figure 4.14, C). These findings are consistent with the documented effect of ruxolitinib induced JAK2 inhibition in monocyte derived DC by Heine *et al.* This study examined demonstrated that JAK2 inhibition significantly impaired DC generation and maturation, with impaired cytokine release, migration and subsequent lack of induction of T cell responses (384).

The experiments described above demonstrate that mesothelioma is capable of altering DC function, with impaired ability to stimulate T cell responses. There was no significant impairment of DC generation or maturation in DC exposed to mesothelioma conditions; however, enhanced STAT3 activity was observed. The reduction of STAT3 signalling, achieved using a targeted STAT3 ASO, led to partial rescue of the DC-T cell interaction, implying that hyperactivation of STAT3 could be implicated in this mechanism. Specific inhibition of STAT3 following hyperactivation may be therefore be a possible mechanism to improve both T cell and DC function in a tumour conditioned environment.

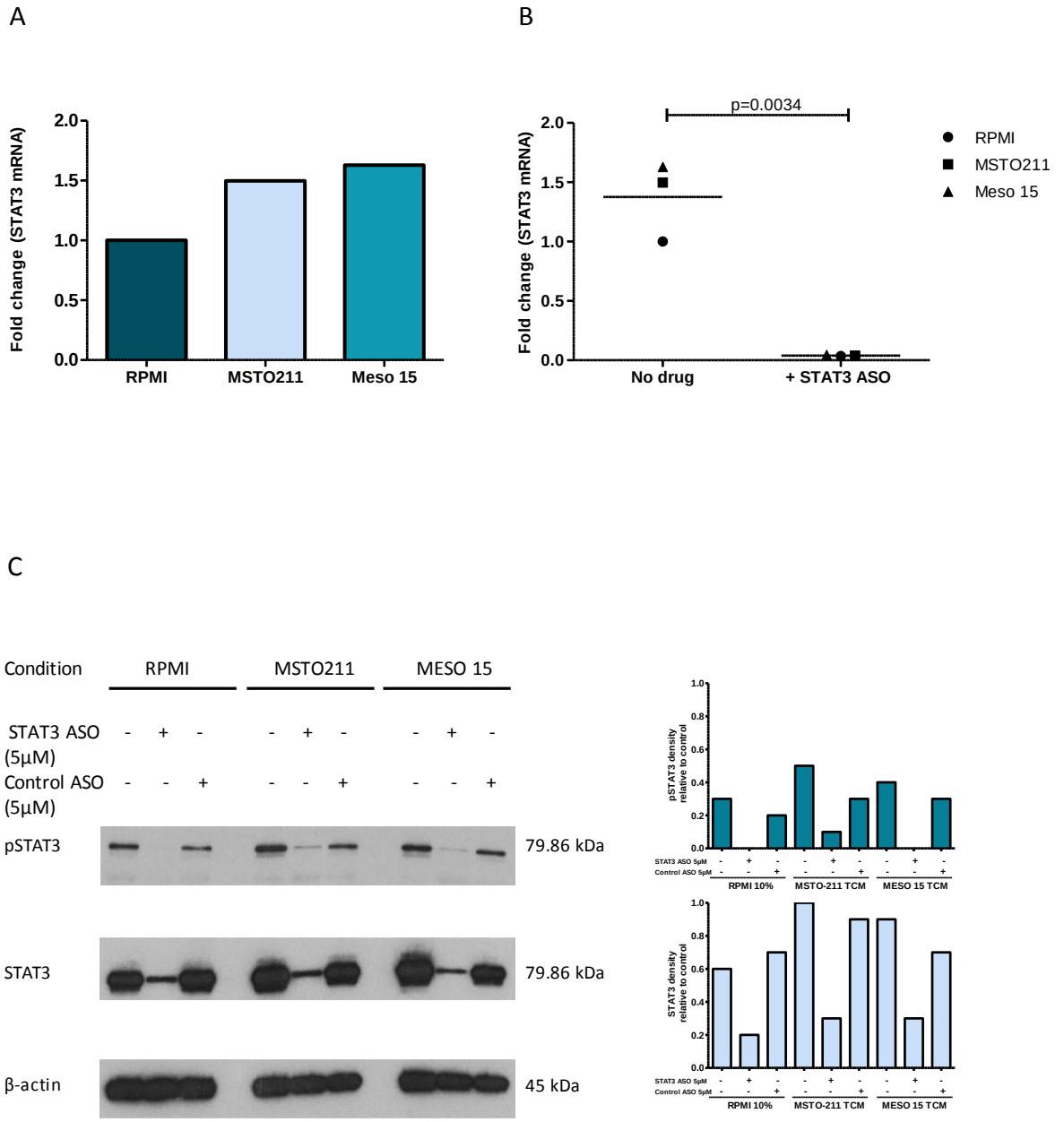

Figure 4. 13. The effect of JAK2 versus STAT3 inhibition on the ability of DC to stimulate T cell proliferation

(A) DC were generated in the presence of RPMI 10% or 25% mesothelioma conditioned media (TCM) from MSTO211-H and Meso 15, as described above. Within DC exposed to TCM, an increase in STAT3 mRNA was observed. These changes did not show significance following replicate experiments. Within parallel experiments DC were generated in the presence of a STAT3 ASO. Significant reductions in STAT3 mRNA (B) and protein (C) were observed in all DC groups, p=0.0034 and p<0.0001, respectively. Statistical analysis was performed using a paired T test.

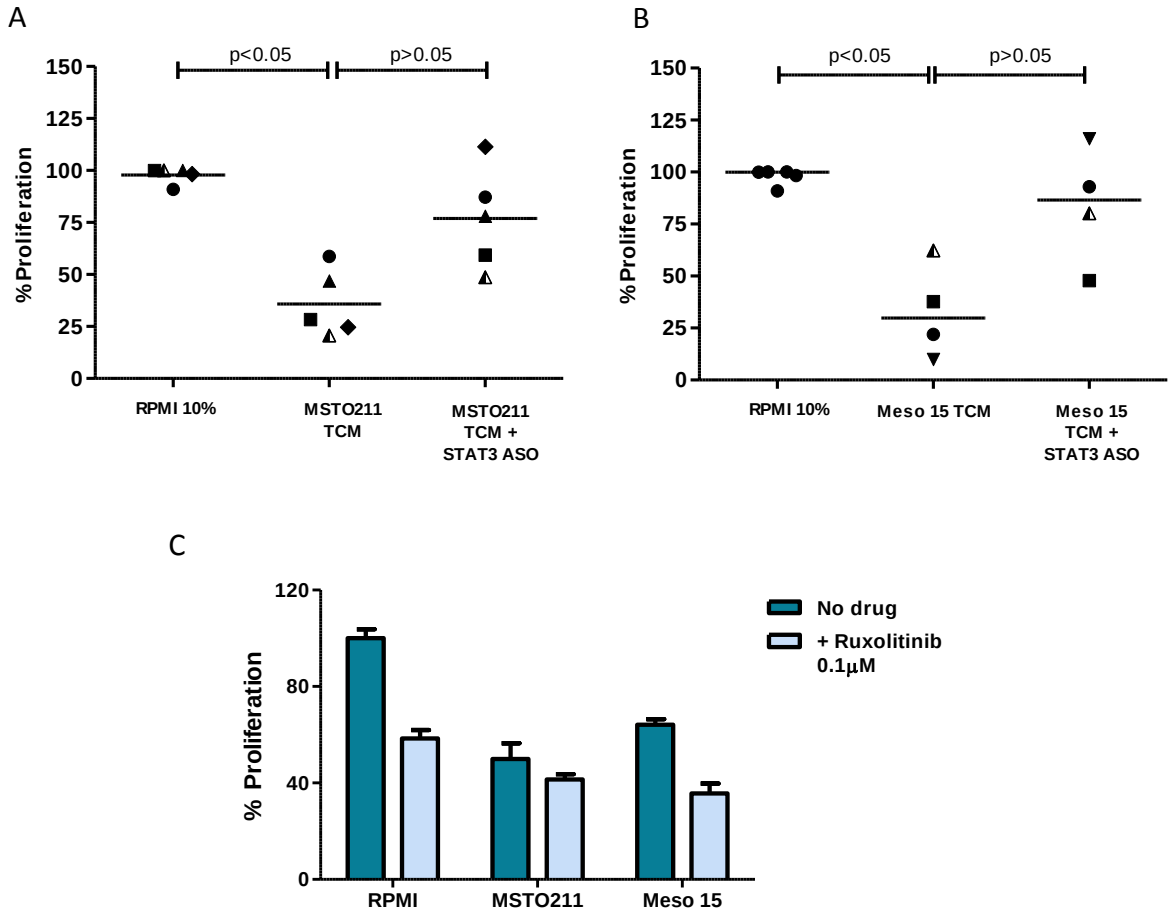

Figure 4. 14 The effect of JAK2 versus STAT3 inhibition on the ability of DC to stimulate T cell proliferation

DC were generated in the presence of RPMI 10% or 25% TCM from mesothelioma cell lines MSTO211-H and Meso 15. Additional DC were cultured for each condition in the presence of the STAT3 ASO and the JAK2 inhibitor, ruxolitinib. Cells were harvested at day 6 and re-plated within T cell proliferation assays. (A, B) STAT3 knockdown led to improvements in T cell proliferation following stimulation by DC cultured with both MSTO211 (n=5) and Meso 15 TCM (n=4). This did not reach significance when replicate experiments were analysed. (C) The addition of ruxolitinib impaired the ability of DC to stimulate T cell proliferation and did not result in improved function of DC cultured with mesothelioma TCM. Statistical analysis was performed using a Kruskal-Wallis ANOVA, with Dunn's correction for multiple comparisons.

4.2 Discussion

This study has demonstrated that in the setting of mesothelioma T cell function is significantly impaired through the actions of tumour related cytokines and this may be a result of STAT3 activation. Within these experiments, the release of IFN-γ, the primary cytokine required for T cell cytotoxic function and driver of cytotoxic T cell differentiation, was reduced through culture in the presence of mesothelioma factors. In addition, this was associated with a remarkable impairment in T cell proliferation, in contrast to un-exposed controls. The early induction of STAT3 phosphorylation and subsequent enhanced STAT3 transcription is of vital importance as a possible mechanism of T cell dysfunction, due to the significant inhibitory effects STAT3 hyperactivation is known to promote in T cells (385). Mesothelioma is known to have a highly inflammatory environment and, as discussed in chapter 3, was proven in this setting to produce cytokines capable of STAT3 activation including IL-6, IL-8 and VEGF. Through individual examination of these cytokines it was demonstrated that IL-6 was the only cytokine capable of inducing the same profile of STAT3 phosphorylation as mesothelioma TCM. In addition, blocking the action of IL-6 using a soluble inhibitor was able to reverse this activation, confirming that IL-6 is the main driver of STAT3 phosphorylation in this setting.

Whether manipulation of STAT3 within T cells could alter the response to mesothelioma was therefore the primary question. We attempted to answer this through the inhibition of STAT3 signalling using an antisense oligonucleotide (ASO), which could specifically target STAT3. During our experiments it became apparent that the effect of the ASO within T cells was limited, with only minor reductions in the expression of STAT3 mRNA and protein being achieved. This was in contrast to levels of reduction observed in other cell types such as the T cell leukaemia cell line, JURKAT, and dendritic cells. Despite attempts to enhance ASO action

via transfection reagents, comparable reductions in T cells were not achieved. This implied that either the uptake of the ASO by T cells was in some way impaired, or that STAT3 activation in this setting could not be so robustly overcome by the ASO. The manufacturer of this oligonucleotide did not describe difficulties in free-uptake of this ASO when tested in a number of solid tumour or haematological cancer cell lines; however, to our knowledge, function in healthy human T cells was not investigated (386). Difficulties in human T cell transfection are commonly encountered (387), leading to the development of transfection methods such as virus-transfection and electroporation to enhance the entry of desired genes, therefore investigation of enhanced ASO function using these methods should be carried out.

Despite the limitations in STAT3 inhibition using this ASO in T cells, improvements in T cell function were observed in treated T cells, implying that partial inhibition of STAT3 in this setting was resulting in partial T cell rescue. In view of these findings, we sought to alter T cell signalling via STAT3 at an alternative point within the pathway, utilising the JAK2 inhibitor ruxolitinib. Use of this inhibitor did not substantially reduce STAT3 expression within treated T cells and did not result in superior rescue. Although marketed as a JAK2 inhibitor, it is known that ruxolitinib is not specific to this tyrosine kinase and is known to inhibit over 30 cellular kinases (388). Of particular relevance, ruxolitinib was shown to cause almost 100% inhibition of both TYK2 and JAK1 (388), which are required within the signalling pathway of STAT1 (389). This therefore accounts for the profound reductions in STAT1 mRNA, which were not observed with the use of the ASO. As discussed within the introduction, STAT1 is a vital component of the signalling cascade during T cell activation, required for T cell proliferation and survival (380,381). These findings therefore support the theory that impaired STAT1

signalling could be the mechanism behind poor T cell rescue achieved with ruxolitinib and support the use of specific inhibitors to target STAT3.

Within dendritic cells, impaired ability to drive T cell proliferation following exposure to mesothelioma conditioned media was also observed. Despite this, generation and maturation of DC did not appear to be significantly altered. The role of STAT3 in this setting was therefore investigated and increases in the transcription of STAT3 mRNA and small changes in STAT3 phosphorylation and protein expression following exposure to mesothelioma conditioned media were observed. In order to demonstrate the functional significance of these subtle changes, DC were generated in the presence of the STAT3 ASO. Interestingly, following treatment of DC with the STAT3 ASO, far greater STAT3 inhibition was induced than that achieved with T cells, despite delivery methods to DC and T cell groups being identical. The observed STAT3 reduction appeared to translate to improvements in DC function, with enhanced T cell stimulation achieved by DC treated with conditioned media from 2 separate cell lines, although these findings did not reach significance upon statistical analysis. In a separate experiment using ruxolitinib, a similar lack of response was observed with DC as had been seen in T cells, likely due to similar effects on the signalling of other STATs. This is not surprising in view of the defects in DC maturation and function that ruxolitinib has proven to induce in vivo (384).

The findings in this study clearly demonstrate that mesothelioma is capable of inducing defects in the function of T cells and DC, and that these effects are mediated by factors released by this tumour into the microenvironment. The data obtained support the theory that within T cells, suppression of their function is due to IL-6 driven STAT3 activation. As shown by others, this IL-6/STAT3 driven phenotype is unable to produce sufficient IFN-γ to

support T cell differentiation, due to the induction of SOCS1 (390), subsequently leading to impaired T cell proliferation and, in a tumour microenvironment, impaired T cell tumour infiltration (385). In addition, STAT3 activation may propagate its own activation through further release of immunosuppressive factors such as IL-10 and TGF-β (391). Further to this, recent work by Cuicci *et al* has demonstrated that STAT3 activation within cytotoxic T cells is also capable of inducing the expression of RORγt which led to blockade of the functions of transcription factors T-bet and Eomesodermin, which are required for successful CD8+ T cell differentiation and function (392).

Within the setting of DC, STAT3 activation also appears to be driving the dysfunction observed. DC dysfunction has been reported in a number of cancer settings, with numbers 2 to 4 times lower than healthy comparators (393,394), along with defects in the expression of co-stimulatory molecules CD80, CD86 and MCH Class II (HLA-DR) (199,395). STAT3 activation within DC, driven by tumour derived factors, in particular IL-6, has been shown to be the main pathway restricting DC development (382,396). This was confirmed through the rescue of DC maturation and function using STAT3 inhibition (397). Such changes in DC profiles have been observed in mesothelioma patients and importantly have prognostic implications, with correlation between the presence of functional DC and patient survival (199).

Taken together, these findings indicate that the mesothelioma tumour environment contains factors which are capable of driving STAT3 activation in both T cells and DC. This activation is likely to propagate the release of further immunosuppressive factors and result in an incompetent immune response. Impaired T cell activation as a result of DC dysfunction is compounded by reduced T cell ability to differentiate and proliferate as effector T cells and a STAT3-high environment, further propagates this phenotype. Further work in this area is

required, particularly to obtain superior reduction in T cell STAT3 expression; however, the targeted inhibition of STAT3 using molecules such as ASOs, may be a new area of targeted immunotherapy which could significantly alter patient outcomes.

Chapter 5: Manipulation of the immune microenvironment through check point blockade

5.1 Introduction

The ability of STAT3 activation to induce cross talk within the tumour micro-environment is further enhanced through its ability to activate the expression of immune check points. The utility of immune check points as a means to alter the host response to cancer has become hugely relevant over the last 10 years owing to the development of effective targeted agents, which have dramatically altered patient outcomes in a number of malignancies. The most prominent targets for check point manipulation are the T cell surface molecules CTLA-4 and PD-1, along with the PD-1 ligand PD-L1, expressed on several different immune cells, as well as tumour tissue.

CTLA-4 was the first immune check point to be successfully targeted within cancer (351). Expressed on T cells, this molecule is rapidly up-regulated following T cell activation and competes with CD28 on T cells for the co-stimulatory molecules CD80 and CD86 (398). This competitive activity slows the T cell response to antigen-specific activation, resulting in reduced proliferation and IL-2 production, therefore muting the immune response (399). Similarly PD-1, expressed on antigen specific T cells, is up-regulated following antigen activation and through engagement with its ligand, PD-L1, results in reduced T cell proliferation, cytokine release and apoptosis (267,400). PD-L1 is expressed on many cell types including macrophages, dendritic cells, B cells and T cells (270,272), in addition to a number of epithelial tissues (268). It's expression is also up-regulated during T cell activation, driven by inflammatory factors such as IFN-γ and TNF-α (401), leading to suppression of the T cell

response. In healthy individuals, the presence of these inhibitory molecules are required to maintain immune system homeostasis; however, it is the aberrant expression of these molecules which have led to the story of their success in the setting of cancer, as tumour tissues manipulate these pathways to create T cell tolerance and immune escape.

PD-L1 is up-regulated in a number of malignancies including lung cancer (402), melanoma (403) and breast cancer (299). There is partial overlap of PD-L1 expression and high mutational load in tumours (404) and, corresponding to this, the relationship between response to PD-1 and PD-L1 blockade and mutational load has been shown to be significant in both melanoma and NSCLC (405). In colorectal cancer, where responses to PD-1 and PD-L1 inhibition have been poor, a sub-group of MMR deficient, mutation-high tumours, have also been shown to have higher response rates to checkpoint inhibition (406,407). There are currently no PD-1 or PD-L1 modulatory therapies licensed for use in the setting of colorectal cancer therefore recent investigations have aimed to detect sub-populations that may benefit from immune blockade. These studies have demonstrated that tumours with deficient expression of mismatch repair proteins, which carry higher mutational burden (408), show higher PD-L1 expression, particularly when both tumour cell and tumour infiltrating immune cell expression is taken into account (409).

The mechanisms of both PD-1 and PD-L1 up-regulation in cancer are complex, owing to their expression on a variety of different cell types. Despite this, throughout the literature there is a prominence of STAT3 involvement. For PD-L1, pathways involving interferon regulatory factor 1 (IGRF1) (292), NMP/ALK signalling via ERK phosphorylation (295) and activation of phosphatidylinositol-3-OH kinase (PI3K) (296) have all been implicated. However, JAK/STAT inhibition was shown to reduce the expression of PD-L1 driven by IGF1 and, an additional

pathway involving NMP/ALK signalling in T cell lymphoma, demonstrated that NMP/ALK activation of STAT3 led to direct binding to the PD-L1 promoter, resulting in enhanced expression (294). In addition, within nasopharyngeal carcinoma, the EBV-induced latent membrane protein 1 (LMP1) was shown to increase PD-L1 expression via STAT3 activation (410). Within APCs, STAT3 was shown to be the primary signalling pathway responsible for PD-L1 up-regulation in populations of immature, tolerogenic DCs (411). Interestingly, this paper also demonstrated that this inhibitory APC population produced immunosuppressive cytokines IL-10 and IL-6, which could therefore both maintain STAT3 expression and lead to inhibitory actions on surrounding T cells.

For PD-1, its major regulator of expression is the transcription factor NFATc1. Activated following TCR stimulation, NFATc1 binds to a conserved region of the Pdcd1 gene regulating PD-1 expression (412), thus providing a self-regulatory circuit within the T cell. Upon identification of additional distal binding sites on the Pdcd1 gene, further regulators STAT3 and STAT4 were identified, activated through IL-6 and IL-12 stimulation of T cells, respectively (413).

Following the expression of PD-1 and PD-L1 on immune populations, significant restriction of the immune system is observed. Interaction of immature DC with CD8+ T cells was shown to induce populations of tolerant, non-activated T cells through the expression of PD-1 and CTLA-4 on their surface. This was confirmed by the removal of PD-1 expression in an identical setting resulting in T cell priming, despite the DC still remaining in an immature state (414). This negative interaction is enhanced in the setting of cancer, demonstrated by significantly increased expression of PD-L1 in monocytic DC extracted from the lymph nodes of patients with ovarian cancer, compared with non-cancerous subjects. These DC released increased

concentrations of the immunosuppressive cytokine IL-10 and led to reciprocal IL-10 release from T cells, which were also suppressed in their proliferative ability (270). Blockade of PD-L1 on DC, reversed this effect, leading to the release of the pro-inflammatory cytokines IL-12 and IL-10, in addition to enhanced T cell proliferation and slowed tumour growth within a murine model (270).

The induction of PD-1 PD-L1 signalling is not restricted to DC however, with evidence that populations of suppressive MDSC, macrophages and neutrophils are also acting via this pathway. MDSC have been shown to reduce the effect of PD-L1 blockade, with evidence that reducing the number and function of G-MDSC in the tumour environment in head and neck cancer, led to an improved response to PD-L1 therapy (415). Reduction in numbers of G-MDSC was achieved through PI3K inhibition, which resulted in reduction of the immunosuppressive factors arginase-I and iNOS, which were believed to be the mechanisms behind improved T cell responsiveness. The expression of PD-L1 on this population of G-MDSC was not assessed, therefore it is unclear whether signalling between G-MDSC and T cells had an impact on outcome. A murine study focussing primarily on tumour infiltrating monocytes confirmed that the use of an inhibitor against the colony stimulating factor receptor 1 (CSF-1), achieved successful reduction in numbers of PD-L1 positive splenic, but not tumoural, suppressive monocytes in tumour bearing mice (416). This was associated with increased numbers of circulating and tumour infiltrating CD8+ T cells, with increased levels of T cell activation, despite no reduction in tumour infiltrating monocytic MDSC. Furthermore, when anti-CSF-1 treatment was used in combination with a PD-L1 inhibitor numbers of tumour infiltrating monocytic MDSC were successfully reduced and a profound improvement in tumour response was observed (416). With the focus changing to granulocytes, Wang *et al*

demonstrated that within gastric cancer, tumour derived GMCSF was capable of enhancing the expression of PD-L1 on tumour associated granulocytes through the activation of JAK2/STAT3. These PD-L1 expressing populations were in turn capable of inhibiting T cell proliferation and IFN-γ production and this affect was reduced by the inhibition of PD-L1 on granulocytes (417). Interestingly, recent research has identified that high patient neutrophil counts, with resultant increases in NLR, have a significant negative effect on the efficacy of immune check point blockade and can predict both response and survival (418-420). From these findings it can be inferred that there is significant interplay between tumour associated and circulating myeloid cells, in particular granulocytes, with enhanced T cell suppression occurring via the PD-1/PD-L1 pathway. Through manipulation of both sides of the suppressive environment with a reduction of both the number of immunosuppressive cells, in addition to inhibiting the PD1/PD-L1 interaction, it can be hypothesised that improvements in therapeutic response to check point inhibitors can be achieved.

In view of the complexity of the cellular cross-talk in cancer described above, we wished to determine whether treatment with either PD-L1 or PD-1 blockade, could lead to a reduction in cancer associated granulocytes in cancer patients, and whether their suppressive activity could be reversed through this mechanism. Within Chapter 1, it was demonstrated that within the tumour microenvironment PD-1 expression is enhanced in intra-tumoural T cells. Although the mechanism by which this up-regulation was regulated was not determined, STAT3 activation could be a prominent driver, as described above. A hypothesis was therefore generated that in addition to the identified suppressive effect of granulocytes, the inflammatory micro-environment within mesothelioma could be activating the PD-1/PD-L1

pathway, further reducing the ability of T cells to effectively detect and respond to tumour growth.

Current clinical trials examining the effects of PD-1 and PD-L1 inhibition are ongoing in a number of cancer types currently; however, within the time constraints of this PhD, access to specimens from a mesothelioma trial was not possible. It was therefore decided to study this mechanism within the setting of NSCLC, as it is possible that the principles of immune evasion are occurring in both tumour types. Samples were accessed from 2 clinical trials, The National Lung MATRIX trial (MATRIX) and PEPS-2, which utilised differing approaches to PD-1 pathway disruption.

MATRIX, which is primarily designed to study precision medicine through providing targeted treatments to patients with NSCLC, incorporated an additional arm to enable those with no activating mutation to obtain a novel therapy. This arm provided a PD-L1 inhibitor, Durvalumab, which has evidence of activity in NSCLC (421). PEPS-2 was designed to assess the efficacy of, and tolerance to, the PD-1 antibody, Pembrolizumab, in performance status 2 patients. Pembrolizumab had previously demonstrated improved PFS and OS in a phase III clinical trial in NSCLC which had not included PS-2 patients (301). In view of the fact that many lung cancer patients present with multiple co-morbid conditions and with advancing age, there is a real clinical need to explore treatments in patients with poorer PS.

In addition to analysing the effect on granulocytes and T cells, a comprehensive exploratory analysis of monocytes was planned. Analysis of cell surface markers at baseline and sequential time points following treatment was planned, along with assessment of the suppressive activity of myeloid populations at baseline and post-treatment time points. Analysis of

changes in blood parameters and their association with patient factors and outcome was also planned.

5.2 Results

5.2.1 The collection of whole blood specimens from patients with lung cancer

The collection of whole blood specimens from patients with NSCLC (adenocarcinoma or squamous cell carcinoma), was carried out as part of the two clinical trials described above, MATRIX and PEPS2. In order for patients to be eligible for participation in MATRIX, they were required to have a histological diagnosis of NSCLC of either stage III or IV, and have failed at least one line of standard treatment, with documented radiological evidence of progressive disease. Patient tumour samples were required to have completed the screening process for actionable mutations and have sufficient tissue for PD-L1 staining by IHC. Performance status was required to be WHO 0-1 to meet eligibility. PEPS2 required patients to have a histologically confirmed diagnosis of NSCLC, with PD-L1 status confirmed by IHC. In contrast to MATRIX, this population were not required to have received prior lines of therapy and were eligible only if their performance status was WHO 2. This variability in patient criteria may lend itself to the enrolment of very different groups of patients, with baseline variations in their inflammatory profile.

From the cohort of patients for MATRIX 20 samples were collected at enrolment, 17 at week 2, 10 at week 6 and 8 at treatment completion. These specimens were not consistently sequential, with only 6 patients with all 4 time points, 9 patients with 3 time points and 14 patients with time-points 1 and 2 (Table 5.1). PEPS2 provided a more extensive patient cohort, providing 46 samples at time point 1, 24 samples at time point 2 and 19 samples at time point 3 (Table 5.2).

Patient characteristics for both trials are displayed in Tables 5.1 & 5.2. For MATRIX, the median age of patients was 65 (range 50-78), 48% were male, 56% had a diagnosis of adenocarcinoma and 32% squamous cell carcinoma, in 12% the histology was unspecified. 28% of patients were stage III and 32% stage IV, 36% did not have their stage recorded. All patients enrolled in the trial were WHO PS 0-1. All MATRIX patients had received at least 1 prior treatment, with 40% having received 2 lines, 16% 3 lines and a further 16% receiving 4 lines before enrolment. Data on tumour PD-L1 positivity was not routinely collected therefore this was not available for inclusion within the analysis.

Within PEPS2, median age of patients was 70.3 (range 43-87) and 55% were male. Data on cancer subtype or stage was not collected upon trial registration. The range of PD-L1 positivity was 0-100%, with a mean of 26.3%. All patients were required to be WHO PS 2. 83.6% of patients had received previous lines of treatment, with 23.6% receiving 1 line of treatment, 32.7% 2 lines, 18.2% 3 lines and 9.1% 4 lines prior to trial enrolment.

Throughout this chapter, for ease of interpretation, all data relating to PEPS2 is represented in black, MATRIX in blue and healthy controls in red.

Table 5. 1. Patient characteristics of National Lung Matrix Trial specimens

Patient Characteristics (n=25)	
Variable	n (%)
Age	
Median (range)	67(50-78)
Sex	
Male	12 (48)
Female	13 (52)
Histology	
Adenocarcinoma	14 (56)
Squamous cell carcinoma	8 (32)
Unknown	3 (12)
PD-L1 Status	
Median (range)	Unknown
Cancer Stage	
III	7 (28)
IV	8 (32)
Unknown	9 (36)
Performance Status	
0-1	25 (100)
2	0 (0)
Previously treated	
Yes	25(100)
No	0(0)
Previous lines of treatment	
1	7(28)
2	10(40)
3	4(16)
4	4(16)
Sample collection	
Time point 1: Pre-treatment	23
Time point 2: 2 weeks	19
Time point 3: 6 weeks	13
Time point 4: End of treatment	12

Table 5. 2 Patient characteristics of PEPS2 trial specimens

Patient Characteristics (n=55)	
Variable	**n (%)**
Age	
Median (range)	70.3 (43-87)
Sex	
Male	30 (55)
Female	25 (45)
Histology	
Adenocarcinoma	Unknown
Squamous cell carcinoma	Unknown
PDL1 Status	
Mean (range)	26.3% (0-100)
Cancer Stage	
III	Unknown
IV	Unknown
Performance Status	
0-1	0
2	55 (100)
Previously treated	
Yes	46 (83.6)
No	9 (16.4)
Previous lines of treatment	
1	13 (23.6)
2	18 (32.7)
3	10 (18.2)
4	5 (9.1)
Sample collection	
Time point 1: Pre-treatment	46
Time point 2: Cycle 2	24
Time point 3: Cycle 4	19

5.2.2 The detection of abnormal immune populations in patients with lung cancer

In order to determine whether the principles of the findings in patients with mesothelioma could be applied to patients with lung cancer, we hypothesised that an abnormal inflammatory environment, equivalent to that demonstrated in patients with mesothelioma, was also likely to exist in patients with lung cancer. It has previously been demonstrated that neutrophil to lymphocyte ratio in NSCLC is significantly increased and has prognostic relevance (422,423), with granulocytes also representing the most abundant tumour infiltrating population in the setting of NSCLC (424), therefore we were confident that the principles applied were comparable. In order to confirm these findings in this setting, relative percentages of whole blood monocytes, granulocytes and lymphocytes were examined, in the blood of patients with NSCLC. Patients enrolled into either MATRIX or PEPS2 provided baseline whole blood samples which were processed as described in chapter 2. Whole blood analysis was performed through flow cytometry to detect the presence of immune populations. Gradient separation with the use of Lymphoprep, was also performed to allow analysis of the PBMC compartment.

In concordance with the findings in mesothelioma patients, abnormal populations of circulating granulocytes were detected in both patient cohorts. Patients within PEPS2 had a median percentage of 60.3% (range 20.1 to 87.6), versus 34.5% (range 15.1 to 66.4) in healthy comparators (Figure 5.1, A). Within patients enrolled in MATRIX a similar distribution was observed with median percentage of whole blood granulocytes of 56.6% (range 21.4 to 84.2), versus 35.9% (range 16.7 to 53.9) in healthy comparators. (Figure 5.1, B). These differences were highly significant with a p value of 0.0001 (analysed using a non-parametric Mann Whitney U test).

Due to the increased percentages of granulocytes, the relative percentage of T cells was significantly reduced in both cohorts (Figure 5.1 C, D), with resultant increases in Neutrophil to Lymphocyte ratios (NLR). Patients within PEPS2 and MATRIX demonstrated average NLR values of 5.7 and 5.4, respectively, compared to 1.2 within healthy donors (Figure 5.1 E, F). These findings imply that, as within patients with mesothelioma, NSCLC is associated with an abnormal inflammatory environment, with higher numbers of whole blood circulating granulocytes and resultant increases in neutrophil to lymphocyte ratios.

In addition to abnormal granulocyte populations, higher percentages of CD14+ monocytic cells were also detected within the blood of patients from both PEPS2 and MATRIX trials. Within patients in PEPS2 and MATRIX, the median percentage of detected CD14+CD11b+ cells was 5.9% and 6.7%, respectively, compared to 3.7% and 3.5% in the comparable healthy samples (Figure 5.2, A and B). These differences were again highly significant when analysed using a Mann Whitney U test, with p values of <0.0001.

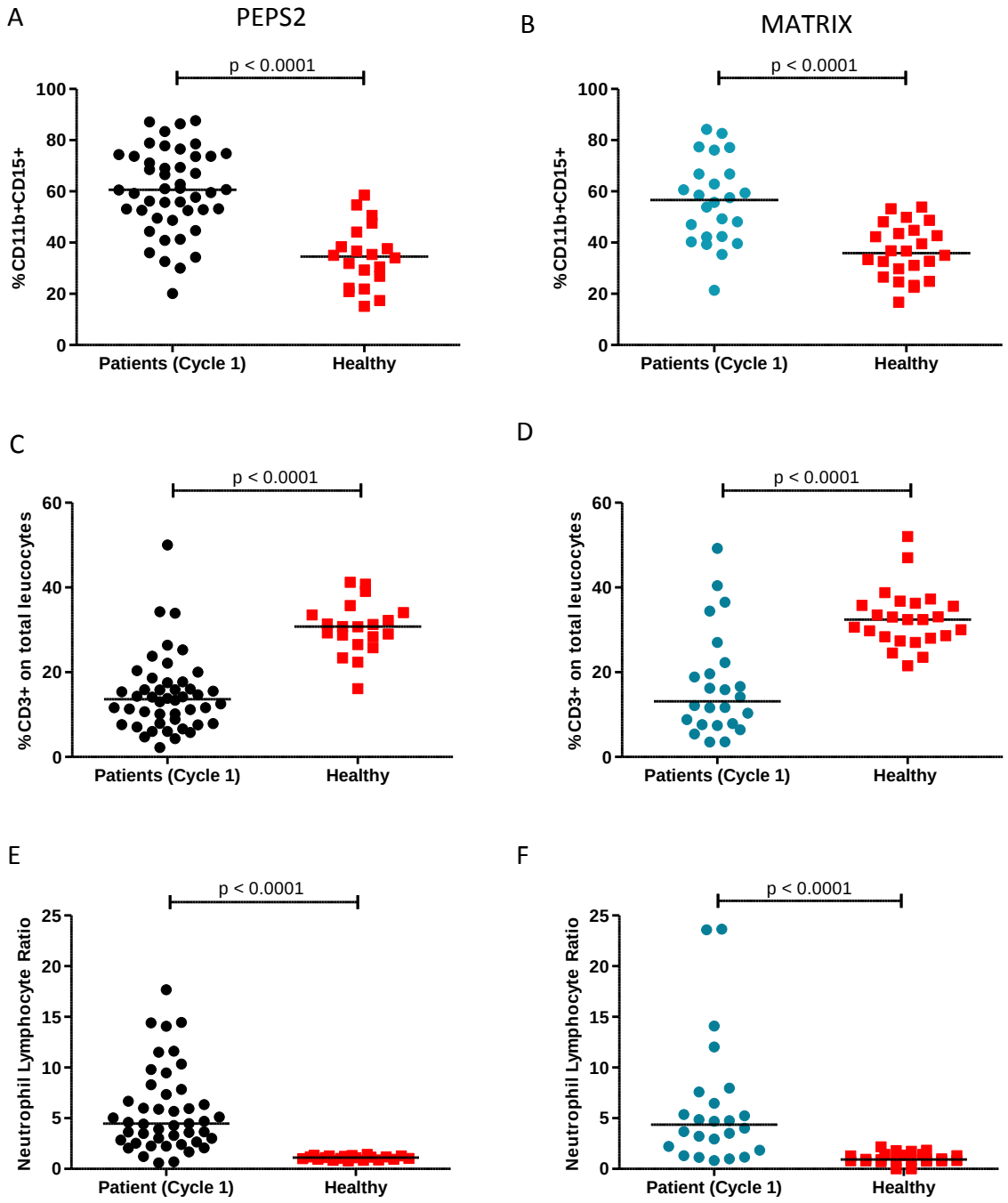

Figure 5. 1. Patients with NSCLC demonstrate abnormal peripheral blood profiles

Blood was sampled from patients with NSCLC participating within PEPS2 (black dots, n=46) and MATRIX (blue dots, n=24) clinical trials. Flow cytometry analysis of whole blood was performed alongside blood samples from healthy controls (red dots, n=20 & n=24, respectively). (A, B) Scatter plots demonstrate percentage of circulating CD11B+CD15+ granulocytes in patients and healthy controls. Increased percentages were observed in NSCLC patients, within both trial cohorts. (C, D) Scatter plots demonstrate percentage of CD3+ lymphocytes. Reduced percentages were observed in NSCLC patients. (E, F) The neutrophil to lymphocyte ratio (NLR) was calculated for trial patients and healthy controls. Scatter plots show an increase in NLR in patients, compared to healthy controls. Horizontal lines represent median values. Statistical analysis was performed using a Mann Whitney U test.

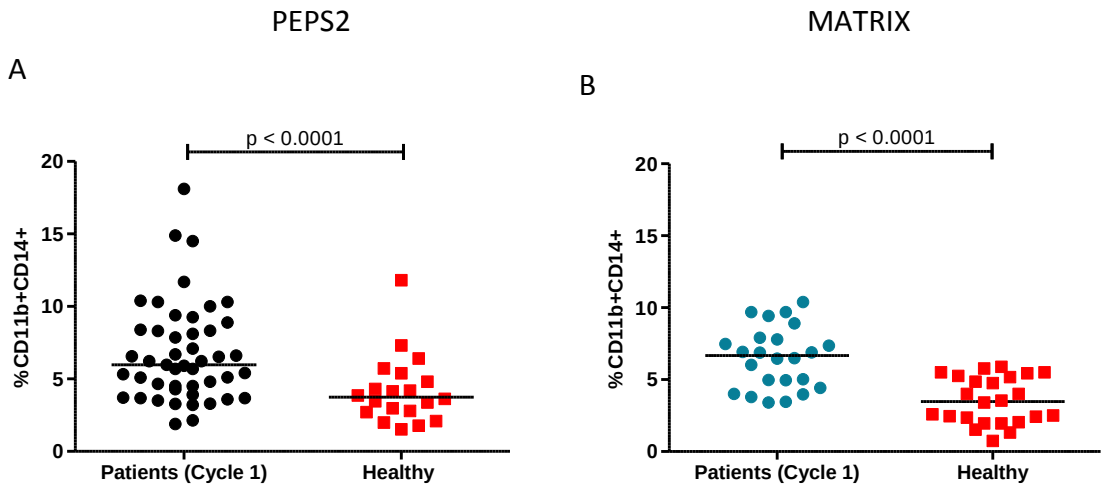

Figure 5. 2. Patients with NSCLC have increased percentages of CD14+ monocytic cells

Blood was sampled from patients with NSCLC participating within PEPS2 (black dots, n=46) and MATRIX (blue dots, n=24) clinical trials. Flow cytometry analysis of whole blood was performed alongside blood samples from healthy controls (red dots, n=20 & n=24, respectively). Scatter plots demonstrate the percentage of CD11b+CD14+ monocytic cells in the blood of patients from both (A) PEPS2, and (B) MATRIX. CD11b+CD14+ percentage was significantly higher than within healthy control samples. Horizontal lines represent median values. Statistical analysis was performed using a Mann Whitney U test.

5.2.3 The expression of cell surface signalling proteins is not significantly altered in circulating immune cells in NSCLC

Further analysis of both circulating granulocytes, monocytes and T cells was carried out to assess their expression of the major histocompatibility complex molecule HLA-DR (Class II MHC), in addition to the checkpoint signalling molecules PD-L1 and PD-1. Both granulocytic and monocytic populations were assessed to determine the presence of HLA-DR negative subgroups, incapable of antigen presentation and immune activation, compared to healthy donors.

As expected, granulocyte populations demonstrated lower HLA-DR expression than monocytic populations; however, there were large variations in expression in both groups. No HLA-DR negative sub-population was identified within patient samples, when compared to healthy controls (Figure 5.3 A-D).

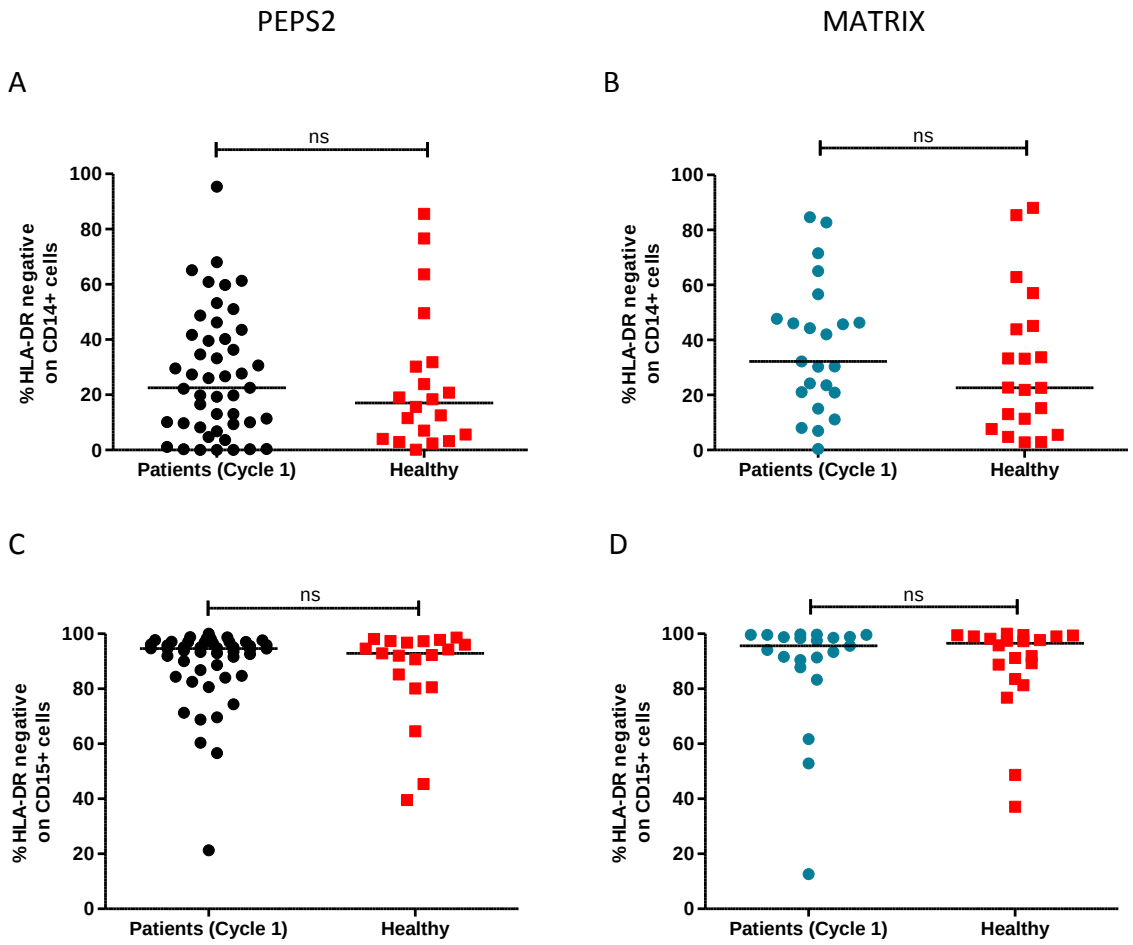

Figure 5. 3. HLA-DR expression is not altered on myeloid populations in patients with NSCLC

(A) Scatter plot demonstrates flow cytometry analysis of whole blood CD14+HLA-DR-. Percentage CD14+HLADR- cells are shown for PEPS2 patients (black dots, n=46) and healthy controls (red dots, n=20). (B) Percentage CD14+HLADR- cells are shown for MATRIX patients (blue dots, n=23) and healthy controls (red dots, n=20). (C, D) Percentage CD15+HLA-DR- cells in PEPS2 and MATRIX patients, alongside healthy controls. Horizontal lines represent median values. Statistical analysis was carried out using a Mann Whitney U test.

Whole blood granulocyte populations did not demonstrate significantly higher expression of PD-L1 when compared to healthy controls in either PEPS2 or MATRIX. The median PD-L1 expression seen on granulocytes obtained from PEPS2 was 10.5%, with a range from 0.5% to 48.8%. Within samples from MATRIX median PD-L1 expression was 5%, with a range from 0.2% to 31.5%. Healthy granulocyte samples showed median PD-L1 expression of 6.6% and 3.3%, respectively (Figure 5.4 A, B). Tumour associated granulocytes could not be assessed due to the nature of the trial samples.

Whole blood monocytes demonstrated overall higher surface expression of PD-L1 although, as seen with HLA-DR expression, PD-L1 expression was widely variable between samples. Within PEPS2 median PD-L1 expression on CD14+ monocytic cells was 68.1%, ranging from 6% to 98.8%. Analysed healthy samples showed a similar range, between 3.8% to 82.6%; however, the median expression was significantly lower at 45.6% ($p=0.0084$, analysed by Mann Whitney U test). Samples obtained from MATRIX showed lower PD-L1 expression than that detected in PEPS2, with median expression of 45.7%, ranging from undetectable (0%) to 97%. This was not statistically different to healthy CD14+ PD-L1 expression of 30.5% (range 0.5-89%) in this cohort. (Figure 5.4 C, D). The two healthy comparator populations were not statistically different.

Circulating T cell expression of PD-1 was also assessed within both trial populations. Within PEPS2 the median level of PD-1 expression on patient T cells was 27.3%, ranging from 2% to 52.5%. This was significantly higher when compared to 18% (range 9.5-24.5%) in healthy comparators, $p=0.0084$ (Mann Whitney U test) (Figure 5.4 E). In patients within MATRIX, there was no statistical difference to healthy comparators in the expression of PD-1 on T cells, consistent with the findings of lower PD-L1 expression on CD14+ cells. Median PD-1

expression on T cells was 19.4%, ranging from 6% to 40%. Healthy samples showed a median expression of 17.2% (range 9.5-33%) (Figure 5.4 F).

In view of the trial design of PEPS2, PD-L1 expression within tumours was also carried out as part of trial enrolment. This was not performed within our laboratory, but results were made available to us as part of the sample analysis. Expression was variable with samples showing ranges from 0 to 100% PD-L1 expression. Median PD-L1 expression within tumour samples was 4%, owing to a large number of samples with very low expression. Of the 55 patients included in this analysis, 24 samples (52.2%) showed no PD-L1 expression, 16 samples (34.8%) showed expression between 1 and 49% and the remaining 14 samples (30.4%) showed PD-L1 expression >50% (Figure 5.5 A). One patient had no recorded tumour PD-L1 expression. When examining the PEPS2 cohort there was no correlation between tumour PD-L1 expression, circulating granulocyte, monocyte or T cell PD-1 expression (Figure 5.5 B-D).

Although patients enrolling into MATRIX were recommended to have their tumour PD-L1 status assessed as part of the trial protocol, this information was not collected at enrolment and therefore could not be obtained.

The notable differences in expression of both PD-1 and PD-L1 on lymphocytes and myeloid cells within the 2 trial cohorts was of interest, therefore patient factors were examined to determine whether age, number of treatment lines, or cancer stage were associated with the higher levels of expression seen within PEPS2. No relationships could be identified to explain these differences. The only factor which stood out as a variation between the 2 populations was performance status, due to the nature of enrolment into each trial. When comparing the 2 trial cohorts, PEPS2 patients showed significantly higher PD-L1 expression on both CD15+

granulocytes and CD14+ monocytes, p=0.027 and p=0.0043, respectively. Significantly higher PD-1 expression on T cells was also detected within PEPS2 patients, with a p value of 0.0129 (Mann Whitney U test). When exploring factors that could account for these differences, only the trial cohort, or performance status appeared to separate these populations (Figure 5.6 A-C).

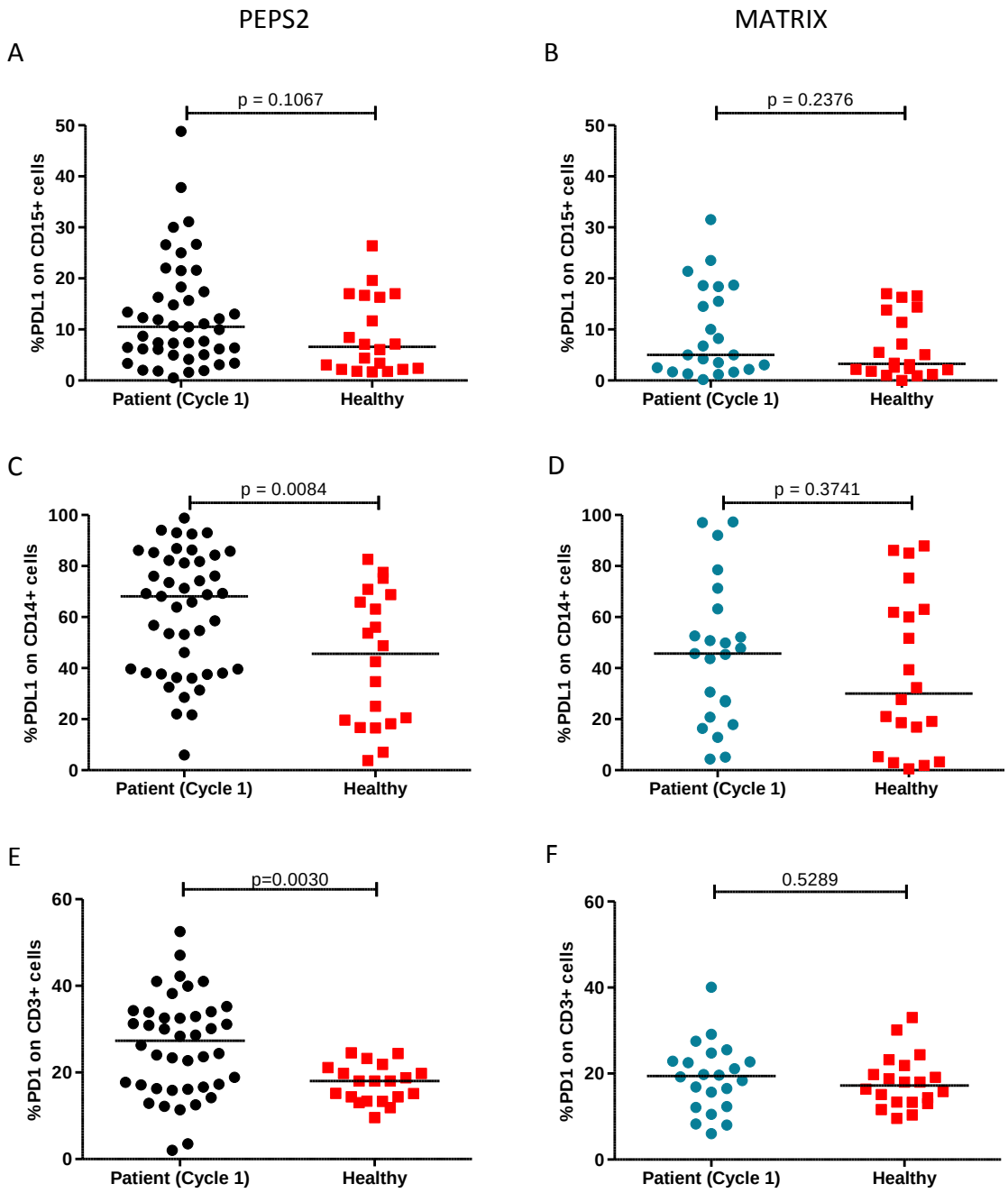

Figure 5. 4. The expression of checkpoints in the peripheral blood of patients with NSCLC

The surface expression of PD-L1 and PD-1 upon whole blood myeloid cells and lymphocytes were examined through flow cytometry for patients within PEPS2 (black dots, n=42) and MATRIX (blue dots, n=22). Samples were compared to healthy controls (red dots, n=20). (A, B) Percentage PD-L1 expression on CD15+ granulocytes is displayed for PEPS2 and MATRIX cohorts. (C) Percentage PD-L1 expression on CD14+ monocytes from patients within PEPS2. PD-L1 percentage was significantly higher when compared to healthy controls (p=0.0084). (D) Percentage PD-L1 expression on CD14+ monocytes from MATRIX trial patients. (E) Percentage PD-1 expression on CD3+ lymphocytes from patients enrolled in PEPS2; percentages were significantly higher when compared to healthy controls (p=0.003). (F) Percentage PD-1 expression on CD3+ lymphocytes within patients enrolled in MATRIX. Horizontal lines represent median values. Statistical analysis carried out using a Mann Whitney U test.

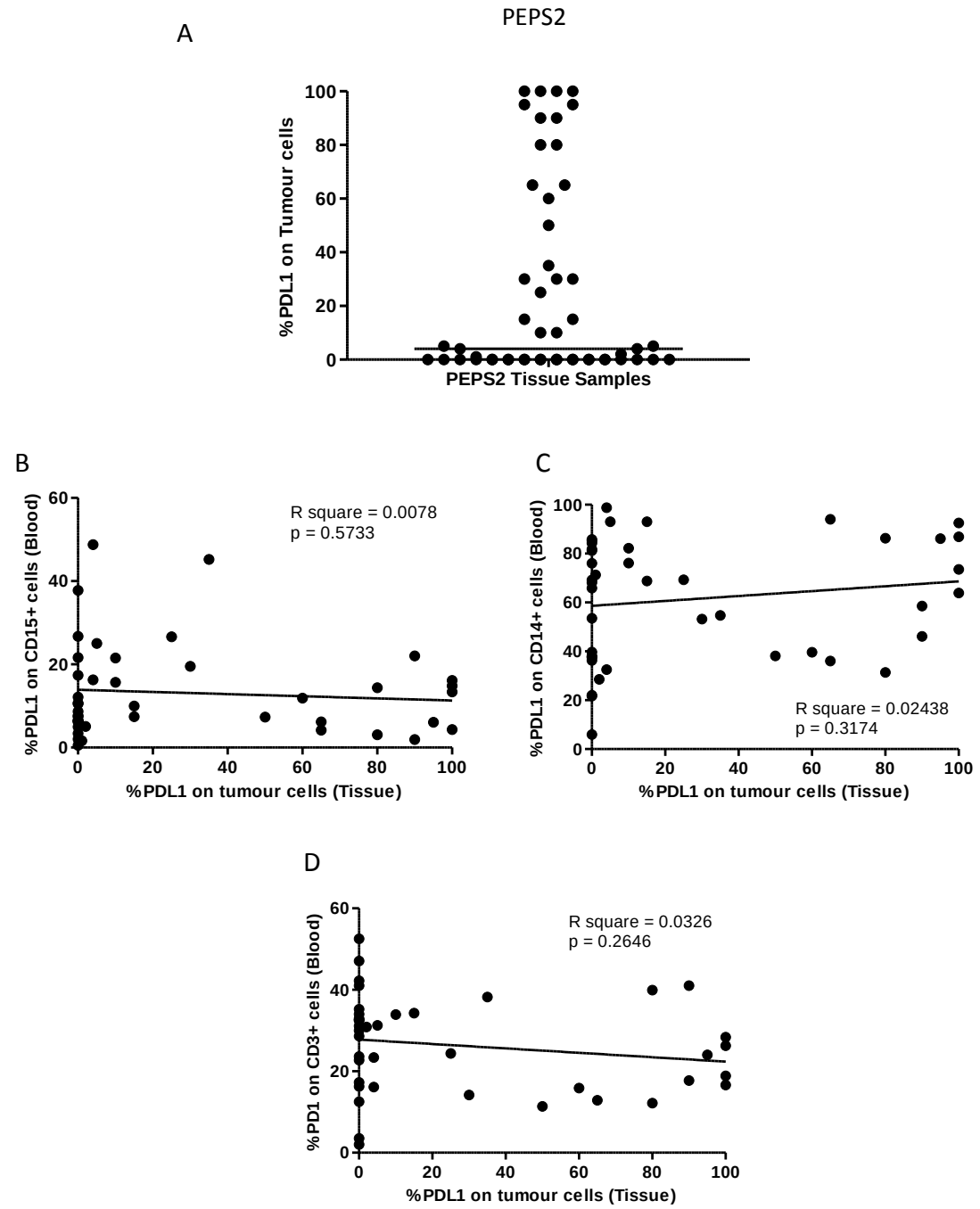

Figure 5. 5. Correlation between checkpoint expression on tumour cells and peripheral blood

(A) Upon enrolment within the PEPS2 trial patient tumour samples were tested by immunohistochemistry to determine PD-L1 expression. These studies were performed within clinical laboratories and results made available to our research for analysis. Scatter plot demonstrates percentage PD-L1 expression on tumour tissues. Median expression was 4%, ranging from 0-100%. Correlation plots were drawn between tumour PD-L1 expression and PD-L1 on whole blood CD14+ (B) and CD15+ cells (C), and expression of PD-1 on CD3+ cells (D). R squared demonstrates goodness of fit, with corresponding p values. No correlations were observed.

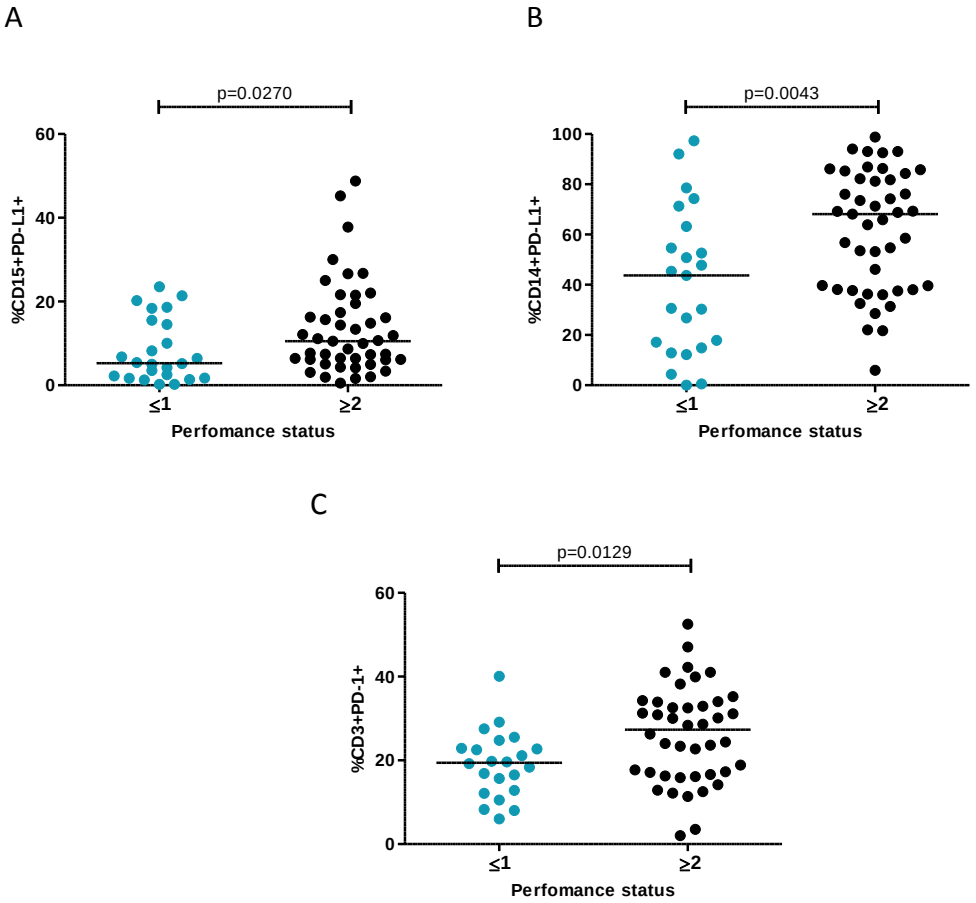

Figure 5. 6. Associations between performance status and PD-L1 expression

In view of the significant differences in PD-L1 and PD-1 expression observed in patients within PEPS2, patient factors were examined to assess for any correlation with higher PD-L1 or PD-1 expression. No association was detected between age, previous treatment lines or cancer stage (not shown). As the two trials were divided by performance status (PS), this factor could account for the differences in PD-L1 and PD-1 expression. Scatter plots demonstrate differences between the PS 1 and PS 2 patients were detected when examining (A) CD15+ PD-L1 expression, (B) CD14+PD-L1 expression and (C) CD3+ PD-1 expression. Horizontal lines represent median values. Statistical analysis was carried out using a Mann Whitney U test.

5.2.4 The effect of PD-1 and PD-L1 blockade on circulating immune populations

Following treatment with either systemic PD-1 or PD-L1 antibodies, we wished to assess whether there was any impact on the number of circulating granulocytes, monocytes and T cells. In addition, the effect of PD-1 and PD-L1 expression on these circulating populations was also examined.

Specimens from PEPS2 were collected at 3 time points; pre-treatment (cycle 1), pre-cycle 2 (cycle 2), and pre-cycle 4 (cycle 4). At the time of analysis, the number of matched samples was low, with only 23 patients having time points 1 and 2, and 10 patients having samples taken for all 3 time points. Two patients were recorded at time point 2 and 3, but not pre-treatment. Fourteen patients were recorded only at time point 1 and eight patients were recorded only at time point 2.

When looking at all samples combined, there were no significant changes in overall numbers of circulating granulocytes following treatment with the PD-1 antibody, Pembrolizumab (Figure 5.7 A). Examining paired samples also showed no change in circulating numbers of granulocytes (consecutive samples are demonstrated in black). Similarly, there were no observed changes in the numbers of circulating CD14+ monocytic cells (Figure 5.7 B). No significant changes were observed in PD-L1 expression upon circulating CD15+ granulocytes or CD14+ monocytes (Figure 5.7 C, D).

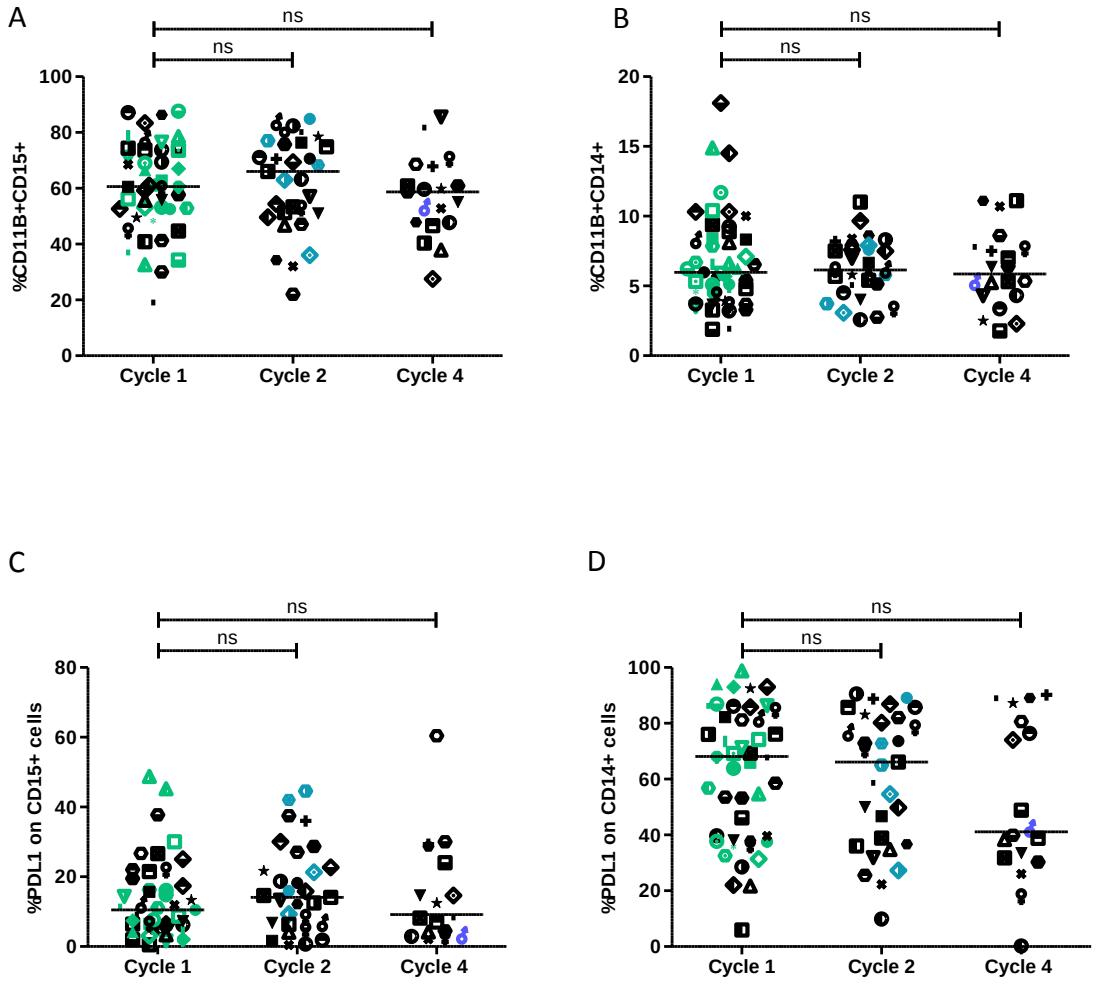

Figure 5. 7. Sequential changes in peripheral myeloid populations in PEPS2 trial patients

Analysis of patient whole blood was carried out by flow cytometry prior to the start of Pembrolizumab treatment (Cycle 1, n=46) and at the point of receiving cycle 2 (n=31) and cycle 4 (n=18). (Treatment cycles were each 3 weeks apart). Patients with consecutive samples are represented in black and single patients in colour. (A, B) Scatter plots demonstrate percentages of circulating CD11b+CD15+ granulocytes and CD11b+CD14+ monocytes at cycles 1, 2 and 4. (C, D) Scatter plots demonstrating percentage PD-L1 expression on CD15+ and CD14+ populations at cycles 1, 2 and 4. No significant changes were observed with sequential cycles. Horizontal lines represent median values, statistical analysis has been carried out using a Kruskal Wallis ANOVA with Dunn's correction for multiple comparisons.

Upon examination of T cell numbers there were again, no changes following the initiation of treatment and T cell percentages within patients remained low. In contrast to this, the levels of detectable PD-1 expression were significantly altered following treatment, with a dramatic reduction in expression from median of 27.3% at cycle 1, to 1.4% and 1.3% at cycles 2 and 4, respectively (Figure 5.8, A, B).

The reduction in detection of Pembrolizumab was believed to be due to concealment of the PD-1 protein on the surface of T cells. The pembrolizumab epitope of PD-1 is made up of several discontinuous segments, with multiple sites of binding between the PD-1 protein and Pembrolizumab within the PD-L1 binding region (425). Pembrolizumab occupies a larger surface area than native PD-L1 and induces conformational changes in the PD-1 protein (425). It is therefore likely that the binding epitope of our antibody is either unable to bind due to concealment by Pembrolizumab, or due to a fundamental change in epitope structure, preventing stable binding. The long half-life of Pembrolizumab at 27 days, will also suggest that at the start of each 21 day cycle, it can be expected that the antibody is still bound to circulating T cells (426).

Information on the exact epitope bound by our antibody was not commercially available.

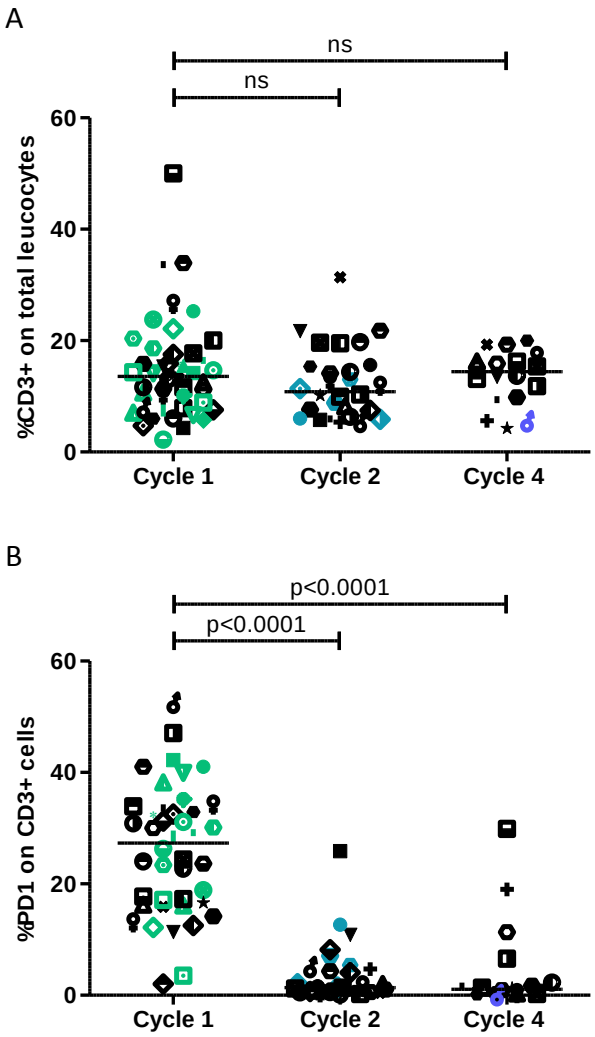

Figure 5. 8. Sequential changes in peripheral lymphocyte populations in PEPS2 trial patients

Analysis of patient whole blood was carried out by flow cytometry prior to the start of Pembrolizumab treatment (Cycle 1, n=46) and at the point of receiving cycle 2 (n=31) and cycle 4 (n=18). (Treatment cycles were each 3 weeks apart). Patients with consecutive samples are represented in black and single patients in colour. (A) Scatter plot demonstrates percentage of CD3+ cells within whole blood at cycles 1, 2 and 4. There were no observed changes with sequential cycles. (B) Scatter plot demonstrates percentage of PD-1+CD3+ cells within whole blood at cycles 1, 2 and 4. A reduction in the level of detectable PD-1 on CD3+ was detected at cycle 2 and sustained at cycle 4. The reduction in PD-1 detection was highly significant ($p<0.0001$). Horizontal lines represent median values, statistical analysis has been carried out using a Kruskal Wallis ANOVA with Dunn's correction for multiple comparisons.

For patients within MATRIX, each received treatment with the PD-L1 antibody, Durvalumab. 20 of 24 patients had consecutive samples. Specimens were collected pre-treatment (Cycle 1), before the second cycle of treatment (Cycle 2) and prior to their fourth treatment (Cycle 4). Each cycle length was 2 weeks. Samples were also collected at the point a patient ended treatment, due to progression or secondary to drug toxicity. These samples are recorded as "end of treatment" (EOT).

As observed within samples from PEPS2, there were no overall significant changes in the percentage of circulating CD15+ granulocytes or CD14+ monocytes in consecutive samples following cycle 1 (Figure 5.9 A, B). An increase the percentage of CD15+CD11b+ was observed at cycle 4 in patients from MATRIX however, with median percentages increasing from 55.7% to 68.5%. In view of this observation, paired analysis was applied to these populations and this revealed a significant relationship, p=0.0211 (Wilcoxon matched pairs singed rank test).

PD-L1 expression on CD15+ cells was low at enrolment and did not significantly change following treatment (Figure 5.9, C). PD-L1 expression on CD14+ cells did not change significantly during treatment (Figure 5.9, D). Although no significant changes were detected, when examining patterns of expression of PD-L1 on CD14+ cells, median expression was seen to be higher at the end of treatment, at 66.4%, compared to 45.7% pre-cycle 1. This is an interesting observation and higher sample numbers are needed to demonstrate whether this could represent a true change in expression.

In contrast to the inhibition of PD-1 binding and detection in patient samples following treatment with Pembrolizumab, PD-L1 continued to be detectable at all time points following administration of Durvalumab. This may be due to our antibody either binding at a different

epitope on the PD-L1 molecule, or due to loss of PD-L1 binding at the time of testing. Durvalumab has been shown to bind at five of six complementarity determining regions (CDRs) on the PD-L1 molecule yet, bound with an individual epitope, when compared to other commercial PD-L1 antibodies (427). It is therefore possible that if Durvalumab remained bound, regions of the molecule would be accessible for additional antibody binding.

The half-life of Durvalumab is approximately 17 days (428), therefore if cells remained viable, it should be expected for antibody to remain present at the start of each cycle. However, the natural life span of many myeloid cells is less than 7 days (429), therefore myeloid cells tested pre-treatment would not be bound by antibody. The binding of Durvalumab within tissues could not be assessed due to the nature of the samples obtained.

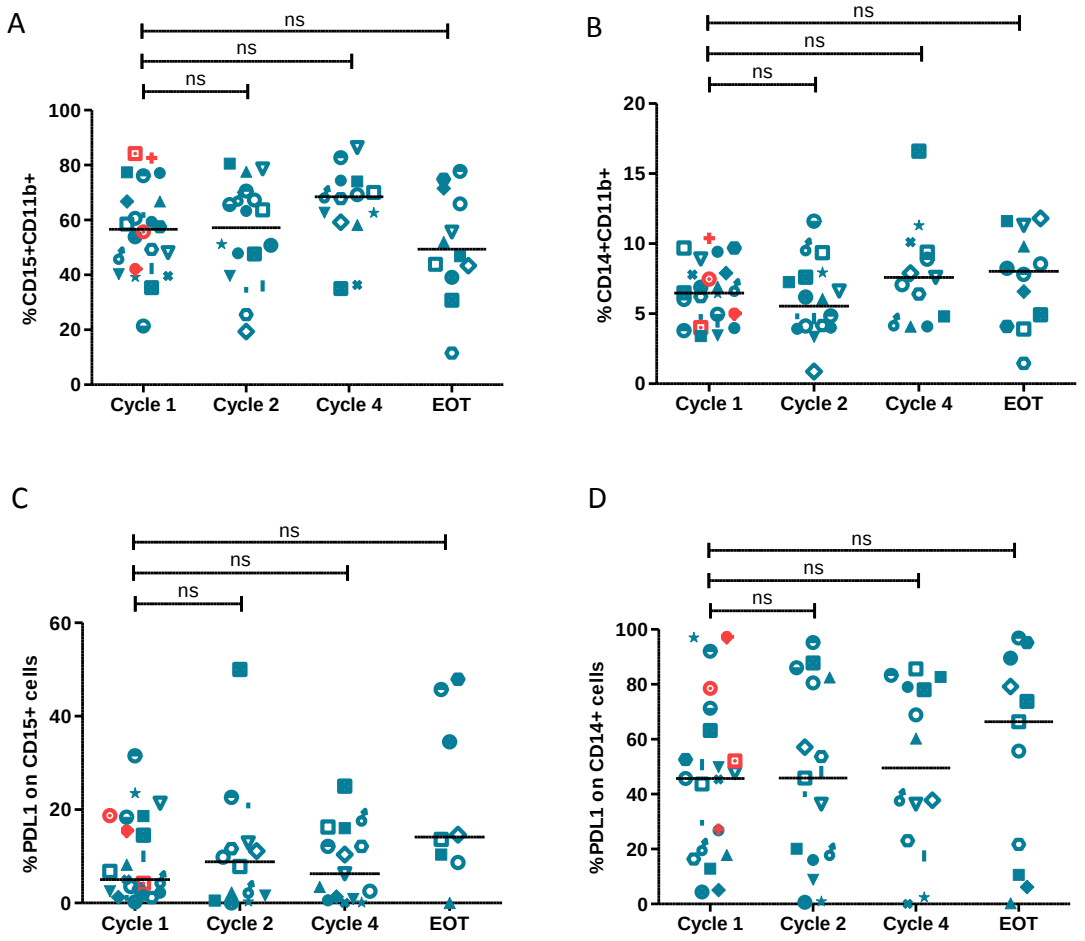

Figure 5. 9. Sequential changes in peripheral myeloid populations in MATRIX trial patients

Within the MATRIX trial, analysis of patient whole blood was carried out by flow cytometry prior to the start of Durvalumab treatment (Cycle 1, n=24), at the point of receiving cycle 2 (n=18), cycle 4 (n=14) and at the end of treatment (EOT, n=12). Treatment cycles were each 2 weeks apart. Patients with consecutive samples are represented in blue and single patients in red. (A, B) Scatter plots demonstrate percentage of circulating CD11b+CD15+ granulocytes and CD11b+CD14+ monocytes at cycles 1, 2, 4 and EOT. (C, D) Scatter plots demonstrate percentage PD-L1 expression on CD15+ granulocytes and CD14+ monocytes. No significant changes were observed with sequential cycles. Horizontal lines represent median values, statistical analysis has been carried out using a Kruskal Wallis ANOVA with Dunn's correction for multiple comparisons.

Following treatment in MATRIX with Durvalumab a reduction in the percentages of circulating CD3+ leucocytes was observed, with median percentage decreasing from 13.2% in week one, to 9.7% and 11.7% at week 2 and 6, respectively. When analysed as a group, this data did not show significance; however, when matched samples were analysed, a significant reduction of CD3+ T cells was detected at week 2 ($p=0.0204$, Wilcoxon matched pairs signed rank test). (Figure 5.10 A, B). The expression of PD-1 on T cells was not significantly altered, although at week 6 there was a suggestion of higher expression seen, with median expression increasing from 19% to 24.4% (Figure 5.10 C). The hypothesis was that the PD-L1 antibody should create an enhanced inflammatory environment therefore, I would have expected to see increasing numbers of circulating T cells and lower expression of PD-1 on such cells.

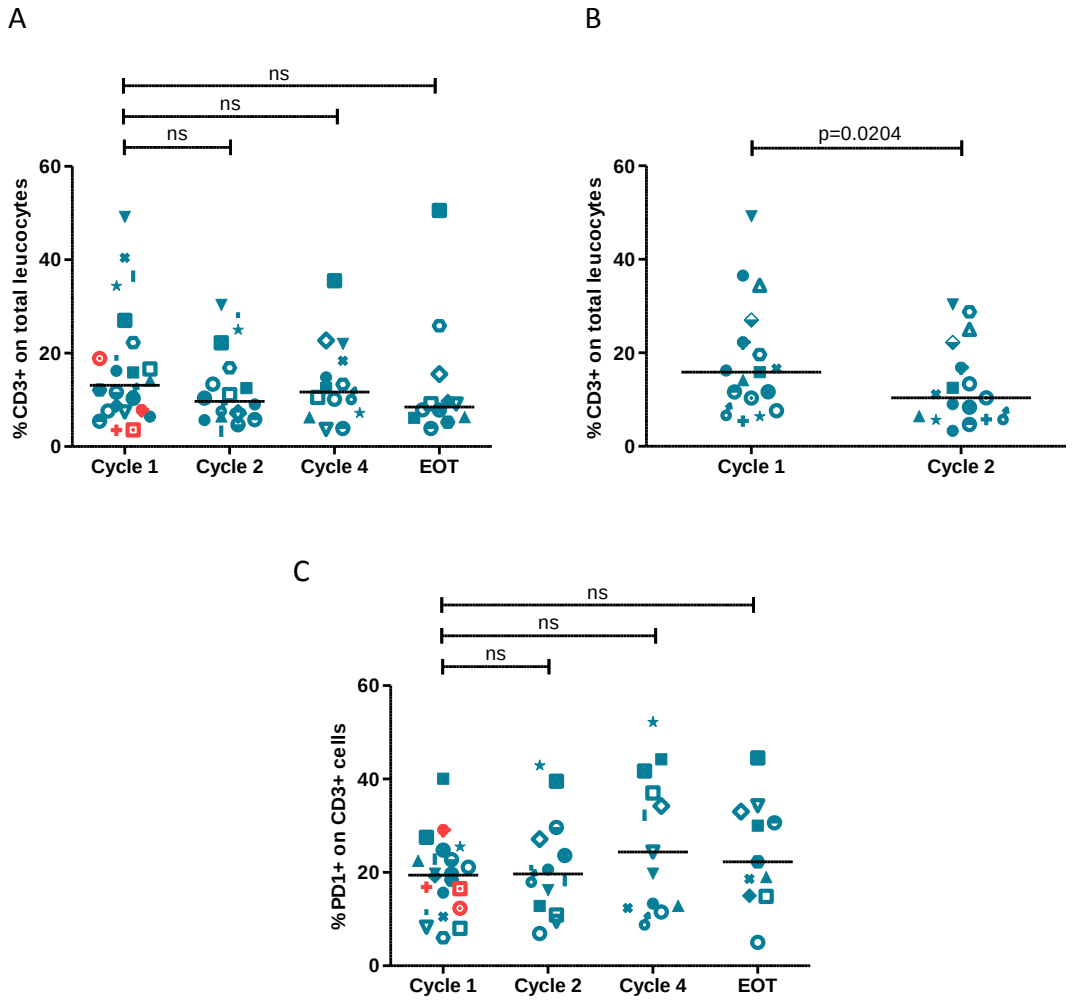

Figure 5. 10. Sequential changes in peripheral lymphocyte populations in MATRIX trial patients

Analysis of patient whole blood was carried out by flow cytometry prior to the start of Durvalumab treatment (Cycle 1, n= 24), at the point of receiving cycle 2 (n=18) and cycle 4 (n=14), and at the end treatment (EOT, n= 12). Treatment cycles were each 2 weeks apart. Patients with consecutive samples are represented in blue and single patients in red. (A) Scatter plot demonstrates percentage of circulating CD3+ lymphocytes at all 4 time points. There were no observed changes in the overall number of circulating CD3+ lymphocytes. (B) Scatter plot showing detection of CD3+ lymphocytes in matched patient samples at cycles 1 and 2 (n=17). A significant reduction in CD3+ lymphocytes was observed at cycle 2, p=0.0204, (Wilcoxon matched pairs signed rank test). (C) Scatter plot demonstrating expression of PD-1 on circulating CD3+ lymphocytes at all 4 time points. No changes were observed with sequential cycles. Horizontal lines represent median values, statistical analysis has been carried out using a Kruskal Wallis ANOVA with Dunn's correction for multiple comparisons.

5.2.5 The effect of PD-1 and PD-L1 inhibition on the suppressive activity of CD15+ and CD14+ cells

Following the detection of high concentrations of circulating CD15+ granulocytes and CD14+ monocytes in patients recruited within both clinical trials, the suppressive function of these populations was assessed through T cell suppression assays. Following gradient separation of blood, CD15+ and CD14+ cells were isolated through magnetic bead separation. Cells were then counted and plated within 96 well plates at 4 concentrations, from $4x10^6$ per ml, reducing to $0.5x10^6$ per ml (Figure 5.11). Allogeneic T cells were plated within the same well and stimulation was achieved through anti-CD3 and anti-CD28. Proliferation was assessed at 96 hours by thymidine incorporation.

High levels of suppression occurred with all populations, including healthy controls, at concentrations of 1 T cell to 1 myeloid cell and this persisted within some healthy controls at 1 T cell to 0.5 myeloid cells, particularly within CD14+ proliferation assays. At lower concentrations sustained T cell proliferation was seen within healthy controls, but persistent T cell suppression in patient samples from both PEPS2 and MATRIX. To ensure that the observed differences were not due to the culture conditions, for example over-crowding of cells within wells preventing T cell expansion, overall differences between suppressive activity were examined at the ratio of 1 T cell to 0.25 myeloid cells.

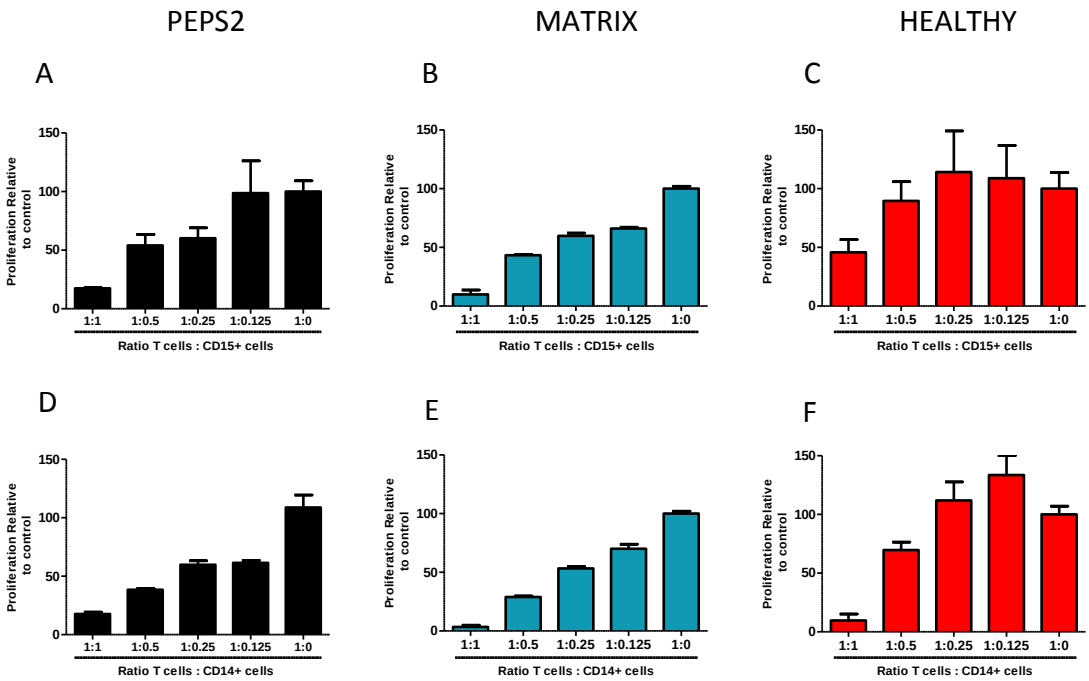

Figure 5. 11. T cell proliferation assays in patients and healthy controls

CD15+ and CD14+ cells were isolated from whole blood obtained from healthy donors and patients within the PEPS2 and MATRIX trials, prior to commencing treatment. Cells were plated with allogeneic T cells at reducing concentrations (1:1 to 1:0.125). T cells were stimulated with anti-CD3 and anti-CD28 antibodies. Thymidine was added to plates after 96 hours of culture and thymidine incorporation was used to determine proliferation. T cells cultured alone, and T cells cultured with CD3 and CD28, were used as internal plate controls. Proliferation was calculated as a percentage of control T cell proliferation. Populations of CD15+ and CD14+ cells from patients enrolled in PEPS2 (A and D) and MATRIX (B and E) were capable of suppressing T cell proliferation at both high and low concentrations. Recovery of T cell proliferation occurred earlier in healthy samples (C and F), as compared to patients.

Consistent with the findings in mesothelioma that circulating granulocytes were suppressive to T cells, it was demonstrated that CD15+ granulocytes isolated from the whole blood of lung cancer patients were capable of T cell suppression. Within both trial populations variable suppression of allogeneic T cells was observed prior to initiation of treatment. Within patients of the PEPS2 trial greater suppressive activity was recorded than within MATRIX (Figure 5.12 A, B). The suppressive activity of CD15+ granulocytes from both PEPS2 and MATRIX patients was significantly different to that of healthy controls, with p values of 0.0003 and 0.0192, respectively (non-parametric Mann Whitney U test).

When examining the function of CD14+ monocytic cells we also observed suppression of allogeneic T cells within proliferation assays in both cohorts, again with samples from PEPS2 showing greater suppressive activity than those of MATRIX (Figure 5.12 C, D). This relationship was again statistically significant when comparing both PEPS2 samples and healthy controls (p=0.0001), and in the comparison of MATRIX samples with healthy controls (p=0.0058).

The question of greater interest, however, was whether following treatment with either PD-1 or PD-L1 blockade the suppressive activity of myeloid populations could be altered. The ability of both cell groups to cause T cell suppression was therefore re-assessed following treatment at multiple time points (Figure 5.12). Within PEPS2 there was no trend towards either reduced or increased suppression between the pre-treatment or cycle 2 samples. There was a slight trend towards greater suppression at cycle 4, however, sample number was low at this time point and no significant relationship could be identified (Figure 5.12, A). There was also no evidence of altered suppressive capability of CD15+ cells within samples of the MATRIX trial at any of the 3 post-treatment time points (Figure 5.12, B). When examining the

suppressive activity of CD14+ cells in both populations, there again appeared to be no change in the suppressive action of cells following treatment (Figure 5.12 C, D).

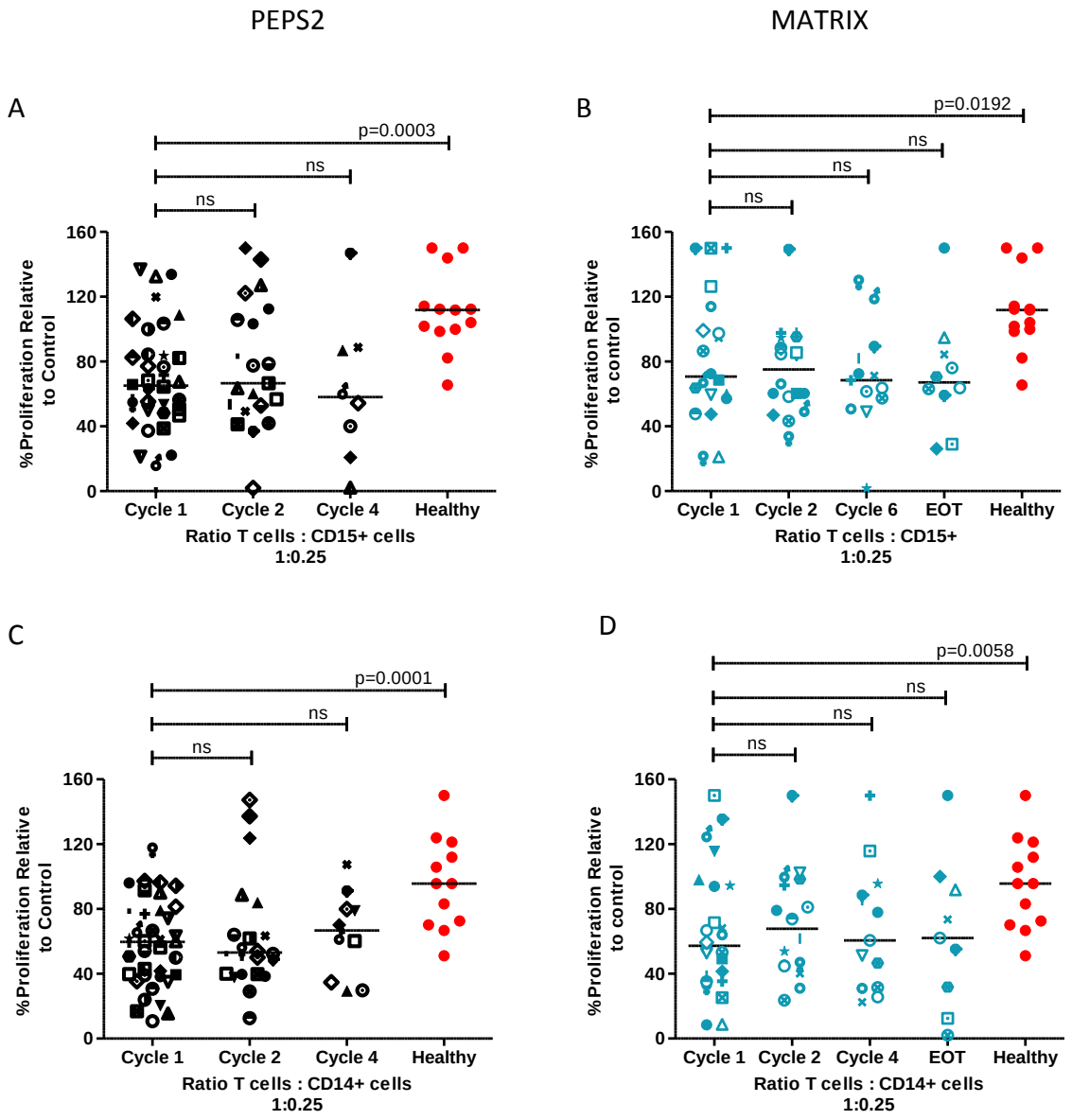

Figure 5. 12. Sequential changes in T cell suppression following PD-1/PD-L1 blockade

The suppressive action of CD15+ and CD14+ cells was assessed at cycle 1 (pre-treatment), cycles 2 and cycle 4 for both PEPS2 and MATRIX trials. An "end of treatment" (EOT) sample was also obtained for MATRIX patients. Scatter plots demonstrate the percentage of T cell proliferation, relative to control. (A, B) Scatter plots represent percentage T cell proliferation, following suppression assays with CD15+ granulocytes from PEPS2 and MATRIX patients at each cycle. Healthy controls are plotted in red. (C, D) Scatter plots represent percentage T cell proliferation, following suppression assays with CD14+ monocytes from PEPS2 and MATRIX patients at each cycle. Healthy controls are plotted in red. CD15+ and CD14+ cells were suppressive within both cohorts, when compared to healthy controls (Mann Whitney U test). No sequential changes in suppressive activity were observed in either cohort (Kruskal-Wallis ANOVA with Dunn's correction for multiple comparisons).

As it was clear that a broad variation in suppressive activity existed, samples which had shown suppressive activity at the pre-treatment time point were analysed separately. Samples were segregated into “suppressive” and “non-suppressive” populations. For CD14+ cells this was defined as a reduction of T cell proliferation of greater than 50%; however, with CD15+ populations this was defined as a reduction of T cell proliferation of greater than 25%, due to the fact that there were insufficient samples which suppressed beyond 50% to complete the analysis. For samples to be included in this analysis they also were required to have at least one matched sample collected at a later time point, in order to perform a paired analysis.

There were 10 samples (28%) obtained from patients enrolled within PEPS2 from time point 1, with matched consecutive time points, which produced T cell suppression of greater than 25%. Within MATRIX there were 8 samples (40%) identified that fit these criteria. At time point 2, prior to the second cycle of treatment, there was evidence of increased T cell proliferation within both trial populations; however, neither relationship reached significance. The small numbers in this analysis are likely to impact on this effect (Figure 5.13 A, B).

Analysis of CD14+ populations demonstrated 8 patients within each trial population with T cell suppression below 50% of control. This accounted for only 22% of patients within the PEPS2 population but 40% within the MATRIX population. An increase in average T cell proliferation was seen within samples from MATRIX patients, but again these changes were non-significant. This increase in T cell proliferation appeared to be sustained at later time points but numbers were too few at these time points to draw conclusions (Figure 5.13 C, D).

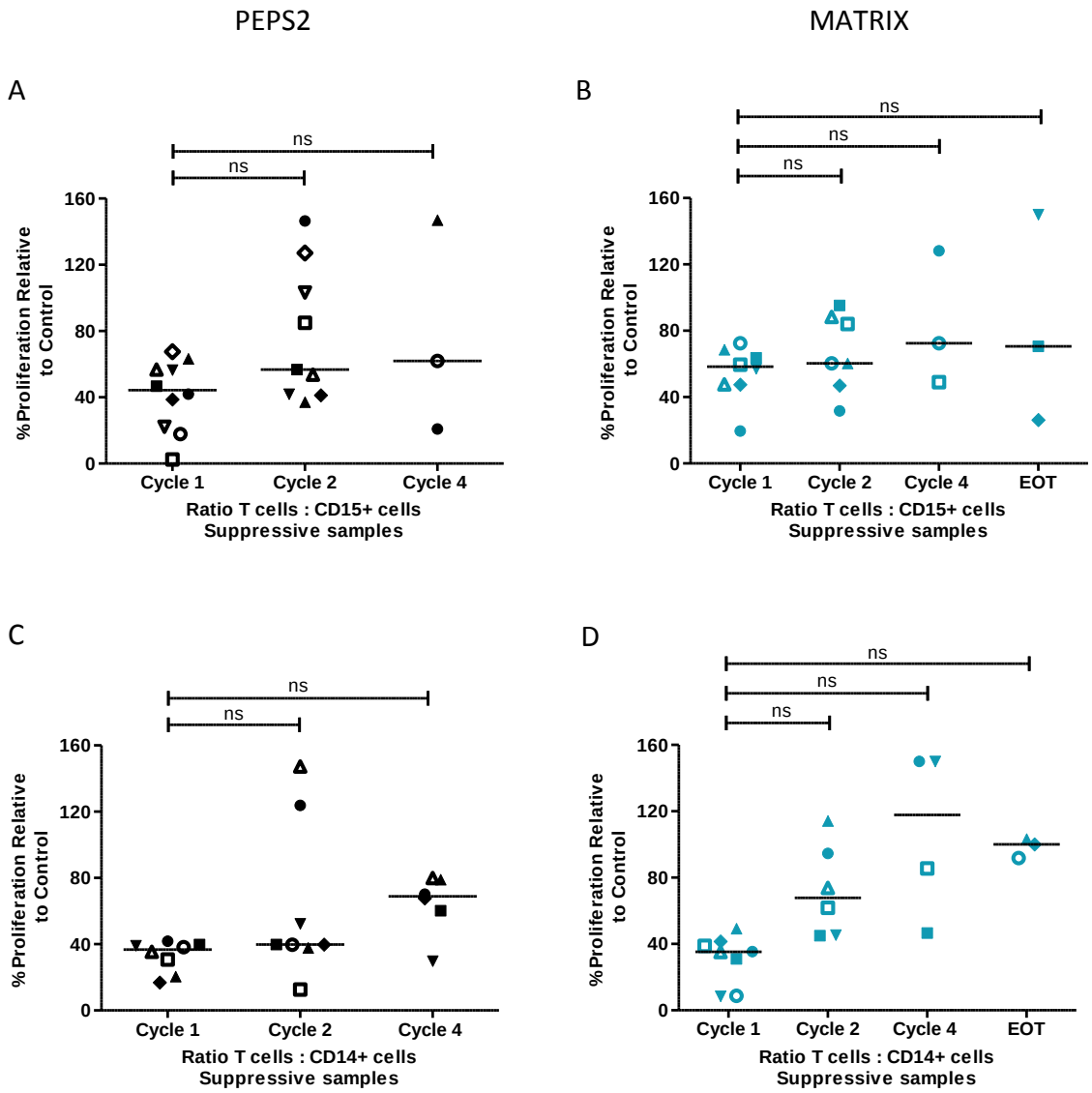

Figure 5. 13. Improvements in suppressive activity following PD-1/PD-L1 blockade

Suppressive samples were selected from both PEPS2 and MATRIX cohorts to determine whether disruption of the PD-1/PD-L1 pathway could lead to rescued T cell proliferation. (A, B) Scatter plots demonstrate T cell proliferation in the presence of CD15+ cells from PEPS2 and MATRIX patients. Only samples with a reduction in T cell proliferation of 25% or higher at cycle 1, are shown. Matched samples are plotted for cycles 2, 4 and EOT. (C, D) Scatter plots demonstrate T cell proliferation in the presence of CD14+ cells, where a reduction in T cell proliferation of 50% or higher, occurred at cycle 1. Matched samples are shown for cycles 2, 4 and EOT. No significant changes were observed. Statistical analysis was performed using Wilcoxon matched pairs signed rank test. Horizontal lines represent median values.

In view of the overall findings of greater T cell suppression within patient cohorts, we wished to establish whether any characteristics of these suppressive subgroups could be attributed to their enhanced suppressive activity. Factors explored included percentage of CD15+ or CD14+ circulating cells, the HLA-DR and PD-L1 status of these cell populations, and patient factors including age, tumour PD-L1 % (within PEPS2 only) and number of previous treatments.

Within PEPS2 patients, there was a trend for higher suppression with higher CD15+ whole blood percentages. When analysed by linear regression, there was a significant relationship between higher CD15% and greater suppressive activity ($p=0.0295$) (Figure 5.14 A). A relationship between CD14% and suppressive activity in PEPS2 samples was not evident (Figure 5.14 B). No relationship could be appreciated between expression of HLA-DR on CD15+ cells; however, HLA-DR positivity on CD14+ cells correlated with greater levels of suppression. This was contrary to the initial hypothesis (Figure 5.14 D). No relationship between PD-L1 positivity and suppressive activity was detected with either population (Figure 5.14 E, F).

Upon the examination of patient factors including age, tumour PD-L1 expression and the number of previous treatments received prior to entering the trial, no significant relationships were observed within the PEPS2 population.

Within MATRIX patients, no significant relationships were observed with any of the tested variables. Interestingly, there appeared to be a trend towards greater suppression in patients with lower percentages of CD15+ cells, the opposite of the relationship observed within PEPS2. For HLA-DR expression, a trend was again seen for greater suppressive activity in

patients with higher HLD-DR positivity on CD14+ cells, this did not reach significance. The small number of samples obtained within MATRIX limited this form of analysis.

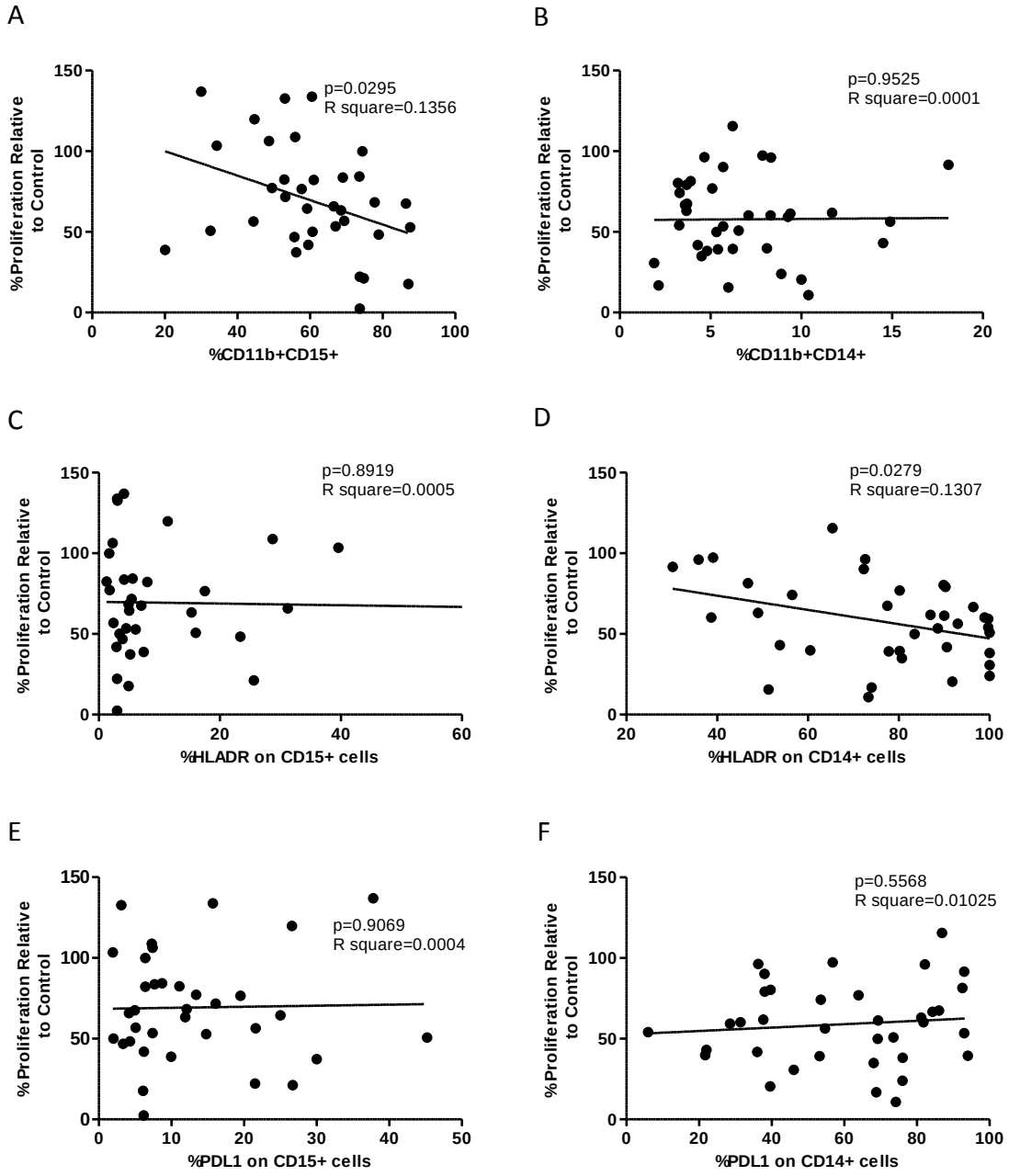

Figure 5. 14. Correlation between peripheral blood profiles and suppressive activity within PEPS2 trial patients

To determine whether there were any identifiable factors associated with increased suppressive activity of either CD15+ and CD14+ populations from PEPS2 patients, correlation plots were created for multiple variables. Plots demonstrate correlation between T cell proliferation and (A) Whole blood CD11b+CD15+ percentage, (B) Whole blood CD11b+CD14+ percentage, (C) HLA-DR expression on CD15+ cells, (D) HLA-DR expression on CD14+ cells, (E) PD-L1 expression on CD15+ cells and (F) PD-L1 expression on CD14+ cells. R squared demonstrates goodness of fit, with corresponding p values.

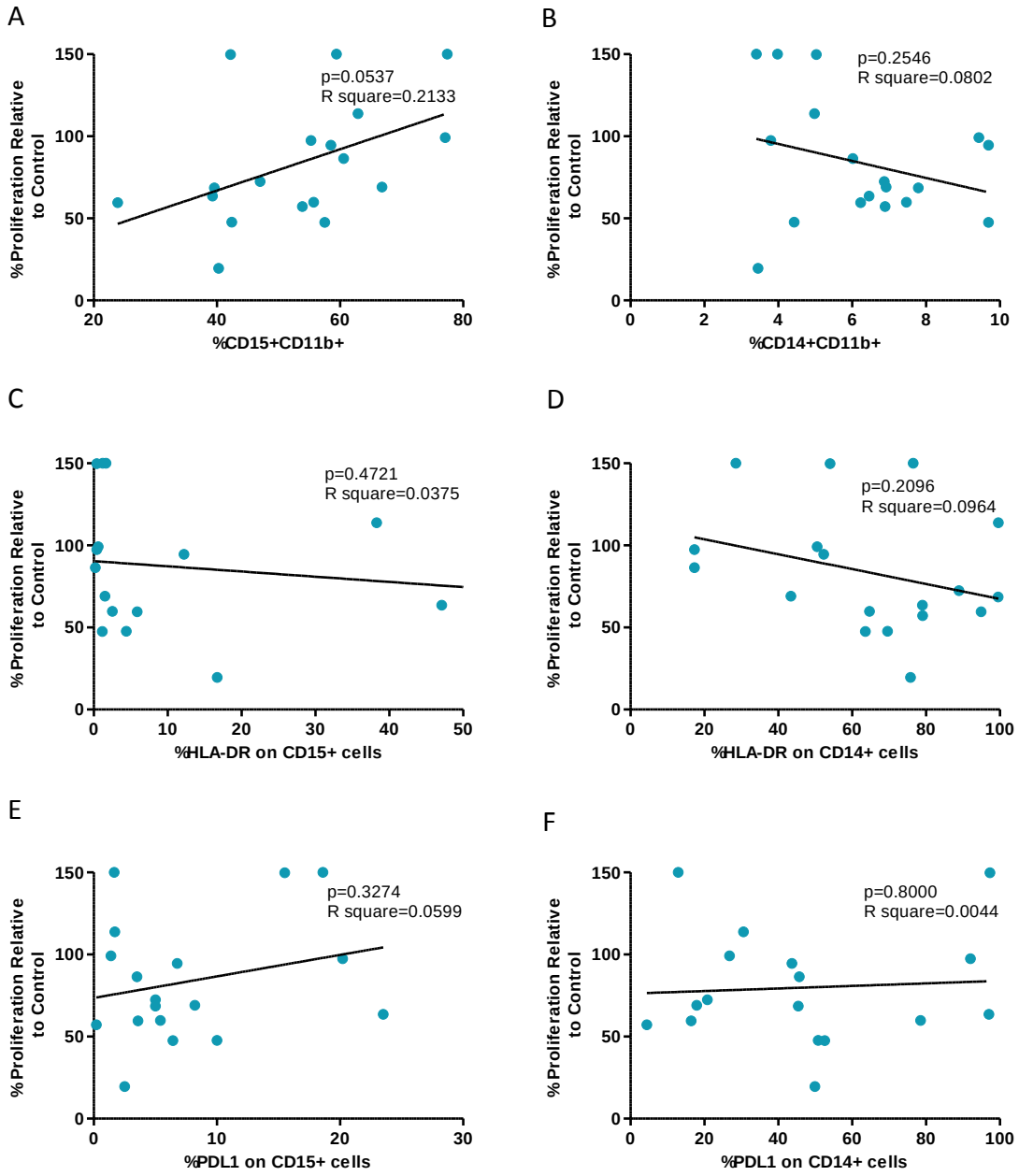

Figure 5. 15. Correlation between peripheral blood profiles and suppressive activity within MATRIX trial patients

To determine whether there were any identifiable factors associated with increased suppressive activity of either CD15+ and CD14+ populations from MATRIX patients, correlation plots were created for multiple variables. Plots demonstrate correlation between T cell proliferation and (A) Whole blood CD11b+CD15+ percentage, (B) Whole blood CD11b+CD14+ percentage, (C) HLA-DR expression on CD15+ cells, (D) HLA-DR expression on CD14+ cells, (E) PD-L1 expression on CD15+ cells and (F) PD-L1 expression on CD14+ cells. R squared demonstrates goodness of fit, with corresponding p values.

5.2.6 Correlation with patient outcome data

Following the analysis of the whole blood profile and suppressive activity, we wished to understand whether either of these factors impacted on patient outcome, in terms of response to treatment and both progression free and overall survival. At the time of completion of this thesis, only data from PEPS2 was available for analysis in this format.

Response and survival data available at the time of writing of this thesis are demonstrated in table 5.3 and 5.4. In terms of response rates, 27% of patients saw response to treatment, with a further 30% having stable disease. These results are comparable to other PD-1/PD-L1 studies (302); however, as these patients had mostly received prior therapies, these outcomes were reduced compared to those seen within the first line phase III trial on Pembrolizumab in NSCLC (143). Median progression free and overall survival were 126 and 250 days, respectively.

Data were examined on whole blood myeloid and T cell percentages, surface marker expression of HLA-DR, PD-1 and PD-L1 and suppressive function of both CD15+ and CD14+ populations to determine whether any factors could be associated with, or predict, patient outcome or survival.

Response to treatment was measured in 3 categories; partial response, stable disease or progressive disease. Outcomes were not available for all patients, leaving a fourth category of unrecorded. No relationships were observed between blood parameters or suppressive activity and response to treatment. The division of baseline markers into 4 categories led to minimal interpretation as numbers in each category were low. This meant that any observed relationship would have to be large in order to be detected. When looking at both PFS and

OS, univariate correlation plots were drawn between each whole blood variable, in addition to suppressive activity. Linear regression was then used to assess for a significant relationship. Non-parametric analysis was applied in view of the nature of the variables.

There were no associations observed between the suppressive activity of CD15+ or CD14+ populations and PFS or overall survival. When examining whole blood parameters neither baseline CD15% or CD14% appeared to influence progression free survival. Further analysis of sub-populations of CD14+ populations including CD14+CD16- classical monocytes, also showed no association with response or survival. As prior associations have been made between populations of HLA-DR low monocytes and outcome following treatment with the CTLA-4 antibody Ipilimumab (317), both total CD11b+CD14+ and CD14+CD16- populations were analysed according to HLA-DR positivity. Levels of HLA-DR positivity were not shown to be associated with outcome following treatment.

Along with the predictive value of myeloid populations, low lymphocyte percentages have also been associated with outcome following PD-1 and CTLA-4 inhibition (317,430). The relative percentages of CD3+ lymphocytes in patients was examined and a significant relationship between low numbers of circulating CD3+ cells and shorter progression free survival was observed, p=0.0458 (Figure 5.16 E). This relationship continued to be observed with overall survival, with lower CD3 percentages again being associated with poorer overall survival, p=0.0408 (Figure 5.16 F). When looking at overall survival times, patients surviving less than one year showed average T cell percentages of 12.8 compared to 17.3 in patients surviving for greater than one year.

Expression of PD-L1 on tumour tissues is an accepted marker of predicting response to treatment with anti-PD-1 therapy (301). However, the relevance of expression of this marker on the wider immune microenvironment is not known. PD-L1 expression on CD15+ and CD14+ myeloid populations was therefore examined. No association was detected between the expression of PD-L1 on CD15+ populations and patient outcome. In contrast, higher PD-L1 expression on CD14+ populations was associated with poorer overall survival (Figure 5.17 B). This relationship was significant with a p value of 0.0231. Exploring this data showed that those patients surviving less than 6 months demonstrated median CD14 PD-L1 expression of 72.7%, compared to 56.8% in those surviving over 6 months. In patients with survival over one year, median PD-L1 expression was 53.2%. Baseline PD-1 expression on CD3+ T cells showed no association with PFS or OS.

In view of the association of low numbers of circulating T cells and OS, we also wished to examine the neutrophil-lymphocyte ratio as a predictor of outcome following treatment as this reflects the relationship between low T cell numbers and high neutrophil counts. The NLR has previously been shown to be an independent marker of PFS and OS in patients with advanced malignancy treated the immunotherapy agents ipilimumab (431) and Nivolumab (418-420), although is not yet an accepted prognostic or predictive marker. Within this study, the NLR at baseline did not appear to show a relationship to PFS; however, there was a visible, but non-significant, trend towards higher baseline NLR predicting poorer overall survival (Figure 5.18 A, B). In addition, when examining those patients with an NLR of < 5 median OS was notably different, with 419 days compared with 207 days in those with an NLR > 5. In view of the observed trend, subsequent time points were examined. At cycle 2, the NLR was significantly associated with poorer progression free and overall survival, p=0.0246 and

p=0.001, respectively. When the cycle 2 subgroup was divided by NLR of < 5, there was a significant improvement in median survival with 515 days versus 246 days in those with an NLR > 5, p=0.0215 (Chi square). This finding of serial measurement of NLR as a predictive marker for both anti-CTLA4 and anti-PD1 therapy has also been observed, with a stronger relationship to outcome demonstrated by the NLR at a 6 week time point by Lalani *et al* (432) and at both 7 and 10 weeks post-treatment by DiGiacomo *et al* (433). These findings perhaps emphasise the importance of the NLR as a prognostic/predictive biomarker, as normalisation of blood parameters in responding patients may allow prediction of better overall outcome (Figure 5.18 C, D).

Table 5. 3. Treatment effect on progression free and overall survival by best response

Best Response	No. (%)	Median PFS, days (range)	Median OS, days (range)
Partial response	17 (27.5)	424 (216-518)	500 (216-643)
Stable disease	19 (30.7)	126 (68-452)	278 (89-714)
Progressive disease	9 (14.5)	57 (48-196)	152 (74-591)
Not recorded	17 (27.5)	47 (13-301)	45 (13-367)

Table 5. 4. Combined progression free and overall survival for all patients

Median PFS, days (range)	126 (13-518)
Median OS, days (range)	250 (13-714)

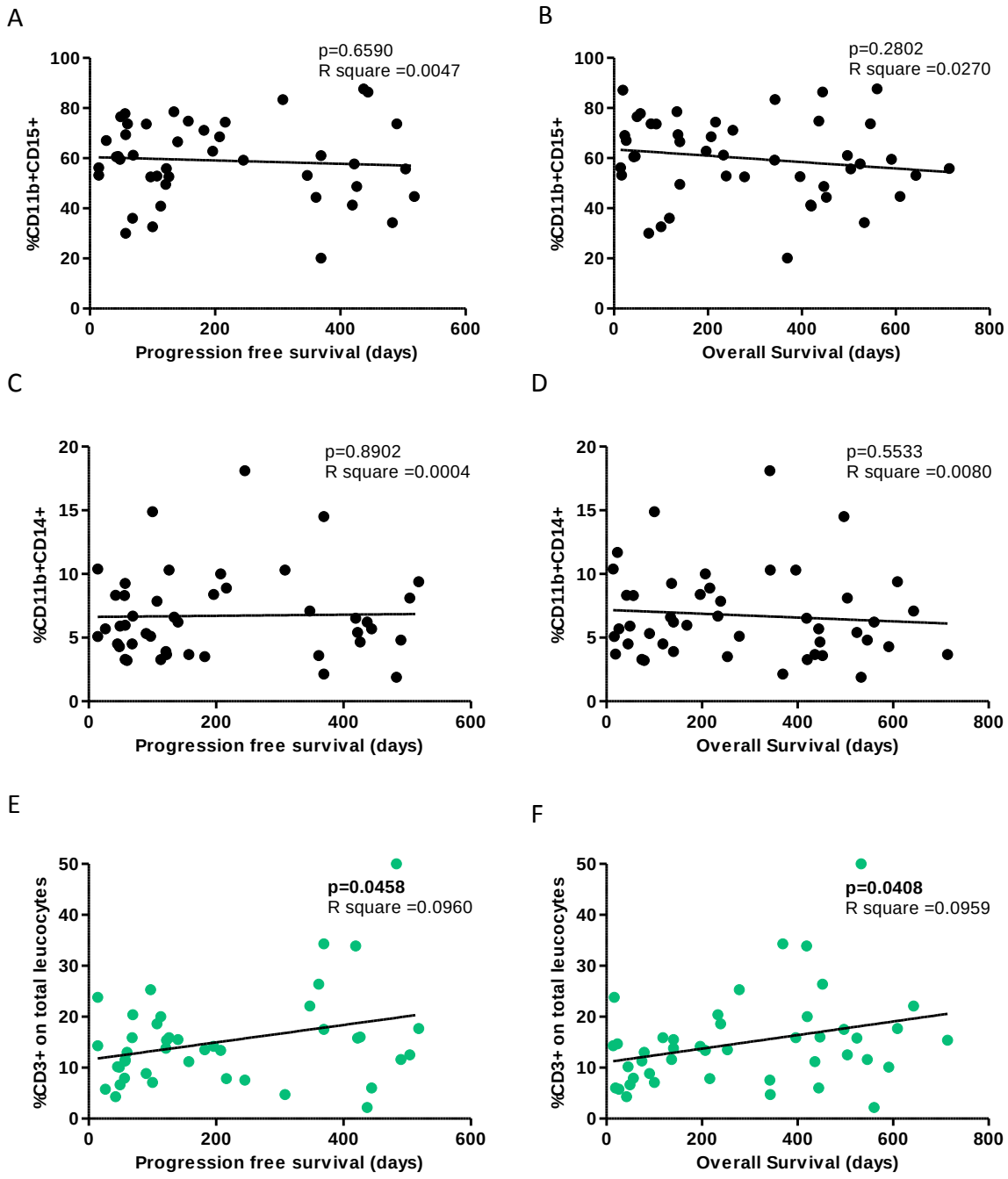

Figure 5. 16. Correlation between peripheral blood profiles and patient survival within the PEPS2 trial

Correlation plots were generated to observe relationships between baseline patient blood profiles and clinical outcome. (A, B) Correlation of baseline CD11b+CD15+ percentage and progression free (PFS) and overall survival (OS), (n=46). (C, D) Correlation of baseline CD11b+CD14+ percentage and PFS and OS, (n=46). (E, F) Correlation of baseline CD3+ percentage and PFS and OS, (n=45). Analysis was performed using non-parametric linear regression. R squared demonstrates goodness of fit, with corresponding p values. Significant relationships are represented in green.

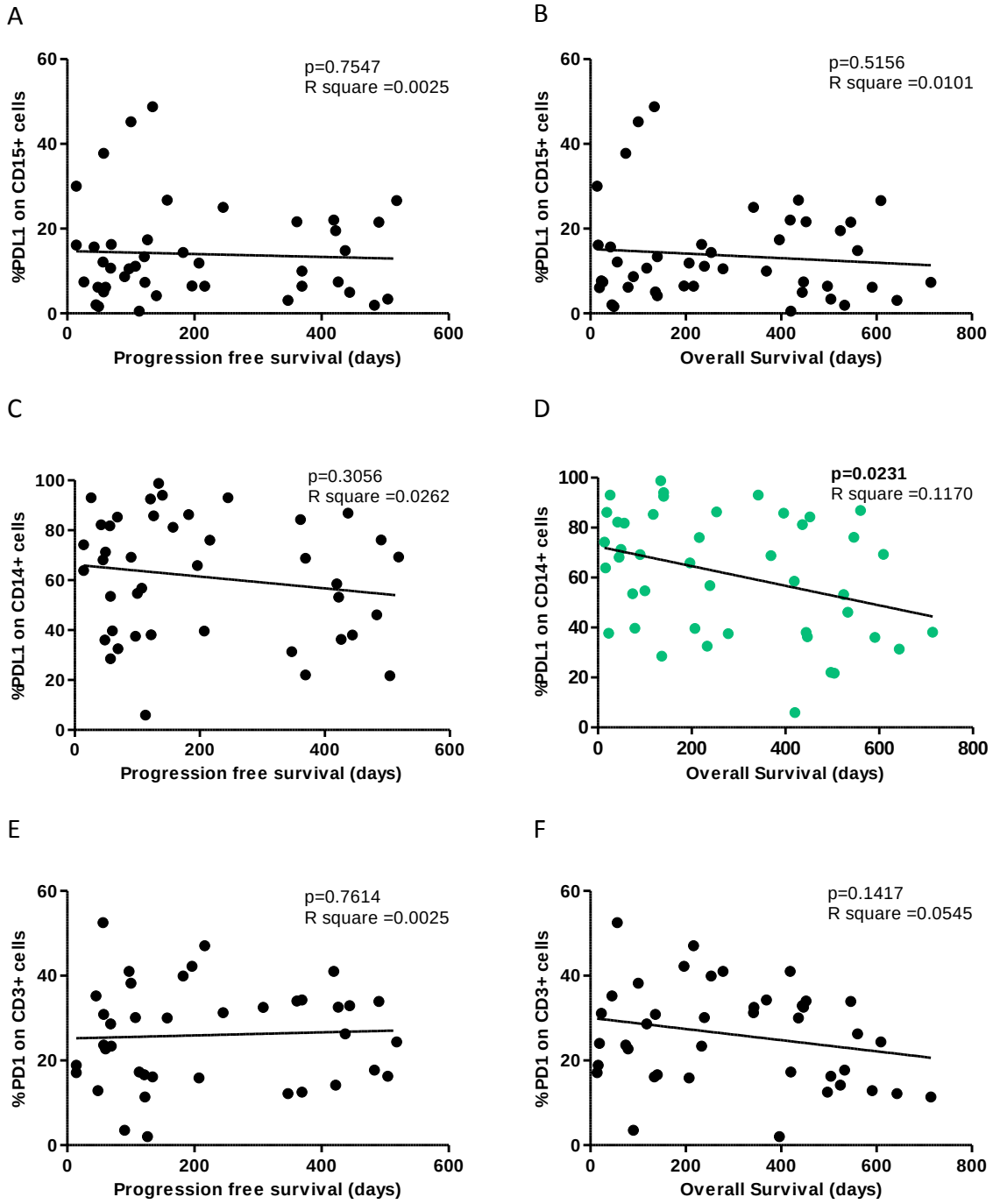

Figure 5. 17. Correlation between checkpoint expression and patient survival within the PEPS2 trial

Association of the expression of the surface markers PD-L1 and PD-1 and progression free survival (PFS) and overall survival (OS) was examined. (A, B) Correlation of % PD-L1 expression on CD15+ cells and PFS and OS, (n=45). (C, D) Correlation of % PD-L1 expression on CD14+ cells and PFS and OS, (n=45). (E, F) Correlation of % PD1 expression on CD3+ lymphocytes and PFS and OS, (n=42). Analysis was performed using non-parametric linear regression. R squared demonstrates goodness of fit, with corresponding p values. Significant relationships are represented in green.

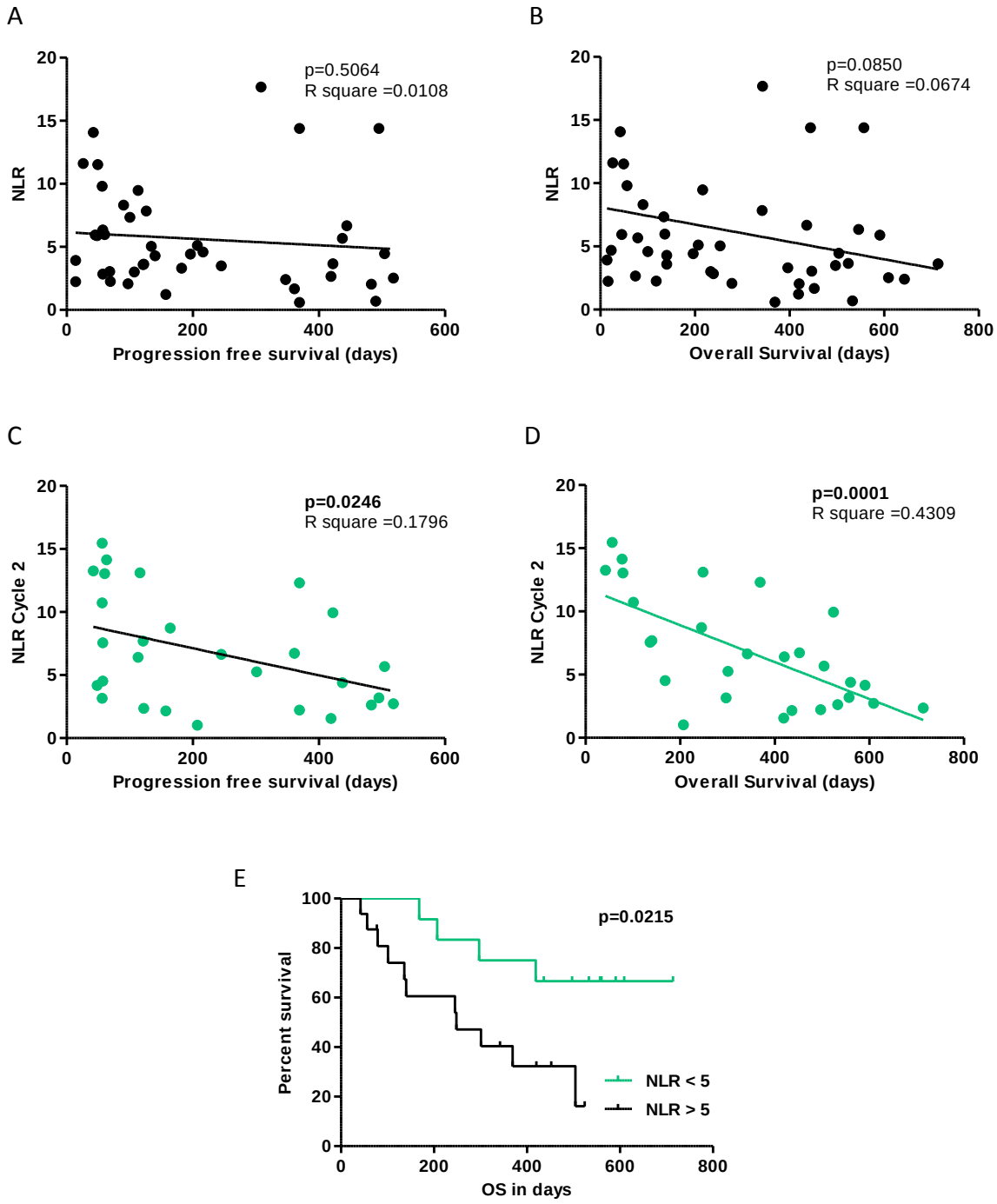

Figure 5. 18. Associations between the NLR and patient survival within the PEPS2 trial

Relationships between the NLR and patient outcome were assessed. (A, B) Correlation plots were produced between baseline NLR and progression free survival (PFS) and overall survival (OS). No significant relationships were observed. (C, D) Correlation between cycle 2 NLR, and PFS and OS. Analysis was performed using non-parametric linear regression. R squared demonstrates goodness of fit, with corresponding p values. Significant relationships are represented in green. (E) Kaplan Meier plot showing survival in relation to cycle 2 NLR. Survival curves show patients grouped by NLR >5 (black) or NLR <5 (green). Statistical analysis has been performed using a log-rank Chi square test. Patients with NLR< 5 at cycle 2 had significantly longer survival times, p=0.0215.

5.3 Discussion

Within this chapter associations between peripheral blood characteristics and outcome following treatment of NSCLC with both PD-1 and PD-L1 inhibitors have been explored. In addition, attempts have been made to bring together hypotheses generated from the findings in chapter 1 and chapter 2 relating to immune dysfunction in the setting of mesothelioma and lung cancer.

Despite the huge progress made in treating cancer through immune modulation, treatments targeting CTLA-4, PD-1 and PD-L1 are not effective in all patients. Most patients will also eventually go on to develop progressive disease, highlighting the importance of establishing both predictive biomarkers of response to immunotherapy, in addition to understanding the mechanisms behind this dysfunction. This research permitted a unique angle of analysis as it allowed the assessment of serial peripheral blood biomarkers in 2 distinct clinical populations of patients with lung cancer, in addition to 2 differing drug mechanisms.

Within this work the longitudinal blood profiles of patients were examined following treatment with either PD-1 or PD-L1 antibodies; in addition to the relationships between blood profiles and patient outcome. It was quickly determined that the blood profiles of patients enrolled within both trials were significantly different to healthy controls, with increased percentages of both monocytic and granulocytic myeloid cells and reduced percentages of CD3+ lymphocytes, consistent with previous studies of the peripheral blood profile in cancer patients (434-437). In serial samples there were no overall significant changes in CD14+ or CD15+ populations. Within the MATRIX population, higher CD15+ percentages were detected at the cycle 4 time point and this may reflect an increasing inflammatory reaction in patients following immune stimulation; however, low numbers

within the analysis limit this assessment. In contrast to increasing CD15+ percentages, a reduction in T cell percentages were observed at both cycles 2 and 4 within patients receiving anti-PD-L1 therapy within MATRIX. This trend was not seen within patients enrolled in PEPS2. This observation is contrary to the original hypothesis that PD-1 or PD-L1 inhibition would improve T cell number and function. No significant changes were observed in surface expression of HLA-DR, PD-L1 or PD-1, on myeloid cells or T cells, except for the concealment of the PD-1 protein in PEPS2 patients leading to marked reductions in detection.

Significant suppressive activity of circulating CD15+ and CD14+ cells was demonstrated within T cell proliferation assays in both trial cohorts. Interestingly, suppression was greater in both cell populations from the PEPS2 trial, when compared to MATRIX. When examining serial samples following treatment, there was no overall suggestion of rescued proliferation; however, when samples were separated by the extent of suppressive activity, a trend towards improved T cell proliferation was observed at cycle 2 in both trial cohorts. This relationship was non-significant but may represent a reduction in the polarising behaviour of myeloid populations following interruption of the PD-1/PD-L1 signalling pathway. Previous studies have demonstrated that through the interruption of PD-L1 signalling suppressive action of both granulocytic cells and monocytes can be reduced, leading to enhanced T cell activation (416,417). The correlation in PEPS2 between higher whole blood CD15+ percentages and greater levels of suppression supports the hypothesis that abnormal granulocyte populations within the peripheral blood of patients create an immunosuppressive environment. High levels of CD15+ granulocytes represent an abnormal inflammatory response (233,237), and their presence is capable of disruption of T cell function through a number of well-defined mechanisms, discussed in detail below.

Overall, the effects of PD-1 or PD-L1 inhibition on the peripheral blood profile were small; however, the observation of lower percentages of CD3+ cells was an unexpected finding and should be considered in the context of patient response and outcome to fully assess its relevance. Through PD-1 blockade it would be expected that T cell function is enhanced and as such, circulating numbers improved; however, a recent investigation of peripheral blood profiles in melanoma patients receiving anti-PD1 therapy demonstrated improved responses in patients with low baseline T cell percentages (438). This finding was believed to reflect a movement of circulating T cells into peripheral tissues as seen in responses to anti-PD-1 therapy (439) although contradicts other studies which demonstrate low baseline T cell numbers to have a negative prognostic impact (317,430). The fact that this observation was not observed within the PEPS2 population may also indicate a chance finding and therefore further data collection is pivotal. The effect on the suppressive function of both CD15+ and CD14+ populations was also minimal, but trends were present to suggest that disruption of the PD-1/PD-L1 signalling pathway was leading to a normalisation of myeloid and T cell interactions. As with peripheral blood markers, this analysis should also be reviewed in the context of response and patient outcome and a significant limitation is the number of samples analysed sequentially, limiting the interpretation of these findings.

For samples obtained from PEPS2, analysis according to response and outcome was possible. Several recent studies have attempted to analyse similar relationships in patients receiving immunotherapy, with two of the most extensive studies performed by Marten's and Weide (317,430). In these studies, a broad range of peripheral blood parameters were analysed in patients receiving the either the CTLA-4 antibody ipilimumab, or the PD-L1 antibody, pembrolizumab. When examining factors associated with CTLA-4 inhibition, Martens *et al*

found that the presence of low numbers of CD14+ monocytes in addition to low percentages of CD14+HLA-DR$^{-/lo}$ MDSC were associated with a high probability of longer survival, with the presence of a low relative lymphocyte count being a negative indicator (317). In contrast, when looking at factors associated with Pembrolizumab Weide and colleagues found no association between patient outcome and monocyte count however, high absolute and relative neutrophil counts were significantly predictive of poorer survival. High basophil, eosinophil and lymphocyte counts were also all predictors of improved OS (430). When examining trends in PEPS2 no relationship was detected between total CD14+ monocytes and patient outcome, consistent with the finding by Weide *et al*. In view of recent work by Kreig *et al*, which showed no relationship between HLA-DR$^{-/lo}$ monocytic MDSC and patient outcome, but demonstrated improved responses in those patients with higher baseline numbers of classical CD14+CD16- monocytes (438), this subpopulation was also assessed, but no relationship could be demonstrated. There was also no correlation found between relative CD15+ percentages and patient PFS or OS.

In agreement with both studies by Martens and Weide, a significant correlation was detected between low CD3 percentages and both poorer PFS and OS, with lower mean CD3 percentages observed in patients living less than 1 year. The biological explanation behind such observations is highly likely to be related to the mechanism of drugs targeting PD-1 and PD-L1 interactions. As signalling between PD-1 and PD-L1 leads to reduced T cell proliferation, cytokine release and apoptosis (267,400), the breakdown of this signalling aims to re-activate T cell function. It has been demonstrated that the presence of higher numbers of infiltrating T cells (440), in addition to early increases in peripheral T cell percentages (318) are predictive of response to PD-1 therapy, consistent with the relationship observed in PEPS2 patients.

This analysis also detected poorer overall survival in patients with higher expression of PD-L1 on CD14+ cells, which is of interest as there is little known about the association of peripheral PD-L1 expression and outcome following PD-1 or PD-L1 therapy. Patients with survival less than 6 months demonstrated median CD14 PD-L1 expression of 72.7%, compared to 56.8% in those surviving over 6 months. This reduced further to 53% in those surviving greater than 1 year. The combined positive score, which takes into account tumour, lymphocyte and macrophage PD-L1 expression, has recently begun to be used to predict response to PD-1 and PD-L1 treatment (314), with higher scores associated with improved response rates and survival. The findings of poorer outcomes in patients with higher peripheral monocyte PD-L1 expression is contrary to this; however, it may be proposed that systemic activation of PD-L1 may have a negative impact on circulating T cells leading to an overall dysfunction which is unable to be overcome despite PD-1 blockade, particularly in those patients with low numbers of functioning T cells at baseline. Research carried out by Mao *et al* supports this theory (416). This group demonstrated within a murine model that a reduction in circulating PD-L1 expressing monocytes led to increased numbers of circulating and tumour infiltrating CD8+ T cells, with increased levels of T cell activation. The association observed should therefore be explored in a wider cohort to establish whether this could be used as a possible predictor of response to PD-1 therapy.

A further point of interest within this investigation is the relationship between NLR and patient outcome. Despite not successfully showing a relationship between whole blood neutrophil percentages and outcome, there was a clear trend to poorer outcome when this variable was represented within the NLR, and a significant correlation when examining the NLR at the cycle 2 time point. At cycle 2 survival was significantly prolonged in those patients

with an NLR less than 5, with median survival of 515 days compared with 246 days. Caution must be applied when interpreting this analysis as numbers were low, with only 28 patients contributing data at this time point. Despite the non-significant difference at time point one, median survival between the two groups was notably different, with a median OS of 419 in patients with an NLR <5, compared to 207 days with NLR >5. Forty-five patients contributed to this analysis. These findings are supported by work by three separate groups examining predictive and prognostic markers of response to Nivolumab therapy in NSCLC (418-420). The largest study performed by Bagley *et al* retrospectively analysed the baseline NLR in 175 patients with NSCLC receiving Nivolumab. Using the same cut-off point of NLR >5, they demonstrated pre-treatment NLR to be an indicator of poor OS. In addition, in a multi-variate model, NLR remained an independent indicator of poor survival, alongside the presence of liver metastases and PS > 2 (420). No serial measurements of NLR were recorded within the study by Bagley *et al*; however, within the setting of renal cell carcinoma Lalani and colleagues performed serial assessment of NLR in patients receiving anti-PD1 therapy (432). They demonstrated that higher baseline NLR showed a trend towards predicting response and survival, but as seen in our findings, a later NLR measurement at 6 weeks was a significant predictor of response, PFS and OS. In addition, those patients who saw a reduction in NLR at the second time point had an improved outcome, independent of their baseline. Similar findings were observed by DiGiacomo when analysing the NLR in patients receiving Ipilimumab in melanoma, with above average NLR at both week 7 and week 10 strongly predictive of poorer survival (433). These findings are consistent with our observation that a high NLR following the first cycle of treatment, was strongly associated with poorer PFS and OS. As discussed in previous sections, the NLR has already been strongly associated with poorer outcome in many cancer types (185,332,422,441) and its importance as an indicator

of response to immunotherapy is now emerging. A high NLR is impacted by high peripheral neutrophil counts and the presence of high numbers of circulating neutrophils indicate systemic inflammation (233). In the setting of cancer, neutrophil chemotactic factors are found to be expressed to higher levels and neutrophil production of MMP-9 and VEGF have been shown to be drivers of angiogenesis (236,245). Alongside this tumour promoting activity, neutrophils also disrupt T cell function through production of ROS (239,240), enhanced arginase activity (244) and via direct induction of apoptosis (235). These actions, leading to poor T cell function and number, are therefore highly likely to impact on the ability of immunotherapies to promote an effective anti-tumour response, as the blockade of immune checkpoint signalling can only create its effect if there is an adequate pool of T cells to engage.

The role of STAT3 within the cancer-immune microenvironment was also discussed within the introduction to this chapter as STAT3 hyperactivation, again promoted by an enhanced inflammatory response, may both induce the expression of immune check points (294,410,413,442) and compromise T cell function by inducing differentiation to regulatory T cells and inhibiting T cell cytotoxic function (385,391,443). Investigation of the role of STAT3 in this setting, particularly in circulating patient T cells, was planned however, due to limitations on the timing of this thesis, this element of the research is yet to be completed.

Further limitations of this study were the way in which trial samples were delivered to the university for analysis. Both trials were UK wide, which meant samples must be taken and posted by multiple centres. Blood samples should by protocol reach our laboratory within 24 hours, which then permitted analysis with good quality specimens. Occasionally samples were delayed at source or during transit, meaning that their condition was not adequate for

analysis on arrival. In addition, some samples which were analysed, but deemed poor quality, were required to be removed from the analysis. Poor quality samples were identified during flow cytometry, when above average cell death was noted. In addition to loss of samples for quality control, some patients failed to have blood sent due to deviations from protocol, or due to inability to obtain adequate blood at venesection. Finally, trial drop-out led to limited numbers of samples at the later time points. The removal of samples from analysis for these reasons, the limited numbers of sequential samples that were obtained during the analysis period.

In addition to the problems with sample acquisition, access to all appropriate patient data was also difficult towards the end of this PhD, since both trials were still active. Within the MATRIX trial we were unable to access patient outcome data to support or refute the findings made in PEPS2. Comparative analysis in both cohorts will provide interesting insights into the relevance of the different observations in peripheral blood profiles. This data will hopefully be collated and published once this trial is complete.

Chapter 6: Final Discussion and Future Directions

6.1 Final Discussion

The identification of associations between immune suppression and the development of cancer prompted great interest in this field, with the view that harnessing the immune system could be a mechanism in which to combat cancer development. These theories have taken many years to come to fruition; however, over the last two decades, there have been huge developments in the understanding of immune dysregulation in cancer and mechanisms in which to overcome this. Treatments which re-direct the body's own immune system to attack cancer cells have shown great promise, with some of the most dramatic clinical outcomes seen in many years. Despite these breakthroughs, there remain many unanswered questions regarding immune biology in the setting of cancer, in terms of both why such deranged immune profiles are seen, in addition to the mechanisms by which they act. This thesis had two main aims. Firstly, to explore the differing immune profile within cancer patients, particularly focussing on myeloid cell populations in mesothelioma; and secondly, to attempt to identify a mechanism by which abnormal immune populations may be altering the function of the host immune system in the presence of cancer.

Multiple studies have demonstrated that within the setting of cancer immune cell profiles are altered. Early observations in mice demonstrated the presence of populations of myeloid cells which seemed to be uniquely triggered by the development of cancer (247-249) and were shown to be capable of inactivating normal immune responses. Strikingly, the removal of tumours from subjects with abnormal immune populations has been associated with a normalisation of these populations (444,445), in addition to observations of reversed immune

suppression (446). These findings highlight the important interactions occurring between the tumour and the immune system, implying that the induced dysfunction continues to rely on tumour feedback. As this field of research has progressed there have been many documented immunosuppressive populations, including regulatory T cells (187,193), immune suppressive dendritic cells (213,214), tumour associated "M2" macrophages (225) and tumour associated neutrophils (233-235). The role of neutrophils is also emerging as an important marker of systemic immune disruption, with many studies demonstrating the presence of increased numbers of neutrophils within the blood of cancer patients. This identification and association with poor outcome was first published by Shoenfeld in 1986 (447) and has since been described as the neutrophil-to-lymphocyte ratio (NLR), with associations with poor outcome seen in many tumour settings (448-451).

The first chapter of this thesis attempted to draw on these principles and examine the role of circulating systemic granulocytes, in addition to tumour infiltrating granulocytes, in patients with mesothelioma. In a UK based population with newly diagnosed mesothelioma, this research demonstrated raised levels of circulating granulocytes and resultant increases in the NLR. The differences observed in the NLR were significant, with ratios in patients showing an average of 6.2, compared with 1.5 in healthy comparators. As described above, the NLR has been demonstrated in a number of solid cancers to be strongly prognostic of poor outcome following surgery and systemic oncological treatments. Importantly, it has also been shown to be predictive of outcome in patients with both mesothelioma and NSCLC. In 2 large cohort studies, NLR was associated with poorer survival in mesothelioma, with marked reductions in survival from 12 to 7.5 months and a reduction in 1 year survival from 60 to 26% (185,332). In a large cohort study by Linton and colleagues the NLR was an independent prognostic factor

in multivariate analysis and was proposed within a new prognostic scoring system (185). The strong association of this variable with patient outcome therefore highlights the complex and vitally important relationship between malignancy and a functional immune system.

Through flow cytometry analysis, the predominant abnormal cell type in our patient population was shown to be whole blood granulocytes. Initial experiments included granulocytes found within the PBMC layer, which would classically be described as G-MDSC (250). This population was less abundant and less potent in terms of their ability to suppress T cell function, therefore our work focussed on high density granulocytes, which form a distinct population from G-MDSC. Within tumour tissues CD15+ granulocytic cells were also identified, consistent with findings of Chee and colleagues, who identified populations of NP57+ neutrophils present in tissue sections derived from a cohort of 302 mesothelioma patients (183). Chee *et al* demonstrated that high NP57 expression within tumours was associated with poorer overall survival (183) and therefore supports our theory that a granulocytic infiltrate may be altering both the immune biology and tumour behaviour. Defining the nomenclature of these immune suppressive or tumour associated neutrophils is challenging. There is not one distinct immunomodulatory neutrophil population and during the malignant process multiple pathways can drive their polarisation and development. The involvement of granulocyte-derived MDSC in immune suppression perhaps occurs during an earlier stage of their development, as one of the most frequently described characteristics of MDSC is their immature nature (250), with morphologically less developed cells showing greater suppressive potential in mouse models (452). In practice, this definition is often contraindicated, as studies demonstrate suppressive neutrophil populations can be activated, with hyper-segmented morphology and higher levels of CD11b and CD66b expression

(238,244). Conversely, both CD16high and CD16low (activated) populations have been shown to demonstrate suppressive activity (235,238). It is not clear within such studies whether these populations represent normal neutrophils with suppressive functions, or a form of MDSC. Pillay *et al* describe a population of mature neutrophils, expressing high surface CD16, CD11b and CD54, with low CD62L. These neutrophils were induced by acute inflammation and had increased maturity in terms of a hyper-segmented morphology. This phenotype therefore does not fit with the classical MDSC yet, neutrophils were found to suppress T cell proliferation through the release of ROS. H_20_2 delivery was found to be delivered directly to T cells through the integrin Mac-1 (238). Hao and colleagues detected this population of $CD62L^{dim}$, $CD16^{bright}$ neutrophils in both cancer and surgery patients, and confirmed that these cells were not found in the blood of normal controls (453). Further to this, de Kleijn *et al* went on to suggest an additional mechanism by which this subset suppresses T cell function (454). Within the research of de Kleijn and colleagues, they demonstrated that in response to IFN-γ, $CD62L^{dim}$ $CD16^{bright}$ neutrophils increase their expression of PD-L1, which led to suppression of T cell proliferation (454). These subsets therefore represent populations of neutrophils that may otherwise be classed within a spectrum of normal cells, rather than classic MDSC. Within both studies whole blood neutrophils were assessed, rather than those residing within the PBMC layer, further distinguishing them from the classic granulocyte-derived MDSC. However, methods of isolation are conflicted within the literature. Rodriguez *et al* report a similarly suppressive, activated population, being selected from the PBMC layer in patients with renal cell carcinoma (244). These activated neutrophils appeared similar in morphology to those described by Pillay *et al*, with a mature, hyper-segmented appearance, but resided within the PBMC layer and were low expressers of CD16. In addition, the mechanism of T cell suppression for this subpopulation was that of arginase I release (362).

The flow cytometry characteristics identified within this thesis did not strongly support previously identified neutrophil phenotypes, with no significant differences in surface marker expression detected between patient and healthy donor granulocytes. A suggestion of lower CD66b and CD11b expression within patient whole blood and PBMC granulocytes was observed and this was greater within the low density (PBMC) population. Within low density granulocytes, lower CD16 expression was also observed, which may support the findings of Rodriguez *et al* (244). In contrast however, Rodriguez and colleagues demonstrated this population of G-MDSC had high CD11b and CD66b expression, which was not a finding within our research. PD-L1 expression within our granulocyte population was low, with a median of 8% of CD15+ cells positive for PD-L1. This was lower than that of healthy controls, where 12% stained CD15+PD-L1+. It is difficult to compare these percentages to the findings of de Kleijn, as within their study enhanced PD-L1 expression was quantified through mean fluorescence intensity, rather than absolute levels of PD-L1 expression (454); however, it is unlikely that PD-L1 played a significant role in the function of our CD15+ granulocytes in view of the lack of differentiation from healthy controls.

Within whole blood high density neutrophils, flow cytometry phenotypic analysis was not sufficient to delineate a population which differed from healthy controls. In addition, due to the nature of the experiments, no detailed flow cytometry analysis of tumour infiltrating CD15+ cells was performed to distinguish a tumour residing population from that in whole blood. Further examination of the gene expression profiles of all 3 neutrophil populations would be of great interest, particularly following recent research by Fridlender *et al* which explored the genetic variations between murine G-MDSC and TAN in depth, demonstrating increased APC functions and chemokine production in both G-MDSC and TAN, and

interestingly, down regulation of pathways required for the respiratory burst (336). Fridlender *et al* demonstrated that healthy murine neutrophils were more aligned to MDSC in their mRNA expression profiles, particularly in regard to cytoskeletal organisation and migration, indicating that the role of neutrophils is altered upon entering the tumour environment (336). No data on cell surface marker expression was given from this study; however, due to this work being carried out in murine cancer models, cell phenotypes would not be comparable to this thesis.

The development of an altered inflammatory profile in mesothelioma is well documented with a wide range of immunomodulatory cytokines produced during the development of both asbestos related disease and mesothelioma (69,76,78), in addition to the production of factors which alter the extra-cellular matrix and promote angiogenesis (74,85,125). The production of factors such as MMP-9, described by Nozawa *et al*, are also implicated in the mechanisms used by tumour infiltrating neutrophils leading to enhanced VEGF production and the "angiogenic switch" in malignancy. This thesis similarly identifies a strong inflammatory profile within mesothelioma, with findings drawn from both primary mesothelioma samples and newly derived mesothelioma cell lines. Consistent with Adachi *et al* (78), high expression of the pro-inflammatory cytokine IL-6 and the angiogenesis driver VEGF was identified. High expression of the neutrophil chemotactic factors IL-8, Midkine and GRO-α, also supports the role of the tumour environment in recruitment and activation of neutrophils. Midkine and GRO-α have both been previously shown to be raised in both asbestos exposed individuals and patients with mesothelioma (222,455) and are implicated in driving inflammation an invasion in this and other cancers (456,457). Further to these findings, GM-CSF was also detected within the supernatants of mesothelioma tissues and cell

lines, which has also been implicated in neutrophil function, with a role in the induction of ROS production, a widely accepted mechanism of neutrophil induced immune suppression (239) . Through co-culture and exposure to TCM it was shown that ROS generation was driven by mesothelioma derived GM-CSF and this was demonstrated to be the mechanism of T cell suppression occurring in neutrophil exposed T cells (342). GM-CSF is implicated in the generation of suppressive myeloid cells and was shown to be a required cytokine for the generation of these populations (207,369,370). Recruitment of suppressive myeloid cells in murine tumour models was shown to be enhanced by the delivery of GM-CSF and also impaired the function of tumour vaccines in this setting (208). Similar effects were also detected within human melanoma patients. GMCSF, used in this setting as an adjunctive therapy to recruit and drive APC function, was shown to enhance populations of immunosuppressive myeloid cells and led to poorer vaccine response (458,459). Patients receiving GM-CSF demonstrated enhanced populations of CD14+HLADRlow MDSC, which were suppressive to T cell proliferation through TGF-β (459). These findings support the role of GM-CSF in the development of immunomodulatory myeloid populations and suggest an additional mechanism that could be targeted alongside the use of more standard therapies. This theory is further supported by data demonstrating that inhibition of GM-CSF and combined chemotherapy treatment can reduce the function of inhibitory populations (371).

The finding that ROS was acting as the primary mechanism of T cell suppression in this setting is also relevant to the wider tumour microenvironment, as ROS has been shown to be an important regulator of cancer associated inflammation (460,461). At moderate levels ROS has been shown to activate the transcription factor NF-κB, a factor typically induced by inflammatory cytokines such as TNF-α and IL-1β (462). NF-κB drives the transcription of

further inflammatory mediators, recruiting and activating inflammatory cells (463). A feedback loop is therefore generated to drive an inflammatory environment. Interestingly, many recent studies have shown that reactive oxygen intermediates are vital for most pathways of NF-κB activation, further highlighting this important mechanism (464). Within a tumour environment, ROS has been shown to promote angiogenesis through activation of the STAT3/VEGF signalling pathways in breast cancer (465), and through activation of the ERK1/2 pathway, inducing expression of both HIF-1α and VEGF (466). A role in the development of metastases has also been documented through activation of the extracellular matrix and drivers of epithelial to mesenchymal transition (467,468).

In support of these complex interactions between ROS and a broader setting of inflammation, our work also detected abnormalities in the wider immune profile of patients with mesothelioma, with alterations in percentages of CD14+ monocytic cells and CD3+ T cells. These findings may also be driven by the enhanced expression of inflammatory cytokines including IL-6, IL-8 and VEGF, widely described in mesothelioma (78,469,470) and confirmed within this work. The reduction in patient T cell percentages may be in part driven through the immunomodulatory properties of IL-6, with inhibition of both CD4+ and CD8+ differentiation driven through the actions of this pleomorphic cytokine (390,471).

In the second chapter of this thesis mesothelioma supernatants were shown to reduce T cell function, with a reduction in their ability to produce the pro-inflammatory cytokine IFN-γ, as previously shown by Diehl *et al* (390). More notably however, was the profound reduction in T cell proliferation that was observed following culture in the presence of mesothelioma TCM, partially driven by STAT3 activation. We demonstrated that IL-6, present within the supernatant of mesothelioma cell lines, induced early STAT3 phosphorylation in T cells.

Reducing STAT3 activation using an antisense oligonucleotide, led to a modest improvement in overall T cell proliferation. In support of the finding that STAT3 may be responsible for maintaining the effective functioning of proliferating T cells, work by Kujawski *et al* demonstrated that through complete knockdown of STAT3 within CD8+ T cells, both T cell tumour infiltration and T cell proliferation were enhanced (385). Both Kujawski and Ozao-Choy further confirmed these observations using the tyrosine kinase inhibitor sunitinib. Sunitinib is known to act through the STAT3 signalling pathway, demonstrating that altering STAT3 signalling could both enhance T cell proliferation, reduce expression of T cell exhaustion markers PD-1 and CTLA-4 and reduce the development of regulatory T cells. The antisense oligonucleotide chosen in this study appeared unable to efficiently enter T cells and inhibit T cell STAT3, which likely explains the limited rescue in T cell function that was observed. Further investigation using molecules such as sunitinib may be a useful method to further assess this hypothesis and confirm the role of STAT3 as a negative regulator of T cell function in the setting of mesothelioma.

Examining the role of STAT3 in T cells in isolation does not reflect the profound role that STAT3 appears to employ within the immune microenvironment, therefore the role of STAT3 in the function of DC was also assessed. Exposure of DC to tumour derived supernatants during generation led to decreased ability to effectively stimulate T cell responses. Although only subtle changes in STAT3 activity were shown in these impaired populations, STAT3 inhibition, confirmed through western blot, led to marked improvements in their ability to stimulate T cell proliferation. This effect is supported by research by both Park and Nefedova, who demonstrate that tumour derived inflammatory factors, in particular IL-6 and VEGF, are capable of inhibiting DC function through the activation of STAT3 (382,396). Both IL-6 and

VEGF were present in high concentrations in mesothelioma supernatants and are therefore highly likely to be driving STAT3 activation within DC in this work. No significant changes in DC maturation markers were detected and the persistence of CD14 and CD33, markers of undifferentiation, were not consistent or significant. The mechanism behind the alteration of DC function is therefore unanswered. One area unexplored is the possibility of the induction of immune checkpoints on DC such as CTLA-4 and PD-L1, which in turn, are capable of impairing T cell function through the induction of T cell tolerance (414). The expression of PD-L1 on DC has been shown to be driven through STAT3 activation, secondary to IL-6 stimulation, and is associated with an inhibitory DC phenotype capable of inducing regulatory T cells (411). Wolfle *et al* demonstrated that this population drove positive feedback through the production of inflammatory cytokines IL-6, TNF and IL-12, along with the immunosuppressive cytokine IL-10. This environment would be capable of ongoing stimulation of STAT3 activation in both DC and T cells, further promoting a suppressive environment. We did not examine the cytokine profiles produced by DC following TCM exposure therefore cannot determine whether these mechanisms of immunosuppression are occurring in this setting. Further work is required to investigate in depth the phenotype of TCM induced DC and the cytokine profile released. Examining the interaction with T cell sub-populations and changes in T cell surface protein expression of regulatory T cell markers such as CD25 and FOXP3, may then determine the mechanisms employed.

The final chapter of this thesis aimed to bring together the findings from both chapters 3 and 4 and further assess their relevance in a larger, real-world population of patients. In addition, it aimed to assess the impact of check-point inhibition on the peripheral blood profile in cancer patients and correlate these findings to treatment response. A limitation of the work

carried out within chapter 3 was that no clinical data associated with patient blood and tissue samples was available for analysis. Findings of higher CD15+ percentages or the NLR could therefore not be correlated with patient factors such as treatment response or survival. A primary study identified in mesothelioma was due to aid in the provision of such data; however, this trial could not be completed due to withdrawal of the proposed study drug. Investigation of similar parameters within two cohorts of lung cancer patients was therefore proposed, as parallels could be drawn between the clinical settings of lung cancer and mesothelioma.

Both lung cancer trials were investigating the efficacy of PD-1/PD-L1 inhibition, however differed in their enrolled cohort and drug target. The PEPS2 trial enrolled exclusively performance status 2 patients, while MATRIX excluded this cohort, and the PEPS2 study drug targeted the PD-1 molecule, while MATRIX targeted PD-L1. These factors had the possibility to provide markedly different patient populations, giving an additional comparative angle during the analysis. Patient samples were collected at the point of entry into clinical trials and serial samples at defined time points, following initiation of treatment. This provided a novel study of whole blood immune populations following treatment with the immunomodulatory checkpoint inhibitors, Pembrolizumab (PEPS2) and Durvalumab (MATRIX).

Consistent with our findings in mesothelioma, abnormal peripheral blood profiles were observed in patients with advanced NSCLC. Patients had high percentages of circulating CD15+ and CD14+ myeloid cells and low percentages of CD3+ lymphocytes. Both populations showed profound differences in CD14+ and CD15+ myeloid percentages when compared with healthy controls. Interestingly, patients within the PEPS2 cohort also displayed significantly higher expression levels of the checkpoint inhibitors PD-L1 and PD-1 on CD14+ and CD3+ cells,

respectively. A number of variables were examined to attempt to explain this variation, including age, number of prior treatments and cancer stage; however, no relationship could be identified. The only differential factor which stood out as a possible explanation was the performance status of patients. It is well documented that performance status is a strong prognostic marker in malignancy and it can be inferred that performance status is also associated with a more profound inflammatory environment. One of the earliest EORTC studies examining prognostic markers in mesothelioma identified both high WBC count and PS to be independently prognostic of poorer survival (472), validated in later work by Edwards *et al* and Fennell *et al* (473,474). Further studies have consistently confirmed an environment of inflammation to be negatively associated with prognosis and the inflammatory based Glasgow Prognostic Score demonstrates that those patients with PS > 2 are more likely to demonstrate raised inflammatory markers such as CRP (475). The presence of systemic inflammation has also been shown to drive the expression of PD-L1 on tumour tissues, with PD-L1 expression being associated with increased plasma CRP levels in lung cancer patients (476). More recently, serum PD-L1 has also been shown to be associated with high levels of CRP in gastric cancer (477). A persistent inflammatory environment also creates an exhausted T cell population with higher PD-1 expression (478). These factors combined could therefore explain the findings observed within the PEPS2 population, who demonstrate poorer performance status, peripheral blood inflammatory profiles and high expression of inhibitory check point markers. The importance of explaining these findings has relevance to the later observations that both low numbers of circulating CD3+ T cells, high expression of PD-L1 on CD14+ cells and NLR were all predictive of poorer overall survival within this population. The association of lymphopenia with poor outcome in cancer patients is well documented and, when represented within the NLR, has been widely associated with both poor outcome in

malignancy (185,332,422,434,436) and poor response to check point inhibition (317,430). The relevance of peripheral PD-L1 expression is more novel and there are few studies that characterise this. A recent extensive exploratory study performed by Krieg *et al* examined the peripheral blood profiles of melanoma patients receiving anti-PD-1 therapy with either nivolumab or pembrolizumab. They performed an extensive assessment of baseline and post-treatment peripheral blood profiles, using mass spectrometry to attempt to determine signatures predictive of patient response. Their analysis examined differences between responders and non-responders and detected a population of CD14+CD16-HLA-DR^{hi} classical monocytes, which were predictive of response. Higher percentages of these populations were detected in responders both at baseline and post-treatment. This population was shown to co-localise with PD-L1 expression, which was seen less frequently in non-responder populations. In addition, Krieg detected that low frequencies of CD3+ T cells were also predictive of responding patients (438). These observations are contrary to the findings in this thesis and are an interesting development within this field as, classically, both high CD3 and low monocyte frequencies have been more aligned with patients with improved outcomes in the setting of lung cancer and mesothelioma (356,479). In agreement with this traditional theory, Weide *et al* examined baseline blood profiles in 616 melanoma patients receiving treatment with the PD-1 antibody pembrolizumab. They found that high baseline lymphocyte counts were significantly predictive of improved overall survival following treatment (430). A similar study by Martens *et al* observed the same associations and found that improved response to treatment was associated with increases in T cell frequencies within 2 to 6 weeks of therapy (317). These findings are also supported by Deylon *et al* who demonstrated improved survival within patients with higher absolute lymphocyte counts prior to their second course of treatment (480). Interestingly, all three studies observed increases in

circulating eosinophils as further predictors of improved response and survival. This finding was not observed by Krieg and colleagues. The numbers studied within the work by Krieg is a limitation, as only 51 samples from a single institution were assessed and this may have led to the introduction of selection or population bias. The findings in this thesis of poorer outcome associated with higher CD14+ PD-L1 expression is also contrary to Krieg *et al*. There is less supportive work assessing these peripheral populations in the setting of immune checkpoint blockade; however, there are associations between serum-detectable PD-L1 and patient outcome. Soluble PD-L1 has been widely identified in cancer patients (481) and has been shown to be preferentially shed by the myeloid compartment within peripheral blood (482). Once present within the circulation its role is not well defined, yet has been shown to negatively impact on T cell function (482). The presence of soluble PD-L1 in patients with NSCLC has also been associated with poorer overall survival (483), confirming its role as a negative regulator of the immune system. Within the tumour microenvironment there remains greater controversy on the functions of both tumour and myeloid expression of PD-L1. High tumour PD-L1 expression has been associated with poor tumour differentiation and poorer patient survival in NSCLC (484); however, higher levels of expression are also a positive predictor of response and outcome following treatment with PD-1 and PD-L1 antibodies (402). Although the role of tumour infiltrating immune cells has begun to be incorporated into scoring systems within other cancer subtypes, including urothelial and gastric cancer (314,485), this has yet to be adopted in NSCLC or mesothelioma, therefore its role as a positive or negative marker in this environment is yet to be defined.

The contradictions observed in associations between peripheral blood profiles and clinical outcome in patients receiving immune checkpoint inhibitors highlights the difficulties faced

in this type of analysis. Often studies are small and focussed on different elements of peripheral and tumour immune populations, leading to difficulties comparing between studies and in concluding which markers are most predictive of response or survival. In conclusion, this thesis raises again the prognostic value of pre-treatment and on treatment NLR in predicting outcome from PD-1 inhibition in NSCLC. In addition, this research presents a more novel finding of the significance of high circulating monocyte PD-L1 expression in predicting poorer overall survival following treatment. The ability to apply these findings in clinical practice would allow improved patient selection and possible early identification of non-responders in regard to the on-treatment NLR. Such markers should be validated within clinical trials to allow them to be widely adopted. In terms of patient benefit, robust predictive biomarkers of response could minimise exposure to ineffective treatments and allow a more stratified approach to treatment selection.

6.2 Future directions

Due to the inclusion of clinical trial samples from an active trial, some elements of research from this PhD are ongoing. Interrogation of patient serum samples is in progress, assessing the presence of a broad group of inflammatory markers, including the pro-inflammatory cytokines GM-CSF, IL-1β, IL-6 and IL-8; along with the immune suppressive cytokines IL-10, IL-4 and IL-13. In view of the findings within chapter 3 of a strong inflammatory profile in the blood of patients with mesothelioma these findings will aid in the ability to draw similarities between these two populations. In addition, information relating to the systemic cytokine profile, will allow further conclusions to be drawn relating to the effect of both circulating myeloid and lymphocyte populations in this setting. For instance, a profile of high inflammation including enhanced levels of IL-6, IL-8 and GM-CSF will support the theory that

the high numbers of circulating neutrophils are driving, or conversely being driven, by a heightened inflammatory environment.

In addition to assessment of serum cytokines, analysis of T cell protein expression is also planned. The primary aim of this element of the research was to assess the activity of STAT3 in the circulating T cell population and determine whether STAT3 activity is affected through the blockade of PD-1 or PD-L1. As described previously, both PD-1 and PD-L1 can be driven through STAT3 activation, primarily stimulated by inflammatory cytokines such as IL-6 and VEGF (411,413). We hypothesise therefore that, within the inflammatory environment of lung cancer, hyperactivation of STAT3 may be contributing to T cell exhaustion, PD-1 expression and poor T cell function. Further analysis of the expression of T cell exhaustion markers CTLA-4, PD-1, LAG-3 and TIM-3 is also proposed. These investigations will allow a comprehensive analysis of the immune microenvironment in advanced NSCLC and provide a novel assessment of the sequential changes that occur within peripheral T cells following check-point blockade.

With the above information gained, as well as building on the research from chapters 3 and 4 of this PhD, a more comprehensive analysis of both the myeloid and lymphocyte populations in patients receiving checkpoint treatment for mesothelioma should then be pursued.

Although it was demonstrated that mesothelioma and lung cancer patients harbour an abnormal granulocyte population, we were unable to determine their precise characteristics, and therefore could not define this population. As highlighted by the work on murine

neutrophils and G-MDSC by Fridlender *et al* (336), differentiation of these populations could be achieved by thorough RNA sequencing analysis.

With the much wider use of next generation sequencing (NGS), the ability to explore the transcribed genome has become far more accessible to research (486). It is now possible to gain an understanding of the dynamic expression of genes and accurately quantify levels of gene expression. In addition, in contrast to pre-determined gene microarrays or qRT-PCR, it is also possible to detect completely new areas of enhanced gene expression, which may provide insights into previously undefined cellular functions or aberrant cellular activity (487). We propose that work alongside a trial of checkpoint blockade in mesothelioma could provide this opportunity. Blood samples should be taken from patients at diagnosis, start of immunomodulatory treatment (e.g. checkpoint blockade) and along a treatment course, and granulocytes from both whole blood and the PBMC compartment assessed. In addition, if granulocytes could be extracted and studied from tumour specimens this would also be of considerable merit.

Transcriptomic analysis of each population of granulocytes would determine whether a predominant population or, multiple granulocyte subsets with differing functions, are present in cancer patients. Specifically, this information may provide evidence of multiple granulocyte populations and insights into the functions of tumour related granulocytes. Possible mechanisms of deregulated immune function may be highlighted, in addition to evidence to support theories on tumour related growth signals (361).

With the information gained from RNA sequencing, it may also be possible to define a novel panel of cell surface markers, capable of differentiating the detected granulocyte populations.

Following detection of regions of surface marker clustering and differentiation between populations, confirmation of protein expression would be carried out through flow cytometry. To allow the study of multiple cell surface markers, mass cytometry (CyTOF) could be applied. Mass cytometry combines the principles of both flow cytometry and mass spectrometry, pushing the restrictions of polychromatic flow cytometry (PFC) and allowing the analysis of over 40 simultaneous parameters on a single cell, without the risk of channel overspill experienced with standard PFC. Once predominant groups of surface markers were identified, these could be limited to allow use in PFC and permit wider application. If this technique were successful, the proposal of a group of differing granulocyte phenotypes, relating to populations such as G-MDSC and TAN, would be hugely influential in this field of research (250).

Finally, if patients' samples could be obtained from a mesothelioma clinical trial of checkpoint blockade, it would be of interest to determine peripheral blood markers for prognostic or predictive relevance in the treatment of this cancer. Although not yet accepted as an official biomarker, the NLR clearly has prognostic relevance and it would be interesting to prospectively assess this marker in a trial of a PD-1 or PD-L1 inhibitor in mesothelioma. Importantly, a validated set of predictive biomarkers needs to be determined in all cancer subtypes, but particularly within those where response to check point inhibition is poorer, such as mesothelioma, colorectal and gastro-oesophageal cancer. Within colorectal cancer, identification that a subset of patients with higher mutational burden will preferentially respond to check point blockade, is one example of this stratification (488).

In the current environment we have been privileged to witness huge advancement in the treatment of cancer, with survival at its highest in many conditions, particularly lung cancer.

Despite the wealth of research into of the immune system and its role in cancer development we are however, still significantly limited by our understanding of the complex interactions occurring within the tumour microenvironment. This limited understanding is highlighted by the conflicting research findings that are discovered within available literature. Further comprehension of the mechanisms driving altered inflammatory profiles in cancer and the mechanisms utilised in immune escape will hopefully lead to ongoing improvements in cancer care and further gains in survival.

Appendix 1

Publication: Tumor-Derived GM-CSF Promotes Granulocyte Immunosuppression in Mesothelioma Patients

Published OnlineFirst March 30, 2018; DOI: 10.1158/1078-0432.CCR-17-3757

Translational Cancer Mechanisms and Therapy

Clinical Cancer Research

Tumor-Derived GM-CSF Promotes Granulocyte Immunosuppression in Mesothelioma Patients

Swati Khanna[1], Suzanne Graef[2], Francis Mussai[2], Anish Thomas[1], Neha Wali[3], Bahar Guliz Yenidunya[4], Constance Yuan[5], Betsy Morrow[1], Jingli Zhang[1], Firouzeh Korangy[1], Tim F. Greten[1], Seth M. Steinberg[6], Maryalice Stetler-Stevenson[5], Gary Middleton[2], Carmela De Santo[2], and Raffit Hassan[1]

Abstract

Purpose: The cross-talk between tumor cells, myeloid cells, and T cells can play a critical role in tumor pathogenesis and response to immunotherapies. Although the etiology of mesothelioma is well understood, the impact of mesothelioma tumor cells on the surrounding immune microenvironment is less well studied. In this study, the effect of the mesothelioma tumor microenvironment on circulating and infiltrating granulocytes and T cells is investigated.

Experimental Design: Tumor tissues and peripheral blood from mesothelioma patients were evaluated for presence of granulocytes, which were then tested for their T-cell suppression potential. Different cocultures of granulocytes and/or mesothelioma tumor cells and/or T cells were set up to identify the mechanism of T-cell inhibition.

Results: Analysis of human tumors showed that the mesothelioma microenvironment is enriched in infiltrating granulocytes, which inhibit T-cell proliferation and activation. Characterization of the whole blood at diagnosis identified similar, circulating, immunosuppressive $CD11b^{+}CD15^{+}HLADR^{-}$ granulocytes at increased frequency compared with healthy controls. Culture of healthy-donor granulocytes with human mesothelioma cells showed that GM-CSF upregulates NOX2 expression and the release of reactive oxygen species (ROS) from granulocytes, resulting in T-cell suppression. Immunohistochemistry and transcriptomic analysis revealed that a majority of mesothelioma tumors express GM-CSF and that higher GM-CSF expression correlated with clinical progression. Blockade of GM-CSF with neutralizing antibody, or ROS inhibition, restored T-cell proliferation, suggesting that targeting of GM-CSF could be of therapeutic benefit in these patients.

Conclusions: Our study presents the mechanism behind the cross-talk between mesothelioma tumors and the immune microenvironment and indicates that targeting GM-CSF could be a novel treatment strategy to augment immunotherapy in patients with mesothelioma. *Clin Cancer Res; 24(12); 2859–72. ©2018 AACR.*

Introduction

Malignant mesothelioma is an aggressive cancer arising from the mesothelial cells lining the pleura, peritoneum, and pericardium (1). The majority of patients present with advanced-stage disease and are not candidates for surgery. Although chemotherapy improves outcome for these patients, the median overall survival is less than 24 months (2). Immunotherapy approaches relying on T-cell anticancer activity, such as peptide vaccines and CAR T cells, have shown only limited efficacy, suggesting that the underlying immune microenvironment may play a role in muting the immune response (3, 4).

Myeloid cells play an important role in the balance of pro- and anticancer T-cell responses. Murine models of mesothelioma have shown that monocytes, macrophages, and dendritic cells may be modulated by the tumor microenvironment (5–7). However, the functional role of granulocytes and their mechanism of action in human mesothelioma are not well understood. Studies in mesothelioma have suggested the ratio between peripheral blood or intratumoral neutrophils and lymphocytes correlates with prognosis, indicating a key interaction between these cells in tumor pathogenesis (8). In other cancers, secreted factors within the tumor microenvironment control the differentiation of granulocytes. In turn, this may promote inflammation within the tumor microenvironment or lead to changes in the interaction with the adaptive immune response. Here, we investigate the mechanisms underlying the cross-talk between mesothelioma tumor cells, granulocytes, and T cells.

[1]Thoracic and GI Oncology Branch, Center for Cancer Research, National Cancer Institute, National Institutes of Health, Bethesda, Maryland. [2]Institute of Immunology and Immunotherapy, University of Birmingham, Birmingham, UK. [3]University of Maryland Baltimore County, Baltimore, Maryland. [4]Koç University, Rumelifeneri, Saryer/İstanbul, Turkey. [5]Laboratory of Pathology, Center for Cancer Research, National Cancer Institute, National Institutes of Health, Bethesda, Maryland. [6]Biostatistics and Data Management Section, Office of the Clinical Director, Center for Cancer Research, National Cancer Institute, National Institutes of Health, Bethesda, Maryland.

Note: Supplementary data for this article are available at Clinical Cancer Research Online (http://clincancerres.aacrjournals.org/).

S. Khanna, S. Graef, F. Mussai; G. Middleton, C. De Santo, and R. Hassan contributed equally to this article.

Corresponding Author: Raffit Hassan, National Cancer Institute, National Institutes of Health, Building 10 Room 4-5553, National Cancer Institute, Bethesda, MD 20892-4264. Phone: 301-451-8742; Fax: 301-402-1344; E-mail: hassanr@mail.nih.gov

doi: 10.1158/1078-0432.CCR-17-3757

Published OnlineFirst March 30, 2018; DOI: 10.1158/1078-0432.CCR-17-3757

Translational Relevance

The functional role of granulocytes and their cross-talk with tumor cells and T cells in human mesothelioma is not well understood. We demonstrated that GM-CSF is expressed by mesothelioma tumor cells and can polarize granulocytes to upregulate reactive oxygen species production, which in turn suppresses the T-cell proliferation and function. As GM-CSF plays a role in driving an immunosuppressive granulocyte phenotype in mesothelioma, targeting GM-CSF could represent an alternative therapeutic approach for these patients.

Materials and Methods

Patients and sample collection

Heparinized blood samples were obtained from patients with malignant mesothelioma ($n = 47$) who were enrolled in IRB-approved protocols at the National Cancer Institute, Bethesda, and the University of Birmingham, UK, before treatment (Table S1). Written informed consent was obtained from all the patients and the study was conducted in accordance with recognized ethical guidelines. Blood from healthy donors was obtained from the NIH Blood Bank ($n = 30$) and at the University of Birmingham, UK ($n = 18$) in heparin tubes. Patients with both histologically confirmed pleural ($n = 24$) and peritoneal ($n = 9$) mesothelioma were included in this study and at the time of enrolment had clinical and/or radiological evidence of disease. A number of patients had received prior treatments including surgery and systemic chemo- or immunotherapy (Table S1). The transcriptomes of 87 mesothelioma tumors diagnosed between 1999 and 2013, held within the R2: Genomics Analysis and Visualisation Platform (http://r2.amc.nl) were analyzed for CSF2 expression. Patients were aged from 28 to 81 years of age at diagnosis. Fifty-six patients had a history of asbestos exposure, 14 had no history, and 17 were not known. Of the 87 patients' samples histologies were distributed as follows: 23 biphasic, 5 diffuse, 57 epithelioid, and 2 sarcomatoid.

Cell lines

Human mesothelioma cell lines [ED (MSTO211)-H, AC-Meso Y9-Meso, MPM15, MPM26, MPM30, MPM34, and MPM43] purchased from the Aichi Cancer Research Centre Institute and Mesobank UK were cultured in RPMI-1640 (Invitrogen) with 10% heat-inactivated fetal bovine serum, glutamine (1×), sodium pyruvate (1×), and penicillin-streptomycin (RPMI 10% = R10%). The cell lines were cultured in a humidified atmosphere at 37°C with 5% CO_2. All cell lines were verified by Northgene DNA short-tandem repeat analysis within the last 6 months. All cell lines were tested of mycoplasma and were negative. Cell lines were used for up to 5 passages.

Flow cytometric analysis of whole blood and tumors

Whole blood and fresh tumor samples from diagnostic surgery were processed within 12 hours of collection. Ten samples from patients with benign pleural pathologies of infectious and inflammatory nature were also included as a comparison. Whole blood was either lysed using ammonium chloride solution according to the manufacturer's instructions (Qiagen) or using a hypertonic ammonium chloride solution (150 mmol/L NH_4Cl, 10 mmol/L $KHCO_3$, 0.1mmol/L EDTA) for 10 minutes at room temperature (maintained at 21°C –23°C) at a ratio of 1:9 (volume of sample: volume of lysing solution) prior to antibody staining. Where indicated peripheral blood was separated using a Lymphoprep density gradient. Tissue samples were digested using type II collagenase (Worthington) for 3 hours at 37°C. Immune populations were identified by staining with anti-CD11b, anti-HLA-DR, anti-CD13, anti-CD14, anti-CD15, anti-CD66b, and anti CD45 antibodies (BD Biosciences) on ice or at room temperature for 30 minutes. Cells were acquired using FACS-Canto II (BD Biosciences) and Cyan (Beckman Coulter) and analyzed either by FCS Express 4 software (DeNovo Software) or FlowJo (TreeStar).

Isolation of granulocytes, T cells, and mesothelioma cells for functional assays

The whole blood from healthy donors and patients were processed as described above. We isolated the low-density granulocytes from the peripheral blood mononuclear layer and high-density granulocytes from the layer of white cells on the red cell pellet following Lymphoprep centrifugation by magnetic bead isolation using anti-CD15 microbeads (BD Pharmingen) and MACS LS separation columns (Miltenyi Biotech) according to the manufacturer's instructions. Cell purity was >98% as confirmed by flow cytometry. Cell populations were similarly isolated from collagenase digested tumors using MACS beads (anti-CD15 for granulocytes and anti-CD14 for monocytes), followed by flow cytometric confirmation of purity. The dose of collagenase selected has previously been established to not affect cell surface marker expression or cell viability.

For isolation of autologous T cells and myeloid cells from the whole blood, the target populations were enriched first using positive selection with CD45 magnetic beads (Miltenyi Biotech) followed by staining with myeloid antibodies (above) and anti-CD3 antibody (BioLegend). Cells were sorted on Astrios (Beckman Coulter) using a 100 μm nozzle. DAPI was used as a viability marker to gate out the dead cells.

Granulocyte polarization

To generate tumor-conditioned media (TCM), cell lines or sorted patients' tumor cells were plated (1.5×10^6 cells) and cultured for 72 hours. The conditioned media were removed and filtered prior to use. Following Lymphoprep isolation high-density granulocytes were enriched by CD15 magnetic bead isolation as above, healthy donor granulocytes were plated in R10% in 24-well plates, at concentrations of 1×10^6 per well. TCM was added as 25% of the total volume as indicated. Granulocytes were harvested following 24 hours of culture and washed twice prior to use in suppression assays. Granulocyte viability was confirmed to be >90% in all cases, by flow cytometry, before further experimentation.

Autologous T-cell proliferation assays

Sorted $CD3^+$ T cells were labeled with 10 μmol/L carboxyfluorescein diacetate succinimidyl ester (CFSE; Life Technologies) and cultured with sorted granulocytes at ratios of 1:0, 1:0.5, 1:1 in complete media at 37°C, 5% CO_2 for 4 days in the presence of 1:1 ratio of anti-CD3/ anti-CD28 dynabeads (Invitrogen). Cells were stained with V450 anti-CD4 (Clone-RPA-T4; BD

Published OnlineFirst March 30, 2018; DOI: 10.1158/1078-0432.CCR-17-3757

Biosciences) and APC-Cy7 anti-CD8 (Clone-RPA-T8; BioLegend) and proliferation was determined by CFSE dilution. Unstimulated T cells were used as a negative control. The effect of the addition of L-NMMA (0.5 mmol/L, NG-Methyl-L-arginine acetate), nor-NOHA (0.5 mmol/L, N-Omega-hydroxy-nor-L-arginine) and iNAC (10 mmol/L; all from Sigma- Aldrich) was similarly tested. The percentage of cells that diluted CFSE (divided cells) was determined.

Peripheral blood lymphocyte cell proliferation assay

Peripheral blood lymphocytes (PBL; 2×10^5) were cultured in 96-well flat bottom plates with coated anti-CD3 antibody (3 μg/mL) and anti-CD28 antibody (2 μg/mL), in 200 μL R10%. Cells were incubated at 37°C, 5% CO_2 for 4 days and then 1 μCi/well ^{3}H-thymidine (Perkin Elmer Life Sciences) was added for 12 to 16 hours. ^{3}H-thymidine incorporation was measured using a TopCount reader (Perkin Elmer). The suppressive ability of autologous or conditioned granulocytes was assessed by coculturing-purified cells together with the PBLs. nor-NOHA (0.5 mmol/L), L-NMMA (0.5 mmol/L), iNAC (10 mmol/L; Sigma-Aldrich) was added to cells in culture. HEPES (25 mmol/L) was added to the medium to maintain the pH after iNAC addition. Data are expressed as a percentage of PBL proliferation driven by antibody costimulation in the presence of MDSC compared with PBL proliferation in the absence of suppressive cells (100%).

Reactive oxygen species (ROS) assay

Sorted granulocytes were stained with 2′, 7′-dichlorofluorescein diacetate (DCFDA) using DCFDA cellular ROS detection assay kit (Abcam) for 30 minutes at 37°C. The stained cells were analyzed on a BD FACS Calibur and Cyan (Beckman Coulter). Cells stained with Tert-butyl hydrogen peroxide (TBHP), TCM polarized granulocytes were also incubated with Phorbol 12-myristate 13-acetate (PMA; concentration need to be added) during the staining with DCFDA, this was used as a positive control.

Quantification of H_2O_2 production was measured using the Amplex Red Hydrogen Peroxidase assay kit (Invitrogen). Following culture in mesothelioma conditioned media for 24 hours, sorted granulocytes were washed twice in R10%, counted and plated in Krebs–Ringer phosphate buffer according to the manufacturer's guidelines. Detection of H_2O_2 was carried out following 30 minutes of incubation at 37°C using a microplate reader at 560 nm.

ELISA

The concentrations of cytokines within conditioned media following culture with T cells, mesothelioma cell lines (1×10^6/mL) or sorted tumor cells were quantified using a competitive enzyme-linked immunoassay according to the manufacturers' instructions. The following molecules were tested GM-CSF (Biolegend), IL13 (BD Biosciences), IL8 (BioLegend), IL6 (BioLegend), G-CSF (R&D Systems), VEGF (R&D Systems), Mesothelin (BioLegend). The concentration of IFNγ in coculture supernatants was determined by Ready Set Go ELISA kit (eBioscience).

RT-Q-PCR analysis

RT-Q-PCR was used to detect NOX2 expression in cell line supernatant-conditioned granulocytes (0, 4, 8, 12, 24 hours' time points). RNA was extracted using an RNeasy Mini kit (Qiagen). cDNA was prepared using SuperScriptTM III Reverse Transcriptase (Invitrogen) following the manufacturer's instructions. RT-Q-PCR was done in duplicate using FAST SYBR Green Master Mix (Applied Biosystems) and the Applied Biosystems 7500 Fast Real-Time PCR system. Analysis of gene expression was calculated according to the $2^{-\Delta T}$ method and plotted as arbitrary units of mRNA relative to GAPDH. Gene specific primer sequences were NOX2 (CAAGATGCGTGGAAACTA, F; TCCCTGCTCCCACTAACA, R) and GAPDH (CCAGCCGAGCCACATCGCTC, F; ATGAGCCCCAGCCTTCTC, R; Eurofins).

Immunohistochemistry

Mesothelioma sections from diagnostic tumor biopsies ($n = 38$) were deparaffinized in Histoclear (National diagnostics) and ethanol and rehydrated in 0.3% hydrogen peroxide for 15 minutes. Antigen retrieval was performed in 10 mmol/L sodium citrate buffer (pH 6.0) for 20 minutes in a microwave oven. Slides were cooled and washed prior to blocking in 5× Caesin (Thermo Fisher Scientific) for 30 minutes at room temperature. Sections were then incubated over night with primary antibody, rabbit anti–GM-CSF (Novus Biologicals), diluted in PBS. Sections were washed and secondary antibody (Universal ImmPRESS antibody, Vector Laboratories) was added at room temperature for 30 minutes followed by further washing and addition of DAB substrate (ImmPACT DAB, Vector Laboratories) for 5 minutes. After counterstaining with Harris hematoxylin (Sigma-Aldrich), slides were dehydrated using ethanol and Histoclear and mounted using Omnimount (National Diagnostics). Slides were examined and photographed using a Nikon Eclipse 400 microscope.

Statistical analysis

Continuous parameter values were compared between two groups using an exact form of a Wilcoxon rank sum test. Paired comparisons were performed using a Wilcoxon signed rank test. Spearman correlation analysis was used to determine the correlation between age and MDSC parameters. The correlations are interpreted as follow: strong if $|r| > 0.70$; moderately strong if $0.50 < |r| < 0.70$; weak to moderately strong if $0.30 < |r| < 0.50$; weak if $|r| < 0.30$. All P values are two-tailed and presented without adjustment for multiple comparisons because all tests performed were considered to be exploratory.

Results

Mesothelioma tumors modulate infiltrating myeloid cells to suppress T-cell responses

The immune microenvironment in mesothelioma has been shown to have strong prognostic implications with infiltration by $CD8^+$ lymphocytes conferring a favorable prognosis (9) and the association of peripheral blood granulocyte-to-lymphocyte ratio with poorer prognosis (10–12). However, our understanding of the biological cross-talk between mesothelioma cells, granulocytes, and T cells in human patients is limited.

Interrogation of the transcriptomic profile of 87 mesothelioma tumors, held within the R2: Genomics Analysis and Visualisation Platform (http://r2.amc.nl), suggested a significant infiltration of immune cells in the tumor microenvironment (Fig. 1A). Flow cytometric analysis of 18 digested human mesothelioma tumors confirmed this data at the cellular level within the tumor microenvironment (mean: CD15 = 8.6%,

Published OnlineFirst March 30, 2018; DOI: 10.1158/1078-0432.CCR-17-3757

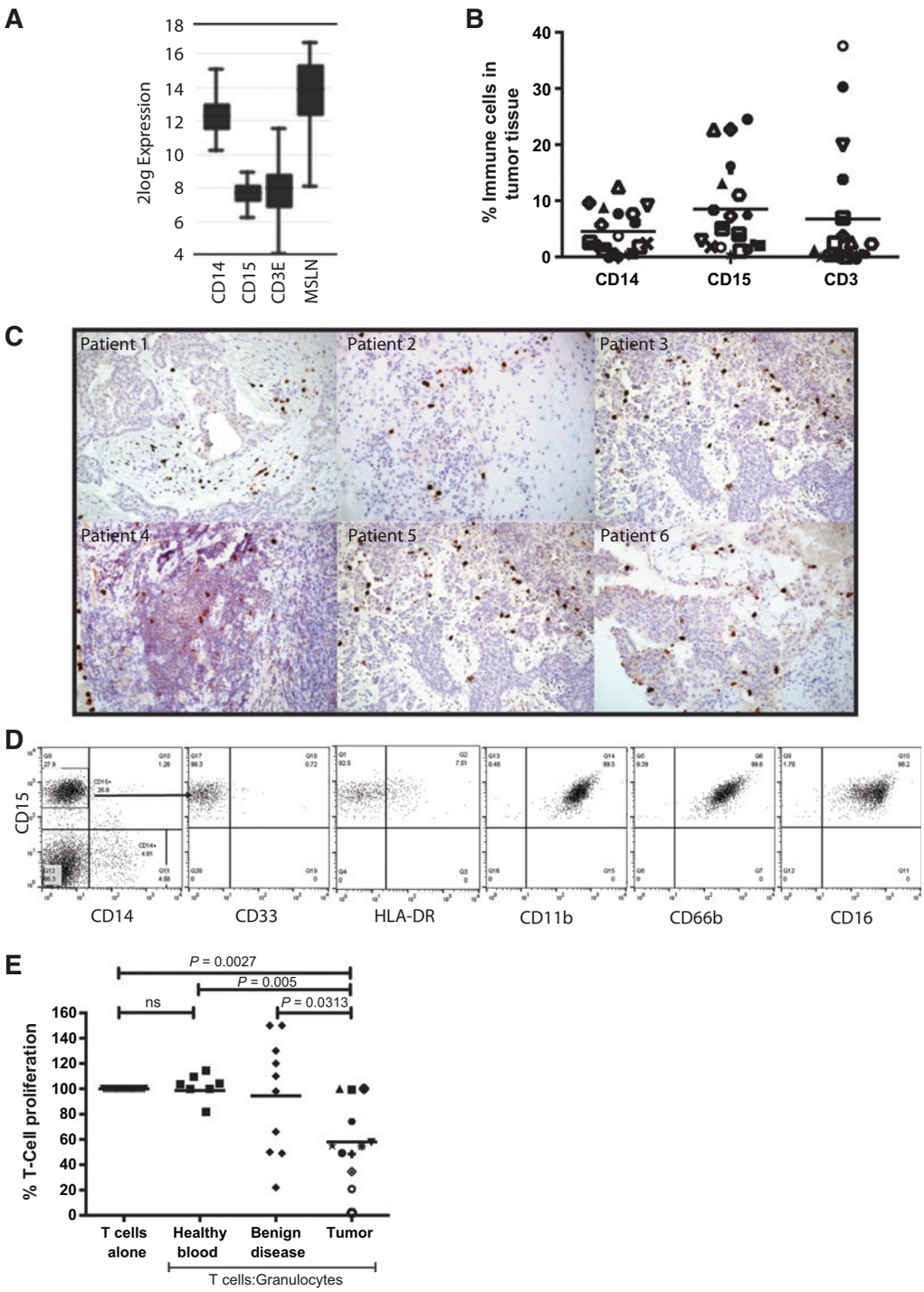

Figure 1.

Granulocytes in tumor tissue suppress T-cell proliferation. **A,** Transcriptomic expression of CD14, CD15, CD3E, and Mesothelin in 87 mesothelioma tumors from the R2: Genomics Analysis and Visualisation Platform (http://r2.amc.nl). **B,** Percentages of $CD15^+$, $CD14^+$, and $CD3^+$ cells detected by flow cytometry in the digested tumor tissue of 18 patients with confirmed mesothelioma. **C,** Representative tumor sections from 6 patients (total stained = 38 tumors) demonstrating infiltration of CD15 expressing cells within mesothelioma tumors. Images were taken at 20× magnification. **D,** Immunophenotype of tumor-associated granulocytes by flow cytometry identified that they expressed CD11b, CD15, with low/absent CD33 expression, and low/absent HLA-DR expression. **E,** T-cell proliferation from healthy donors is suppressed following culture with $CD15^+$ granulocytes (representative 1:0.5 ratio) sorted from mesothelioma tumors, compared with those cultured in complete media alone, with $CD15^+$ granulocytes from the blood of healthy donors, or from pleural tissue with benign pathologies.

Published OnlineFirst March 30, 2018; DOI: 10.1158/1078-0432.CCR-17-3757

CD14 = 4.8%, CD3 = 6.7%; Fig. 1B). Immuno-histochemical staining of a further 38 mesothelioma tumors supported the findings, with identification of granulocytes in all samples at diagnosis (Fig. 1C). characterization of tumor-associated granulocytes by flow cytometry showed that they expressed CD11b, CD15, with low/absent CD33 expression, and low/absent HLA-DR expression (Fig. 1D). Murine model of mesothelioma recently identified that the immune-regulatory transcriptome of granulocytes may be altered within the tumor microenvironment with potential effects on surrounding T cells and tumor cells (13). To investigate the effects of granulocytes on T cells, $CD15^+$ granulocytes were sorted from mesothelioma tumors at the time of resection and cocultured with T cells from healthy donors. Tumor-derived granulocytes suppressed T-cell proliferation to a greater extent compared with those from healthy-donor blood or those extracted from pleural tissue with benign pathologies (Fig. 1E). Similarly, $CD14^+$ monocytes from mesothelioma tumors were sorted and also found to suppress T-cell proliferation ($P = 0.0002$; Supplementary Fig. S1A). Therefore, the tumor microenvironment is able to locally modulate infiltrating myeloid cells to inhibit T-cell proliferation.

Mesothelioma creates a systemic immunosuppressive environment through circulating granulocytes

The effects of mesothelioma tumors on the immune system may be limited to the local tissue microenvironment or could also lead to systemic alteration. To test this, we compared T cells from the blood of patients at diagnosis to those from healthy donors and observed that mesothelioma patients' T cells have a reduced proliferation capacity compared with those in healthy donors (Fig. 2A). We have previously identified that tumor metabolism of arginine can create a systemic environment inhibitory to T-cell responses. As mesotheliomas are known to be arginine auxotrophs, we measured the arginase activity of mesothelioma cell lines (14). No significant arginase activity was identified suggesting an alternative mechanism must be responsible (Supplementary Fig. S1B). As we identified immunosuppressive granulocytes infiltrating mesothelioma tumors, we hypothesized that the T-cell suppression may be due to the presence of these circulating immunosuppressive myeloid cells.

To investigate the hypothesis, the frequency of granulocytic and monocytic cells was characterized in the whole blood of healthy donors and mesothelioma patients ($n = 33$) at diagnosis (Table S2). There were significant increases in the percentage of HLA-DR-granulocytes ($CD14^-CD15^+CD11b^+HLADR^-$) in the whole blood compared with healthy controls ($P = 0.013$; Fig. 2B). Subpopulation analysis revealed only a marginal difference in HLA-DR- monocytes ($CD14^+$CD15-$CD11b^+$HLADR-) compared with healthy donors ($P = 0.05$; Fig. 2C) and no difference in the frequency of $HLA\text{-}DR^+$ monocytes ($CD14^+CD11b^+HLADR^+$; median 7.0% vs. 8.9%; $P = 0.14$) or $HLA\text{-}DR^+$ granulocytes ($CD15^+CD14^-CD11b^+HLADR^+$) cells (median 0.83% vs. 1.46%; $P = 0.29$) between healthy donors and mesothelioma patients. Consistent with reports of increased granulocyte:lymphocyte ratios in mesothelioma patients, granulocytes were the most predominant population overall (median frequency: $CD14^+$ monocytes: 0.198% vs. $CD15^+$ granulocytes: 66.8%). Immunophenotyping revealed significant differences in the relative expressions of granulocyte markers CD11b and CD66b compared with those from healthy donors (Fig. 2D; Supplementary Fig. S1C).

As $CD15^+$ granulocytes are the major population of circulating myeloid cells in mesothelioma patients and shared the same immunophenotype as tumor-infiltrating granulocytes described above, their functional effects on T cells was examined further. Coculture of sorted whole blood granulocytes from patients decreased both autologous $CD4^+$ and $CD8^+$ T-cell proliferation at ratios of 1:1 and1:0.5 (T cells:granulocytes; Fig. 2E; Supplementary Fig. S1D) and activation ($P = 0.0078$, Fig. 2F).

Immunosuppressive granulocytes may be methodologically identified in the PBMC layer (classical G-MDSC; low-density) and on the red cell pellet (high density) following density gradient centrifugation of whole blood. Analysis of separated whole blood identified a significant increase in the frequency of granulocytes within the PBMC layer; however, the frequency is extremely low (median <10%) with 90% of the granulocytes lying on the red cell pellet (Fig. 3A). This small population of granulocytes had only a weak ability to suppress T-cell proliferation (Fig. 3B). Only the high-density granulocytes, which had increased frequency in the patients, had suppressive activity (Fig. 3B). Granulocytes from healthy donors had minimal effects on T-cell proliferation (Fig. 1E; Supplementary Fig. S2A) or IFNγ release (Supplementary Fig. S2B). Therefore, granulocytes within the blood and tumors of mesothelioma patients share the same immunophenotype and functional capacity to suppress T-cell proliferation and activation, thus extending the immunosuppressive microenvironment.

Mesothelioma-conditioned granulocytes suppress T-cell proliferation by generation of ROS

Granulocytes can impair T-cell proliferation through a number of mechanisms including arginine depletion, nitric oxide species or ROS production, and release of immunosuppressive cytokines (15–19). We examined iNOS and arginase I expression in patients' granulocytes and those from healthy donors identifying no significant differences in expression (Fig. 3C). The addition of the arginase or iNOS inhibitors, nor-NOHA or L-NMMA respectively, to sorted patients' granulocytes did not rescue T-cell proliferation thus excluding these mechanisms (Fig. 3D). No evidence for immunosuppressive cytokine release from these cells was identified in patient plasma by ELISA (IL10, IL1β, IL4, IL13; Supplementary Fig. 2C). In a mesothelioma murine model, ROS have been demonstrated to suppress T-cell responses (20). Gating on granulocytes identified that mesothelioma patients upregulate ROS compared with healthy controls ($P = 0.03$; Fig. 3E; Supplementary Fig. S2D). Addition of the ROS inhibitor iNAC to sorted patients' granulocytes restored both autologous $CD4^+$ and $CD8^+$ T-cell proliferation (Fig. 3F; Supplementary Fig. S2E) and IFNγ release (Fig. 3G). We confirmed that ROS production was reduced by the addition of the inhibitor iNAC ($P = 0.031$; Fig. 3H). PDL1 is another mechanism that myeloid cells may use to modulate T cells. There was no significant difference in the frequency of $CD15^+PDL1^+$ cells in the blood or tumors of patients compared with those from healthy controls (Supplementary Fig. S2F). Correlating the frequency of $PDL1^+CD15^+$ cells with $CD3^+$ frequency revealed no significant correlation in the blood ($P = 0.4976$, $r = -0.3214$; Supplementary Fig. S2F), but there was a significant correlation in the tumor ($P = 0.0583$, $r = 0.8286$; Supplementary Fig S2G and S2H). The findings

Published OnlineFirst March 30, 2018; DOI: 10.1158/1078-0432.CCR-17-3757

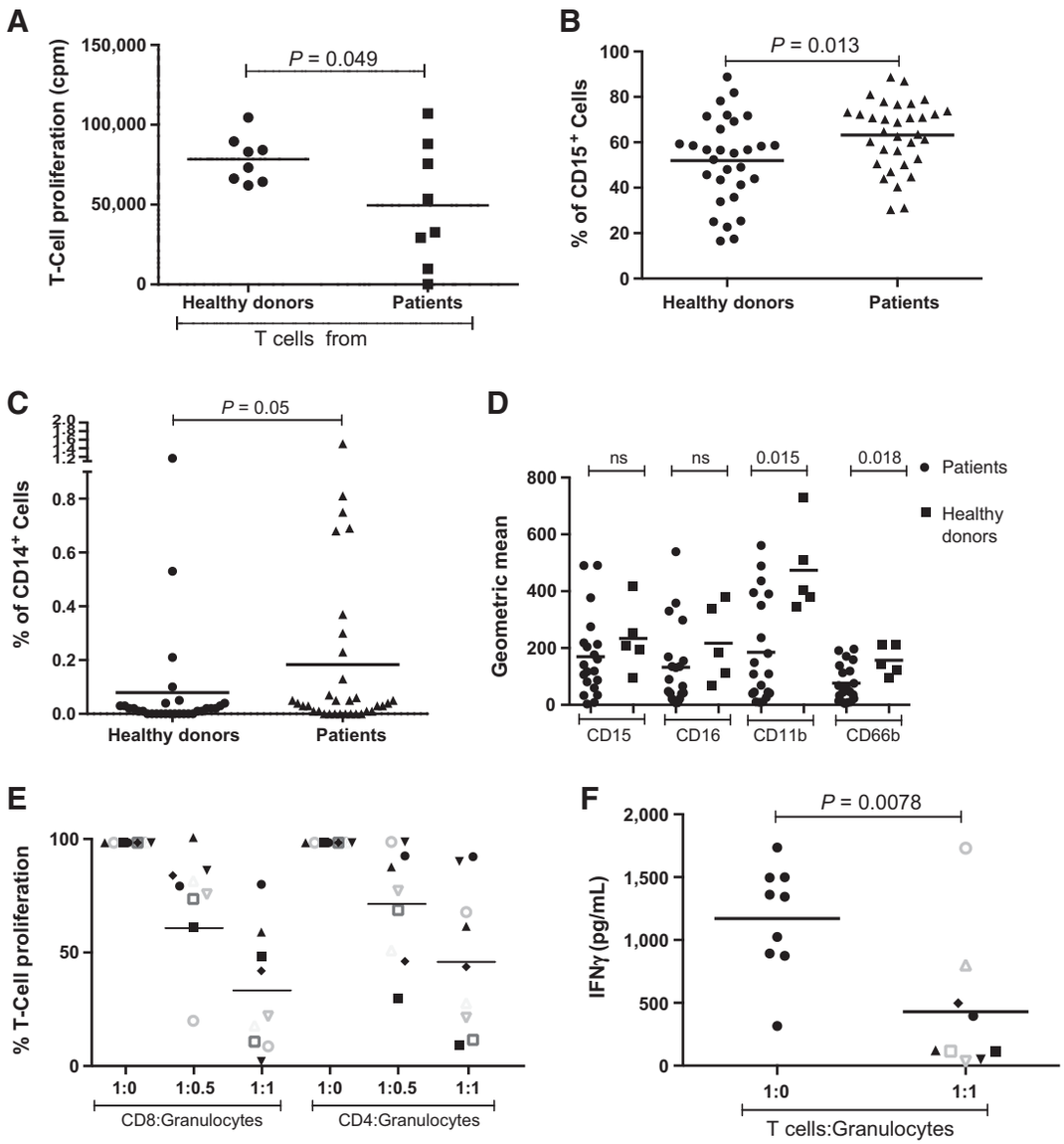

Figure 2.

Granulocytes are elevated in peripheral blood of mesothelioma patients and suppress T-cell proliferation and activation. **A**, Sorted $CD3^+$ T cells from the blood of mesothelioma patients (6 untreated, 2 with prior therapy) have reduced proliferative capacity compared with those sorted from the blood of healthy donors. **B,** Increased frequency of $CD15^+$ granulocytes in the peripheral blood of mesothelioma patients ($n = 33$) and healthy donors ($n = 30$) at diagnosis. **C,** Marginal increased frequency of $CD14^+HLADR^-$ monocytes in the peripheral blood of mesothelioma patients ($n = 33$) and healthy donors ($n = 30$). **D,** Expression of CD15, CD16, CD11b, and CD66b markers on granulocytes of healthy donors and mesothelioma patients, as detected by flow cytometry. **E,** Autologous $CD4^+$ and $CD8^+$ T-cell proliferation is suppressed following culture with $CD15^+$ granulocytes sorted from the blood of patients at diagnosis. T cells and granulocytes were cocultured at ratios of 1:0.5 and 1:1, respectively, and compared with T cells alone (1:0). **F,** T-cell–derived IFNγ release in culture supernatants is significantly impaired following coculture with $CD15^+$ granulocytes sorted from the blood of patients at diagnosis.

suggest that in the tumor, granulocyte PDL1 may be a secondary mechanism of modulating T-cell numbers inside the tumor microenvironment, but not peripherally.

GM-CSF from mesothelioma tumor cells drives granulocyte ROS production

Although it is recognized that mesothelioma tumors release G-CSF, which may contribute to granulocyte expansion and recruitment, the mechanism by which granulocytes are polarized to upregulate ROS production and suppress T cells is unknown (21, 22). Granulocytes produce ROS through the activity of NADPH oxidase enzyme (NOX2) expression. Consistent with this, we demonstrated that NOX2 is expressed in patients' granulocytes and healthy donors (Fig. 4A). To examine the effect of the mesothelioma microenvironment on granulocytes, healthy-donor–derived granulocytes were cultured in the conditioned

Published OnlineFirst March 30, 2018; DOI: 10.1158/1078-0432.CCR-17-3757

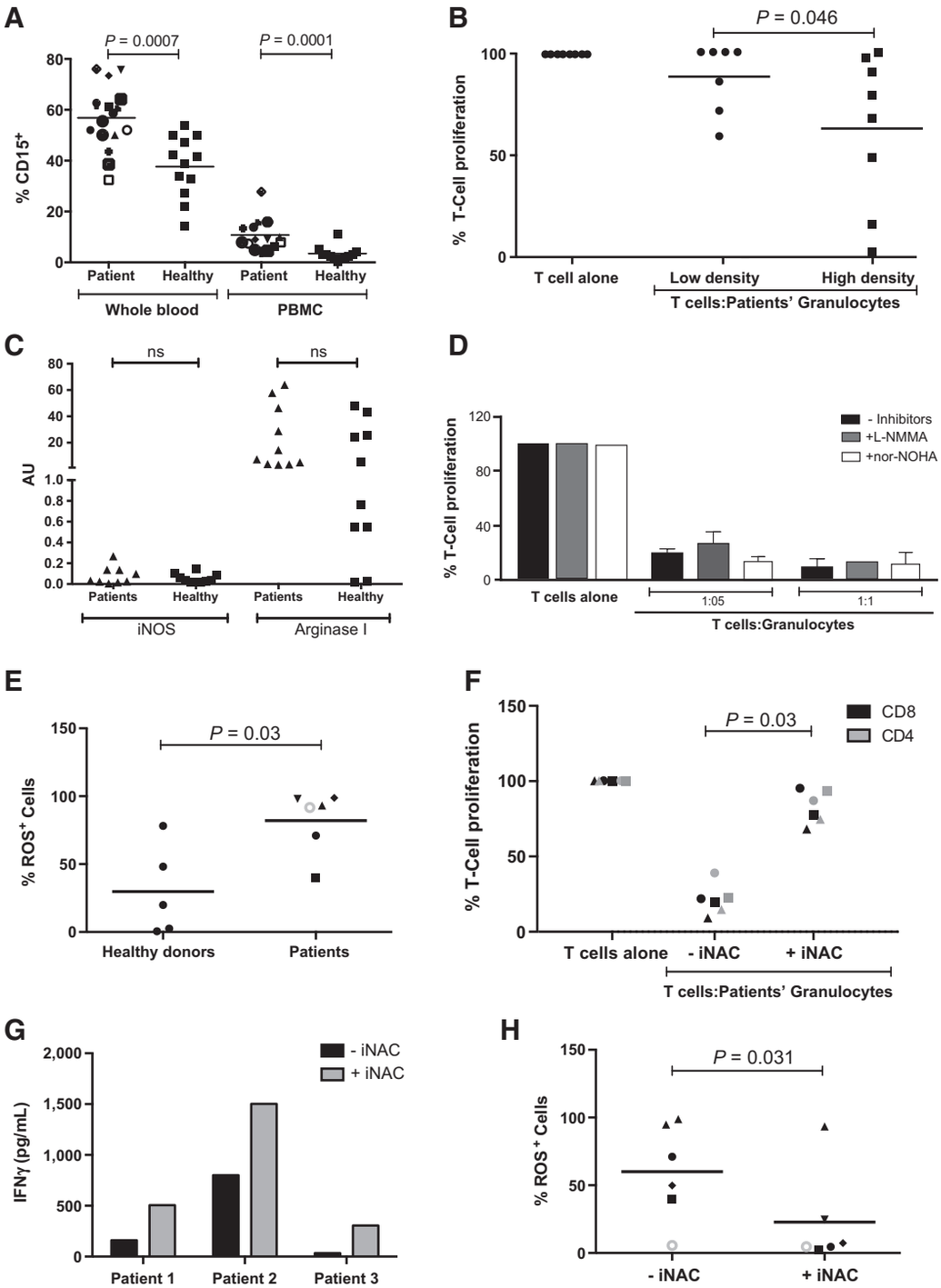

Figure 3.

Granulocytes from mesothelioma patients suppress T-cell proliferation through ROS. **A,** The frequency of $CD11b^{+}CD15^{+}$ cells was compared in the whole blood and PBMC layer following Lymphoprep separation for 18 mesothelioma patients and 12 healthy donors. The majority of $CD15^{+}$ granulocytes lie on the red cell pellet following Lymphoprep separation. **B,** Healthy donor T-cell proliferation is most suppressed following culture in the presence of blood $CD15^{+}$ granulocytes from mesothelioma patients which have been collected from the red cell pellet (high density) after Lymphoprep separation. Low-density granulocytes isolated in the PBMC layer of the same blood samples were comparatively less suppressive to T-cell proliferation. **C**, QPCR analysis of the expression of iNOS and arginase in granulocytes sorted from healthy donors or patients. **D**, T-cell proliferation is not restored by the addition of L-NMMA or nor-NOHA to the cultures in the presence of $CD15^{+}$ granulocytes from patients. Two representative patients are shown. **E,** Increased frequency of ROS^{+} $CD15^{+}$ granulocytes in the blood of patients from mesothelioma patients compared with healthy donors. **F**, Inhibition of NOX2 activity with iNAC reversed the suppressive effect of granulocytes on CD4 and CD8 T-cell proliferation. **G,** Inhibition of NOX2 activity with iNAC restored T-cell activation, as measured by IFNγ release into cell supernatants. **H,** Culture of patients' granulocytes with iNAC reduced the intracellular production of ROS confirming the known specificity of drug action.

Published OnlineFirst March 30, 2018; DOI: 10.1158/1078-0432.CCR-17-3757

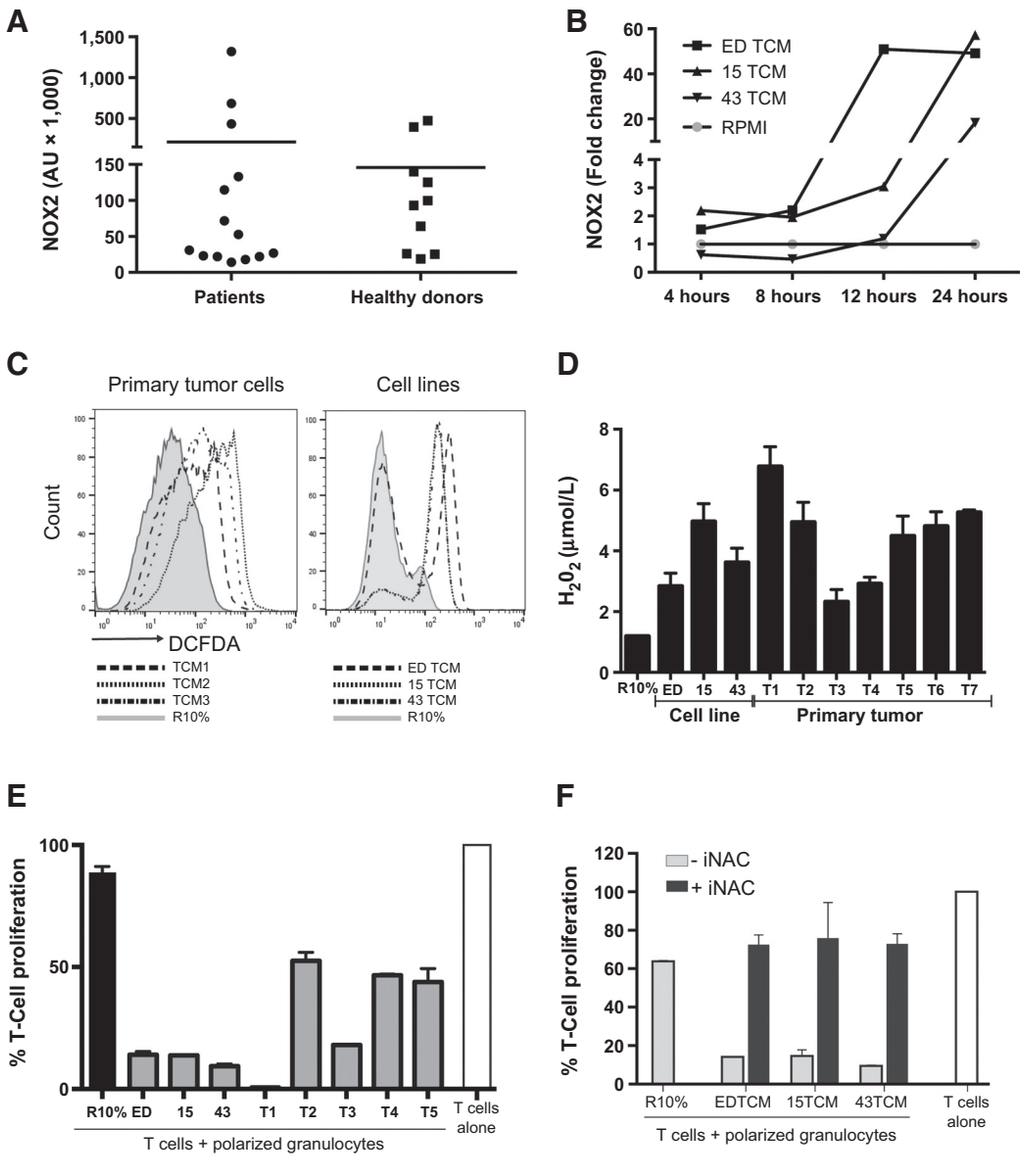

Figure 4.

ROS generation by granulocytes is upregulated by the mesothelioma microenvironment. **A**, Expression of NOX2 by qRT-PCR in $CD15^+$ cells from the blood of healthy donors and mesothelioma patients. **B,** NOX2 expression in $CD15^+$ granulocytes is upregulated over time following coculture with mesothelioma cell lines, as assessed by qRT-PCR. **C,** ROS production is upregulated in healthy-donor–derived granulocytes following culture in conditioned media from sorted mesothelioma malignant cells or mesothelioma cell lines, compared with complete RPMI. ROS species are detected by DCFDA staining and flow cytometry. **D,** Release of ROS from $CD15^+$ granulocytes is upregulated after culture with mesothelioma cell lines or sorted mesothelioma malignant cells as detected by hydrogen peroxide species, using a colorimetric assay. **E,** T-cell proliferation is significantly inhibited following culture with cell line conditioned- or tumor-conditioned granulocytes. Comparison made with T cells cultured with granulocytes conditioned by completed media alone. **F,** Treatment of mesothelioma cell line conditioned granulocytes with iNAC prevents suppression of T-cell proliferation.

supernatants of mesothelioma cell lines or primary tumors. Conditioned supernatants led to an upregulation of NOX2 expression over time (Fig. 4B), with accompanying increase in the production (Fig. 4C; Supplementary Fig. S3A and S3B) and release of ROS (Fig. 4D). PMA was used as positive control for ROS induction in granulocytes upregulation, confirming the mesothelioma specific mechanism (Supplementary Fig. S3C). The mesothelioma-conditioned granulocytes showed a strong ability to suppress T-cell proliferation (Fig. 4E), which could be rescued by the addition of iNAC (Fig. 4F). LOX-1 has been reported to be a marker for some granulocytic MDSCs (23). Conditioned media led to no change in LOX-1 on healthy-donor granulocytes (Supplementary Fig. 3D). Therefore, mesothelioma cells signal to granulocytes to modulate their function.

To identify the nature of the mesothelioma-granulocyte cross-talk, mesothelioma-conditioned supernatant was first

Published OnlineFirst March 30, 2018; DOI: 10.1158/1078-0432.CCR-17-3757

boiled to denature all proteins. Boiled supernatant lost the ability to polarize granulocytes to suppress T-cell proliferation (Supplementary Fig. S3E) consistent with the release of a soluble molecule from the mesothelioma cells. Arginine depletion, a potential mechanism of polarization due to mesothelioma arginine auxotrophism, similarly did not polarize healthy-donor granulocytes to produce ROS consistent with this finding (Supplementary Fig. 3F).

ELISAs for cytokines involved in granulocyte signaling were performed of supernatants from mesothelioma cell lines and mesothelioma human primary tumor cells identified a number of key molecules were highly expressed—G-CSF, GM-CSF, IL13, IL6, IL8, VEGF, PGE2, mesothelin (Fig. 5a). In particular mesothelioma cells release IL8 (neutrophil chemotactic protein; mean concentration 981 pg/mL) and G-CSF (mean concentration 283 pg/mL), which are known to attract granulocytes into the

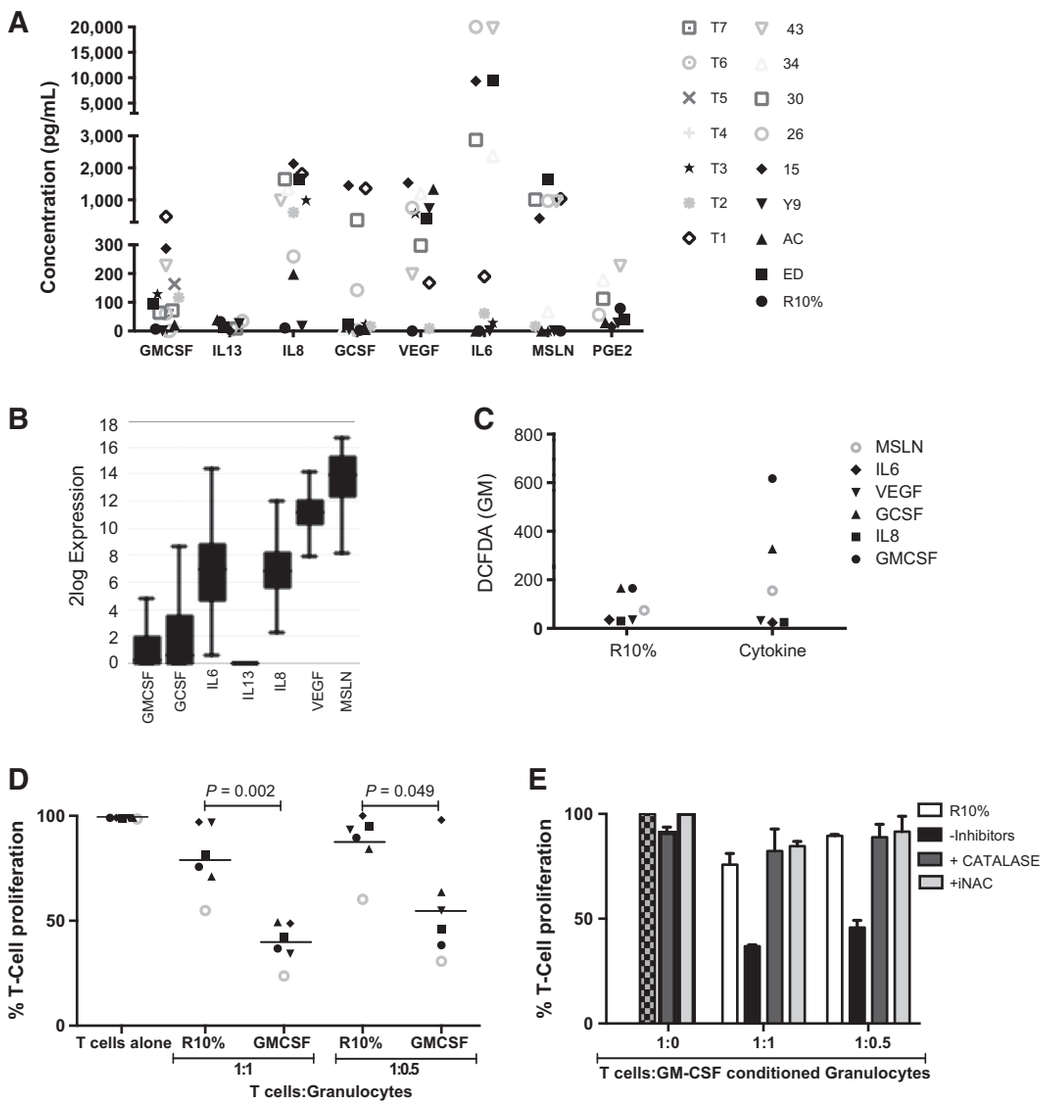

Figure 5.

Mesothelioma cells release GM-CSF to upregulate granulocyte ROS and suppressive activity. **A,** Cytokine multiplex assay determined the cytokine profile of tumor cell supernatants and cell line supernatants. Increased concentrations of GM-CSF, IL8, GCSF, VEGF, IL6, and mesothelin are found. Low concentrations of prostaglandin E2 and IL13 were detected. **B,** Transcriptomic expression of GMCSF, GCSF, IL6, IL13, IL8, VEGF, and mesothelin in 87 mesothelioma tumors from the R2: Genomics and Visualisation Platform. **C**, ROS production (DCFDA staining) by healthy donor $CD15^{+}$ cells treated with detected cytokines to determine which were capable of enhancing ROS production. GM-CSF increased ROS production most prominently. **D,** T-cell proliferation was significantly suppressed by granulocytes conditioned with recombinant GM-CSF, compared with control granulocytes. Ratios of 1:1 and 1:0.5 T cells:granulocytes shown. **E**, Inhibition of granulocyte ROS production (iNAC) or accumulation (catalase) after healthy-donor granulocytes were conditioned with GM-CSF restores T-cell proliferation compared with controls.

Published OnlineFirst March 30, 2018; DOI: 10.1158/1078-0432.CCR-17-3757

tumor microenvironment. No evidence of serum amyloid-A release from mesothelioma cells was found. Interrogation of the R2 database confirmed a similar cytokine expression profile from 87 human tumors (Fig. 5B). Culture of healthy-donor granulocytes with individual recombinant cytokines identified above showed that GM-CSF led to the highest upregulation of ROS production (Fig. 5C) with associated upregulation in NOX2 expression (Supplementary Fig. S3G). Granulocytes treated with recombinant GM-CSF inhibited T-cell proliferation (Fig. 5D and E), and T-cell proliferation was rescued by the inhibitor (iNAC) or removal of ROS with catalase (Fig. 5E). No increases in plasma GM-CSF concentrations are identified in patients at diagnosis, suggesting that the intratumoral release of GM-CSF drives the ROS upregulation in granulocytes (Supplementary Fig. S4A). Addition of anti-GM-CSF–neutralizing antibody to mesothelioma cell line cocultures inhibited ROS upregulation (Fig. 6A and B) and the release of peroxide species in conditioned granulocyte supernatants (Supplementary Fig. S4B) confirming mesothelioma-released GM-CSF drives granulocyte ROS production and T-cell–suppressive activity. The addition of anti-GM-CSF–neutralizing antibody rescued T-cell proliferation, confirming the mechanism of mesothelioma polarization of granulocytes (Fig. 6C).

ROS production from conditioned healthy granulocytes correlated with the concentration of GM-CSF in tumor-conditioned media ($r = 0.438$, $P = 0.0118$; Fig. 6D). Immunohistochemistry of mesothelioma tumors confirmed that GM-CSF is expressed within the tumor microenvironment of patients (Fig. 6E; Supplementary Fig. S4C) and transcriptomic analysis of 87 primary tumor samples within the R2: database demonstrated that GM-CSF is expressed in over 50% of the samples and does not correlate with histological subtype (Fig. 6F).

In summary, mesothelioma creates an immunosuppressive microenvironment locally and systemically through the release of GM-CSF from tumor cells, which induces granulocyte ROS production to inhibit T-cell function.

Discussion

Although the role of monocytes and macrophages in mesotheliomas has previously been well documented in human tissue and murine models, granulocytes have received little attention. In this study, we focused on human mesotheliomas, identifying the mechanism by which tumor cells modulate granulocyte function to suppress T-cell responses. A previous immune-histochemical study identified that high CD4 T-cell counts or low neutrophil counts within mesothelioma tumors are linked to better patient outcomes (24). To evaluate the seemingly reciprocal relationship between granulocytes and T lymphocytes, we first confirmed that granulocytes make up a significant proportion of infiltrating immune cells with relatively fewer T cells. To date, granulocyte function in mesotheliomas has almost exclusively been studied in murine cell line xenografts. Murine granulocytes may be alternatively activated in mesotheliomas (N1 vs. N2) or characterized as granulocytic MDSCs (G-MDSC; refs. 13, 20, 25). In all of these murine cases, the granulocytic cells express ROS—a well-established mechanism of T-cell suppression (26). We carefully considered whether our tumor-infiltrating and -circulating granulocytes could be G-MDSC according to recent guidelines for nomenclature which define MDSCs based on immunophenotype, density, and suppressive activity (27). In our mesothelioma patients, both circulating and tumor-associated granulocytes were $CD11b^{+}CD14^{-}CD15^{+}/CD66b^{+}$ fitting with the G-MDSC phenotype. However, blood G-MDSCs are classically described as being low-density cells following separation with density centrifugation. We showed that in mesothelioma patients' blood, low-density granulocytes are a minority population within the PBMC layer and have minimal T-cell suppressive activity—thus the two populations are distinct. In addition, no evidence of altered LOX-1 expression, a marker recently identified on low-density G-MDSCs, was found after mesothelioma conditioning of healthy-donor granulocytes (23). The most suppressive granulocytes are those of high density and act through ROS release. The intratumoral granulocytes we studied share the same immunophenotype and suppressive mechanism. As discussed in the consensus recommendations based on current technology, there is no unique marker to distinguish suppressive granulocytes from G-MDSC, particularly for intratumoral cells. Notably, the need to use cell density on separation as a method to define immune cell subsets is extremely limited, and alternative methodologies will be developed for the future characterization of these cells. Our findings highlight the plasticity of granulocytes in humans and their place in regulating the tumor-associated immune microenvironment (13). Similar examples of human cancer–associated, immunosuppressive granulocytes, as opposed to G-MDSC, have been identified in melanoma and non–small lung cancer, driven through the release of tumor-derived factors (15, 28).

Our analysis of the supernatants of mesothelioma cell lines and primary tumor tissue revealed a cytokine profile consistent with granulocyte attraction and modulation within the tumor microenvironment. A number of factors have been reported to modulate granulocyte function in murine models of mesothelioma. In a murine model of mesothelioma, prostaglandin inhibition reduced the number of granulocytic MDSCs (20). TGFβ within murine mesothelioma tumors also drives the expression of the chemokines CCL3, CCL5, and CCL2 in protumoral granulocytes (29). For humans, no direct mechanism of mesothelioma modulation of granulocytes has been shown although the mesothelioma-inducing mineral erionite can directly stimulate ROS production in healthy-donor–derived neutrophils (30). IL8 (CXCL8) is a potent proinflammatory cytokine and is primarily known for its chemotactic and activating action on neutrophils, along with inhibition of normal neutrophil apoptosis (31–33). Our finding of moderate levels of IL8 released from mesothelioma cells may contribute to the enhanced granulocytes infiltration of mesothelioma tumors. Targeting of IL8 in models of tumors such as fibrosarcoma and prostate carcinoma prevents the influx of host neutrophils (34). IL8 is also an autocrine growth factor in a number of cancer types (35–37) including mesothelioma (38).

We identified that meostheliomas can also release G-CSF, a second well-established cytokine that induces granulocyte infiltration. Notably, G-CSF production by mesothelioma is reported to confer a more aggressive phenotype (39–41). Although we confirmed mesothelioma tumors release IL8 and G-CSF or prostaglandins, these factors had no impact in generating suppressive granulocytes. Instead, we demonstrated that GM-CSF is expressed by mesothelioma tumor cells and can polarize granulocytes to upregulate ROS production. No differences in the effect of granulocyte-derived ROS was found on

Published OnlineFirst March 30, 2018; DOI: 10.1158/1078-0432.CCR-17-3757

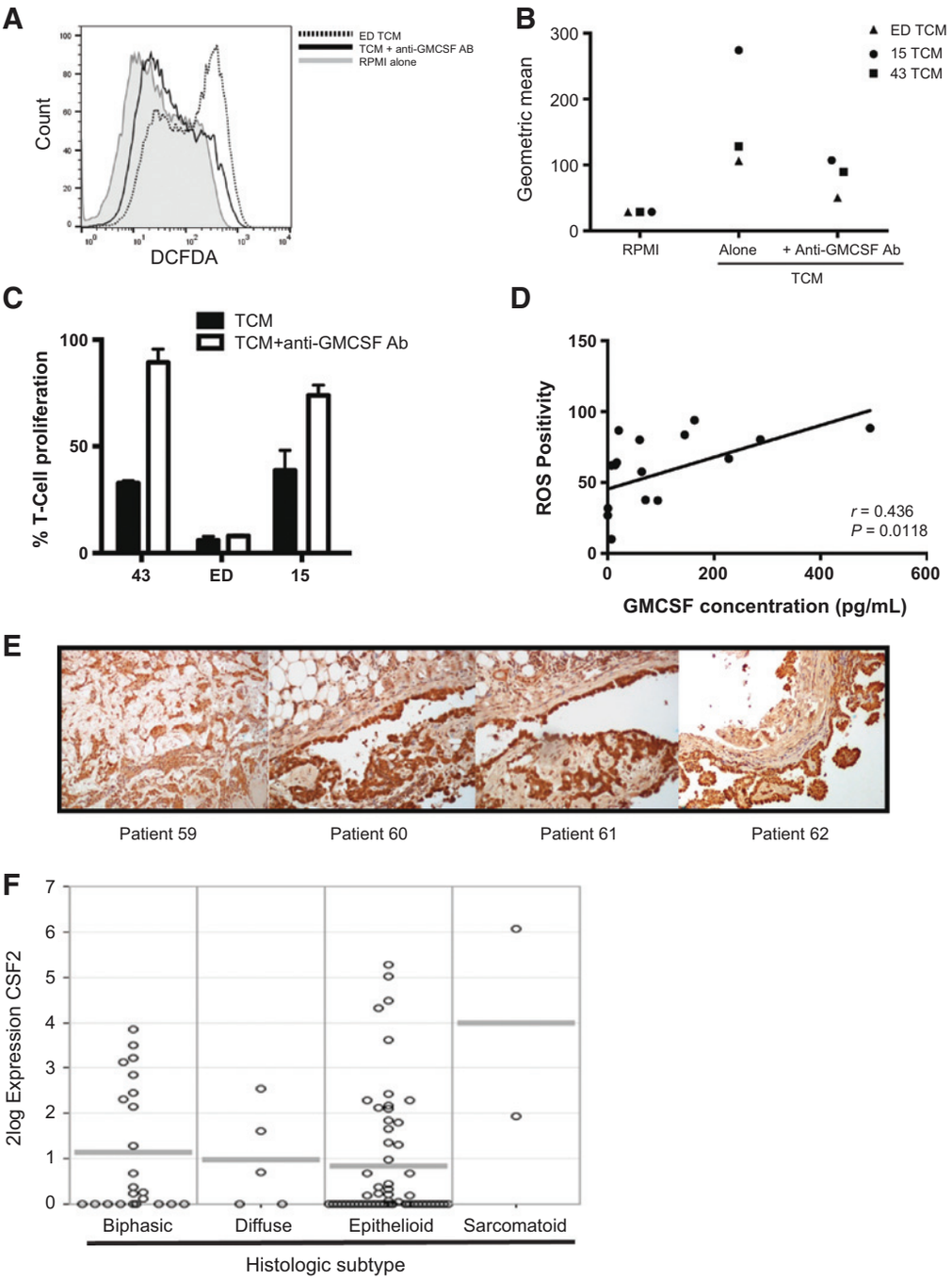

Figure 6.

Anti-GM-CSF–neutralizing antibody can prevent granulocyte suppressive function. **A**, The addition of anti-GM-CSF–neutralizing antibody to mesothelioma cell line conditioned media prevents granulocyte ROS expression, as measured by DCFDA staining. Representative histograms for ED cell line shown. **B,** The addition of anti-GM-CSF–neutralizing antibody to mesothelioma cell line conditioned media prevents granulocyte ROS expression. Geometric means for DCFDA staining shown following flow cytometric detection. **C,** The addition of anti-GM-CSF–neutralizing antibody to mesothelioma cell line conditioned media prevents granulocyte-suppressive activity compared with granulocytes cultured in tumor-conditioned media alone. **D,** Correlation between GM-CSF concentrations in tumor-conditioned media and expression of ROS in conditioned granulocytes, as measured by DCFDA mean fluorescence intensity by flow cytometry. Linear correlation line shown. **E,** Immunohistochemistry staining demonstrating the presence of GM-CSF in mesothelioma tumor sections. Mesothelioma of epithelioid (first image), adenomatoid (second and third images), and mixed/biphasic (fourth image) type demonstrated cytoplasmic positivity of tumor cells in a diffuse pattern. Images taken at 20× magnification. **F**, Interrogation of 87 primary tumor samples within the R2: database demonstrated that GM-CSF is expressed in over 50% of the samples and did not correlate with histological subtype.

Published OnlineFirst March 30, 2018; DOI: 10.1158/1078-0432.CCR-17-3757

$CD4^+$ versus $CD8^+$ T cells. Establishment of cell lines from primary mesotheliomas has reported significant production of GM-CSF (42) and this cytokine can drive suppressive granulocyte activity in murine models for a number of solid tumors (43–45). Although we identified GM-CSF was widely expressed in our samples studied, the effects of prior therapies in our patient population on GM-CSF expression is unknown.

Clinically, GM-CSF has been used as an alternative to G-CSF to support myeloid cell recovery postchemotherapy in mesothelioma patients (46, 47). No differences in outcome were reported for the two growth factors, although the effects on immune parameters are not available. Recombinant GM-CSF has also been administered alongside a tumor vaccine in this patient group (48–50) and used alongside immunotherapy approaches in neuroblastoma. In the mesothelioma studies, GM-CSF was administered to patients in all study arms, regardless of whether they received the investigational tumor/peptide vaccines or not. Although responses are noted, it is not possible to understand whether the cytokine had any effect on outcomes both within the trial populations or compared with historical controls. It is possible that administration of GM-CSF may inhibit antitumor T-cell responses, through the induction of G-MDSC, contributing to the lack of clinically relevant T-cell responses seen in these patients. In two trials where GM-CSF was administered intralesionally to mesothelioma, neutrophil infiltration and maturation were enhanced; however, this was not associated with tumor responses in the majority of patients (51, 52). Indeed, a phase II clinical trial in neuroblastoma demonstrated difference in prognosis if GM-CSF is administered intravenously versus subcutaneously, which could affect the dose-dependent effects of this cytokine on granulocyte phenotype (53, 54).

Preclinical studies that block GM-CSF have resulted in reversal of T-cell inhibition by MDSCs in the setting of pancreatic tumors and improvements in phenotype in inflammatory disease models (55, 56). Our data suggest that targeting the GM-CSF pathway may be of benefit in mesothelioma. Clinically relevant approaches to target GM-CSF have been focused on inflammatory diseases (57). Mavrilimumab (CAM-3001) is a human anti–GM-CSF receptor—an antibody that has completed phase I and II clinical trials in the setting of rheumatoid arthritis (58). Our findings suggest that anti–GM-CSF or anti–GM-CSF receptor antibodies could play a critical role in mesothelioma treatment, particularly alongside T-cell immunotherapies.

Disclosure of Potential Conflicts of Interest

No potential conflicts of interest were disclosed.

Authors' Contributions

Conception and design: S. Khanna, S. Graef, F. Mussai, G. Middleton, C.D. Santo, R. Hassan

Development of methodology: S. Khanna, S. Graef, N. Wali, J. Zhang, M. Stetler-Stevenson, C.D. Santo, R. Hassan

Acquisition of data (provided animals, acquired and managed patients, provided facilities, etc.): S. Khanna, S. Graef, F. Mussai, A. Thomas, N. Wali, B.G. Yenidunya, C. Yuan, B. Morrow, M. Stetler-Stevenson, C.D. Santo, R. Hassan

Analysis and interpretation of data (e.g., statistical analysis, biostatistics, computational analysis): S. Khanna, S. Graef, F. Mussai, A. Thomas, N. Wali, B.G. Yenidunya, C. Yuan, F. Korangy, T.F. Greten, S.M. Steinberg, M. Stetler-Stevenson, G. Middleton, C.D. Santo, R. Hassan

Writing, review, and/or revision of the manuscript: S. Khanna, S. Graef, F. Mussai, A. Thomas, B.G. Yenidunya, F. Korangy, T.F. Greten, S.M. Steinberg, G. Middleton, C.D. Santo, R. Hassan

Administrative, technical, or material support (i.e., reporting or organizing data, constructing databases): S. Khanna, T.F. Greten, C.D. Santo, R. Hassan

Study supervision: F. Mussai, G. Middleton, C.D. Santo, R. Hassan

Acknowledgments

This work was supported by the Intramural Research Program of the Center for Cancer Research, National Cancer Institute, NIH, Cancer Research UK, the British Lung Foundation, and the June Hancock Mesothelioma Research Fund.

The authors thank the patients who contributed samples to the study. Thank you to research nurses for collection of patient samples. Thank you to Dean Fennell at the University of Leicester for the provision of mesothelioma samples.

The costs of publication of this article were defrayed in part by the payment of page charges. This article must therefore be hereby marked *advertisement* in accordance with 18 U.S.C. Section 1734 solely to indicate this fact.

Received December 18, 2017; revised February 9, 2018; accepted March 23, 2018; published first March 30, 2018.

References

1. Yap TA, Aerts JG, Popat S, Fennell DA. Novel insights into mesothelioma biology and implications for therapy. Nat Rev Cancer 2017;17:475–88.
2. Zalcman G, Mazieres J, Margery J, Greillier L, Audigier-Valette C, Moro-Sibilot D, et al. Bevacizumab for newly diagnosed pleural mesothelioma in the Mesothelioma Avastin Cisplatin Pemetrexed Study (MAPS): a randomised, controlled, open-label, phase 3 trial. Lancet 2016;387:1405–14.
3. Adusumilli PS, Cherkassky L, Villena-Vargas J, Colovos C, Servais E, Plotkin J, et al. Regional delivery of mesothelin-targeted CAR T cell therapy generates potent and long-lasting CD4-dependent tumor immunity. Sci Transl Med 2014;6:261ra151.
4. Zauderer MG, Tsao AS, Dao T, Panageas KS, Lai WV, Rimner A, et al. A Randomized Phase II trial of adjuvant galinpepimut-S, WT-1 analog peptide vaccine, after multimodality therapy for patients with malignant pleural mesothelioma. Clin Cancer Res 2017;23:7483–9.
5. Cornwall SM, Wikstrom M, Musk AW, Alvarez J, Nowak AK, Nelson DJ. Human mesothelioma induces defects in dendritic cell numbers and antigen-processing function which predict survival outcomes. Oncoimmunology 2016;5:e1082028.
6. Veltman JD, Lambers ME, van Nimwegen M, Hendriks RW, Hoogsteden HC, Hegmans JP, et al. Zoledronic acid impairs myeloid differentiation to tumour-associated macrophages in mesothelioma. Br J Cancer 2010;103:629–41.
7. Chene AL, d'Almeida S, Blondy T, Tabiasco J, Deshayes S, Fonteneau JF, et al. Pleural effusions from patients with mesothelioma induce recruitment of monocytes and their differentiation into M2 macrophages. J Thorac Oncol 2016;11:1765–73.
8. Hooper CE, Lyburn ID, Searle J, Darby M, Hall T, Hall D, et al. The south west area mesothelioma and pemetrexed trial: a multicentre prospective observational study evaluating novel markers of chemotherapy response and prognostication. Br J Cancer 2015;112:1175–82.
9. Yamada N, Oizumi S, Kikuchi E, Shinagawa N, Konishi-Sakakibara J, Ishimine A, et al. CD8+ tumor-infiltrating lymphocytes predict favorable prognosis in malignant pleural mesothelioma after resection. Cancer Immunol Immunother 2010;59:1543–9.
10. Kao SC, Pavlakis N, Harvie R, Vardy JL, Boyer MJ, van Zandwijk N, et al. High blood neutrophil-to-lymphocyte ratio is an indicator of poor

prognosis in malignant mesothelioma patients undergoing systemic therapy. Clin Cancer Res 2010;16:5805–13.
11. Linton A, Pavlakis N, O'Connell R, Soeberg M, Kao S, Clarke S, et al. Factors associated with survival in a large series of patients with malignant pleural mesothelioma in New South Wales. Br J Cancer 2014;111:1860–9.
12. Pinato DJ, Mauri FA, Ramakrishnan R, Wahab L, Lloyd T, Sharma R. Inflammation-based prognostic indices in malignant pleural mesothelioma. J Thorac Oncol 2012;7:587–94.
13. Shaul ME, Levy L, Sun J, Mishalian I, Singhal S, Kapoor V, et al. Tumor-associated neutrophils display a distinct N1 profile following TGFbeta modulation: A transcriptomics analysis of pro- vs. antitumor TANs. Oncoimmunology 2016;5:e1232221.
14. Szlosarek PW, Klabatsa A, Pallaska A, Sheaff M, Smith P, Crook T, et al. In vivo loss of expression of argininosuccinate synthetase in malignant pleural mesothelioma is a biomarker for susceptibility to arginine depletion. Clin Cancer Res 2006;12:7126–31.
15. De Santo C, Arscott R, Booth S, Karydis I, Jones M, Asher R, et al. Invariant NKT cells modulate the suppressive activity of IL-10-secreting neutrophils differentiated with serum amyloid A. Nat Immunol 2010;11:1039–46.
16. Movahedi K, Guilliams M, Van den Bossche J, Van den Bergh R, Gysemans C, Beschin A, et al. Identification of discrete tumor-induced myeloid-derived suppressor cell subpopulations with distinct T cell-suppressive activity. Blood 2008;111:4233–44.
17. Rodriguez PC, Ernstoff MS, Hernandez C, Atkins M, Zabaleta J, Sierra R, et al. Arginase I-producing myeloid-derived suppressor cells in renal cell carcinoma are a subpopulation of activated granulocytes. Cancer Res 2009;69:1553–60.
18. Schmielau J, Finn OJ. Activated granulocytes and granulocyte-derived hydrogen peroxide are the underlying mechanism of suppression of t-cell function in advanced cancer patients. Cancer Res 2001;61:4756–60.
19. Zea AH, Rodriguez PC, Atkins MB, Hernandez C, Signoretti S, Zabaleta J, et al. Arginase-producing myeloid suppressor cells in renal cell carcinoma patients: a mechanism of tumor evasion. Cancer Res 2005;65:3044–8.
20. Veltman JD, Lambers ME, van Nimwegen M, Hendriks RW, Hoogsteden HC, Aerts JG, et al. COX-2 inhibition improves immunotherapy and is associated with decreased numbers of myeloid-derived suppressor cells in mesothelioma. Celecoxib influences MDSC function. BMC Cancer 2010;10:464.
21. Oka K, Sarashina G, Yonekawa N, Watanabe O, Miyao Y, Hashimoto T, et al. G-CSF-producing malignant pleural mesothelioma: an autopsy case report with literature review. Int J Surg Pathol 2012;20:272–5.
22. Demetri G, Zenzie B, Rheinwald J, Griffin JD. Expression of colony-stimulating factor genes by normal human mesothelial cells and human malignant mesothelioma cells lines in vitro. Blood 1989;74:940–6.
23. Condamine T, Gabrilovich DI. Molecular mechanisms regulating myeloid-derived suppressor cell differentiation and function. Trends Immunol 2011;32:19–25.
24. Chee SJ, Lopez M, Mellows T, Gankande S, Moutasim KA, Harris S, et al. Evaluating the effect of immune cells on the outcome of patients with mesothelioma. Br J Cancer 2017;190:148–58.
25. Mishalian I, Bayuh R, Levy L, Zolotarov L, Michaeli J, Fridlender G. Tumor-associated neutrophils (TAN) develop pro-tumorigenic properties during tumor progression. Cancer Immunol Immunother 2013;62:1745–56.
26. Corzo CA, Cotter MJ, Cheng P, Cheng F, Kusmartsev S, Sotomayor E, et al. Mechanism regulating reactive oxygen species in tumor-induced myeloid-derived suppressor cells. J Immunol 2009;182:5693–701.
27. Bronte V, Brandau S, Chen SH, Colombo MP, Frey AB, Greten TF, et al. Recommendations for myeloid-derived suppressor cell nomenclature and characterization standards. Nat Commun 2016;7:12150.
28. Rotondo R, Barisione G, Mastracci L, Grossi F, Orengo AM, Costa R, et al. IL-8 induces exocytosis of arginase 1 by neutrophil polymorphonuclears in nonsmall cell lung cancer. Int J Cancer 2009;125:887–93.
29. Fridlender ZG, Sun J, Kim S, Kapoor V, Cheng G, Ling L, et al. Polarization of tumor-associated neutrophil phenotype by TGF-beta: "N1" versus "N2" TAN. Cancer cell 2009;16:183–94.
30. Urano N, Yano E, Evans PH. Reactive oxygen metabolites produced by the carcinogenic fibrous mineral erionite. Environ Res 1991;54:74–81.
31. Achcar Rde O, Cagle PT, Jagirdar J. Expression of activated and latent signal transducer and activator of transcription 3 in 303 non-small cell lung carcinomas and 44 malignant mesotheliomas: possible role for chemotherapeutic intervention. Arch Pathol Lab Med 2007;131:1350–60.
32. Baggiolini M, Walz A, Kunkel SL. Neutrophil-activating peptide-1/interleukin 8, a novel cytokine that activates neutrophils. J Clin Invest 1989;84:1045–9.
33. Glynn PC, Henney E, Hall IP. The selective CXCR2 antagonist SB272844 blocks interleukin-8 and growth-related oncogene-alpha-mediated inhibition of spontaneous neutrophil apoptosis. Pulmon Pharmacol Ther 2002;15:103–10.
34. Bekes EM, Schweighofer B, Kupriyanova TA, Zajac E, Ardi VC, Quigley JP, et al. Tumor-recruited neutrophils and neutrophil TIMP-free MMP-9 regulate coordinately the levels of tumor angiogenesis and efficiency of malignant cell intravasation. Am J Pathol 2011;179:1455–70.
35. Brew R, Erikson JS, West DC, Kinsella AR, Slavin J, Christmas SE. Interleukin-8 as an autocrine growth factor for human colon carcinoma cells in vitro. Cytokine 2000;12:78–85.
36. Luppi F, Longo AM, de Boer WI, Rabe KF, Hiemstra PS. Interleukin-8 stimulates cell proliferation in non-small cell lung cancer through epidermal growth factor receptor transactivation. Lung Cancer 2007;56:25–33.
37. Takamori H, Oades ZG, Hoch OC, Burger M, Schraufstatter IU. Autocrine growth effect of IL-8 and GROalpha on a human pancreatic cancer cell line, Capan-1. Pancreas 2000;21:52–6.
38. Galffy G, Mohammed KA, Nasreen N, Ward MJ, Antony VB. Inhibition of interleukin-8 reduces human malignant pleural mesothelioma propagation in nude mouse model. Oncol Res 1999;11:187–94.
39. Kasuga I, Ishizuka S, Minemura K, Utsumi K, Serizawa H, Ohyashiki K. Malignant pleural mesothelioma produces functional granulocyte-colony stimulating factor. Chest 2001;119:981–3.
40. Rikimaru T, Ichikawa Y, Ogawa Y, Higuchi E, Kinosita M, Oizumi K, et al. Production of granulocyte colony-stimulating factor by malignant mesothelioma. Eur Respir J 1995;8:183–4.
41. Fujiwara A, Higashiyama M, Kanou T, Okami J, Tokunaga T, Tomita Y, et al. Granulocyte-colony stimulating factor (G-CSF) producing malignant pleural mesothelioma: Report of a case. Thoracic Cancer 2015;6:105–9.
42. Pass H, Stevens E, Oie H, Tsokos M, Abati A, Fetsch P, et al. Characteristics of nine newly derived mesothelioma cell lines. Ann Thorac Surg 1995;59:835–44.
43. Dolcetti L, Peranzoni E, Ugel S, Marigo I, Fernandez Gomez A, Mesa C, et al. Hierarchy of immunosuppressive strength among myeloid-derived suppressor cell subsets is determined by GM-CSF. Eur J Immunol 2010;40:22–35.
44. Solito S, Falisi E, Diaz-Montero CM, Doni A, Pinton L, Rosato A, et al. A human promyelocytic-like population is responsible for the immune suppression mediated by myeloid-derived suppressor cells. Blood 2011;118:2254–65.
45. Youn JI, Collazo M, Shalova IN, Biswas SK, Gabrilovich DI. Characterization of the nature of granulocytic myeloid-derived suppressor cells in tumor-bearing mice. J Leukoc Biol 2012;91:167–81.
46. Dirix LY, van Meerbeeck J, Schrijvers D, Corthouts B, Prove A, van Marck E, et al. A phase II trial of dose-escalated doxorubicin and ifosfamide/mesna in patients with malignant mesothelioma. Ann Oncol 1994;5:653–5.
47. Kosty MP, Herndon JE 2nd, Vogelzang NJ, Kindler HL, Green MR. High-dose doxorubicin, dexrazoxane, and GM-CSF in malignant mesothelioma: a phase II study-Cancer and Leukemia Group B 9631. Lung Cancer 2001;34:289–95.
48. Powell A, Creaney J, Broomfield S, Van Bruggen I, Robinson B. Recombinant GM-CSF plus autologous tumor cells as a vaccine for patients with mesothelioma. Lung Cancer 2006;52:189–97.
49. Krug LM, Dao T, Brown AB, Maslak P, Travis W, Bekele S, et al. WT1 peptide vaccinations induce CD4 and CD8 T cell immune responses in patients with mesothelioma and non-small cell lung cancer. Cancer Immunol Immunother 2010;59:1467–79.
50. Zauderer MG, Tsao AS, Dao T, Panageas K, Lai WV, Rimner A, et al. A randomized phase II trial of adjuvant galinpepimut-S, WT-1 analogue peptide vaccine, after multimodality therapy for patients with malignant pleural mesothelioma. Clin Cancer Res 2017;23:7483–9.
51. Davidson JA, Musk AW, Wood BR, Morey S, Ilton M, Yu LL, et al. Intralesional cytokine therapy in cancer: a pilot study of GM-CSF infusion in mesothelioma. J Immunother 1998;21:389–98.

Published OnlineFirst March 30, 2018; DOI: 10.1158/1078-0432.CCR-17-3757

52. Robinson BW, Mukherjee SA, Davidson A, Morey S, Musk AW, Ramshaw I, et al. Cytokine gene therapy or infusion as treatment for solid human cancer. J Immunother 1998;21:211–7.
53. Cheung NK, Cheung IY, Kramer K, Modak S, Kuk D, Pandit-Taskar N, et al. Key role for myeloid cells: phase II results of anti-G(D2) antibody 3F8 plus granulocyte-macrophage colony-stimulating factor for chemoresistant osteomedullary neuroblastoma. Int J Cancer 2014;135:2199–205.
54. Peters WP, Stuart A, Affronti ML, Kim CS, Coleman RE. Neutrophil migration is defective during recombinant human granulocyte-macrophage colony-stimulating factor infusion after autologous bone marrow transplantation in humans. Blood 1988;72:1310–5.
55. Gargett T, Christo SN, Hercus TR, Abbas N, Singhal N, Lopez AF, et al. GM-CSF signalling blockade and chemotherapeutic agents act in concert to inhibit the function of myeloid-derived suppressor cells in vitro. Clin Transl Immunol 2016;5:e119.
56. Cook AD, Louis C, Robinson MJ, Saleh R, Sleeman MA, Hamilton JA. Granulocyte macrophage colony-stimulating factor receptor alpha expression and its targeting in antigen-induced arthritis and inflammation. Arthritis Res Ther 2016;18:287.
57. Wicks IP, Roberts AW. Targeting GM-CSF in inflammatory diseases. Nat Rev Rheumatol 2016;12:37–48.
58. Burmester GR, McInnes IB, Kremer J, Miranda P, Korkosz M, Vencovsky J, et al. A randomised phase IIb study of mavrilimumab, a novel GM-CSF receptor alpha monoclonal antibody, in the treatment of rheumatoid arthritis. Ann Rheum Dis 2017;76:1020–30.

Published OnlineFirst March 30, 2018; DOI: 10.1158/1078-0432.CCR-17-3757

Clinical Cancer Research

Tumor-Derived GM-CSF Promotes Granulocyte Immunosuppression in Mesothelioma Patients

Swati Khanna, Suzanne Graef, Francis Mussai, et al.

Clin Cancer Res 2018;24:2859-2872. Published OnlineFirst March 30, 2018.

References

(1) Greenberg M, Lloyd Davies TA. Mesothelioma Register 1967-68. British Journal of Industrial Medicine 1974 Apr 1,;31(2):91-104.

(2) Wagner JC, Sleggs CA, Marchand P. Diffuse Pleural Mesothelioma and Asbestos Exposure in the North Western Cape Province. British Journal of Industrial Medicine 1960 Oct 1,;17(4):260-271.

(3) Tossavainen A. Global use of asbestos and the incidence of mesothelioma. International journal of occupational and environmental health 2004 Jan 1,;10(1):22-25.

(4) Metintas M, Metintas S, Özdemir N, Hillerdal G, Uçgun I, Baykul C, et al. Environmental asbestos exposure and malignant pleural mesothelioma. Respiratory Medicine 1999;93(5):349-355.

(5) McElvenny DM, Darnton AJ, Price MJ, Hodgson JT. Mesothelioma mortality in Great Britain from 1968 to 2001. Occup Med (Oxf) 2005 Mar;55(2):79-87.

(6) Peto J, Matthews FE, Hodgson JT, Jones JR. Continuing increase in mesothelioma mortality in Britain. The Lancet 1995;345(8949):535-539.

(7) Ferrante D, Bertolotti M, Todesco A, Mirabelli D, Terracini B, Magnani C. Cancer mortality and incidence of mesothelioma in a cohort of wives of asbestos workers in Casale Monferrato, Italy. Environ Health Perspect 2007 Oct;115(10):1401-1405.

(8) Sakellariou K, Malamou-Mitsi V, Haritou A, Koumpaniou C, Stachouli C, Dimoliatis ID, et al. Malignant pleural mesothelioma from nonoccupational asbestos exposure in Metsovo (north-west Greece): slow end of an epidemic? European Respiratory Journal 1996 Jun 1,;9(6):1206-1210.

(9) Hodgson DC, Gilbert ES, Dores GM, Schonfeld SJ, Lynch CF, Storm H, et al. Long-Term Solid Cancer Risk Among 5-Year Survivors of Hodgkin's Lymphoma. Journal of Clinical Oncology 2007 Apr 20,;25(12):1489-1497.

(10) Takahashi K, Karjalainen A. A cross-country comparative overview of the asbestos situation in ten Asian countries. Int J Occup Environ Health 2003;9(3):244-248.

(11) Walgate R. European nations agree to improve environmental health. The Lancet 2010;375(9719):969.

(12) Park EK, Takahashi K, Hoshuyama T, Cheng TJ, Delgermaa V, Vinh Le G, et al. Global Magnitude of Reported and Unreported Mesothelioma. Environmental Health Perspectives 2011 Apr 1,;119(4):514-518.

(13) Demirer E, Ghattas CF, Radwan MO, Elamin EM. Clinical and Prognostic Features of Erionite-Induced Malignant Mesothelioma. Yonsei Medical Journal 2015 Mar 1,;56(2):311-323.

(14) Goodman JE, Nascarella MA, Valberg PA. Ionizing Radiation: A Risk Factor for Mesothelioma. Cancer Causes & Control 2009 Oct 1,;20(8):1237-1254.

(15) Carbone M, Pass HI, Rizzo P, Marinetti MR, Di Muzio M, Mew D, et al. Simian virus 40-like DNA sequences in human pleural mesothelioma. Oncogene 1994 Jan 1,;9(6):1781-1790.

(16) Baris I, Simonato L, Artvinli M, Pooley F, Saracci R, Skidmore J, et al. Epidemiological and environmental evidence of the health effects of exposure to erionite fibres: a four-year study in the Cappadocian region of Turkey. International journal of cancer 1987 Jan 15,;39(1):10-17.

(17) Van Gosen B, Blitz T, Plumlee G, Meeker G, Pierson M. Geologic occurrences of erionite in the United States: an emerging national public health concern for respiratory disease. Environ Geochem Health 2013 Aug;35(4):419-430.

(18) Beaucham C, King B, Feldmann K, Harper M, Dozier A. Assessing occupational erionite and respirable crystalline silica exposure among outdoor workers in Wyoming, South Dakota, and Montana. Journal of Occupational and Environmental Hygiene 2018 Jun 3,;15(6):455-465.

(19) Travis LB, Fosså SD, Schonfeld SJ, McMaster ML, Lynch CF, Storm H, et al. Second Cancers Among 40 576 Testicular Cancer Patients: Focus on Long-term Survivors. Journal of the National Cancer Institute 2005 Sep 21,;97(18):1354-1365.

(20) Hilleman MR. Discovery of simian virus 40 (SV40) and its relationship to poliomyelitis virus vaccines. Dev Biol Stand. 1998;94:183-90.

(21) Carbone M, Stach R, Di Resta I, Pass HI, Rizzo P. Simian virus 40 oncogenesis in hamsters. Developments in biological standardization 1998;94:273.

(22) Poulin DL, DeCaprio JA. Is There a Role for SV40 in Human Cancer? Journal of Clinical Oncology 2006 Sep 10,;24(26):4356-4365.

(23) Cancer Research UK. [Online]. 2018; Available at: https://www.cancerresearchuk.org/health-professional/cancer-statistics/statistics-by-cancer-type/mesothelioma/incidence. Accessed November, 2018.

(24) Hasan B, Greillier L, Pallis A, Menis J, Gaafar R, Sylvester R, et al. Progression free survival rate at 9 and 18 weeks predict overall survival in patients with malignant pleural mesothelioma: an individual patient pooled analysis of 10 European Organisation for Research and Treatment of Cancer Lung Cancer Group studies and an independent study validation. European journal of cancer (Oxford, England : 1990) 2014 Nov;50(16):2771.

(25) De Angelis R, Sant M, Coleman MP, Francisci S, Baili P, Pierannunzio D, et al. Cancer survival in Europe 1999–2007 by country and age: results of EUROCARE-5—a population-based study. Lancet oncology 2014;15(1):23-34.

(26) Mutsaers SE. The mesothelial cell. International Journal of Biochemistry and Cell Biology 2004;36(1):9-16.

(27) Ferrandez-Izquierdo A, Navarro-Fos S, Gonzalez-Devesa M, Gil-Benso R, Llombart-Bosch A. Immunocytochemical typification of mesothelial cells in effusions: in vivo and in vitro models. Diagnostic cytopathology 1994;10(3):256-262.

(28) Ohtani O, Ohtani Y, Li RX. Phylogeny and ontogeny of the lymphatic stomata connecting the pleural and peritoneal cavities with the lymphatic system--a review. Italian journal of anatomy and embryology = Archivio italiano di anatomia ed embriologia 2001;106(2 Suppl 1):251.

(29) Visser CE, Tekstra J, Brouwer-Steenbergen JJE, Tuk CW, Boorsma DM, Sampat-Sardjoepersad SC, et al. Chemokines produced by mesothelial cells: huGRO-alpha, IP-10, MCP-1 and RANTES. Clinical & Experimental Immunology 1998 May;112(2):270-275.

(30) Hausmann MJ, Rogachev B, Weiler M, Chaimovitz C, Douvdevani A. Accessory role of human peritoneal mesothelial cells in antigen presentation and T-cell growth. Kidney International 2000 Feb;57(2):476-486.

(31) Mutsaers SE, McAnulty RJ, Laurent GJ, Versnel MA, Whitaker D, Papadimitriou JM. Cytokine regulation of mesothelial cell proliferation in vitro and in vivo. European journal of cell biology 1997 Jan;72(1):24.

(32) Mutsaers SE, Whitaker D, Papadimitriou JM. Stimulation of mesothelial cell proliferation by exudate macrophages enhances serosal wound healing in a murine model. Am J Pathol 2002 Feb;160(2):681-692.

(33) Foley-Comer AJ, Herrick SE, Al-Mishlab T, Prele CM, Laurent GJ, Mutsaers SE. Evidence for incorporation of free-floating mesothelial cells as a mechanism of serosal healing. Journal of Cell Science 2002 Apr 1,;115(7):1383.

(34) Yanez-Mo M, Lara-Pezzi E, Selgas R, Ramirez-Huesca M, Dominguez-Jimenez C, Jimenez-Heffernan JA, et al. Peritoneal Dialysis and Epithelial-to-Mesenchymal Transition of Mesothelial Cells. The New England Journal of Medicine 2003 Jan 30,;348(5):403-413.

(35) Aroeira LS, Aguilera A, Sánchez-Tomero JA, Bajo MA, del Peso G, Jiménez-Heffernan JA, et al. Epithelial to Mesenchymal Transition and Peritoneal Membrane Failure in Peritoneal Dialysis Patients: Pathologic Significance and Potential Therapeutic Interventions. J Am Soc Nephrol 2007;18(7):2004-2013.

(36) Lippmann M, Yeates DB, Albert RE. The effects of inflammation on the pulmonary deposition, retention and clearance of inhaled particles. Br J Ind Med 1980;37(4):337-62.

(37) Stayner L, Smith R, Bailer J, Gilbert S, Steenland K, Dement J, et al. Exposure-Response Analysis of Risk of Respiratory Disease Associated with Occupational Exposure to Chrysotile Asbestos. Occupational and Environmental Medicine 1997 Sep 1,;54(9):646-652.

(38) Kanarek MS. Mesothelioma from Chrysotile Asbestos: Update. Annals of Epidemiology 2011;21(9):688-697.

(39) Suzuki Y, Yuen SR. Asbestos Tissue Burden Study on Human Malignant Mesothelioma. Industrial Health 2001;39(2):150-160.

(40) Paris C, Aurélie Martin A, Letourneux M, Wild P. Modelling prevalence and incidence of fibrosis and pleural plaques in asbestos-exposed populations for screening and follow-up: a cross-sectional study. Environmental health : a global access science source 2008 Jun 20,;7(1):30.

(41) Hillerdal G. Pleural plaques and risk for bronchial carcinoma and mesothelioma. A prospective study. Chest 1994 Jan 1,;105(1):144-150.

(42) American Thoracic Society. Diagnosis and initial management of nonmalignant diseases related to asbestos. American journal of respiratory and critical care medicine 2004 Sep 15,;170(6):691-715.

(43) Roggli VL, Gibbs AR, Attanoos R, Churg A, Popper H, Cagle P, et al. Pathology of asbestosis-An update of the diagnostic criteria: Report of the asbestosis committee of the college of american pathologists and pulmonary pathology society. Archives of pathology & laboratory medicine 2010 Mar;134(3):462.

(44) Zhang Y, Lee TC, Guillemin B, Yu MC, Rom WN. Enhanced IL-1 beta and tumor necrosis factor-alpha release and messenger RNA expression in macrophages from idiopathic pulmonary fibrosis or after asbestos exposure. The Journal of Immunology 1993 May 1,;150(9):4188-4196.

(45) Kamp DW, Dunne M, Weitzman SA, Dunn MM. The interaction of asbestos and neutrophils injures cultured human pulmonary epithelial cells: role of hydrogen peroxide. The Journal of laboratory and clinical medicine 1989 Nov 1,;114(5):604-612.

(46) Vallyathan V, Mega JF, Shi X, Dalal NS. Enhanced generation of free radicals from phagocytes induced by mineral dusts. American journal of respiratory cell and molecular biology 1992 Apr 1,;6(4):404-413.

(47) Mossman BT, Hansen K, Marsh JP, Brew ME, Hill S, Bergeron M, et al. Mechanisms of fibre-induced superoxide release from alveolar macrophages and induction of superoxide dismutase in the lungs of rats inhaling crocidolite. IARC scientific publications 1989 Jan 1,(90):81-92.

(48) Kamp DW, Weitzman SA. The molecular basis of asbestos induced lung injury. Thorax 1999 Jul 1,;54(7):638-652.

(49) Thomas G, Ando T, Verma K, Kagan E. Asbestos fibers and interferon-gamma up-regulate nitric oxide production in rat alveolar macrophages. American Journal of Respiratory Cell and Molecular Biology 1994 Dec 1,;11(6):707-715.

(50) Choe N, Tanaka S, Kagan E. Asbestos Fibers and Interleukin-1 Upregulate the Formation of Reactive Nitrogen Species in Rat Pleural Mesothelial Cells. American Journal of Respiratory Cell and Molecular Biology 1998 Aug 1,;19(2):226-236.

(51) Vandervliet A, Eiserich JP, Oneill CA, Halliwell B, Cross CE. Tyrosine Modification by Reactive Nitrogen Species: A Closer Look. Archives of Biochemistry and Biophysics 1995;319(2):341-349.

(52) Zanella CL, Posada J, Tritton TR, Mossman BT. Asbestos Causes Stimulation of the Extracellular Signal-regulated Kinase 1 Mitogen-activated Protein Kinase Cascade after Phosphorylation of the Epidermal Growth Factor Receptor. Cancer Research 1996 Dec 1,;56(23):5334-5338.

(53) Ramos-Nino ME, Timblin CR, Mossman BT. Mesothelial Cell Transformation Requires Increased AP-1 Binding Activity and ERK-dependent Fra-1 Expression. Cancer Research 2002 Nov 1,;62(21):6065-6069.

(54) Popescu NC, Chahinian AP, DiPaolo JA. Nonrandom Chromosome Alterations in Human Malignant Mesothelioma. Cancer Research 1988 Jan 1,;48(1):142.

(55) Ruosaari ST, Nymark PEH, Aavikko MM, Kettunen E, Knuutila S, Hollmén J, et al. Aberrations of chromosome 19 in asbestos-associated lung cancer and in asbestos-induced micronuclei of bronchial epithelial cells in vitro. Carcinogenesis 2008 May;29(5):913-917.

(56) Dopp E, Schiffmann D. Analysis of chromosomal alterations induced by asbestos and ceramic fibers. Toxicology Letters 1998;96(1-2):155-162.

(57) Zhang T, Lv L, Huang Y, Ren X, Shi Q. Chromosome nondisjunction during bipolar mitoses of binucleated intermediates promote aneuploidy formation along with multipolar mitoses rather than chromosome loss in micronuclei induced by asbestos. Oncotarget 2016 Dec 25,.

(58) Flejter WL, Li FP, Antman KH, Testa JR. Recurring loss involving chromosomes 1, 3, and 22 in malignant mesothelioma: possible sites of tumor suppressor genes. Genes, chromosomes & cancer 1989 Nov;1(2):148-154.

(59) Taguchi T, Jhanwar SC, Siegfried JM, Keller SM, Testa JR. Recurrent Deletions of Specific Chromosomal Sites in 1p, 3p, 6q, and 9p in Human Malignant Mesothelioma. Cancer Research 1993 Sep 15,;53(18):4349.

(60) Wikman H, Rousaari S, Nymark P, Sarhadi VK, Saharinen J, Vanhala E, Karjalainen A, Hollme J, Knuutila S, Anttila S. Gene expression and copy number profiling suggests the importance of allelic imbalance in 19p in asbestos-associated lung cancer. Oncogene 2007;26:4730-4737.

(61) Bianchi AB, Mitsunaga SI, Cheng JQ, Klein WM, Jhanwar SC, Seizinger B, et al. High Frequency of Inactivating Mutations in the Neurofibromatosis Type 2 Gene (NF2) in Primary Malignant Mesotheliomas. Proceedings of the National Academy of Sciences of the United States of America 1995 Nov 21,;92(24):10854-10858.

(62) Sekido Y, Pass HI, Bader S, Mew DJY, Christman MF, Gazdar AF, et al. Neurofibromatosis Type 2 (NF2) Gene Is Somatically Mutated in Mesothelioma but not in Lung Cancer. Cancer Research 1995 Mar 15,;55(6):1227-1231.

(63) Guo G, Chmielecki J, Goparaju C, Heguy A, Dolgalev I, Carbone M, et al. Whole-exome sequencing reveals frequent genetic alterations in BAP1, NF2, CDKN2A, and CUL1 in malignant pleural mesothelioma. Cancer research 2015 Jan 15,;75(2):264-269.

(64) Bueno R, Stawiski EW, Goldstein LD, Durinck S, De Rienzo A, Modrusan Z, et al. Comprehensive genomic analysis of malignant pleural mesothelioma identifies recurrent mutations, gene fusions and splicing alterations. Nature Genetics 2016 Apr 1,;48(4):407.

(65) Sherr CJ. The INK4a/ARF network in tumour suppression. Nature Reviews Molecular Cell Biology 2001;2:731.

(66) Illei PB, Rusch VW, Zakowski MF, Ladanyi M. Homozygous Deletion of CDKN2A and Codeletion of the Methylthioadenosine Phosphorylase Gene in the Majority of Pleural Mesotheliomas. Clinical Cancer Research 2003 Jun 1,;9(6):2108.

(67) Rusch V, Reva B, Shimizu S, Shen R, Olshen A, Ito T, et al. The nuclear deubiquitinase BAP1 is commonly inactivated by somatic mutations and 3p21.1 losses in malignant pleural mesothelioma. Nature Genetics 2011 Jul;43(7):668-672.

(68) Yu H, Pak H, Hammond-Martel I, Ghram M, Rodrigue A, Daou S, et al. Tumor suppressor and deubiquitinase BAP1 promotes DNA double-strand break repair. Proceedings of the National Academy of Sciences of the United States of America 2014 Jan 7,;111(1):285-290.

(69) Yang H, Rivera Z, Jube S, Nasu M, Bertino P, Goparaju C, et al. Programmed necrosis induced by asbestos in human mesothelial cells causes high-mobility group box 1 protein release and resultant inflammation. Proceedings of the National Academy of Sciences of the United States of America 2010 Jul 13,;107(28):12611-12616.

(70) Driscoll KE, Maurer JK, Higgins J, Poynter J. Alveolar macrophage cytokine and growth factor production in a rat model of crocidolite-induced pulmonary inflammation and fibrosis. Journal of toxicology and environmental health 1995 Oct 1,;46(2):155-169.

(71) Simeonova PP, Luster MI. Iron and reactive oxygen species in the asbestos-induced tumor necrosis factor-alpha response from alveolar macrophages. American Journal of Respiratory Cell and Molecular Biology 1995 Jun 1,;12(6):676-683.

(72) Dostert C, Petrilli V, Van Bruggen R, Steele C, Mossman BT, Tschopp J. Innate Immune Activation Through Nalp3 Inflammasome Sensing of Asbestos and Silica. Science 2008 May 2,;320(5876):674-677.

(73) Partanen R, Hemminki K, Koskinen H, Luo J. The Detection of Increased Amounts of the Extracellular Domain of the Epidermal Growth Factor Receptor in Serum During Carcinogenesis in Asbestosis Patients. JOM. Journal of Occupational Medicine 1994 Dec 1,;36(12):1324-1328.

(74) Zhong J, Cornelsen Gencay MM, Bubendorf L, Burgess JK, Parson H, Robinson BWS, et al. ERK1/2 and p38 MAP kinase control MMP-2, MT1-MMP, and TIMP action and affect cell migration: A comparison between mesothelioma and mesothelial cells. Journal of Cellular Physiology 2006 May;207(2):540-552.

(75) Lasky JA, Coin PG, Lindroos PM, Ostrowski LE, Brody AR, Bonner JC. Chrysotile asbestos stimulates platelet-derived growth factor-AA production by rat lung fibroblasts in vitro: evidence for an autocrine loop. American Journal of Respiratory Cell and Molecular Biology 1995 Feb 1,;12(2):162-170.

(76) Acencio M, Soares B, Marchi E, Silva C, Teixeira L, Broaddus V. Inflammatory Cytokines Contribute to Asbestos-Induced Injury of Mesothelial Cells. Lung 2015 Oct;193(5):831-837.

(77) Yang H, Bocchetta M, Kroczynska B, Elmishad AG, Chen Y, Liu Z, et al. TNF-α Inhibits Asbestos-Induced Cytotoxicity via a NF-κB-Dependent Pathway, a Possible Mechanism for Asbestos-Induced Oncogenesis. Proceedings of the National Academy of Sciences of the United States of America 2006 Jul 5,;103(27):10397-10402.

(78) Adachi Y, Aoki C, Yoshio-Hoshino N, Takayama K, Curiel DT, Nishimoto N. Interleukin-6 induces both cell growth and VEGF production in malignant mesotheliomas. International Journal of Cancer 2006 Sep 15,;119(6):1303-1311.

(79) Strizzi L, Catalano A, Vianale G, Orecchia S, Casalini A, Tassi G, et al. Vascular endothelial growth factor is an autocrine growth factor in human malignant mesothelioma. The Journal of Pathology 2001 Apr;193(4):468-475.

(80) Lippman SM, Gibson N, Subbaramaiah K, Dannenberg AJ. Combined targeting of the epidermal growth factor receptor and cyclooxygenase-2 pathways. Clinical cancer research : an official journal of the American Association for Cancer Research 2005 Sep 1,;11(17):6097-6099.

(81) Topley N, Petersen MM, Mackenzie R, Neubauer A, Stylianou E, Kaever V, et al. Human peritoneal mesothelial cell prostaglandin synthesis: Induction of cyclooxygenase mRNA by peritoneal macrophage-derived cytokines. Kidney International 1994 Sep;46(3):900-909.

(82) Edwards JG, Faux SP, Plummer SM, Abrams KR, Walker RA, Waller DA, et al. Cyclooxygenase-2 Expression Is a Novel Prognostic Factor in Malignant Mesothelioma. Clinical Cancer Research 2002 Jun 1,;8(6):1857.

(83) Baldi A, Santini D, Vasaturo F, Santini M, Vicidomini G, Di Marino MP, et al. Prognostic significance of cyclooxygenase-2 (COX-2) and expression of cell cycle inhibitors p21 and p27 in human pleural malignant mesothelioma. Thorax 2004 May;59(5):428-433.

(84) Demirag F, Ünsal E, Yilmaz A, çağlar A. Prognostic Significance of Vascular Endothelial Growth Factor, Tumor Necrosis, and Mitotic Activity Index in Malignant Pleural Mesothelioma. Chest 2005 Nov;128(5):3382-3387.

(85) Yasumitsu A, Tabata C, Tabata R, Hirayama N, Murakami A, Yamada S, et al. Clinical Significance of Serum Vascular Endothelial Growth Factor in Malignant Pleural Mesothelioma. Journal of Thoracic Oncology 2010 Apr;5(4):479-483.

(86) Achcar Rde O, Cagle PT, Jagirdar J. Expression of activated and latent signal transducer and activator of transcription 3 in 303 non-small cell lung carcinomas and 44 malignant

mesotheliomas: possible role for chemotherapeutic intervention. Archives of pathology & laboratory medicine 2007 Sep;131(9):1350.

(87) Nicholson SE, De Souza D, Fabri LJ, Corbin J, Willson TA, Zhang J, et al. Suppressor of cytokine signaling-3 preferentially binds to the SHP-2-binding site on the shared cytokine receptor subunit gp130. Proc Natl Acad Sci USA 2000;97(12):6493-6498.

(88) Iwahori K, Serada S, Fujimoto M, Nomura S, Osaki T, Lee CM, et al. Overexpression of SOCS3 exhibits preclinical antitumor activity against malignant pleural mesothelioma. Int J Cancer 2011 Aug 15;129(4):1005-1017.

(89) Canino C, Mori F, Cambria A, Diamantini A, Germoni S, Alessandrini G, et al. SASP mediates chemoresistance and tumor-initiating-activity of mesothelioma cells. Oncogene 2012 Jun 28,;31(26):3148-3163.

(90) Berry G, de Klerk NH, Reid A, Ambrosini GL, Fritschi L, Olsen NJ, et al. Malignant pleural and peritoneal mesotheliomas in former miners and millers of crocidolite at Wittenoom, Western Australia. Occupational and environmental medicine 2004 Apr 1,;61(4):e14.

(91) Robinson BWS, Musk AW, Lake RA. Malignant mesothelioma. The Lancet 2015 Jul 30,;366(9483):397-408.

(92) Robinson BWS, Lake RA. Advances in Malignant Mesothelioma. N Engl J Med 2005;353(15):1591-1603.

(93) Huncharek M. Miliary Mesothelioma. Chest 1994 Aug;106(2):605-606.

(94) Livasy CA, Tishko DJ, Maygarden SJ. Miliary pulmonary metastases from a clinically occult pleural mesothelioma. Annals of Diagnostic Pathology 2003;7(4):249-253.

(95) Purek L, Laroumagne S, Dutau H, Maldonado F, Astoul P. Miliary Mesothelioma: A New Clinical and Radiological Presentation in Mesothelioma Patients with Prolonged Survival After Trimodality Therapy. Journal of Thoracic Oncology 2011 Oct;6(10):1753-1756.

(96) Baratti D, Kusamura S, Deraco M. Diffuse malignant peritoneal mesothelioma: Systematic review of clinical management and biological research. Journal of Surgical Oncology 2011 Jun 15,;103(8):822-831.

(97) Ramachandran R, Radhan P, Santosham R, Rajendiran S. A Rare Case of Primary Malignant Pericardial Mesothelioma. Journal of Clinical Imaging Science 2014 Jul 1,;4(3):47.

(98) Suman S, Schofield P, Large S. Primary pericardial mesothelioma presenting as pericardial constriction: a case report. Heart (British Cardiac Society) 2004 Jan;90(1):4.

(99) Abe K, Kato N, Miki K, Nimura S, Suzuki M, Kiyota H, et al. Malignant mesothelioma of testicular tunica vaginalis. International Journal of Urology 2002 Oct;9(10):602-603.

(100) Paintal A, Raparia K, Zakowski MF, Nayar R. The diagnosis of malignant mesothelioma in effusion cytology: a reappraisal and results of a multi-institution survey. Cancer cytopathology 2013 Dec;121(12):703-707.

(101) Chirieac LR, Pinkus GS, Pinkus JL, Godleski J, Sugarbaker DJ, Corson JM. The immunohistochemical characterization of sarcomatoid malignant mesothelioma of the pleura. American Journal of Cancer Research 2010;1(1):14-24.

(102) Rusch V. A Proposed New International TNM Staging System for Malignant Pleural Mesothelioma. Chest 1995 Oct;108(4):1122-1128.

(103) Edge SB, Bird DR, Compton CC. AJCC Cancer Staging Atlas. 2nd ed. ed. DE: Springer Verlag; 2012.

(104) Wilcox BE, Subramaniam RM, Peller PJ, Aughenbaugh GL, Nichols FC, Aubry MC, et al. Utility of Integrated Computed Tomography—Positron Emission Tomography for Selection of Operable Malignant Pleural Mesothelioma. Clinical Lung Cancer 2009 Jul 1,;10(4):244-248.

(105) Cao C, Akhunji Z, Fu B, Wilcox C, Novis E, Tian DH, et al. Surgical Management of Malignant Pleural Mesothelioma: An Update of Clinical Evidence. Seminars in thoracic and cardiovascular surgery 2015;27(1):6-8.

(106) Rintoul RC, Ritchie AJ, Edwards JG, Waller DA, Coonar AS, Bennett M, et al. Efficacy and cost of video-assisted thoracoscopic partial pleurectomy versus talc pleurodesis in patients with malignant pleural mesothelioma (MesoVATS): an open-label, randomised, controlled trial. The Lancet 2014 Sep 20,;384(9948):1118-1127.

(107) Bovolato P, Casadio C, Billè A, Ardissone F, Santambrogio L, Ratto G, et al. Does Surgery Improve Survival of Patients with Malignant Pleural Mesothelioma?: A Multicenter Retrospective Analysis of 1365 Consecutive Patients. Journal of Thoracic Oncology 2014 Mar;9(3):390-396.

(108) Friedberg JS. The state of the art in the technical performance of lung-sparing operations for malignant pleural mesothelioma. Seminars in thoracic and cardiovascular surgery 2013;25(2):125.

(109) Cao C, Tian D, Park J, Allan J, Pataky KA, Yan TD. A systematic review and meta-analysis of surgical treatments for malignant pleural mesothelioma. Lung cancer (Amsterdam, Netherlands) 2014 Feb;83(2):240-245.

(110) Treasure T, Lang-Lazdunski L, Waller D, Bliss JM, Tan C, Entwisle J, et al. Extra-pleural pneumonectomy versus no extra-pleural pneumonectomy for patients with malignant pleural mesothelioma: clinical outcomes of the Mesothelioma and Radical Surgery (MARS) randomised feasibility study. Lancet Oncology 2011;12(8):763-772.

(111) Vogelzang NJ, Rusthoven JJ, Symanowski J, Denham C, Kaukel E, Ruffie P, et al. Phase III study of pemetrexed in combination with cisplatin versus cisplatin alone in patients with malignant pleural mesothelioma. J Clin Oncol 2003 Jul 15;21(14):2636-2644.

(112) Zalcman G, Mazieres J, Margery J, Greillier L, Audigier-Valette C, Moro-Sibilot D, et al. Bevacizumab for newly diagnosed pleural mesothelioma in the Mesothelioma Avastin Cisplatin Pemetrexed Study (MAPS): a randomised, controlled, open-label, phase 3 trial. The Lancet 2016 Apr 8,;387(10026):1405-1414.

(113) Baldini EH. Radiation Therapy Options for Malignant Pleural Mesothelioma. Seminars in Thoracic and Cardiovascular Surgery 2009;21(2):159-163.

(114) Garland LL, Rankin C, Gandara DR, Rivkin SE, Scott KM, Nagle RB, et al. Phase II Study of Erlotinib in Patients With Malignant Pleural Mesothelioma: A Southwest Oncology Group Study. Journal of Clinical Oncology 2007 Jun 10,;25(17):2406-2413.

(115) Krug LM, Kindler HL, Calvert H, Manegold C, Tsao AS, Fennell D, et al. Vorinostat in patients with advanced malignant pleural mesothelioma who have progressed on previous chemotherapy (VANTAGE-014): a phase 3, double-blind, randomised, placebo-controlled trial. lancet oncology 2015;16(4):447-456.

(116) Ou S, Moon J, Garland L, Mack P, Testa J, Tsao A, et al. SWOG S0722: Phase II Study of mTOR Inhibitor Everolimus (RAD001) in Advanced Malignant Pleural Mesothelioma (MPM). Journal of Thoracic Oncology 2015 Feb;10(2):387-391.

(117) Mikulski SM, Costanzi JJ, Vogelzang NJ, McCachren S, Taub RN, Chun H, et al. Phase II trial of a single weekly intravenous dose of ranpirnase in patients with unresectable malignant mesothelioma. Journal of clinical oncology : official journal of the American Society of Clinical Oncology 2002 Jan 1,;20(1):274-281.

(118) Janne PA, Taffaro ML, Salgia R, Johnson BE. Inhibition of Epidermal Growth Factor Receptor Signaling in Malignant Pleural Mesothelioma. Cancer Research 2002 Sep 15,;62(18):5242-5247.

(119) Normanno N, De Luca A, Bianco C, Strizzi L, Mancino M, Maiello MR, et al. Epidermal growth factor receptor (EGFR) signaling in cancer. Gene 2006 Jan 17;366(1):2-16.

(120) Govindan R, Kratzke RA, Herndon II JE, Niehans GA, Vollmer R, Watson D, et al. Gefitinib in Patients with Malignant Mesothelioma: A Phase II Study by the Cancer and Leukemia Group B. Clinical Cancer Research 2005 Mar 15,;11(6):2300-2304.

(121) Paik P, Krug L. Histone Deacetylase Inhibitors in Malignant Pleural Mesothelioma: Preclinical Rationale and Clinical Trials. Journal of Thoracic Oncology 2010 Feb;5(2):275-279.

(122) O'Brien ME, Gaafar RM, Popat S, Grossi F, Price A, Talbot DC, et al. Phase II study of first-line bortezomib and cisplatin in malignant pleural mesothelioma and prospective validation of progression free survival rate as a primary end-point for mesothelioma clinical trials (European Organisation for Research and Treatment of Cancer 08052). European journal of cancer (Oxford, England : 1990) 2013 Sep 1,;49(13):2815-2822.

(123) Hassan R, Remaley AT, Sampson ML, Zhang J, Cox DD, Pingpank J, et al. Detection and Quantitation of Serum Mesothelin, a Tumor Marker for Patients with Mesothelioma and Ovarian Cancer. Clinical Cancer Research 2006 Jan 15,;12(2):447-453.

(124) Chang K, Pastan I. Molecular Cloning of Mesothelin, a Differentiation Antigen Present on Mesothelium, Mesotheliomas, and Ovarian Cancers. Proceedings of the National Academy of Sciences of the United States of America 1996 Jan 9,;93(1):136-140.

(125) Servais EL, Colovos C, Rodriguez L, Bograd AJ, Nitadori J, Sima C, et al. Mesothelin overexpression promotes mesothelioma cell invasion and MMP-9 secretion in an orthotopic mouse model and in epithelioid pleural mesothelioma patients. Clinical cancer research : an official journal of the American Association for Cancer Research 2012 May 1,;18(9):2478-2489.

(126) Rump A, Morikawa Y, Tanaka M, Minami S, Umesaki N, Takeuchi M, et al. Binding of Ovarian Cancer Antigen CA125/MUC16 to Mesothelin Mediates Cell Adhesion. Journal of Biological Chemistry 2004 Mar 5,;279(10):9190-9198.

(127) Bharadwaj U, Marin-Muller C, Li M, Chen C, Yao Q. Mesothelin overexpression promotes autocrine IL-6/sIL-6R trans-signaling to stimulate pancreatic cancer cell proliferation. Carcinogenesis 2011;32(7):1013-1024.

(128) Hassan R, Cohen SJ, Phillips M, Pastan I, Sharon E, Kelly RJ, et al. Phase I clinical trial of the chimeric anti-mesothelin monoclonal antibody MORAb-009 in patients with mesothelin-expressing cancers. Clinical cancer research : an official journal of the American Association for Cancer Research 2010 Dec 15,;16(24):6132-6138.

(129) Blumenschein GR, Hassan R, Moore KN, Santin A, Kindler HL, Nemunaitis JJ, et al. Phase I study of anti-mesothelin antibody drug conjugate anetumab ravtansine (AR). Journal of Clinical Oncology 2016 34:15_suppl, 2509-2509.

(130) Hassan R, Sharon E, Thomas A, Zhang J, Ling A, Miettinen M, et al. Phase 1 study of the antimesothelin immunotoxin SS1P in combination with pemetrexed and cisplatin for front-line therapy of pleural mesothelioma and correlation of tumor response with serum mesothelin, megakaryocyte potentiating factor, and cancer antigen 125. Cancer 2014 Nov 1,;120(21):3311-3319.

(131) Le DT, Brockstedt DG, Nir-Paz R, Hampl J, Mathur S, Nemunaitis J, et al. A Live-Attenuated Listeria Vaccine (ANZ-100) and a Live-Attenuated Listeria Vaccine Expressing Mesothelin (CRS-207) for Advanced Cancers: Phase I Studies of Safety and Immune Induction. Clinical Cancer Research 2012 Feb 1,;18(3):858-868.

(132) Partha S. Chowdhury, Jaye L. Viner, Richard Beers, Ira Pastan. Isolation of a High-Affinity Stable Single-Chain Fv Specific for Mesothelin from DNA-Immunized Mice by Phage Display and Construction of a Recombinant Immunotoxin with Anti-Tumor Activity. Proceedings of the National Academy of Sciences of the United States of America 1998 Jan 20,;95(2):669-674.

(133) Kreitman RJ, Hassan R, FitzGerald DJ, Pastan I. Phase I Trial of Continuous Infusion Anti-Mesothelin Recombinant Immunotoxin SS1P. Clinical Cancer Research 2009 Aug 15,;15(16):5274-5279.

(134) Hassan R, Miller AC, Sharon E, Thomas A, Reynolds JC, Ling A, et al. Major Cancer Regressions in Mesothelioma After Treatment with an Anti-Mesothelin Immunotoxin and Immune Suppression. Science Translational Medicine 2013 Oct 23,;5(208):208ra147.

(135) Hassan R, Alewine C, Pastan I. New Life for Immunotoxin Cancer Therapy. Clinical cancer research : an official journal of the American Association for Cancer Research 2016 Mar 1,;22(5):1055-1058.

(136) Calabro L, Morra A, Fonsatti E, Cutaia O, Amato G, Giannarelli D, et al. Tremelimumab for patients with chemotherapy-resistant advanced malignant mesothelioma: an open-label, single-arm, phase 2 trial. Lancet Oncol 2013 Oct;14(11):1104-1111.

(137) Alley EW, Lopez J, Santoro A, Morosky A, Saraf S, Piperdi B, et al. Clinical safety and activity of pembrolizumab in patients with malignant pleural mesothelioma (KEYNOTE-028): preliminary results from a non-randomised, open-label, phase 1b trial. Lancet Oncology 2017 May 1,;18(5):623.

(138) Scherpereel A, Mazieres J, Greillier L, Dô P, Bylicki O, Monnet I. Second- or third-line nivolumab (Nivo) versus nivo plus ipilimumab (Ipi) in malignant pleural mesothelioma (MPM) patients: Results of the IFCT-1501 MAPS2 randomized phase II trial. ournal of Clinical Oncology 2017;35(18_suppl).

(139) Zalcman G, Mazieres J, Greillier L, Lantuejoul S, Do P, Bylicki O, et al. Second or 3rd line nivolumab (Nivo) versus nivo plus ipilimumab (Ipi) in malignant pleural mesothelioma (MPM) patients: Updated results of the IFCT-1501 MAPS2 randomized phase II trial. Annals of Oncology 2017;28 (suppl_5):v605-v649.

(140) Robert C, Long GV, Brady B, Dutriaux C, Maio M, Mortier L, et al. Nivolumab in Previously Untreated Melanoma without BRAF Mutation. The New England Journal of Medicine 2015 Jan 22,;372(4):320-330.

(141) Robert C, Schachter J, Long GV, Arance A, Grob JJ, Mortier L, et al. Pembrolizumab versus Ipilimumab in Advanced Melanoma. The New England Journal of Medicine 2015 Jun 25,;372(26):2521-2532.

(142) Wolchok JD, Chiarion-Sileni V, Gonzalez R, Rutkowski P, Grob J, Cowey CL, et al. Overall Survival with Combined Nivolumab and Ipilimumab in Advanced Melanoma. The New England Journal of Medicine 2017 Oct 5,;377(14):1345-1356.

(143) Reck M, Rodriguez-Abreu D, Robinson AG, Hui R, Csoszi T, Fulop A, et al. Pembrolizumab versus Chemotherapy for PD-L1-Positive Non-Small-Cell Lung Cancer. N Engl J Med 2016 Nov 10;375(19):1823-1833.

(144) Hellmann MD, Ciuleanu T, Pluzanski A, Lee JS, Otterson GA, Audigier-Valette C, et al. Nivolumab plus Ipilimumab in Lung Cancer with a High Tumor Mutational Burden. The New England Journal of Medicine 2018 May 31,;378(22):2093-2104.

(145) Brahmer J, Rodríguez-Abreu D, Robinson A, Hui R, Csőszi T, Fülöp A, et al. OA 17.06 Updated Analysis of KEYNOTE-024: Pembrolizumab vs Platinum-Based Chemotherapy for Advanced NSCLC With PD-L1 TPS ≥50. Journal of Thoracic Oncology 2017 Nov;12(11):S1793-S1794.

(146) Motzer RJ, Tannir NM, McDermott DF, Arén Frontera O, Melichar B, Choueiri TK, et al. Nivolumab plus Ipilimumab versus Sunitinib in Advanced Renal-Cell Carcinoma. The New England Journal of Medicine 2018 Apr 5,;378(14):1277-1290.

(147) Hegmans, Joost P J J, Hemmes A, Aerts JG, Hoogsteden HC, Lambrecht BN. Immunotherapy of Murine Malignant Mesothelioma Using Tumor Lysate-pulsed Dendritic Cells. American Journal of Respiratory and Critical Care Medicine 2005 May 15,;171(10):1168-1177.

(148) Hegmans JP, Veltman JD, Lambers ME, de Vries IJ, Figdor CG, Hendriks RW, et al. Consolidative dendritic cell-based immunotherapy elicits cytotoxicity against malignant mesothelioma. Am J Respir Crit Care Med 2010 Jun 15;181(12):1383-1390.

(149) Joris D. Veltman, Margaretha E. H. Lambers, Menno van Nimwegen, Sanne de Jong, Rudi W. Hendriks, Henk C. Hoogsteden, et al. Low-Dose Cyclophosphamide Synergizes with Dendritic Cell-Based Immunotherapy in Antitumor Activity. Journal of Biomedicine and Biotechnology 2010;2010:1-10.

(150) Ziegler-Heitbrock L, Ancuta P, Crowe S, Dalod M, Grau V, Hart DN, et al. Nomenclature of monocytes and dendritic cells in blood. Blood 2010 Oct 21,;116(16):e74-e80.

(151) Villani A, Satija R, Reynolds G, Sarkizova S, Shekhar K, Fletcher J, et al. Single-cell RNA-seq reveals new types of human blood dendritic cells, monocytes, and progenitors. Science (New York, N.Y.) 2017 Apr 21,;356(6335):eaah4573.

(152) Siegal FP, Kadowaki N, Shodell M, Fitzgerald-Bocarsly PA, Shah K, Ho S, et al. The Nature of the Principal Type 1 Interferon-Producing Cells in Human Blood. Science 1999 Jun 11,;284(5421):1835-1837.

(153) Sapoznikov A, Fischer JAA, Zaft T, Krauthgamer R, Dzionek A, Jung S. Organ-dependent in vivo priming of naive CD4+,but not CD8+,T cells by plasmacytoid dendritic cells. The Journal of experimental medicine 2007 Aug 6,;204(8):1923-1933.

(154) Klechevsky E, Morita R, Liu M, Cao Y, Coquery S, Thompson-Snipes L, et al. Functional Specializations of Human Epidermal Langerhans Cells and CD14 + Dermal Dendritic Cells. Immunity 2008;29(3):497-510.

(155) Penel-Sotirakis K, Simonazzi E, Péguet-Navarro J, Rozières A. Differential Capacity of Human Skin Dendritic Cells to Polarize CD4+T Cells into IL-17, IL-21 and IL-22 Producing Cells. PLoS One 2012 Nov 1,;7(11):e45680.

(156) Ochoa MT, Loncaric A, Krutzik SR, Becker TC, Modlin RL. "Dermal Dendritic Cells" Comprise Two Distinct Populations: CD1 Dendritic Cells and CD209 Macrophages. Journal of Investigative Dermatology 2008 Sep;128(9):2225-2231.

(157) Matzinger P. Tolerance, Danger, and the Extended Family. Annu Rev Immunol 1994;12(1):991-1045.

(158) Gallucci S, Lolkema M, Matzinger P. Natural adjuvants: Endogenous activators of dendritic cells. Nat Med 1999;5:1249.

(159) Garg AD, Galluzzi L, Apetoh L, Baert T, Birge RB, Bravo-San Pedro JM, et al. Molecular and Translational Classifications of DAMPs in Immunogenic Cell Death. Frontiers in immunology 2015;6:588.

(160) Kroemer G, Galluzzi L, Kepp O, Zitvogel L. Immunogenic Cell Death in Cancer Therapy. Annual Review of Immunology 2013 Mar 21,;31(1):51-72.

(161) Denkert C, Loibl S, Noske A, Roller M, Müller BM, Komor M, et al. Tumor-Associated Lymphocytes As an Independent Predictor of Response to Neoadjuvant Chemotherapy in Breast Cancer. Journal of Clinical Oncology 2010 Jan 1,;28(1):105-113.

(162) Halama N, Michel S, Kloor M, Zoernig I, Benner A, Spille A, et al. Localization and Density of Immune Cells in the Invasive Margin of Human Colorectal Cancer Liver Metastases Are Prognostic for Response to Chemotherapy. Cancer research 2011 Sep 1,;71(17):5670-5677.

(163) Basu S, Binder RJ, Suto R, Anderson KM, Srivastava PK. Necrotic but not apoptotic cell death releases heat shock proteins, which deliver a partial maturation signal to dendritic cells and activate the NF-kappa B pathway. Int Immunol 2000 Nov;12(11):1539-1546.

(164) Scaffidi P, Misteli T, Bianchi ME. Release of chromatin protein HMGB1 by necrotic cells triggers inflammation. Nature 2002 Jul 11;418(6894):191-195.

(165) Ishii KJ, Suzuki K, Coban C, Takeshita F, Itoh Y, Matoba H, et al. Genomic DNA released by dying cells induces the maturation of APCs. J Immunol 2001 Sep 01;167(5):2602-2607.

(166) Preynat-Seauve O, Schuler P, Contassot E, Beermann F, Huard B, French LE. Tumor-Infiltrating Dendritic Cells Are Potent Antigen-Presenting Cells Able to Activate T Cells and Mediate Tumor Rejection. J Immunol 2006;176(1):61-67.

(167) Salio M, Cella M, Vermi W, Facchetti F, Palmowski M, Smith C, et al. Plasmacytoid dendritic cells prime IFN-γ-secreting melanoma-specific CD8 lymphocytes and are found in primary melanoma lesions. Eur J Immunol 2003;33(4):1052-1062.

(168) Fuertes MB, Kacha AK, Kline J, Woo S, Kranz DM, Murphy KM, et al. Host type I IFN signals are required for antitumor $CD8^+$ T cell responses through $CD8\alpha^+$ dendritic cells. J Exp Med 2011;208(10):2005-2016.

(169) Verdijk P, Aarntzen E, Lesterhuis WJ, Boullart AC, Kok E, van Rossum MM, et al. Limited Amounts of Dendritic Cells Migrate into the T-Cell Area of Lymph Nodes but Have High Immune Activating Potential in Melanoma Patients. Clinical Cancer Research 2009 Apr 1,;15(7):2531-2540.

(170) Lesterhuis WJ, de Vries I, Jolanda M, Schreibelt G, Lambeck AJA, Aarntzen E, Jacobs JFM, et al. Route of administration modulates the induction of dendritic cell vaccine-induced antigen-specific T cells in advanced melanoma patients. Clinical cancer research 2011;17(17):5725-5735.

(171) Anguille S, Smits EL, Lion E, van Tendeloo VF, Berneman ZN. Clinical use of dendritic cells for cancer therapy. Lancet Oncology, The 2014;15(7):e257-e267.

(172) Apel M, Brüning M, Granzin M, Essl M, Stuth J, Blaschke J, et al. Integrated Clinical Scale Manufacturing System for Cellular Products Derived by Magnetic Cell Separation, Centrifugation and Cell Culture. Chemie Ingenieur Technik 2013 Feb;85(1-2):103-110.

(173) Tel J, Aarntzen E, Baba T, Schreibelt G, Schulte BM, Benitez-Ribas D, et al. Natural Human Plasmacytoid Dendritic Cells Induce Antigen-Specific T-Cell Responses in Melanoma Patients. Cancer Res 2013;73(3):1063-1075.

(174) Bol KF, Schreibelt G, Rabold K, Wculek SK, Schwarze JK, Dzionek A, et al. The clinical application of cancer immunotherapy based on naturally circulating dendritic cells. Journal for immunotherapy of cancer 2019 Apr 18,;7(1):109.

(175) Andtbacka RHI, Kaufman HL, Collichio F, Amatruda T, Senzer N, Chesney J, et al. Talimogene Laherparepvec Improves Durable Response Rate in Patients With Advanced Melanoma. Journal of clinical oncology : official journal of the American Society of Clinical Oncology 2015 Sep 1,;33(25):2780-2788.

(176) Schreibelt G, Bol KF, Westdorp H, Wimmers F, Aarntzen E, Duiveman-de Boer T, et al. Effective Clinical Responses in Metastatic Melanoma Patients after Vaccination with Primary Myeloid Dendritic Cells. Clinical cancer research 2016;22(9):2155-2166.

(177) Brocker T, Riedinger M, Karjalainen K. Targeted expression of major histocompatibility complex (MHC) class II molecules demonstrates that dendritic cells can induce negative but not positive selection of thymocytes in vivo. Journal of Experimental Medicine 1997 Feb 1,;185(3):541-550.

(178) Kurts C, Kosaka H, Carbone FR, Miller JF, Heath WR. Class I-restricted cross-presentation of exogenous self-antigens leads to deletion of autoreactive CD8(+) T cells. The Journal of experimental medicine 1997 Jul 21,;186(2):239-245.

(179) Bruce AT, Ikeda H, Dunn GP, Old LJ, Schreiber RD. Cancer immunoediting: from immunosurveillance to tumor escape. Nature Immunology 2002 Nov;3(11):991-998.

(180) Hanahan D, Weinberg R. Hallmarks of Cancer: The Next Generation. Cell 2011;144(5):646-674.

(181) Vajdic CM, van Leeuwen MT. Cancer incidence and risk factors after solid organ transplantation. International journal of cancer 2009 Oct 15,;125(8):1747-1754.

(182) Kim R, Emi M, Tanabe K. Cancer immunoediting from immune surveillance to immune escape. Immunology 2007 May;121(1):1-14.

(183) Chee SJ, Lopez M, Mellows T, Gankande S, Moutasim KA, Harris S, et al. Evaluating the effect of immune cells on the outcome of patients with mesothelioma. Br J Cancer 2017 Oct 24;117(9):1341-1348.

(184) Yamada N, Oizumi S, Kikuchi E, Shinagawa N, Konishi-Sakakibara J, Ishimine A, et al. CD8+ tumor-infiltrating lymphocytes predict favorable prognosis in malignant pleural mesothelioma after resection. Cancer Immunol Immunother 2010 Oct;59(10):1543-1549.

(185) Linton A, Pavlakis N, O'Connell R, Soeberg M, Kao S, Clarke S, et al. Factors associated with survival in a large series of patients with malignant pleural mesothelioma in New South Wales. Br J Cancer 2014 Oct 28;111(9):1860-1869.

(186) Kao SC, Vardy J, Chatfield M, Corte P, Pavlakis N, Clarke C, et al. Validation of prognostic factors in malignant pleural mesothelioma: a retrospective analysis of data from patients seeking compensation from the New South Wales Dust Diseases Board. Clinical lung cancer 2013 Jan;14(1):70.

(187) Mottram P, Wei S, Zhang L, Conejo-Garcia JR, Zou L, Coukos G, et al. Specific recruitment of regulatory T cells in ovarian carcinoma fosters immune privilege and predicts reduced survival. Nature Medicine 2004 Sep;10(9):942-949.

(188) Ghiringhelli F, Puig PE, Roux S, Parcellier A, Schmitt E, Solary E, et al. Tumor cells convert immature myeloid dendritic cells into TGF-beta-secreting cells inducing CD4+CD25+ regulatory T cell proliferation. The Journal of experimental medicine 2005 Oct 3,;202(7):919.

(189) Ghiringhelli F, Ménard C, Terme M, Flament C, Taieb J, Chaput N, et al. CD4+CD25+ regulatory T cells inhibit natural killer cell functions in a transforming growth factor-beta-dependent manner. The Journal of experimental medicine 2005 Oct 17,;202(8):1075-1085.

(190) Chen ML, Pittet MJ, Gorelik L, Flavell RA, Weissleder R, von Boehmer H, et al. Regulatory T Cells Suppress Tumor-Specific CD8 T Cell Cytotoxicity through TGF-β Signals in vivo. Proceedings of the National Academy of Sciences of the United States of America 2005 Jan 11,;102(2):419-424.

(191) Alegre M, Fallarino F, Fioretti MC, Puccetti P, Vacca C, Orabona C, et al. Modulation of tryptophan catabolism by regulatory T cells. Nature Immunology 2003 Dec;4(12):1206-1212.

(192) Kryczek I, Wei S, Zou L, Zhu G, Mottram P, Xu H, et al. Cutting Edge: Induction of B7-H4 on APCs through IL-10: Novel Suppressive Mode for Regulatory T Cells. The Journal of Immunology 2006 Jul 1,;177(1):40.

(193) Shang B, Liu Y, Jiang S, Liu Y. Prognostic value of tumor-infiltrating FoxP3+ regulatory T cells in cancers: a systematic review and meta-analysis. Scientific reports 2015;5:15179.

(194) Yokokawa J, Cereda V, Remondo C, Gulley JL, Arlen PM, Schlom J, et al. Enhanced Functionality of CD4+CD25highFoxP3+ Regulatory T Cells in the Peripheral Blood of Patients with Prostate Cancer. Clinical Cancer Research 2008 Feb 15,;14(4):1032-1040.

(195) Sutmuller RPM, van Duivenvoorde LM, van Elsas A, Schumacher TNM, Wildenberg ME, Allison JP, et al. Synergism of Cytotoxic T Lymphocyte–Associated Antigen 4 Blockade and Depletion of $Cd25^{+}$ Regulatory T Cells in Antitumor Therapy Reveals Alternative Pathways for Suppression of Autoreactive Cytotoxic T Lymphocyte Responses. J Exp Med 2001;194(6):823-832.

(196) Ghiringhelli F, Menard C, Puig PE, Ladoire S, Roux S, Martin F, et al. Metronomic cyclophosphamide regimen selectively depletes CD4+CD25+ regulatory T cells and restores T and NK effector functions in end stage cancer patients. Cancer Immunol Immunother 2007 May;56(5):641-648.

(197) van der Most R, Currie A, Mahendran S, Prosser A, Darabi A, Robinson B, et al. Tumor eradication after cyclophosphamide depends on concurrent depletion of regulatory T cells: a role for cycling TNFR2-expressing effector-suppressor T cells in limiting effective chemotherapy. Cancer Immunol Immunother 2009 Aug;58(8):1219-1228.

(198) Ni K, O'Neill HC. The role of dendritic cells in T cell activation. Immunol Cell Biol 1997;75(3):223-230.

(199) Cornwall SMJ, Wikstrom M, Musk AW, Alvarez J, Nowak AK, Nelson DJ. Human mesothelioma induces defects in dendritic cell numbers and antigen-processing function which predict survival outcomes. OncoImmunology 2016 Feb 1,;5(2):e1082028.

(200) Almand B, Resser JR, Lindman B, Nadaf S, Clark JI, Kwon ED, et al. Clinical Significance of Defective Dendritic Cell Differentiation in Cancer. Clinical Cancer Research 2000 May 1,;6(5):1755.

(201) Saito H, Tsujitani S, Ikeguchi M, Maeta M, Kaibara N. Relationship between the expression of vascular endothelial growth factor and the density of dendritic cells in gastric adenocarcinoma tissue. British Journal of Cancer 1998 Dec;78(12):1573-1577.

(202) Lissoni P, Malugani F, Bonfanti A, Bucovec R, Secondino S, Brivio F, et al. Abnormally enhanced blood concentrations of vascular endothelial growth factor (VEGF) in metastatic cancer patients and their relation to circulating dendritic cells, IL-12 and endothelin-1. Journal of biological regulators and homeostatic agents 2001 Apr;15(2):140.

(203) Gabrilovich D, Ishida T, Oyama T, Ran S, Kravtsov V, Nadaf S, et al. Vascular endothelial growth factor inhibits the development of dendritic cells and dramatically affects the differentiation of multiple hematopoietic lineages in vivo. Blood 1998 Dec 1;92(11):4150-4166.

(204) Park S, Nakagawa T, Kitamura H, Atsumi T, Kamon H, Sawa S, et al. IL-6 Regulates In Vivo Dendritic Cell Differentiation through STAT3 Activation. The Journal of Immunology 2004 Sep 15,;173(6):3844-3854.

(205) Mach N, Gillessen S, Wilson SB, Sheehan C, Mihm M, Dranoff G. Differences in Dendritic Cells Stimulated in Vivo by Tumors Engineered to Secrete Granulocyte-Macrophage Colony-stimulating Factor or Flt3-Ligand. Cancer Research 2000 Jun 1,;60(12):3239.

(206) Leong SP, Enders-Zohr P, Zhou YM, Stuntebeck S, Habib FA, Allen J, R E, et al. Recombinant human granulocyte macrophage-colony stimulating factor (rhGM-CSF) and autologous melanoma vaccine mediate tumor regression in patients with metastatic melanoma. Journal of immunotherapy (Hagerstown, Md. : 1997) 1999 Mar;22(2):166-174.

(207) Lechner MG, Liebertz DJ, Epstein AL. Characterization of cytokine-induced myeloid-derived suppressor cells from normal human peripheral blood mononuclear cells. Journal of immunology (Baltimore, Md. : 1950) 2010 Aug 15,;185(4):2273.

(208) Serafini P, Carbley R, Noonan KA, Tan G, Bronte V, Borrello I. High-dose granulocyte-macrophage colony-stimulating factor-producing vaccines impair the immune response through the recruitment of myeloid suppressor cells. Cancer Res 2004 Sep 1;64(17):6337-6343.

(209) Marrogi A, Pass HI, Khan M, Metheny-Barlow LJ, Harris CC, Gerwin BI. Human Mesothelioma Samples Overexpress Both Cyclooxygenase-2 (COX-2) and Inducible Nitric Oxide Synthase (NOS2): In Vitro Antiproliferative Effects of a COX-2 Inhibitor. Cancer Research 2000 Jul 1,;60(14):3696-3700.

(210) O'Kane SL, Cawkwell L, Campbell A, Lind MJ. Cyclooxygenase-2 expression predicts survival in malignant pleural mesothelioma. European Journal of Cancer 2005;41(11):1645-1648.

(211) Wolff H, Saukkonen K, Anttila S, Karjalainen A, Vainio H, Ristimaki A. Expression of Cyclooxygenase-2 in Human Lung Carcinoma. Cancer Research 1998 Nov 15,;58(22):4997-5001.

(212) Obermajer N, Muthuswamy R, Lesnock J, Edwards RP, Kalinski P. Positive feedback between PGE2 and COX2 redirects the differentiation of human dendritic cells toward stable myeloid-derived suppressor cells. Blood 2011 Nov 17;118(20):5498-5505.

(213) Berggren R, Mottram P, Wei S, Zimmermann MC, Dong H, Daniel B, et al. Blockade of B7-H1 improves myeloid dendritic cell-mediated antitumor immunity. Nature Medicine 2003 May;9(5):562-567.

(214) Krempski J, Karyampudi L, Behrens MD, Erskine CL, Hartmann L, Dong H, et al. Tumor-Infiltrating Programmed Death Receptor-1+ Dendritic Cells Mediate Immune Suppression in Ovarian Cancer. Journal of Immunology 2011 Jun 15,;186(12):6905-6913.

(215) Sica GL, Choi I, Zhu G, Tamada K, Wang S, Tamura H, et al. B7-H4, a Molecule of the B7 Family, Negatively Regulates T Cell Immunity. Immunity 2003;18(6):849-861.

(216) Munn DH, Shafizadeh E, Attwood JT, Bondarev I, Pashine A, Mellor AL. Inhibition of T cell proliferation by macrophage tryptophan catabolism. The Journal of experimental medicine 1999 May 3,;189(9):1363-1372.

(217) Calcinaro F, Candeloro P, Fallarino F, Puccetti P, Vacca C, Orabona C, et al. CTLA-4-Ig regulates tryptophan catabolism in vivo. Nature Immunology 2002 Nov;3(11):1097-1101.

(218) Munn DH, Sharma MD, Lee JR, Jhaver KG, Johnson TS, Keskin DB, et al. Potential Regulatory Function of Human Dendritic Cells Expressing Indoleamine 2,3-Dioxygenase. Science 2002;297(5588):1867-1870.

(219) Choe N, Tanaka S, Xia W, Hemenway DR, Roggli VL, Kagan E. Pleural Macrophage Recruitment and Activation in Asbestos-Induced Pleural Injury. Environmental Health Perspectives 1997 Sep 1,;105(Suppl 5):1257-1260.

(220) Negus RP, Stamp GW, Relf MG, Burke F, Malik ST, Bernasconi S, et al. The detection and localization of monocyte chemoattractant protein-1 (MCP-1) in human ovarian cancer. J Clin Invest 1995;95(5):2391-2396.

(221) Saji H, Koike M, Yamori T, Saji S, Seiki M, Matsushima K, et al. Significant correlation of monocyte chemoattractant protein-1 expression with neovascularization and progression of breast carcinoma. Cancer 2001 Sep 1,;92(5):1085-1091.

(222) Fox SA, Loh SS, Mahendran SK, Garlepp MJ. Regulated chemokine gene expression in mouse mesothelioma and mesothelial cells: TNF-α upregulates both CC and CXC chemokine genes. Oncology Reports 2012 Aug;28(2):707-713.

(223) Dalton DK, Pitts-Meek S, Keshav S, Figari IS, Bradley A, Stewart TA. Multiple defects of immune cell function in mice with disrupted interferon-gamma genes. Science 1993 Mar 19,;259(5102):1739-1742.

(224) Xing Z, Zganiacz A, Santosuosso M. Role of IL-12 in macrophage activation during intracellular infection: IL-12 and mycobacteria synergistically release TNF-α and nitric oxide from macrophages via IFN-γ induction. Journal of Leukocyte Biology 2000 Dec 1,;68(6):897-902.

(225) Mantovani A, Sozzani S, Locati M, Allavena P, Sica A. Macrophage polarization: tumor-associated macrophages as a paradigm for polarized M2 mononuclear phagocytes. Trends in Immunology 2002;23(11):549-555.

(226) Biswas SK, Gangi L, Paul S, Schioppa T, Saccani A, Sironi M, et al. A distinct and unique transcriptional program expressed by tumor-associated macrophages (defective NF-kappaB and enhanced IRF-3/STAT1 activation). Blood 2006 Mar 1,;107(5):2112-2122.

(227) Talks KL, Turley H, Gatter KC, Maxwell PH, Pugh CW, Ratcliffe PJ, et al. The Expression and Distribution of the Hypoxia-Inducible Factors HIF-1α and HIF-2α in Normal Human Tissues, Cancers, and Tumor-Associated Macrophages. The American Journal of Pathology 2000;157(2):411-421.

(228) Lewis JS, Landers RJ, Underwood JCE, Harris AL, Lewis CE. Expression of vascular endothelial growth factor by macrophages is up-regulated in poorly vascularized areas of breast carcinomas. The Journal of Pathology 2000 Oct;192(2):150-158.

(229) Crowther M, Brown NJ, Bishop ET, Lewis CD. Microenvironmental influence on macrophage regulation of angiogenesis in wounds and malignant tumors. Journal of Leukocyte Biology 2001 Oct 1,;70(4):478-490.

(230) Lee CG, Homer RJ, Zhu Z, Lanone S, Wang X, Koteliansky V, et al. Interleukin-13 induces tissue fibrosis by selectively stimulating and activating transforming growth factor beta(1). The Journal of experimental medicine 2001 Sep 17,;194(6):809.

(231) Teramukai S, Kitano T, Kishida Y, Kawahara M, Kubota K, Komuta K, et al. Pretreatment neutrophil count as an independent prognostic factor in advanced non-small-cell lung cancer: An analysis of Japan Multinational Trial Organisation LC00-03. European Journal of Cancer 2009;45(11):1950-1958.

(232) Schmidt H, Suciu S, Punt CJ, Gore M, Kruit W, Patel P, et al. Pretreatment Levels of Peripheral Neutrophils and Leukocytes As Independent Predictors of Overall Survival in Patients With American Joint Committee on Cancer Stage IV Melanoma: Results of the EORTC 18951 Biochemotherapy Trial. Journal of Clinical Oncology 2007 Apr 20,;25(12):1562-1569.

(233) Trellakis S, Bruderek K, Dumitru CA, Gholaman H, Gu X, Bankfalvi A, et al. Polymorphonuclear granulocytes in human head and neck cancer: Enhanced inflammatory activity, modulation by cancer cells and expansion in advanced disease. International Journal of Cancer 2011 Nov 1,;129(9):2183-2193.

(234) De Santo C, Arscott R, Booth S, Karydis I, Jones M, Asher R, et al. Invariant NKT cells modulate the suppressive activity of IL-10-secreting neutrophils differentiated with serum amyloid A. Nature Immunology 2010;11:1039.

(235) Choi J, Suh B, Ahn Y, Kim T, Lee J, Lee S, et al. CD15+/CD16low human granulocytes from terminal cancer patients: granulocytic myeloid-derived suppressor cells that have suppressive function. Tumor Biol 2012 Feb;33(1):121-129.

(236) Nozawa H, Chiu C, Hanahan D. Infiltrating Neutrophils Mediate the Initial Angiogenic Switch in a Mouse Model of Multistage Carcinogenesis. Proceedings of the National Academy of Sciences of the United States of America 2006 Aug 15,;103(33):12493-12498.

(237) Trellakis S, Farjah H, Bruderek K, Dumitru CA, Hoffmann TK, Lang S, et al. Peripheral Blood Neutrophil Granulocytes from Patients with Head and Neck Squamous Cell Carcinoma Functionally Differ from Their Counterparts in Healthy Donors. International Journal of Immunopathology and Pharmacology 2011 Jul;24(3):683-693.

(238) Pillay J, Kamp VM, Hoffen EV, Visser T, Tak T, Lammers JW, et al. A subset of neutrophils in human systemic inflammation inhibits T cell responses through Mac-1. Journal of Clinical Investigation 2012;122(1):327-336.

(239) Schmielau J, Finn OJ. Activated granulocytes and granulocyte-derived hydrogen peroxide are the underlying mechanism of suppression of t-cell function in advanced cancer patients. Cancer Res 2001 Jun 15;61(12):4756-4760.

(240) Kusmartsev S, Nefedova Y, Yoder D, Gabrilovich DI. Antigen-Specific Inhibition of CD8+ T Cell Response by Immature Myeloid Cells in Cancer Is Mediated by Reactive Oxygen Species. The Journal of Immunology 2004 Jan 15,;172(2):989.

(241) Ando T, Mimura K, Johansson CC, Hanson MG, Mougiakakos D, Larsson C, et al. Transduction with the Antioxidant Enzyme Catalase Protects Human T Cells against Oxidative Stress. The Journal of Immunology 2008 Dec 15,;181(12):8382-8390.

(242) Shen L, Smith JM, Shen Z, Eriksson M, Sentman C, Wira CR. Inhibition of human neutrophil degranulation by transforming growth factor-β1. Clinical & Experimental Immunology 2007;149(1):155-161.

(243) Fridlender ZG, Sun J, Kim S, Kapoor V, Cheng G, Ling L, et al. Polarization of Tumor-Associated Neutrophil Phenotype by TGF-beta: N1 versus N2 TAN. Cancer Cell 2009 Sept 08,;16(3):183-194.

(244) Rodriguez PC, Ernstoff MS, Hernandez C, Atkins M, Zabaleta J, Sierra R, et al. Arginase I–Producing Myeloid-Derived Suppressor Cells in Renal Cell Carcinoma Are a Subpopulation of Activated Granulocytes. Cancer Res 2009;69(4):1553-1560.

(245) Mishalian I, Bayuh R, Levy L, Zolotarov L, Michaeli J, Fridlender Z. Tumor-associated neutrophils (TAN) develop pro-tumorigenic properties during tumor progression. Cancer Immunol Immunother 2013 Nov;62(11):1745-1756.

(246) Jablonska E, Puzewska W, Grabowska Z, Jablonski J, Talarek L. VEGF, IL-18 and NO production by neutrophils and their serum levels in patients with oral cavity cancer. Cytokine 2005;30(3):93-99.

(247) Young MR, Newby M, Wepsic HT. Hematopoiesis and suppressor bone marrow cells in mice bearing large metastatic Lewis lung carcinoma tumors. Cancer Res 1987 Jan 1;47(1):100-105.

(248) Almand B, Clark JI, Nikitina E, van Beynen J, English NR, Knight SC, et al. Increased production of immature myeloid cells in cancer patients: a mechanism of immunosuppression in cancer. J Immunol 2001 Jan 1;166(1):678-689.

(249) Gabrilovich DI, Velders MP, Sotomayor EM, Kast WM. Mechanism of Immune Dysfunction in Cancer Mediated by Immature Gr-1+ Myeloid Cells. The Journal of Immunology 2001 May 1,;166(9):5398-5406.

(250) Bronte V, Brandau S, Chen S, Colombo MP, Frey AB, Greten TF, et al. Recommendations for myeloid-derived suppressor cell nomenclature and characterization standards. Nature Communications 2016;7:12150.

(251) Bronte V, Apolloni E, Cabrelle A, Ronca R, Serafini P, Zamboni P, et al. Identification of a CD11b(+)/Gr-1(+)/CD31(+) myeloid progenitor capable of activating or suppressing CD8(+) T cells. Blood 2000 Dec 1;96(12):3838-3846.

(252) Hestdal K, Ruscetti FW, Ihle JN, Jacobsen SE, Dubois CM, Kopp WC, et al. Characterization and regulation of RB6-8C5 antigen expression on murine bone marrow cells. The Journal of Immunology 1991 Jul 1,;147(1):22-28.

(253) Fleming TJ, Fleming ML, Malek TR. Selective expression of Ly-6G on myeloid lineage cells in mouse bone marrow. RB6-8C5 mAb to granulocyte-differentiation antigen (Gr-1) detects members of the Ly-6 family. The Journal of Immunology 1993 Sep 1,;151(5):2399-2408.

(254) Zhu B, Bando Y, Xiao S, Yang K, Anderson AC, Kuchroo VK, et al. CD11b+Ly-6C(hi) suppressive monocytes in experimental autoimmune encephalomyelitis. Journal of immunology (Baltimore, Md. : 1950) 2007 Oct 15,;179(8):5228.

(255) Schwartz RH. Costimulation of T lymphocytes: the role of CD28, CTLA-4, and B7/BB1 in interleukin-2 production and immunotherapy. Cell 1992 Dec 24;71(7):1065-1068.

(256) Lindstein T, June CH, Ledbetter JA, Stella G, Thompson CB. Regulation of lymphokine messenger RNA stability by a surface-mediated T cell activation pathway. Science 1989 Apr 21;244(4902):339-343.

(257) Turka LA, Ledbetter JA, Lee K, June CH, Thompson CB. CD28 is an inducible T cell surface antigen that transduces a proliferative signal in CD3+ mature thymocytes. J Immunol 1990 Mar 01;144(5):1646-1653.

(258) Linsley PS, Bradshaw J, Urnes M, Grosmaire L, Ledbetter JA. CD28 engagement by B7/BB-1 induces transient down-regulation of CD28 synthesis and prolonged unresponsiveness to CD28 signaling. J Immunol 1993 Apr 15;150(8 Pt 1):3161-3169.

(259) Linsley PS, Greene JL, Tan P, Bradshaw J, Ledbetter JA, Anasetti C, et al. Coexpression and functional cooperation of CTLA-4 and CD28 on activated T lymphocytes. J Exp Med 1992 Dec 01;176(6):1595-1604.

(260) Tivol EA, Boyd SD, McKeon S, Borriello F, Nickerson P, Strom TB, et al. CTLA4Ig prevents lymphoproliferation and fatal multiorgan tissue destruction in CTLA-4-deficient mice. J Immunol 1997 Jun 01;158(11):5091-5094.

(261) Takahashi T, Tagami T, Yamazaki S, Uede T, Shimizu J, Sakaguchi N, et al. Immunologic self-tolerance maintained by CD25(+)CD4(+) regulatory T cells constitutively expressing cytotoxic T lymphocyte-associated antigen 4. J Exp Med 2000 Jul 17;192(2):303-310.

(262) Nishimura H, Nose M, Hiai H, Minato N, Honjo T. Development of lupus-like autoimmune diseases by disruption of the PD-1 gene encoding an ITIM motif-carrying immunoreceptor. Immunity 1999 Aug;11(2):141-151.

(263) Nishimura H, Okazaki T, Tanaka Y, Nakatani K, Hara M, Matsumori A, et al. Autoimmune dilated cardiomyopathy in PD-1 receptor-deficient mice. Science 2001 Jan 12;291(5502):319-322.

(264) Vibhakar R, Juan G, Traganos F, Darzynkiewicz Z, Finger LR. Activation-induced expression of human programmed death-1 gene in T-lymphocytes. Exp Cell Res 1997 Apr 10;232(1):25-28.

(265) Agata Y, Kawasaki A, Nishimura H, Ishida Y, Tsubata T, Yagita H, et al. Expression of the PD-1 antigen on the surface of stimulated mouse T and B lymphocytes. Int Immunol 1996 May;8(5):765-772.

(266) Freeman GJ, Long AJ, Iwai Y, Bourque K, Chernova T, Nishimura H, et al. Engagement of the PD-1 immunoinhibitory receptor by a novel B7 family member leads to negative regulation of lymphocyte activation. J Exp Med 2000 Oct 02;192(7):1027-1034.

(267) Carter L, Fouser LA, Jussif J, Fitz L, Deng B, Wood CR, et al. PD-1:PD-L inhibitory pathway affects both CD4(+) and CD8(+) T cells and is overcome by IL-2. European journal of immunology 2002 Mar;32(3):634.

(268) Tamada K, Zhu G, Dong H, Chen L. B7-H1, a third member of the B7 family, co-stimulates T-cell proliferation and interleukin-10 secretion. Nature Medicine 1999 Dec;5(12):1365-1369.

(269) Riley JL. PD-1 signaling in primary T cells. Immunol Rev 2009 May;229(1):114-125.

(270) Alvarez X, David O, Cheng P, Dhurandhar N, Curiel DT, Zimmermann MC, et al. Blockade of B7-H1 improves myeloid dendritic cell-mediated antitumor immunity. Nature Medicine 2003 May;9(5):562-567.

(271) Yamazaki T, Akiba H, Iwai H, Matsuda H, Aoki M, Tanno Y, et al. Expression of programmed death 1 ligands by murine T cells and APC. J Immunol 2002 Nov 15;169(10):5538-5545.

(272) Ishida M, Iwai Y, Tanaka Y, Okazaki T, Freeman GJ, Minato N, et al. Differential expression of PD-L1 and PD-L2, ligands for an inhibitory receptor PD-1, in the cells of lymphohematopoietic tissues. Immunology Letters 2002;84(1):57-62.

(273) Stanciu LA, Bellettato CM, Laza-Stanca V, Coyle AJ, Papi A, Johnston SL. Expression of Programmed Death–1 Ligand (PD-L) 1, PD-L2, B7-H3, and Inducible Costimulator Ligand on Human Respiratory Tract Epithelial Cells and Regulation by Respiratory Syncytial Virus and Type 1 and 2 Cytokines. The Journal of Infectious Diseases 2006;193(3):404-412.

(274) Pinchuk IV, Saada JI, Beswick EJ, Boya G, Qiu SM, Mifflin RC, et al. PD-1 ligand expression by human colonic myofibroblasts/fibroblasts regulates CD4+ T-cell activity. Gastroenterology 2008;135(4):1228-1237.e12372.

(275) Nazareth MR, Broderick L, Simpson-Abelson MR, Kelleher RJ, Yokota SJ, Bankert RB. Characterization of Human Lung Tumor-Associated Fibroblasts and Their Ability to Modulate the Activation of Tumor-Associated T Cells. J Immunol 2007;178(9):5552-5562.

(276) Huard B, Prigent P, Tournier M, Bruniquel D, Triebel F. CD4/major histocompatibility complex class II interaction analyzed with CD4- and lymphocyte activation gene-3 (LAG-3)-Ig fusion proteins. Eur J Immunol 1995 Sep;25(9):2718-2721.

(277) Workman CJ, Cauley LS, Kim I, Blackman MA, Woodland DL, Vignali DAA. Lymphocyte activation gene-3 (CD223) regulates the size of the expanding T cell population following antigen activation in vivo. J Immunol 2004 May 01;172(9):5450-5455.

(278) Workman CJ, Vignali DAA. Negative regulation of T cell homeostasis by lymphocyte activation gene-3 (CD223). J Immunol 2005 Jan 15;174(2):688-695.

(279) Monney L, Sabatos CA, Gaglia JL, Ryu A, Waldner H, Chernova T, et al. Th1-specific cell surface protein Tim-3 regulates macrophage activation and severity of an autoimmune disease. Nature 2002 Jan 31;415(6871):536-541.

(280) Sanchez-Fueyo A, Tian J, Picarella D, Domenig C, Zheng XX, Sabatos CA, et al. Tim-3 inhibits T helper type 1-mediated auto- and alloimmune responses and promotes immunological tolerance. Nat Immunol 2003 Nov;4(11):1093-1101.

(281) Sabatos CA, Chakravarti S, Cha E, Schubart A, Sanchez-Fueyo A, Zheng XX, et al. Interaction of Tim-3 and Tim-3 ligand regulates T helper type 1 responses and induction of peripheral tolerance. Nat Immunol 2003 Nov;4(11):1102-1110.

(282) Zhu C, Anderson AC, Schubart A, Xiong H, Imitola J, Khoury SJ, et al. The Tim-3 ligand galectin-9 negatively regulates T helper type 1 immunity. Nat Immunol 2005 Dec;6(12):1245-1252.

(283) Chiba S, Baghdadi M, Akiba H, Yoshiyama H, Kinoshita I, Dosaka-Akita H, et al. Tumor-infiltrating DCs suppress nucleic acid-mediated innate immune responses through interactions between the receptor TIM-3 and the alarmin HMGB1. Nat Immunol 2012 Sep;13(9):832-842.

(284) Joller N, Hafler JP, Brynedal B, Kassam N, Spoerl S, Levin SD, et al. Cutting edge: TIGIT has T cell-intrinsic inhibitory functions. J Immunol 2011 Feb 01;186(3):1338-1342.

(285) Joller N, Lozano E, Burkett PR, Patel B, Xiao S, Zhu C, et al. Treg cells expressing the coinhibitory molecule TIGIT selectively inhibit proinflammatory Th1 and Th17 cell responses. Immunity 2014 Apr 17;40(4):569-581.

(286) Yu X, Harden K, Gonzalez LC, Francesco M, Chiang E, Irving B, et al. The surface protein TIGIT suppresses T cell activation by promoting the generation of mature immunoregulatory dendritic cells. Nat Immunol 2009 Jan;10(1):48-57.

(287) Pardoll DM. The blockade of immune checkpoints in cancer immunotherapy. Nature Reviews: Cancer 2012 Mar 1,;12(4):252-264.

(288) Konishi J, Yamazaki K, Azuma M, Kinoshita I, Dosaka-Akita H, Nishimura M. B7-H1 expression on non-small cell lung cancer cells and its relationship with tumor-infiltrating lymphocytes and their PD-1 expression. Clin Cancer Res 2004 Aug 01;10(15):5094-5100.

(289) Daud AI, Wolchok JD, Robert C, Hwu W, Weber JS, Ribas A, et al. Programmed Death-Ligand 1 Expression and Response to the Anti-Programmed Death 1 Antibody Pembrolizumab in Melanoma. Journal of clinical oncology : official journal of the American Society of Clinical Oncology 2016;34(34):4102-4109.

(290) Nakanishi J, Wada Y, Matsumoto K, Azuma M, Kikuchi K, Ueda S. Overexpression of B7-H1 (PD-L1) significantly associates with tumor grade and postoperative prognosis in human urothelial cancers. Cancer Immunol Immunother 2007 Aug;56(8):1173-1182.

(291) Seo AN, Kang BW, Kwon OK, Park KB, Lee SS, Chung HY, et al. Intratumoural PD-L1 expression is associated with worse survival of patients with Epstein-Barr virus-associated gastric cancer. Br J Cancer 2017 Dec 05;117(12):1753-1760.

(292) Lee S, Lee S, Jang B, Yang Y, Suh S, Park Y, et al. Interferon regulatory factor-1 is prerequisite to the constitutive expression and IFN-γ-induced upregulation of B7-H1 (CD274). FEBS Letters 2006;580(3):755-762.

(293) Zhang Q, Raghunath PN, Xue L, Majewski M, Carpentieri DF, Odum N, et al. Multilevel Dysregulation of STAT3 Activation in Anaplastic Lymphoma Kinase-Positive T/Null-Cell Lymphoma. J Immunol 2002;168(1):466-474.

(294) Marzec M, Zhang Q, Goradia A, Raghunath PN, Liu X, Paessler M, et al. Oncogenic Kinase NPM/ALK Induces through STAT3 Expression of Immunosuppressive Protein CD274 (PD-L1, B7-H1). Proceedings of the National Academy of Sciences of the United States of America 2008 Dec 30,;105(52):20852-20857.

(295) Yamamoto R, Nishikori M, Tashima M, Sakai T, Ichinohe T, Takaori-Kondo A, et al. B7-H1 expression is regulated by MEK-ERK signaling pathway in anaplastic large cell lymphoma and Hodgkin lymphoma. Cancer Science 2009 Nov 1,;100(11):2093-2100.

(296) Parsa AT, Waldron JS, Panner A, Crane CA, Parney IF, Barry JJ, et al. Loss of tumor suppressor PTEN function increases B7-H1 expression and immunoresistance in glioma. Nature Medicine 2006;13:84.

(297) Lastwika KJ, Wilson W, Li QK, Norris J, Xu H, Ghazarian SR, et al. Control of PD-L1 Expression by Oncogenic Activation of the AKT–mTOR Pathway in Non–Small Cell Lung Cancer. Cancer Res 2016;76(2):227-238.

(298) Wu C, Zhu Y, Jiang J, Zhao J, Zhang X, Xu N. Immunohistochemical localization of programmed death-1 ligand-1 (PD-L1) in gastric carcinoma and its clinical significance. Acta Histochem 2006;108(1):19-24.

(299) Polonia A, Pinto R, Cameselle-Teijeiro JF, Schmitt FC, Paredes J. Prognostic value of stromal tumour infiltrating lymphocytes and programmed cell death-ligand 1 expression in breast cancer. J Clin Pathol 2017 Oct;70(10):860-867.

(300) Ritprajak P, Azuma M. Intrinsic and extrinsic control of expression of the immunoregulatory molecule PD-L1 in epithelial cells and squamous cell carcinoma. Oral Oncology 2015;51(3):221-228.

(301) Herbst RS, Baas P, Kim D, Felip E, Perez-Gracia JL, Han J, et al. Pembrolizumab versus docetaxel for previously treated, PD-L1-positive, advanced non-small-cell lung cancer (KEYNOTE-010): a randomised controlled trial. Lancet 2016 Apr 09;387(10027):1540-1550.

(302) Horn L, Spigel DR, Vokes EE, Holgado E, Ready N, Steins M, et al. Nivolumab Versus Docetaxel in Previously Treated Patients With Advanced Non-Small-Cell Lung Cancer: Two-Year Outcomes From Two Randomized, Open-Label, Phase III Trials (CheckMate 017 and CheckMate 057). J Clin Oncol 2017 Dec 10;35(35):3924-3933.

(303) Gandhi L, Rodríguez-Abreu D, Gadgeel S, Esteban E, Felip E, De Angelis F, et al. Pembrolizumab plus Chemotherapy in Metastatic Non–Small-Cell Lung Cancer. N Engl J Med 2018;378(22):2078-2092.

(304) Radzikowska E, Glaz P, Roszkowski K. Lung cancer in women: age, smoking, histology, performance status, stage, initial treatment and survival. Population-based study of 20 561 cases. Ann Oncol 2002 Jul;13(7):1087-1093.

(305) Lilenbaum R, Axelrod R, Thomas S, Dowlati A, Seigel L, Albert D, et al. Randomized phase II trial of erlotinib or standard chemotherapy in patients with advanced non-small-cell lung cancer and a performance status of 2. J Clin Oncol 2008 Feb 20;26(6):863-869.

(306) Zukin M, Barrios CH, Pereira JR, Ribeiro RDA, Beato, Carlos Augusto de Mendonca, do Nascimento YN, et al. Randomized phase III trial of single-agent pemetrexed versus carboplatin and pemetrexed in patients with advanced non-small-cell lung cancer and Eastern Cooperative Oncology Group performance status of 2. J Clin Oncol 2013 Aug 10;31(23):2849-2853.

(307) Pao W, Hutchinson KE. Chipping away at the lung cancer genome. Nat Med 2012 Mar 06;18(3):349-351.

(308) Oxnard GR, Binder A, Janne PA. New targetable oncogenes in non-small-cell lung cancer. J Clin Oncol 2013 Mar 10;31(8):1097-1104.

(309) Oxnard GR, Binder B, Jänne PA. New Targetable Oncogenes in Non–Small-Cell Lung Cancer. Journal of Clinical Oncology 2013 Mar 10,;31(8):1097-1104.

(310) Topalian SL, Hodi FS, Brahmer JR, Gettinger SN, Smith DC, McDermott DF, et al. Safety, activity, and immune correlates of anti-PD-1 antibody in cancer. N Engl J Med 2012 Jun 28;366(26):2443-2454.

(311) Gettinger S, Rizvi NA, Chow LQ, Borghaei H, Brahmer J, Ready N, et al. Nivolumab Monotherapy for First-Line Treatment of Advanced Non-Small-Cell Lung Cancer. J Clin Oncol 2016 09 01;34(25):2980-2987.

(312) Hodi FS, Chesney J, Pavlick AC, Robert C, Grossmann KF, McDermott DF, et al. Combined nivolumab and ipilimumab versus ipilimumab alone in patients with advanced melanoma: 2-year overall survival outcomes in a multicentre, randomised, controlled, phase 2 trial. Lancet Oncol 2016 Nov;17(11):1558-1568.

(313) Herbst RS, Soria J, Kowanetz M, Fine GD, Hamid O, Gordon MS, et al. Predictive correlates of response to the anti-PD-L1 antibody MPDL3280A in cancer patients. Nature 2014 Nov 27;515(7528):563-567.

(314) Balar AV, Castellano D, O'Donnell PH, Grivas P, Vuky J, Powles T, et al. First-line pembrolizumab in cisplatin-ineligible patients with locally advanced and unresectable or metastatic urothelial cancer (KEYNOTE-052): a multicentre, single-arm, phase 2 study. The Lancet Oncology 2017;18(11):1483-1492.

(315) Bellmunt J, de Wit R, Vaughn DJ, Fradet Y, Lee J, Fong L, et al. Pembrolizumab as Second-Line Therapy for Advanced Urothelial Carcinoma. N Engl J Med 2017;376(11):1015-1026.

(316) Shitara K, Ozguroglu M, Bang Y, Di Bartolomeo M, Mandala M, Ryu M, et al. Pembrolizumab versus paclitaxel for previously treated, advanced gastric or gastro-oesophageal junction cancer (KEYNOTE-061): a randomised, open-label, controlled, phase 3 trial. Lancet 2018 07 14;392(10142):123-133.

(317) Martens A, Wistuba-Hamprecht K, Geukes Foppen M, Yuan J, Postow MA, Wong P, et al. Baseline Peripheral Blood Biomarkers Associated with Clinical Outcome of Advanced Melanoma Patients Treated with Ipilimumab. Clin Cancer Res 2016 06 15;22(12):2908-2918.

(318) Martens A, Wistuba-Hamprecht K, Yuan J, Postow MA, Wong P, Capone M, et al. Increases in Absolute Lymphocytes and Circulating CD4+ and CD8+ T Cells Are Associated with Positive Clinical Outcome of Melanoma Patients Treated with Ipilimumab. Clin Cancer Res 2016 Oct 01;22(19):4848-4858.

(319) Mussai F, De Santo C, Abu-Dayyeh I, Booth S, Quek L, McEwen-Smith RM, et al. Acute myeloid leukemia creates an arginase-dependent immunosuppressive microenvironment. Blood 2013 Aug 1,;122(5):749-758.

(320) Milano MT, Zhang H. Malignant pleural mesothelioma: a population-based study of survival. J Thorac Oncol 2010 Nov;5(11):1841-1848.

(321) Health and Safety Executive. Mesothelioma in Great Britain 2016. Mesothelioma mortality in Great Britain 1968-2014. 2017; Available at: www.hse.gov.uk/statistics/causdis/mesothelioma. Accessed January, 2018.

(322) Sequist LV, Yang JC, Yamamoto N, O'Byrne K, Hirsh V, Mok T, et al. Phase III study of afatinib or cisplatin plus pemetrexed in patients with metastatic lung adenocarcinoma with EGFR mutations. J Clin Oncol 2013 Sep 20;31(27):3327-3334.

(323) Rosell R, Carcereny E, Gervais R, Vergnenegre A, Massuti B, Felip E, et al. Erlotinib versus standard chemotherapy as first-line treatment for European patients with advanced EGFR mutation-positive non-small-cell lung cancer (EURTAC): a multicentre, open-label, randomised phase 3 trial. Lancet Oncol 2012 Mar;13(3):239-246.

(324) Chapman PB, Hauschild A, Robert C, Haanen JB, Ascierto P, Larkin J, et al. Improved survival with vemurafenib in melanoma with BRAF V600E mutation. N Engl J Med 2011 Jun 30;364(26):2507-2516.

(325) Calabro L, Morra A, Fonsatti E, Cutaia O, Fazio C, Annesi D, et al. Efficacy and safety of an intensified schedule of tremelimumab for chemotherapy-resistant malignant mesothelioma: an open-label, single-arm, phase 2 study. Lancet Respir Med 2015 Apr;3(4):301-309.

(326) Hassan R, Thomas A, Patel M, Nemunaitis J, Bennouna J, Powderly J. Avelumab (MSB0010718C; anti-PD-L1) in patients with advanced unresectable mesothelioma from the JAVELIN solid tumor phase Ib trial: safety, clinical activity, and PD-L1 expression. . J Clin Oncol 2016;34((suppl; abstr 8503)).

(327) Adusumilli PS, Cherkassky L, Villena-Vargas J, Colovos C, Servais E, Plotkin J, et al. Regional delivery of mesothelin-targeted CAR T cell therapy generates potent and long-lasting CD4-dependent tumor immunity. Sci Transl Med 2014 Nov 05;6(261):261ra151.

(328) Schuberth PC, Hagedorn C, Jensen SM, Gulati P, van den Broek M, Mischo A, et al. Treatment of malignant pleural mesothelioma by fibroblast activation protein-specific re-directed T cells. J transl med 2013 Aug 12;11:187.

(329) Klampatsa A, Achkova DY, Davies DM, Parente-Pereira AC, Woodman N, Rosekilly J, et al. Intracavitary 'T4 immunotherapy' of malignant mesothelioma using pan-ErbB re-targeted CAR T-cells. Cancer Lett 2017 May 01;393:52-59.

(330) Zauderer MG, Tsao AS, Dao T, Panageas K, Lai WV, Rimner A, et al. A Randomized Phase II Trial of Adjuvant Galinpepimut-S, WT-1 Analogue Peptide Vaccine, After Multimodality Therapy for Patients with Malignant Pleural Mesothelioma. Clinical Cancer Research : An Official Journal of the American Association for Cancer Research 2017 Dec 15,;23(24):7483-7489.

(331) Tan Z, Zhou J, Cheung AKL, Yu Z, Cheung K, Liang J, et al. Vaccine-elicited CD8+ T cells cure mesothelioma by overcoming tumor-induced immunosuppressive environment. Cancer Res 2014 Nov 01;74(21):6010-6021.

(332) Kao SCH, Pavlakis N, Harvie R, Vardy JL, Boyer MJ, van Zandwijk N, et al. High blood neutrophil-to-lymphocyte ratio is an indicator of poor prognosis in malignant mesothelioma patients undergoing systemic therapy. Clin Cancer Res 2010 Dec 01;16(23):5805-5813.

(333) Veltman J, Lambers M, Nimwegen M, Heniks R, Hoogsteden H, Hegmans J, et al. Zoledronic acid impairs myeloid differentiation to tumour-associated macrophages in mesothelioma. British Journal of Cancer 2010 Aug 1,;103(5):629-641.

(334) Chene A, d'Almeida S, Blondy T, Tabiasco J, Deshayes S, Fonteneau J, et al. Pleural Effusions from Patients with Mesothelioma Induce Recruitment of Monocytes and Their Differentiation into M2 Macrophages. J Thorac Oncol 2016 Oct;11(10):1765-1773.

(335) Shaul ME, Levy L, Sun J, Mishalian I, Singhal S, Kapoor V, et al. Tumor-associated neutrophils display a distinct N1 profile following TGFβ modulation: A transcriptomics analysis of pro- vs. antitumor TANs. OncoImmunology 2016 Nov 1,;5(11):e1232221.

(336) Fridlender ZG, Sun J, Mishalian I, Singhal S, Cheng G, Kapoor V, et al. Transcriptomic Analysis Comparing Tumor-Associated Neutrophils with Granulocytic Myeloid-Derived Suppressor Cells and Normal Neutrophils. PLoS One 2012 Feb 1,;7(2):e31524.

(337) Yu Z, Tan Z, Lee BK, Tang J, Wu X, Cheung K, et al. Antigen spreading-induced CD8+T cells confer protection against the lethal challenge of wild-type malignant mesothelioma by eliminating myeloid-derived suppressor cells. Oncotarget 2015 Oct 20;6(32):32426-32438.

(338) Orr Y, Taylor JM, Bannon PG, Geczy C, Kritharides L. Circulating CD10/CD16low neutrophils provide a quantitative index of active bone marrow neutrophil release. British Journal of Haematology 2005 Nov;131(4):508-519.

(339) Wagner C, Deppisch R, Denefleh B, Hug F, Andrassy K, Hänsch GM. Expression patterns of the lipopolysaccharide receptor CD14, and the FCgamma receptors CD16 and CD64 on polymorphonuclear neutrophils: data from patients with severe bacterial infections and lipopolysaccharide-exposed cells. Shock (Augusta, Ga.) 2003 Jan;19(1):5.

(340) Zhang Y, Velez-Delgado A, Mathew E, Li D, Mendez FM, Flannagan K, et al. Myeloid cells are required for PD-1/PD-L1 checkpoint activation and the establishment of an immunosuppressive environment in pancreatic cancer. Gut 2017;66(1):124-136.

(341) Zea AH, Rodriguez PC, Atkins MB, Hernandez C, Signoretti S, Zabaleta J, et al. Arginase-producing myeloid suppressor cells in renal cell carcinoma patients: a mechanism of tumor evasion. Cancer Res 2005 Apr 15;65(8):3044-3048.

(342) Khanna S, Graef S, Mussai F, Thomas A, Wali N, Yenidunya BG, et al. Tumor-Derived GM-CSF Promotes Granulocyte Immunosuppression in Mesothelioma Patients. Clin Cancer Res 2018.

(343) Babior BM. NADPH Oxidase: An Update. Blood 1999;93(5):1464-1476.

(344) El-Benna J, Dang PM, Gougerot-Pocidalo M. Priming of the neutrophil NADPH oxidase activation: role of p47phox phosphorylation and NOX2 mobilization to the plasma membrane. Semin Immunopathol 2008 Jul;30(3):279-289.

(345) Baggiolini M, Walz A, Kunkel SL. Neutrophil-activating peptide-1/interleukin 8, a novel cytokine that activates neutrophils. J Clin Invest 1989;84(4):1045-1049.

(346) Massena S, Christoffersson G, Vågesjö E, Seignez C, Gustafsson K, Binet F, et al. Identification and characterization of VEGF-A–responsive neutrophils expressing CD49d, VEGFR1, and CXCR4 in mice and humans. Blood 2015;126(17):2016-2026.

(347) Dangaj D, Abbott KL, Mookerjee A, Zhao A, Kirby PS, Sandaltzopoulos R, et al. Mannose Receptor (MR) Engagement by Mesothelin GPI Anchor Polarizes Tumor-Associated Macrophages and Is Blocked by Anti-MR Human Recombinant Antibody. PLoS One 2011 Dec 1,;6(12):e28386.

(348) Oppenheim JJ, Zachariae CO, Mukaida N, Matsushima K. Properties of the novel proinflammatory supergene "intercrine" cytokine family. Annu Rev Immunol 1991;9:617-648.

(349) Weckbach LT, Gola A, Winkelmann M, Jakob SM, Groesser L, Borgolte J, et al. The cytokine midkine supports neutrophil trafficking during acute inflammation by promoting adhesion via β2 integrins (CD11/CD18). Blood 2014 Mar 20,;123(12):1887.

(350) Koster J. R2: Genomics Analysis and Visualization Platform. 2008; Available at: https://r2platform.com. Accessed January, 2018.

(351) Hodi FS, O'Day SJ, McDermott DF, Weber RW, Sosman JA, Haanen JB, et al. Improved survival with ipilimumab in patients with metastatic melanoma. N Engl J Med 2010 Aug 19;363(8):711-723.

(352) Weber JS, D'Angelo SP, Minor D, Hodi FS, Gutzmer R, Neyns B, et al. Nivolumab versus chemotherapy in patients with advanced melanoma who progressed after anti-CTLA-4 treatment (CheckMate 037): a randomised, controlled, open-label, phase 3 trial. Lancet Oncol 2015 Apr;16(4):375-384.

(353) Alley EW, Lopez J, Santoro A, Morosky A, Saraf S, Piperdi B, et al. Clinical safety and activity of pembrolizumab in patients with malignant pleural mesothelioma (KEYNOTE-028): preliminary results from a non-randomised, open-label, phase 1b trial. Lancet Oncol 2017 May;18(5):623-630.

(354) Hsu C, Lee S, Ejadi S, Even C, Cohen RB, Le Tourneau C, et al. Safety and Antitumor Activity of Pembrolizumab in Patients With Programmed Death-Ligand 1–Positive Nasopharyngeal Carcinoma: Results of the KEYNOTE-028 Study. JCO 2017;35(36):4050-4056.

(355) Bert H O'Neil, John M Wallmark, David Lorente, Elena Elez, Judith Raimbourg, Carlos Gomez-Roca, et al. Safety and antitumor activity of the anti–PD-1 antibody pembrolizumab in patients with advanced colorectal carcinoma. PLoS One 2017 Dec 1,;12(12):e0189848.

(356) Yamagishi T, Fujimoto N, Nishi H, Miyamoto Y, Hara N, Asano M, et al. Prognostic significance of the lymphocyte-to-monocyte ratio in patients with malignant pleural mesothelioma. Lung Cancer 2015;90(1):111-117.

(357) Ujiie H, Kadota K, Nitadori JI, Aerts JG, Woo KM, Sima CS, et al. The tumoural and stromal immune
microenvironment in malignant pleural mesothelioma: A comprehensive analysis reveals prognostic immune markers. Oncoimmunology 2015;4(6):e1009285.

(358) McLean MH, Murray GI, Stewart KN, Norrie G, Mayer C, Hold GL, et al. The Inflammatory Microenvironment in Colorectal Neoplasia. PLoS One 2011 Jan 1,;6(1):e15366.

(359) Kuang D, Zhao Q, Wu Y, Peng C, Wang J, Xu Z, et al. Peritumoral neutrophils link inflammatory response to disease progression by fostering angiogenesis in hepatocellular carcinoma. Journal of Hepatology 2011;54(5):948-955.

(360) Bekes EM, Schweighofer B, Kupriyanova TA, Zajac E, Ardi VC, Quigley JP, et al. Tumor-Recruited Neutrophils and Neutrophil TIMP-Free MMP-9 Regulate Coordinately the Levels of

Tumor Angiogenesis and Efficiency of Malignant Cell Intravasation. The American Journal of Pathology 2011;179(3):1455-1470.

(361) Strell C, Lang K, Niggemann B, Zaenker KS, Entschladen F. Neutrophil granulocytes promote the migratory activity of MDA-MB-468 human breast carcinoma cells via ICAM-1. Experimental Cell Research 2010;316(1):138-148.

(362) Rodriguez PC, Quiceno DG, Zabaleta J, Ortiz B, Zea AH, Piazuelo MB, et al. Arginase I production in the tumor microenvironment by mature myeloid cells inhibits T-cell receptor expression and antigen-specific T-cell responses. Cancer Res 2004 Aug 15;64(16):5839-5849.

(363) Bronte V, Serafini P, De Santo C, Marigo I, Tosello V, Mazzoni A, et al. IL-4-Induced Arginase 1 Suppresses Alloreactive T Cells in Tumor-Bearing Mice. The Journal of Immunology 2003 Jan 1,;170(1):270-278.

(364) Otsuji M, Kimura Y, Aoe T, Okamoto Y, Saito T. Oxidative stress by tumor-derived macrophages suppresses the expression of CD3 zeta chain of T-cell receptor complex and antigen-specific T-cell responses. Proceedings of the National Academy of Sciences of the United States of America 1996 Nov 12,;93(23):13119.

(365) Nagaraj S, Gupta K, Pisarev V, Kinarsky L, Sherman S, Kang L, et al. Altered recognition of antigen is a novel mechanism of CD8(+) T cell tolerance in cancer. Nat Med 2007;13(7):828-835.

(366) Demirci U, Coskun U, Sancak B, Ozturk B, Bahar B, Benekli M, Buyukberber S. Serum Granulocyte Macrophage-Colony Stimulating Factor: a Tumor Marker in Colorectal Carcinoma? Asian Pac J Cancer Prev. 2009;10(6):1021-1024.

(367) Dang P, Elbim C, Marie J, Chiandotto M, Gougerot-Pocidalo M, El-Benna J. Anti-inflammatory effect of interleukin-10 on human neutrophil respiratory burst involves inhibition of GM-CSF-induced p47 super(PH0X)phosphorylation through a decrease in ERK1/2 activity. FASEB Journal 2006 Jul 1,;20(9):1504-1506.

(368) Gougerot-Pocidalo MA, el Benna J, Elbim C, Chollet-Martin S, Dang MC. Regulation of human neutrophil oxidative burst by pro- and anti-inflammatory cytokines. Journal de la Société de biologie 2002;196(1):37.

(369) Bayne LJ, Beatty GL, Jhala N, Clark CE, Rhim AD, Stanger BZ, et al. Tumor-Derived Granulocyte-Macrophage Colony-Stimulating Factor Regulates Myeloid Inflammation and T Cell Immunity in Pancreatic Cancer. Cancer Cell 2012 Jun 12,;21(6):822-835.

(370) Dolcetti L, Peranzoni E, Ugel S, Marigo I, Fernandez Gomez A, Mesa C, et al. Hierarchy of immunosuppressive strength among myeloid-derived suppressor cell subsets is determined by GM-CSF. European journal of immunology 2010 Jan;40(1):22-35.

(371) Gargett T, Christo SN, Hercus TR, Abbas N, Singhal N, Lopez AF, et al. GM-CSF signalling blockade and chemotherapeutic agents act in concert to inhibit the function of myeloid-derived suppressor cells in vitro. Clinical & Translational Immunology 2016 Dec;5(12):e119-n/a.

(372) Kosty MP, Herndon JE, Vogelzang NJ, Kindler HL, Green MR. High-dose doxorubicin, dexrazoxane, and GM-CSF in malignant mesothelioma: a phase II study—Cancer and Leukemia Group B 9631. Lung Cancer 2001;34(2):289-295.

(373) Dirix LY, van Meerbeeck J, Schrijvers D, Corthouts B, Prové A, van Marck E, et al. A phase II trial of dose-escalated doxorubicin and ifosfamide/mesna in patients with malignant mesothelioma. Annals of oncology : official journal of the European Society for Medical Oncology 1994 Sep 1,;5(7):653-655.

(374) Powell A, Creaney J, Broomfield S, Van Bruggen I, Robinson B. Recombinant GM-CSF plus autologous tumor cells as a vaccine for patients with mesothelioma. Lung Cancer 2006;52(2):189-197.

(375) Davidson JA, Musk AW, Wood BR, Morey S, Ilton M, Yu LL, et al. Intralesional cytokine therapy in cancer: a pilot study of GM-CSF infusion in mesothelioma. Journal of immunotherapy (Hagerstown, Md. : 1997) 1998 Sep 1,;21(5):389-398.

(376) Staar S, Rudat V, Stuetzer H, Dietz A, Volling P, Schroeder M, et al. Intensified hyperfractionated accelerated radiotherapy limits the additional benefit of simultaneous chemotherapy—results of a multicentric randomized German trial in advanced head-and-neck cancer. International Journal of Radiation Oncology, Biology, Physics 2001;50(5):1161-1171.

(377) Gutschalk CM, Herold-Mende CC, Fusenig NE, Mueller MM. Granulocyte Colony-Stimulating Factor and Granulocyte-Macrophage Colony-Stimulating Factor Promote Malignant Growth of Cells from Head and Neck Squamous Cell Carcinomas In vivo. Cancer Research 2006 Aug 15,;66(16):8026-8036.

(378) Burmester GR, McInnes IB, Kremer J, Miranda P, Korkosz M, Vencovsky J, et al. A randomised phase IIb study of mavrilimumab, a novel GM–CSF receptor alpha monoclonal antibody, in the treatment of rheumatoid arthritis. Annals of the Rheumatic Diseases 2017 Jun;76(6):1020-1030.

(379) Heinrich PC, Behrmann I, Haan S, Hermanns HM, Müller-Newen G, Schaper F. Principles of interleukin (IL)-6-type cytokine signalling and its regulation. The Biochemical journal 2003 Aug 15,;374(Pt 1):1-20.

(380) Quigley M, Huang X, Yang Y. STAT1 Signaling in CD8 T Cells Is Required for Their Clonal Expansion and Memory Formation Following Viral Infection In Vivo. J Immunol 2008;180(4):2158-2164.

(381) Tymoszuk P, Doppler W. Impact of STAT1 and CD8(+) T cells on the antineoplastic activity of lapatinib and doxorubicin against spontaneous mammary tumors. Oncoimmunology 2013 Dec 1;2(12):e26689.

(382) Nefedova Y, Huang M, Kusmartsev S, Bhattacharya R, Cheng P, Salup R, et al. Hyperactivation of STAT3 Is Involved in Abnormal Differentiation of Dendritic Cells in Cancer. The Journal of Immunology 2004 Jan 1,;172(1):464-474.

(383) Banchereau J, Steinman RM. Dendritic cells and the control of immunity. Nature 1998 Mar 19;392(6673):245-252.

(384) Heine A, Held SAE, Daecke SN, Wallner S, Yajnanarayana SP, Kurts C, et al. The JAK-inhibitor ruxolitinib impairs dendritic cell function in vitro and in vivo. Blood 2013 Aug 15,;122(7):1192.

(385) Kujawski M, Zhang C, Herrmann A, Reckamp K, Scuto A, Jensen M, et al. Targeting STAT3 in Adoptively Transferred T Cells Promotes Their In Vivo Expansion and Antitumor Effects. Cancer Research 2010 Dec 1,;70(23):9599-9610.

(386) Hong D, Kurzrock R, Kim Y, Woessner R, Younes A, Nemunaitis J, et al. AZD9150, a next-generation antisense oligonucleotide inhibitor of STAT3 with early evidence of clinical activity in lymphoma and lung cancer. Science translational medicine 2015 Nov 18,;7(314):314ra185.

(387) McManus MT, Haines BB, Dillon CP, Whitehurst CE, van Parijs L, Chen J, et al. Small Interfering RNA-Mediated Gene Silencing in T Lymphocytes. The Journal of Immunology 2002 Nov 15,;169(10):5754-5760.

(388) Zhou T, Georgeon S, Moser R, Moore DJ, Caflisch A, Hantschel O. Specificity and mechanism-of-action of the JAK2 tyrosine kinase inhibitors ruxolitinib and SAR302503. Leukemia 2014 Feb 1,;28(2):471-472.

(389) Khodarev N, Roizman B, Weichselbaum RR. Molecular Pathways: Interferon/Stat1 Pathway: Role in the Tumor Resistance to Genotoxic Stress and Aggressive Growth. Clin Cancer Res. 2012 Jun 1;18(11):3015-21.

(390) Diehl S, Anguita J, Hoffmeyer A, Zapton T, Ihle JN, Fikrig E, et al. Inhibition of Th1 Differentiation by IL-6 Is Mediated by SOCS1. Immunity 2000;13(6):805-815.

(391) Ozao-Choy J, Ma G, Kao J, Wang GX, Meseck M, Sung M, et al. The novel role of tyrosine kinase inhibitor in the reversal of immune suppression and modulation of tumor microenvironment for immune-based cancer therapies. Cancer Res 2009 Mar 15;69(6):2514-2522.

(392) Ciucci T, Vacchio MS, Bosselut R. A STAT3-dependent transcriptional circuitry inhibits cytotoxic gene expression in T cells. Proceedings of the National Academy of Sciences of the United States of America 2017 Dec 12,;114(50):13236.

(393) Almand B, Resser JR, Lindman B, Nadaf S, Clark JI, Kwon ED, et al. Clinical significance of defective dendritic cell differentiation in cancer. Clin Cancer Res 2000 May;6(5):1755-1766.

(394) Wojas K, Tabarkiewicz J, Jankiewicz M, Rolinski J. Dendritic cells in peripheral blood of patients with breast and lung cancer - a pilot study. Folia Histochemica et Cytobiologica 2004 Jan 1,;42(1):45-48.

(395) Troy A, Davidson P, Atkinson C, Hart D. Phenotypic characterisation of the dendritic cell infiltrate in prostate cancer. The Journal of Urology 1998;160(1):214-219.

(396) Park S, Nakagawa T, Kitamura H, Atsumi T, Kamon H, Sawa S, et al. IL-6 Regulates In Vivo Dendritic Cell Differentiation through STAT3 Activation. The Journal of Immunology 2004 Sep 15,;173(6):3844-3854.

(397) Nefedova Y, Cheng P, Gilkes D, Blaskovich M, Beg AA, Sebti SM, et al. Activation of dendritic cells via inhibition of Jak2/STAT3 signaling1. Journal of immunology (Baltimore, Md. : 1950) 2005 Oct 1,;175(7):4338-4346.

(398) Engelhardt JJ, Sullivan TJ, Allison JP. CTLA-4 Overexpression Inhibits T Cell Responses through a CD28-B7-Dependent Mechanism. The Journal of Immunology 2006 Jul 15,;177(2):1052-1061.

(399) Brunner MC, Chambers CA, Chan FK, Hanke J, Winoto A, Allison JP. CTLA-4-Mediated Inhibition of Early Events of T Cell Proliferation. The Journal of Immunology 1999 May 15,;162(10):5813-5820.

(400) Shi F, Shi M, Zeng Z, Qi R, Liu Z, Zhang J, et al. PD-1 and PD-L1 upregulation promotes CD8+ T-cell apoptosis and postoperative recurrence in hepatocellular carcinoma patients. International Journal of Cancer 2011 Feb 15,;128(4):887-896.

(401) Mazanet MM, Hughes CCW. B7-H1 Is Expressed by Human Endothelial Cells and Suppresses T Cell Cytokine Synthesis. J Immunol 2002;169(7):3581-3588.

(402) Garon EB, Rizvi NA, Hui R, Leighl N, Balmanoukian AS, Eder JP, et al. Pembrolizumab for the treatment of non-small-cell lung cancer. The New England journal of medicine 2015 May 21,;372(21):2018-2028.

(403) Bruggemann C, Kirchberger MC, Goldinger SM, Weide B, Konrad A, Erdmann M, et al. Predictive value of PD-L1 based on mRNA level in the treatment of stage IV melanoma with ipilimumab. J Cancer Res Clin Oncol 2017 Oct;143(10):1977-1984.

(404) Carbone DP, Reck M, Paz-Ares L, Creelan B, Horn L, Steins M, et al. First-Line Nivolumab in Stage IV or Recurrent Non–Small-Cell Lung Cancer. N Engl J Med 2017;376(25):2415-2426.

(405) Goodman AM, Kato S, Bazhenova L, Patel SP, Frampton GM, Miller V, et al. Tumor Mutational Burden as an Independent Predictor of Response to Immunotherapy in Diverse Cancers. Mol Cancer Ther 2017 Nov;16(11):2598-2608.

(406) Bilgin B, Sendur MAN, Bulent Akinci M, Sener Dede D, Yalcin B. Targeting the PD-1 pathway: a new hope for gastrointestinal cancers. Curr Med Res Opin 2017;33(4):749-759.

(407) Le DT, Uram JN, Wang H, Bartlett BR, Kemberling H, Eyring AD, et al. PD-1 Blockade in Tumors with Mismatch-Repair Deficiency. N Engl J Med 2015 Jun 25;372(26):2509-2520.

(408) Llosa NJ, Cruise M, Tam A, Wicks EC, Hechenbleikner EM, Taube JM, et al. The vigorous immune microenvironment of microsatellite instable colon cancer is balanced by multiple counter-inhibitory checkpoints. Cancer Discovery 2015 Jan;5(1):43-51.

(409) El Jabbour T, Ross JS, Sheehan CE, Affolter KE, Geiersbach KB, Boguniewicz A, et al. PD-L1 protein expression in tumour cells and immune cells in mismatch repair protein-deficient and -proficient colorectal cancer: the foundation study using the SP142 antibody and whole section immunohistochemistry. J Clin Pathol 2018;71(1):46-51.

(410) Fang W, Zhang J, Hong S, Zhan J, Chen N, Qin T, et al. EBV-driven LMP1 and IFN-γ up-regulate PD-L1 in nasopharyngeal carcinoma: Implications for oncotargeted therapy. Oncotarget 2014 Dec 15,;5(23):12189.

(411) Wolfle SJ, Strebovsky J, Bartz H, Sahr A, Arnold C, Kaiser C, et al. PD-L1 expression on tolerogenic APCs is controlled by STAT-3. European Journal of Immunology 2011 Feb 1,;41(2):413-424.

(412) Bally APR, Austin JW, Boss JM. Genetic and Epigenetic Regulation of PD-1 Expression. Journal of immunology (Baltimore, Md. : 1950) 2016 Mar 15,;196(6):2431.

(413) Austin JW, Lu P, Majumder P, Ahmed R, Boss JM. STAT3, STAT4, NFATc1, and CTCF regulate PD-1 through multiple novel regulatory regions in murine T cells. Journal of immunology (Baltimore, Md. : 1950) 2014 May 15,;192(10):4876.

(414) Probst HC, McCoy K, Honjo T, van den Broek M, Okazaki T. Resting dendritic cells induce peripheral CD8 + T cell tolerance through PD-1 and CTLA-4. Nature Immunology 2005 Mar;6(3):280-286.

(415) Davis RJ, Moore EC, Clavijo PE, Friedman J, Cash H, Chen Z, et al. Anti-PD-L1 Efficacy Can Be Enhanced by Inhibition of Myeloid-Derived Suppressor Cells with a Selective Inhibitor of PI3K delta / gamma. Cancer Research 2017 May 15,;77(10):2607-2619.

(416) Mao Y, Eissler N, Blanc KL, Johnsen JI, Kogner P, Kiessling R. Targeting Suppressive Myeloid Cells Potentiates Checkpoint Inhibitors to Control Spontaneous Neuroblastoma. Clinical Cancer Research 2016 Aug 1,;22(15):3849-3859.

(417) Wang T, Zhao Y, Peng L, Chen N, Chen W, Lv Y, et al. Tumour-activated neutrophils in gastric cancer foster immune suppression and disease progression through GM-CSF-PD-L1 pathway. Gut 2017;66(11):1900-1911.

(418) Nakaya A, Kurata T, Yoshioka H, Takeyasu Y, Niki M, Kibata K, et al. Neutrophil-to-lymphocyte ratio as an early marker of outcomes in patients with advanced non-small-cell lung cancer treated with nivolumab. International Journal of Clinical Oncology 2018.

(419) Diem S, Schmid S, Krapf M, Flatz L, Born D, Jochum W, et al. Neutrophil-to-Lymphocyte ratio (NLR) and Platelet-to-Lymphocyte ratio (PLR) as prognostic markers in patients with non-small cell lung cancer (NSCLC) treated with nivolumab. Lung Cancer 2017;111:176-181.

(420) Bagley SJ, Kothari S, Aggarwal C, Bauml JM, Alley EW, Evans TL, et al. Pretreatment neutrophil-to-lymphocyte ratio as a marker of outcomes in nivolumab-treated patients with advanced non-small-cell lung cancer. Lung Cancer 2017;106:1-7.

(421) Uemura T, Hida T. Durvalumab showed long and durable effects after chemoradiotherapy in stage III non-small cell lung cancer: results of the PACIFIC study. Journal of Thoracic Disease 2018;10:S1108-S1112.

(422) Ozyurek BA, Ozdemirel TS, Ozden SB, Erdogan Y, Kaplan B, Kaplan T. Prognostic Value of the Neutrophil to Lymphocyte Ratio (NLR) in Lung Cancer Cases. Asian Pacific Journal of Cancer Prevention : APJCP 2017;18(5):1417-1421.

(423) Yu Y, Qian L, Cui J. Value of neutrophil-to-lymphocyte ratio for predicting lung cancer prognosis: A meta-analysis of 7,219 patients. Molecular and Clinical Oncology 2017;7(3):498-506.

(424) Kargl J, Busch SE, Yang GHY, Kim K, Hanke ML, Metz HE, et al. Neutrophils dominate the immune cell composition in non-small cell lung cancer. Nature Communications 2017;8:14381.

(425) Lee JY, Lee HT, Shin W, Chae J, Choi J, Kim SH, et al. Structural basis of checkpoint blockade by monoclonal antibodies in cancer immunotherapy. Nature communications 2016 Oct 31,;7(1):13354.

(426) Longoria TC, Tewari KS. Evaluation of the pharmacokinetics and metabolism of pembrolizumab in the treatment of melanoma. Expert Opinion on Drug Metabolism & Toxicology 2016 Oct 2,;12(10):1247-1253.

(427) Lee HT, Lee JY, Lim H, Lee SH, Moon YJ, Pyo HJ, et al. Molecular mechanism of PD-1/PD-L1 blockade via anti-PD-L1 antibodies atezolizumab and durvalumab. Scientific reports 2017 Jul 17,;7(1):5532-12.

(428) Syed Y. Durvalumab: First Global Approval. Drugs 2017 Aug;77(12):1369-1376.

(429) Patel AA, Zhang Y, Fullerton JN, Boelen L, Rongvaux A, Maini AA, et al. The fate and lifespan of human monocyte subsets in steady state and systemic inflammation. The Journal of experimental medicine 2017 Jul 3,;214(7):1913-1923.

(430) Weide B, Martens A, Hassel JC, Berking C, Postow MA, Bisschop K, et al. Baseline Biomarkers for Outcome of Melanoma Patients Treated with Pembrolizumab. Clinical Cancer Research 2016 Nov 15,;22(22):5487-5496.

(431) Ferrucci PF, Gandini S, Battaglia A, Alfieri S, Di Giacomo AM, Giannarelli D, et al. Baseline neutrophil-to-lymphocyte ratio is associated with outcome of ipilimumab-treated metastatic melanoma patients. The British Journal of Cancer 2015 Jun 9,;112(12):1904-1910.

(432) Lalani AA, Xie W, Martini DJ, Steinharter JA, Norton CK, Krajewski KM, et al. Change in neutrophil-to-lymphocyte ratio (NLR) in response to immune checkpoint blockade for metastatic renal cell carcinoma. Journal for ImmunoTherapy of Cancer 2018 Dec;6(1).

(433) Di Giacomo AM, Calabro L, Danielli R, Fonsatti E, Bertocci E, Pesce I, et al. Long-term survival and immunological parameters in metastatic melanoma patients who responded to ipilimumab 10 mg/kg within an expanded access programme. Cancer Immunol Immunother 2013 Jun;62(6):1021-1028.

(434) Milne K, Alexander C, Webb JR, Sun W, Dillon K, Kalloger SE, et al. Absolute lymphocyte count is associated with survival in ovarian cancer independent of tumor-infiltrating lymphocytes. Journal of Translational Medicine 2012 Jan 1,;10(1):33.

(435) He J, Shen G, Ren Z, Qin H, Cui C, Zhang Y, et al. Pretreatment levels of peripheral neutrophils and lymphocytes as independent prognostic factors in patients with nasopharyngeal carcinoma. Head & Neck 2012 Dec;34(12):1769-1776.

(436) Ray-Coquard I, Cropet C, Van Glabbeke M, Sebban C, Le Cesne A, Judson I, et al. Lymphopenia as a Prognostic Factor for Overall Survival in Advanced Carcinomas, Sarcomas, and Lymphomas. Cancer Research 2009 Jul 1,;69(13):5383-5391.

(437) H Schmidt, L Bastholt, P Geertsen, I J Christensen, S Larsen, J Gehl, et al. Elevated neutrophil and monocyte counts in peripheral blood are associated with poor survival in patients with metastatic melanoma: a prognostic model. British Journal of Cancer 2005 Aug 8,;93(3):273-278.

(438) Krieg C, Nowicka M, Guglietta S, Schindler S, Hartmann FJ, Weber LM, et al. High-dimensional single-cell analysis predicts response to anti-PD-1 immunotherapy. Nature Medicine 2018 Feb 1,;24(2):144-153.

(439) Daud AI, Loo K, Pauli ML, Sanchez-Rodriguez R, Sandoval PM, Taravati K, et al. Tumor immune profiling predicts response to anti–PD-1 therapy in human melanoma. Journal of Clinical Investigation 2016 Sep 1,;126(9):3447.

(440) Tumeh PC, Harview CL, Yearley JH, Shintaku IP, Taylor EJM, Robert L, et al. PD-1 blockade induces responses by inhibiting adaptive immune resistance. Nature 2014 Nov 27,;515(7528):568-571.

(441) Walsh SR, Cook EJ, Goulder F, Justin TA, Keeling NJ. Neutrophil-lymphocyte ratio as a prognostic factor in colorectal cancer. Journal of Surgical Oncology 2005 Sep 1,;91(3):181-184.

(442) Wolfle SJ, Strebovsky J, Bartz H, Sahr A, Arnold C, Kaiser C, et al. PD-L1 expression on tolerogenic APCs is controlled by STAT-3. European Journal of Immunology 2011 Feb 1,;41(2):413-424.

(443) Pallandre J, Brillard E, Crehange G, Radlovic A, Remy-Martin J, Saas P, et al. Role of STAT3 Disease and Antitumor Immunity. The Journal of Immunology 2007 Dec 1,;179(11):7593-604.

(444) Salvadori S, Martinelli G, Zier K. Resection of Solid Tumors Reverses T Cell Defects and Restores Protective Immunity. The Journal of Immunology 2000 Feb 15,;164(4):2214-2220.

(445) Rashid OM, Nagahashi, M, Ramachandran, S, Graham, L, Yamada A, Spiegel S, Bear HD, Takabe K. Resection of the primary tumor improves survival in metastatic breast cancer by reducing overall tumor burden. Surgery: Official Journal of the Society of University Surgeons, Central Surgical Association, and the American Association of Endocrine Surgeons 2013;153(6):771-778.

(446) Danna EA, Sinha P, Gilbert M, Clements VK, Pulaski BA, Ostrand-Rosenberg S. Surgical Removal of Primary Tumor Reverses Tumor-Induced Immunosuppression Despite the Presence of Metastatic Disease. Cancer Research 2004 Mar 15,;64(6):2205-2211.

(447) Shoenfeld Y, Tal A, Berliner S, Pinkhas J. Leukocytosis in non hematological malignancies?A possible tumor-associated marker. Journal of cancer research and clinical oncology 1986;111(1):54-58.

(448) Cho H, Hur H, Kim S, Kim S, Kim J, Kim Y, et al. Pre-treatment neutrophil to lymphocyte ratio is elevated in epithelial ovarian cancer and predicts survival after treatment. Cancer Immunol Immunother 2009 Jan;58(1):15-23.

(449) Shimada H, Takiguchi N, Kainuma O, Soda H, Ikeda A, Cho A, et al. High preoperative neutrophil-lymphocyte ratio predicts poor survival in patients with gastric cancer. Gastric Cancer 2010 Aug;13(3):170-176.

(450) An X, Ding P, Wang F, Jiang W, Li Y. Elevated neutrophil to lymphocyte ratio predicts poor prognosis in nasopharyngeal carcinoma. Tumor Biol 2011 Apr;32(2):317-324.

(451) Proctor MJ, Mcmillan DC, Morrison DS, Fletcher CD, Horgan PG, Clarke SJ. A derived neutrophil to lymphocyte ratio predicts survival in patients with cancer. The British Journal of Cancer 2012 Aug 7,;107(4):695-699.

(452) Greifenberg V, Ribechini E, Rössner S, Lutz MB. Myeloid-derived suppressor cell activation by combined LPS and IFN-gamma treatment impairs DC development. European journal of immunology 2009 Oct;39(10):2865-2876.

(453) Hao S, Andersen M, Yu H. Detection of immune suppressive neutrophils in peripheral blood samples of cancer patients. American journal of blood research 2013;3(3):239-245.

(454) Kleijn SD, Langereis JD, Leentjens J, Kox M, Netea MG, Koenderman L, et al. IFN-gamma-Stimulated Neutrophils Suppress Lymphocyte Proliferation through Expression of PD-L1. PLoS One 2013;8(8):e72249.

(455) Ak G, Tada Y, Shimada H, Metintas S, Ito M, Hiroshima K, et al. Midkine is a potential novel marker for malignant mesothelioma with different prognostic and diagnostic values from mesothelin. BMC Cancer 2017 Jan 1,;17(1):212.

(456) Zhang L, Song X, Shao Y, Wu C, Jiang J. Prognostic value of Midkine expression in patients with solid tumors: a systematic review and meta-analysis. Oncotarget 2018 May 15,;9(37):24821-24829.

(457) Maeda S, Shinchi H, Kurahara H, Mataki Y, Noma H, Maemura K, et al. Clinical significance of midkine expression in pancreatic head carcinoma. British Journal of Cancer 2007 Aug 6,;97(3):405-411.

(458) Pilla L, Patuzzo R, Rivoltini L, et al. A phase II trial of vaccination with autologous, tumor-derived heat-shock protein peptide complexes Gp96, in combination with GM-CSF and

interferon-α in metastatic melanoma patients. Cancer Immunol Immunother 2006 Aug;55(8):958-968.

(459) Filipazzi P, Valenti R, Huber V, Pilla L, Canese P, Iero M, et al. Identification of a New Subset of Myeloid Suppressor Cells in Peripheral Blood of Melanoma Patients With Modulation by a Granulocyte-Macrophage Colony-Stimulation Factor–Based Antitumor Vaccine. Journal of Clinical Oncology 2007 Jun 20,;25(18):2546-2553.

(460) Reuter S, Gupta SC, Chaturvedi MM, Aggarwal BB. Oxidative stress, inflammation, and cancer: How are they linked? Free Radical Biology and Medicine 2010;49(11):1603-1616.

(461) Wu Y, Antony S, Meitzler JL, Doroshow JH. Molecular mechanisms underlying chronic inflammation-associated cancers. Cancer Letters 2013;345(2):164-173.

(462) Schreck R, Albermann K, Baeuerle PA. Nuclear Factor Kb: An Oxidative Stress-Responsive Transcription Factor of Eukaryotic Cells (A Review). Free Radical Research 1992;17(4):221-237.

(463) Bonizzi G, Karin M. The two NF-κB activation pathways and their role in innate and adaptive immunity. Trends in Immunology 2004;25(6):280-288.

(464) Gloire G, Legrand-Poels S, Piette J. NF-kappaB activation by reactive oxygen species: fifteen years later. Biochemical pharmacology 2006 Nov 30,;72(11):1493.

(465) Zhu D, Shen Z, Liu J, Chen J, Liu Y, Hu C, et al. The ROS-mediated activation of STAT-3/VEGF signaling is involved in the 27-hydroxycholesterol-induced angiogenesis in human breast cancer cells. Toxicology Letters 2016 Dec 15,;264:79-86.

(466) Wang N, Zhan T, Ke T, Huang X, Ke D, Wang Q, et al. Increased expression of RRM2 by human papillomavirus E7 oncoprotein promotes angiogenesis in cervical cancer. British journal of cancer 2014 Feb 18,;110(4):1034-1044.

(467) Lee SY, Ju MK, Jeon HM, Lee YJ, Kim CH, Park HG, et al. Reactive oxygen species induce epithelial-mesenchymal transition, glycolytic switch, and mitochondrial repression through the Dlx-2/Snail signaling pathways in MCF-7 cells. Molecular medicine reports 2019 Sep;20(3):2339.

(468) Sun H, Yang X, Zhao Y, Tian Q, Chen M, Zhao Y, et al. Loss of TMEM126A promotes extracellular matrix remodeling, epithelial-to-mesenchymal transition, and breast cancer metastasis by regulating mitochondrial retrograde signaling. Cancer Letters 2019 Jan;440-441:189-201.

(469) Galffy G, Mohammed KA, Dowling PA, Nasreen N, Ward MJ, Antony VB. Interleukin 8: An Autocrine Growth Factor for Malignant Mesothelioma. Cancer Research 1999 Jan 1,;59(2):367.

(470) Monti G, Jaurand M, Monnet I, Chretien P, Saint-Etienne L, Zeng L, et al. Intrapleural production of interleukin 6 during mesothelioma and its modulation by gamma -interferon treatment. Cancer Research 1994 Jan 1,;54(16):4419-4423.

(471) Rincón M, Anguita J, Nakamura T, Fikrig E, Flavell RA. Interleukin (IL)-6 directs the differentiation of IL-4-producing CD4+ T cells. The Journal of experimental medicine 1997 Feb 3,;185(3):461-470.

(472) Curran D, Sahmoud T, Therasse P, van Meerbeeck J, Postmus PE, Giaccone G. Prognostic factors in patients with pleural mesothelioma: the European Organization for Research and Treatment of Cancer experience. Journal of Clinical Oncology 1998 Jan 1,;16(1):145-152.

(473) Edwards JG, Abrams KR, Leverment JN, Spyt TJ, Waller DA, O'Byrne KJ. Prognostic factors for malignant mesothelioma in 142 patients: validation of CALGB and EORTC prognostic scoring systems. Thorax 2000 Sep;55(9):731-735.

(474) Fennell DA, Parmar A, Shamash J, Evans MT, Sheaff MT, Sylvester R, et al. Statistical Validation of the EORTC Prognostic Model for Malignant Pleural Mesothelioma Based on Three Consecutive Phase II Trials. Journal of Clinical Oncology 2005 Jan 1,;23(1):184-189.

(475) McMillan DC. An inflammation-based prognostic score and its role in the nutrition-based management of patients with cancer. Proceedings of the Nutrition Society 2008 Aug 1,;67(3):257-262.

(476) Akamine T, Takada K, Toyokawa G, Kinoshita F, Matsubara T, Kozuma Y, et al. Association of preoperative serum CRP with PD-L1 expression in 508 patients with non-small cell lung cancer: A comprehensive analysis of systemic inflammatory markers. Surgical Oncology 2018 Mar;27(1):88-94.

(477) Ito M, Oshima Y, Yajima S, Suzuki T, Nanami T, Shiratori F, et al. Is high serum programmed death ligand 1 level a risk factor for poor survival in patients with gastric cancer? Annals of Gastroenterological Surgery 2018 Jul;2(4):313-318.

(478) Wang J, Xu Y, Huang Z, Lu X. T cell exhaustion in cancer: Mechanisms and clinical implications. Journal of Cellular Biochemistry 2018 Jun;119(6):4279-4286.

(479) Hu P, Shen H, Wang G, Zhang P, Liu Q, Du J. Prognostic Significance of Systemic Inflammation-Based Lymphocyte- Monocyte Ratio in Patients with Lung Cancer: Based on a Large Cohort Study. PLoS One 2014 Oct 1,;9(10):e108062.

(480) Delyon J, Mateus C, Lefeuvre D, Lanoy E, Zitvogel L, Chaput N, et al. Experience in daily practice with ipilimumab for the treatment of patients with metastatic melanoma: an early increase in lymphocyte and eosinophil counts is associated with improved survival. Annals of oncology : official journal of the European Society for Medical Oncology 2013 Jun 1,;24(6):1697-1703.

(481) Zhu X, Lang J. Soluble PD-1 and PD-L1: predictive and prognostic significance in cancer. Oncotarget 2017 Nov 14,;8(57):97671-97682.

(482) Frigola X, Inman BA, Krco CJ, Liu X, Harrington S, Bulur PA, Dietz AB, Dong H, Kwon ED. Soluble B7-H1: Differences in production between dendritic cells and T cells. Immunology Letters 2011;142(1):78-82.

(483) Okuma Y, Hosomi Y, Nakahara Y, Watanabe K, Sagawa Y, Homma S. High plasma levels of soluble programmed cell death ligand 1 are prognostic for reduced survival in advanced lung cancer. Lung Cancer 2016;104:1-6.

(484) Wang A, Wang HY, Liu Y, Zhao MC, Zhang HJ, Lu ZY, Fang YC, Chen XF, Liu GT. The prognostic value of PD-L1 expression for non-small cell lung cancer patients: A meta-analysis. European Journal of Surgical Oncology 2015;41(4):450-456.

(485) Guerrero L, Kulangara K, Truong Y, Schwefel S, Hanks D. Abstract LB-218: Pathologist reproducibility of combined positive score (CPS) for the evaluation of PD-L1 in gastric or gastroesophageal junction adenocarcinoma tumors. Cancer Research 2018 Jul 1,;78(13 Supplement):LB-218.

(486) Milos PM, Ozsolak F. RNA sequencing: advances, challenges and opportunities. Nature Reviews Genetics 2011 Feb;12(2):87-98.

(487) Byron SA, Van Keuren-Jensen KR, Engelthaler DM, Carpten JD, Craig DW. Translating RNA sequencing into clinical diagnostics: opportunities and challenges. Nature reviews. Genetics 2016 May;17(5):257-271.

(488) Le DT, Durham JN, Smith KN, Wang H, Bartlett BR, Aulakh LK, et al. Mismatch repair deficiency predicts response of solid tumors to PD-1 blockade. Science 2017 Jul 28,;357(6349):409.